

Cellular mechanism of contractile dysfunction in the diabetic heart

Nicolas Keith Bracken, BSc (Hons)

A thesis submitted for the Degree of
Doctor of Philosophy



2003

TABLE OF CONTENTS

ACKNOWLEDGEMENTS	vi
DEDICATION	vii
DECLARATION	viii
ABSTRACT	ix
ABBREVIATIONS	xii
1 GENERAL INTRODUCTION	1
1.1 History of diabetes	2
1.1.1 The search for an extract	2
1.2 Diabetes Mellitus	3
1.2.1 A worldwide disease	4
1.2.2 Type 1 diabetes mellitus.....	4
1.3 Animal model of diabetes	6
1.3.1 Chemically-induced type 1 model of diabetes mellitus.....	6
1.4 The normal heart	8
1.4.1 The mechanical events of the cardiac cycle	9
1.4.2 Ultra structure of the heart	10
1.4.3 The working myocyte	13
1.4.4 Cardiac action potential.....	14
1.4.5 Rat ventricular action potentials	15
1.4.6 Electrical conductance within the heart	17
1.4.7 Excitation-contraction coupling in the normal heart	21
1.4.8 Calcium sparks underlying local control in heart cells.....	22
1.5 Diabetic cardiomyopathy and cardiovascular disease	23
1.5.1 Contractile dysfunction in the diabetic heart.....	24
1.6 Cardiac myocyte in the resting state	24
1.7 Mediators of calcium influx	25
1.7.1 Sarcolemmal calcium channels	25
1.7.2 Sarcolemmal sodium/calcium exchanger.....	26
1.7.3 Adrenergic response and calcium mobilisation in the heart	27
1.8 Mediators of systolic calcium	29
1.8.1 Ryanodine receptor activation and sarcoplasmic reticulum release	29
1.8.2 Myofilament interaction.....	30

1.9	Mediators of relaxation	31
1.9.1	Sarcoplasmic reticulum uptake.....	32
1.9.1.1	Phospholamban.....	33
1.9.2	Sodium calcium exchanger	33
1.9.3	PMCA pump.....	34
1.10	The story so far	35
1.11	Changes in Cation distribution within the diabetic heart.....	36
1.12	The effect of halothane on the heart	38
1.13	Aims of the study	40
2	MATERIALS AND METHODS.....	42
2.1	Materials	43
2.2	Induction of diabetes	43
2.2.1	Measurement of blood glucose, plasma osmolarity and plasma insulin.....	43
2.3	Preparation of heart tissue for cation analysis	44
2.4	Cardiac myocyte isolation for contractility study and calcium measurement 44	
2.4.1	Isolation of ventricular myocytes	45
2.4.2	Isolation of sub-endocardial and sub-epicardial myocytes.	45
2.5	Measurement of total cardiac calcium, copper, iron, magnesium and zinc	49
2.6	Measurement of contraction in cardiac myocytes.....	49
2.6.1	Effects of insulin and STZ on contraction	50
2.6.2	Effect of halothane, glucose and perturbation of external calcium on contraction	50
2.7	Measurement of intracellular calcium transients in cardiac myocytes	50
2.7.1	Effect of halothane and calcium on cardiac calcium transients	51
2.8	Simultaneous measurement of contraction and calcium in cardiac myocytes	51
2.9	Effect of caffeine on fractional calcium release in cardiac myocytes.....	52
2.10	Effects of nickel chloride on caffeine-induced calcium release	52
2.11	Voltage dependence of contraction and calcium current in cardiac myocytes	53
2.11.1	Effects of halothane on calcium current and voltage dependence of contraction	54
2.12	Data analysis and statistics.....	54

3	GENERAL CHARACTERISTICS OF THE STREPTOZOTOCIN-INDUCED DIABETIC RAT HEART.....	55
3.1	General characteristics of the streptozotocin-induced diabetic rat heart and ventricular myocytes at differing treatment times.....	56
3.1.1	Introduction	56
3.1.2	Methods.....	57
3.1.3	Results.....	57
3.1.4	Discussion	61
3.1.5	Conclusion.....	62
3.2	Distribution of specific divalent cation within the streptozotocin-induced diabetic rat heart.....	63
3.2.1	Introduction	63
3.2.1.1	Magnesium	63
3.2.1.2	Calcium	64
3.2.1.3	Copper.....	64
3.2.1.4	Iron.....	65
3.2.1.5	Zinc	65
3.2.2	Method	65
3.2.3	Results.....	66
3.2.4	Discussion	69
3.2.4.1	Magnesium content.....	69
3.2.4.2	Calcium content.....	70
3.2.4.3	Copper content.....	70
3.2.4.4	Iron content.....	71
3.2.4.5	Zinc content.....	71
3.2.5	Conclusion.....	71
4	EFFECTS OF STREPTOZOTOCIN-INDUCED DIABETES ON CONTRACTION IN RAT CARDIOMYOCYTES	73
4.1	Time dependent effects of streptozotocin-induced diabetes on the kinetics of contraction in ventricular myocytes isolated from rat heart.....	74
4.1.1	Introduction	74
4.1.2	Method	75
4.1.3	Results.....	75
4.1.4	Discussion	79
4.2	Post rest potentiation in STZ-induced diabetic heart	81
4.2.1	Introduction	81
4.2.2	Method	81
4.2.3	Results.....	82
4.2.4	Discussion	85
4.3	Effects of chronic streptozotocin-induced diabetes on contraction-frequency relationships in ventricular myocytes isolated from rat heart	87
4.3.1	Introduction	87
4.3.2	Method	87
4.3.3	Results.....	88
4.3.4	Discussion	91

4.4	Effect of insulin, streptozotocin and perturbation of external calcium concentration on the contractility of streptozotocin-induced diabetic ventricular myocytes.	92
4.4.1	Introduction	92
4.4.2	Method	93
4.4.3	Results	93
	Shortening	97
	(% RCL)	97
4.4.4	Discussion	98
4.5	Effects of varying glucose concentrations on the kinetics of contraction in ventricular myocytes isolated from streptozotocin-induced diabetic rat heart	100
4.5.1	Introduction	100
4.5.2	Method	101
4.5.3	Results	101
4.5.4	Discussion	105
4.6	Regional differences in the streptozotocin –induced diabetic heart	107
4.6.1	Introduction	107
4.6.2	Method	107
4.6.3	Results	108
4.6.4	Discussion	111
4.7	Conclusion	112
5	EFFECTS OF STREPTOZOTOCIN-INDUCED DIABETES ON CALCIUM HOMEOSTASIS IN RAT CARDIOMYOCYTES	113
5.1	General introduction	114
5.2	Effect of perturbation of extracellular calcium on calcium transients in the streptozotocin induced ventricular myocytes in the diabetic heart	116
5.2.1	Introduction	116
5.2.2	Method	116
5.2.3	Results	117
5.2.4	Discussion	121
5.3	Time dependent effects of STZ-induced diabetes	122
5.3.1	Results	122
5.4	The effects of caffeine-induced calcium transients in isolated ventricular myocytes from streptozotocin-induced diabetic rat heart	127
5.4.1	Introduction	127
5.4.2	Method	127
5.4.3	Results	128
5.4.4	Discussion	131
5.5	Effects of nickel on caffeine-induced calcium transients in the isolated ventricular myocytes from streptozotocin-induced diabetic rat heart	134
5.5.1	Introduction	134
5.5.2	Method	134
5.5.3	Results	135

5.5.3.1	Comparison of rate of decay.....	137
5.5.4	Discussion	139
6	EFFECTS OF HALOTHANE ON $I_{Ca,L}$, $[Ca^{2+}]_i$ AND CONTRACTION IN THE STREPTOZOTOCIN-INDUCED DIABETIC AND AGE-MATCHED CONTROL CARDIOMYOCYTE.....	140
6.1	Introduction	141
6.2	Results	143
6.2.1	Current function.....	145
6.2.2	Current Amplitude	145
6.2.3	Current/ voltage relationship	147
6.2.4	Voltage dependence of contraction.....	149
6.2.5	Contraction	151
6.2.6	Calcium	155
6.2.7	Myofilament calcium sensitivity	159
6.3	Discussion.....	162
6.3.1	$I_{Ca,L}$ amplitude and t_{pk}	162
6.3.2	Current voltage relationship	162
6.3.3	Voltage dependence of contraction.....	163
6.3.4	Contraction	165
6.3.5	Calcium	165
6.3.6	Myofilament sensitivity	166
7	GENERAL DISCUSSION AND FINAL COMMENTS	168
7.1	Final conclusion	173
8	APPENDIX.....	175
8.1	Solutions.....	176
8.1.1	Isolation solution	176
8.1.2	Normal Tyrode (NT) solution	176
8.1.3	Patch pipette solution.....	176
8.1.4	Halothane solution	176
9	REFERENCES.....	177
9.1	References sited within this thesis.....	178
9.2	List of publications arising from work which has been undertaken	217

ACKNOWLEDGEMENTS

I would like to extend my thanks to my Director of Studies, Professor Jaipaul Singh and my supervisors Dr. Chris Howarth and Professor Bill Winlow for their help, interest and general guidance throughout my research studies.

I would also like to acknowledge the support of the British Heart Foundation for their financial funding of this PhD and the Physiological Society and the British Council for financial funding which has enabled me to attend meetings and to work at the United Arab Emirates (UAE) University in Al Ain, UAE.

I would like to thank and acknowledge the contribution of my colleague Dr. Alyson Woodall, whose advice, encouragement and friendship has helped me enormously with my research programme. I would also wish to acknowledge Mr. Anwar Qureshi at the UAE University in Al Ain, UAE, whose technical expertise has helped me tremendously.

Special thanks go to Miss. Christine Woodcock for setting up and looking after the animal's models I used and to Dr. George Lees at the University of Sunderland for all his help and encouragement with the patch clamp experiments.

My thanks and appreciation is extended to the technical staff within the department and to fellow research students who have helped me throughout my studies.

Most of all I would like to thank my whole family, especially my wife Emily who has been a constant source of encouragement, support and understanding throughout my research studies.

DEDICATION

This thesis is dedicated to Emily and James with all my love.

DECLARATION

I declare that this thesis has been composed by myself and while registered as a candidate for the degree for which submission is made, I have not been a registered candidate for any other higher research degree at this or any other University or other institution of learning. No material in this thesis has been used in any other submission for an academic qualification.

A handwritten signature in black ink, consisting of a large, stylized initial 'S' followed by a cursive name.

Abstract

The aim of this study was to investigate the cellular mechanism(s) that underpins contractile dysfunction in the streptozotocin (STZ)-induced diabetic rat heart compared to age-matched control heart. In some experiments, a clinically relevant concentration of the volatile anaesthetic halothane (0.6 mM) was used to examine its effect on contractile properties of STZ-induced diabetic heart. Diabetes was induced in male Wistar rats by a single i.p. injection of STZ (60 mg Kg⁻¹, body weight) which, resulted in an experimental model of type 1 diabetes that was characterised by hypoinsulinaemia, hyperglycaemia, increases in osmolarity and decreases in body and heart weights. Total cation contents (Ca²⁺, Cu²⁺, Zn²⁺ and Fe²⁺) were significantly (P<0.05) increased in the STZ-induced diabetic heart compared to age-matched controls. The majority of experiments were carried out on ventricular myocytes following 8-12 weeks of STZ treatment. L-type calcium (Ca²⁺) current ($I_{Ca,L}$) was measured in patch clamped ventricular myocytes in whole cell mode, using a cesium-based pipette solution and a holding potential of -40 mV and test potentials between -30 and 50 mV. The amplitude of $I_{Ca,L}$ was significantly (P<0.05) decreased in the STZ-induced diabetic myocytes compared to age-matched control. Furthermore, halothane further reduced the peak $I_{Ca,L}$ to levels in both age-matched control and STZ-induced diabetic myocytes. Contraction was measured in electrically-stimulated myocytes via a video-edge detector and results showed that the amplitude of contraction as a percentage of resting cell length (% RCL) was significantly (P<0.01) greater in STZ-induced diabetic myocytes (6.8 ± 0.5 %, n=32) compared to that of age-matched control (4.1 ± 1.04 %, n=27). Moreover, the t_{pk} of contraction was found to be significantly (P<0.01) longer in diabetic myocytes (164.1 ± 7.4 ms, n=30 *Vs.* 132.3 ± 5.9 ms, n=27) compared to control, respectively. Halothane evoked significant (P<0.05) reductions in the amplitude of contraction in control myocytes. The amplitude of

contraction was significantly ($P < 0.01$) reduced further in STZ-induced myocytes compared to the response in the absence of halothane. In voltage clamped myocytes however, contraction was peak amplitude of contraction was greater in control compared to STZ-induced myocytes. Since contraction is ultimately dependent on cytosolic Ca^{2+} , it was relevant to measured free intracellular Ca^{2+} concentrations ($[\text{Ca}^{2+}]_i$) using the fluorescent dye fura-2. Basal resting Ca^{2+} (measure by fluorescence ratio units) was significantly ($P < 0.01$) increased in STZ-induced diabetic myocytes following 8 weeks of treatment compared to age-matched control (0.599 ± 0.009 ratio units, $n=23$ Vs. 0.521 ± 0.012 ratio units, $n=23$), respectively. Electrically stimulated cardiac myocytes (1 Hz) induced Ca^{2+} transients that had a longer time from the peak (t_{pk}) of Ca^{2+} transient to half decay ($t_{1/2 \text{ decay}}$). Moreover, in the presence of halothane, the amplitude of electrically stimulated Ca^{2+} transient release was significantly ($P < 0.05$) decreased in control and STZ-induced myocytes but was not significantly altered between control and STZ-induced myocytes. Following a caffeine-induced Ca^{2+} release, $t_{1/2 \text{ decay}}$ of Ca^{2+} decay was significantly ($P < 0.01$) longer (43%) in myocytes obtained from STZ-induced compared to age-matched controls. However, in the presence of 10 mM nickel chloride (NiCl_2), the rate of Ca^{2+} efflux out of the cell was similar in both control and diabetic myocyte. Myofilament sensitivity was studied by plotting the relationship between contraction and Ca^{2+} in control and STZ-induced diabetic myocytes. The results show that myofilament sensitivity for Ca^{2+} is increased in the STZ-induced myocytes but is significantly ($P < 0.05$) reduced following the application of halothane.

In conclusion, the results have shown that in electrically stimulated STZ-induced diabetic myocytes, the increase in contraction is primarily caused by an increase in myofilament Ca^{2+} sensitivity, and not through an increase in Ca^{2+} release from the SR. Moreover, in the STZ-induced diabetic myocytes an alteration in $\text{Na}^+/\text{Ca}^{2+}$ -exchanger may contribute to a

prolonged Ca^{2+} transient. It is suggested that prolonged Ap duration in the diabetic heart leads to increased Ca^{2+} influx albeit a reduced $I_{\text{Ca,L}}$, which may overcompensate for a decrease in SERCA function (that has been reported in the diabetic heart, Misra *et al.* 1999) and may lead to similar SR Ca^{2+} load and release in both diabetic and control myocytes. Following, SR Ca^{2+} release it is suggested that the increased myofilament Ca^{2+} sensitivity in STZ-induced myocytes leads to an increase in contraction that has been reported in this study.

In voltage clamped STZ-induced diabetic myocytes, a decrease in $I_{\text{Ca,L}}$ was mirrored by a decrease in the peak amplitude of contraction. It is suggested that in voltage clamped myocytes from STZ-induced hearts, that are not influenced by the Ap, decreased $I_{\text{Ca,L}}$, may lead to a reduced Ca^{2+} influx and subsequent SR Ca^{2+} release. Reduced Ca^{2+} release from the SR, may not be compensated for by the increase in myofilament Ca^{2+} sensitivity in the diabetic heart, and may ultimately lead to a reduction in the amplitude of contraction that has been reported in this study.

It has also been shown that, following the application of halothane, the $I_{\text{Ca,L}}$, Ca^{2+} transient and amplitude of contraction were significantly more decreased in STZ-induced myocytes compared to that of control. It is suggested that reduced myofilament Ca^{2+} sensitivity in the presence of halothane contributes to the changes in contraction. However, it is also likely that another mechanism such as fractional Ca^{2+} release and/or SR Ca^{2+} load may also be affected by the actions of halothane in the diabetic heart.

ABBREVIATIONS

Adenosine 3',5'-cyclic-monophosphate	cAMP
Adenosine 5' diphosphate	ADP
Adenosine 5' monophosphate	AMP
Adenosine 5' tri phosphate	ATP
American Diabetes Association	ADA
Aortic output	AO
Atrio-ventricular	AV
Calcium-induced calcium release	CICR
Celsius	°C
Congestive heart failure	CHF
Copper	Cu ²⁺
Coronary heart disease	CHD
Current	<i>I</i>
Deoxyribonucleic acid	DNA
Diabetes mellitus	DM
Electrocardiograph	ECG
End diastolic volume	EDV
Ethylene glycol-bis (2-aminoethylether)-N,N,N',N'-tetraacetic acid	EGTA
Excitation-contraction	E-C
grams	g
Halothane	HAL
Hertz	Hz
Human leukocyte antigen	HLA
Insulin dependent diabetes mellitus	IDDM

Intracellular calcium	$[Ca^{2+}]_i$
Intracellular magnesium	$[Mg^{2+}]_i$
Intracellular potassium	$[K^+]_i$
Intracellular sodium	$[Na^+]_i$
Ionised calcium	Ca^{2+}
Ionised chloride	Cl^-
Ionised iron	Fe^{2+}
Ionised magnesium	Mg^{2+}
Ionised potassium	K^+
Ionised sodium	Na^+
Ionised Zinc	Zn^{2+}
Ischemic heart disease	IHD
L-type calcium channel current	$I_{Ca,L}$
Membrane potential	E_m
Messenger ribose nucleic acid	mRNA
milligrammes	mg
millimolar	mM
millimoles	mmol
milliosmoles	mosmol
millivolts	mV
Molecular weight	MW
Myocardial infarction	MI
Myosin heavy chain	MHC
Myosin light chain	MLC
Nano amp	nA

Nickel chloride	NiCl ₂
Nicotinamide adenine dinucleotide phosphate	NADP ⁺
Nitric oxide	NO
Non-esterified fatty acids	NEFA
Non-Insulin dependent diabetes mellitus	NIDDM
Normal Tyrode solution	NT
Per kilogram	Kg ⁻¹
Per litre	l ⁻¹
Phospholamban	PLB
Plasma membrane calcium-ATPase pump	PMCA
Protein kinase	PK
Ribose nucleic acid	RNA
Ryanodine receptor	RyR
Sarcoplasmic reticulum	SR
Sarcoplasmic reticulum calcium-ATPase pump	SERCA
Sino-atrial	SA
Streptozotocin	STZ
Stroke volume	SV
Sub-endocardial myocytes	Endo
Sub-epicardial myocytes	Epi
Time to half relaxation	<i>t</i> _{1/2 relax}
Time to peak	<i>t</i> _{pk}
Voltage activated calcium release	VACR

Chapter 1

General introduction

1.1 History of diabetes

Diabetes has been recognised as a disease state since ancient times. The Ebers papyrus discovered by a German Egyptologist in 1862, dates from 1550 BC and describes a state of polyuria resembling diabetes. For thousands of years, no one knew how to live with, let alone correct diabetes. Children with the disease died quickly, often within days of onset, and older people struggled with devastating complications (Williams & Pickup, 1999).

In 1869, Paul Langerhans, a German medical student in his doctoral thesis, was the first to describe a small cluster of cells in teased preparation of the pancreas, but he was not able to explain their function, and it was Edouard Laguesse in 1893 who named the cells the 'Islets of Langerhans' and suggested the function of the cells to be endocrine in origin. In 1889 twenty years after Paul Langerhans discovery, Oscar Minkowski and Josef von Mering, using dog experiments showed that if the pancreas was removed from the body, the animal displayed typical signs of diabetes, with polydipsia, polyuria and muscle wasting, which were associated with glycosuria and hyperglycaemia (Williams & Pickup, 1999).

1.1.1 The search for an extract

The link between the pancreas and diabetes had now been recognised. This led to research focusing on treating the disease with pancreatic extracts. It was the discovery of insulin in 1921 at the University of Toronto, Canada through collaboration of Frederick Banting and his assistant Charles Best, the biochemist James Collip and physiologist John Macleod that would prove to be one of the greatest breakthroughs in the understanding of diabetes. Banting and Best made chilled extracts of dog pancreas (called isletin by Banting and Best

but later changed to insulin by the request of Macleod, the name given to the hormone in 1909 by Belgium researcher Jean de Meyer) and injected them in pancreatectomised, diabetic dogs. Following the administration of the pancreas the blood sugar of the dogs declined. Macleod and Banting were awarded the Nobel Prize in 1923, which they later shared with Best, and Collip (Joslin, 1948). Collip (1922) later developed an improved extraction procedure, and the first diabetic patient was treated on 1st January 1922. A commercially viable extraction method was then developed in collaboration with chemists at Eli Lilly and Co. and insulin then became widely available in North America and Europe from around 1923 (Williams & Pickup, 1999).

Later developments in insulin research came with the discovery of the primary structure of insulin by Frederick Sanger in 1955 and in 1969 when Dorothy Hodgkin and colleagues described its three dimensional structure (Williams & Pickup, 1999).

1.2 Diabetes Mellitus

Diabetes Mellitus, once considered of minor significance to world health is now ranked amongst the main targets of human health in the 21st century (Zimmet, 2000). The increased attention to diabetes stems from the rising number of people who are diagnosed with the disease (King *et al.* 1998). The disease is recognised as a group of heterogeneous population disorders characterised by fasting hyperglycaemia and glucose intolerance, due to insulin deficiency, impaired effectiveness of insulin action or both (Harris & Zimmet, 1997). It is classified on the basis of aetiology, natural history and clinical presentation of the disease. In 1997 the American Diabetes Association (ADA) classified diabetes in terms of aetiology and not by treatment, and to date, diabetes is classified into two main types; type 1 diabetes mellitus (previously known as insulin-dependent diabetes mellitus (IDDM)

or juvenile onset) and type 2 diabetes mellitus (previously known as non-insulin-dependent diabetes mellitus (NIDDM) and maturity onset) (Williams & Pickup, 1999).

1.2.1 A worldwide disease

Diabetes is a major global health problem. In 1997, an estimated 124 million people worldwide had diabetes, 97 % of these having type 2 diabetes (Amos *et al.* 1997). This figure has now increased to an estimated 160 million today, and is expected to reach a level of 221 million in 2010 (Amos *et al.* 1997) and 300 million world-wide by 2025 (King *et al.* 1998). Within the U.K. alone, type 2 diabetes affects in excess of 1 million people.

1.2.2 Type 1 diabetes mellitus

Type 1 diabetes can occur at all ages but is predominant in children and young adults, with a peak incidence before school age (Williams & Pickup, 1999). The exact cause of the disease is multiple in nature and still imperfectly understood, but is thought to be a consequence of the cellular mediated autoimmune degeneration of pancreatic islet-beta (β) cells and/or environmental factors (Schaffer, 1991). Much evidence suggests that type 1 diabetes has geographical, ethnic or seasonal differences. The highest world incidence of type 1 diabetes is found in Finland where there is reported to be 35 cases per 100,000 people (Tuomilehto *et al.* 1992a), however, in other Baltic states such as Estonia, the incidence is only one third that of Finland, although the country is made up of people of similar linguistic and ethnic background (Tuomilehto *et al.* 1992b). This would suggest that environmental agents have a strong control in the induction of type 1 diabetes. However, despite strong epidemiological evidence it has been difficult to trace particular environmental factors that trigger the disease in genetically susceptible individuals

(Zimmet *et al.* 2001). Comparable with other disease states, a growing number of factors have reported to be involved in triggering diabetes, which includes exposure of viruses (mumps, rubella). Weaning on cows milk and ingestion of smoked meat products have also been reported as induction agents (Williams & Pickup, 1999). The difficulty in identifying environmental factors comes about because of the time difference between being exposed to the triggering agent and the initial onset of hyperglycaemia (Zimmet *et al.* 2001). One new report targets a macrolide antibiotic bafilomycin A1 (bafA1) derived from the *Streptomyces* species as an agent that disrupts pancreatic insulin secretion in mice (Myers *et al.* 2001). *Streptomyces* species are found in soil and some vegetables including, potatoes and sugar beet (Myers *et al.* 2001). Therefore, it has been suggested that everyday common food sources or soil derivatives may be the trigger for the disease (Myers *et al.* 2001). The interesting thing is that a *Streptomyces* species is also the source of STZ, the agent that is widely used to induce pancreatic β -cell necrosis in many experimental rodent models of type 1 diabetes.

The commonest cause of type 1 diabetes is the autoimmune destruction of the pancreatic β -cells in the islets of Langerhans. The exact aetiology is complex and not thoroughly understood. As has been suggested, it is thought that environmental factors may trigger the response in people who have an inherent genetic susceptibility for the disease. Inherited susceptibility to type 1 diabetes depends on several genes at different loci. A major component of the genetic predisposition is encoded within the human leukocyte antigen (HLA) genes lying within the region of the short arm chromosome 6 (Newly called the 'type 1 diabetes locus'). HLA antigens are cell surface glycoproteins and certain HLA-DR (3 and 4) and DQ alleles encoding antigen-presenting molecules have been established to be involved in the susceptibility of type 1 diabetes (Thorsby *et al.* 1998).

Type 1 diabetes is characterised by the loss of insulin production, resulting in a decrease in circulating plasma insulin. This insulin deficiency in the presence of catabolic counter-regulatory hormones such as catecholamines, cortisol, glucagon and growth hormones increase lipolysis within the adipose tissue. The consequence of this is the release of non-esterified fatty acids (NEFA) into the circulation. Within the liver the fatty acids (FA) are partially oxidised to produce ketone bodies, acetoacetic acid and 3-hydroxybutyric acid. All of these contribute to the state of acidosis (Williams & Pickup, 1999). The symptoms of ketoacidosis include polydipsia, polyuria, weight loss, leg cramps and weakness and if not dealt with, can soon lead to diabetic coma and eventual death (Amos *et al.* 1997). Therefore, type 1 diabetic patients have an absolute requirement for insulin, to prevent the life threatening consequences of hyperglycaemia and ketoacidosis (Schaffer, 1991).

1.3 Animal model of diabetes

Most of the experimental data regarding the pathogenesis of diabetic complications have been accumulated using animal models of diabetes, which can be characterised into two main types: experimentally-induced diabetes and spontaneously, genetically determined diabetes (Dhalla *et al.* 1985).

1.3.1 Chemically-induced type 1 model of diabetes mellitus.

Experimental-induction of diabetes frequently involves the administration of an agent, which will induce β -cell necrosis of the pancreas. Two widely used diabetogenic agents are alloxan and STZ (2-deoxy-2-[[[(methylnitrosamino)carbonyl]amino]-D-lucopyranose). STZ appears to be highly specific to β -cells whereas alloxan has been shown to elicit non-

specific necrotic effects. STZ is synthesized by the bacterium *Streptomyces achromogenes* (Szkudelski, 2001). Doses of STZ between 40-60 mg Kg⁻¹ are used to induce an experimental model of type 1 diabetes (Szkudelski 2001). Following administration, STZ is taken up by the pancreatic β -cells via the glucose transporter GLUT2. STZ then causes alkylation (Elsner *et al.* 2000) of deoxyribonucleic acid (DNA), which in turn leads to the activation of poly adenosine 5' diphosphate (ADP)-ribosylation (Sandler & Swenne, 1983). The consequence of this is the cellular depletion of nicotinamide adenine dinucleotide phosphate (NADP⁺) and adenosine tri-phosphate (ATP) (Heller *et al.* 1994). Increased ATP de-phosphorylation following STZ-treatment offers a substrate for xanthine oxide and in doing so results in the formation of super oxide radicals, hydrogen peroxide and hydroxyl radicals (Nukatsuka *et al.* 1988). STZ induction also raises nitric oxide (NO), an inhibitor of aconitase activity, which also participates in DNA damage (Kroncke *et al.* 1995). The outcome of STZ derangement in the β -cells of the pancreas, is the inhibition of insulin synthesis (Nukatsuka *et al.* 1990), which leads to severe insulinopaenia, hyperglycaemia, glycosuria, polydipsia and muscle wasting (features associated with type 1 diabetes) (Bracken *et al.* 2003).

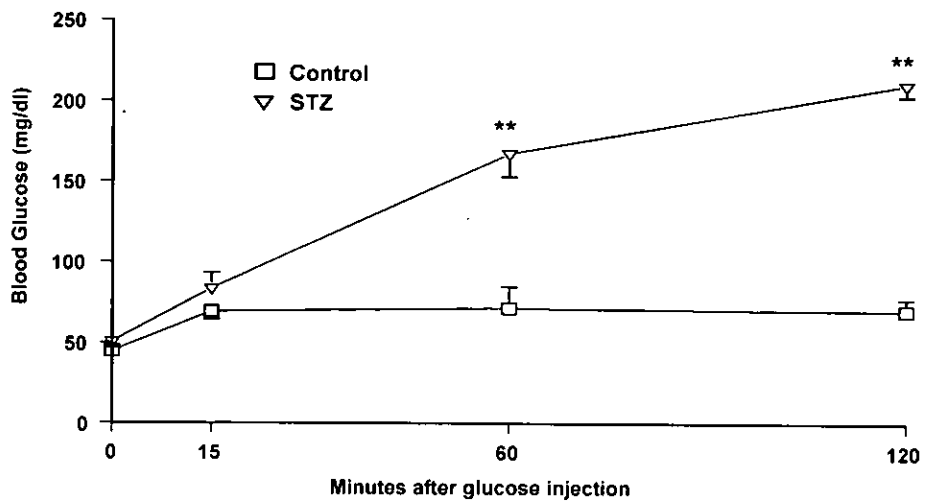


Figure 1.1. Whole blood glucose concentrations in response to an intraperitoneal (i.p.) glucose challenge test (2 g glucose (Kg body weight)⁻¹) in six-month-old STZ type 2 treated and control (n=6) Wistar rats following a 16 hour fast. Values represent the mean ± SEM (** P< 0.01) (unpublished work).

1.4 The normal heart

The mammalian heart is situated in the thoracic cavity, and is a muscular structure encapsulated by a fibrous pericardium layer. It contains four muscular compartments that include the right and left atria and ventricles, which are built upon a fibrotendinous, ring containing four apertures each with valves (Levick, 1995; Vander *et al.* 1999). The papillary muscles within the heart (see Figure 1.3) anchor the bi and tricuspid valves via the chordae tendinae. The purpose of the heart is to deliver oxygenated blood to the cells of the body and to pump the waste products of metabolism away from the cells.

1.4.1 The mechanical events of the cardiac cycle

The continuous pumping action of the heart's cardiac cycle is divided into systole (contraction) and diastole (relaxation), and these two processes are called the cardiac cycle. Ventricular diastole lasts for around 2 thirds of the cardiac cycle at rest. This enables the time period needed for ample ventricular filling. At first, the atria are in diastole too. Therefore, blood flows passively from the superior and inferior vena cava through the atria, atrio-ventricular (AV) valve and into the ventricles. As the ventricles begin to fill up, the rate of flow slows down and ventricular pressure begins to rise. The final part of filling is associated with atrial contraction, which adds only a small amount of additional blood to the ventricles. The volume of blood (130 ml) in the ventricles at the end of ventricular filling is called the end diastolic volume (EDV). At this point ventricular systole begins. At the beginning of systole, the pressure within the ventricles quickly exceeds that within the atria. This causes the closure of the AV valves. At this stage the aortic and pulmonary valves are not open and therefore no ejection of blood occurs out of the ventricle. This phase is therefore known as isovolumetric ventricular contraction. Ventricular pressure then continues to rise until ventricular pressures exceed aortic and pulmonary trunk pressures, this causes the opening of the aortic and pulmonary valves, and the rapid ejection of blood out of the ventricles (stroke volume (SV) = 70 ml). The ventricles then begin to relax at the beginning of diastole, which in turn causes a significant fall in ventricular pressure, below those in the aorta and pulmonary trunk, which coincides with the closure of the aortic and pulmonary valves. At this stage the AV valves are also still closed, therefore no change in ventricular volume occurs. When the pressure within the ventricles fall below that of the atrias, the AV valves open and blood enters the ventricles again to begin another cycle (Litwin *et al.* 1998; Vander *et al.* 1994; Katz, 1977).

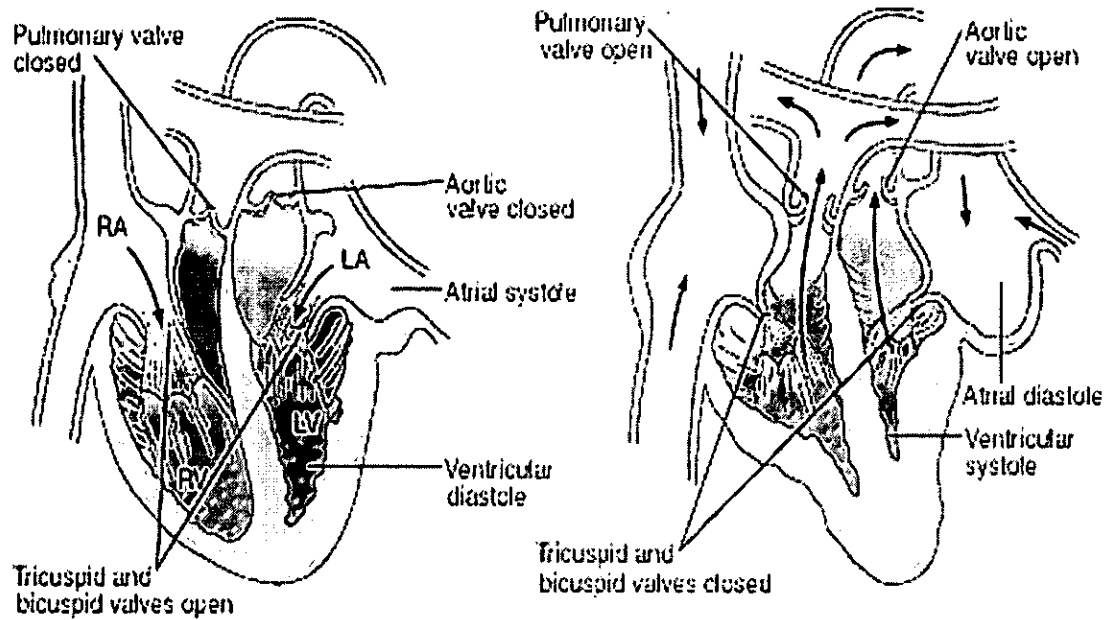


Figure 1.2. A schematic overview of the mechanical events and the direction of blood flow involved in a cardiac cycle of a normal mammalian heart (Taken from Vander *et al.* 1999).

1.4.2 Ultra structure of the heart

The heart wall consists of three distinct layers; the epicardium, endocardium and myocardium. The epicardium makes up the outer layer of the heart wall and contains mainly connective tissue and forms the inner membrane portion of the pericardium. The endocardium, which is the inner most layer of the wall consists of a simple squamous epithelial layer overlying a thinner areola tissue. The middle portion, and the thickest section of the heart wall, the myocardium contains several types of specialised cells, which include ventricular, and atrial cells or myocytes, nodal cells and Purkinje fibres (Litwin *et al.* 1998).

The myocytes form one of the largest portions of cells within the heart. These individual contractile cells have a single central nucleus (although some are bi-nucleated). Myocytes are attached to other myocytes by end junctions called intercalated discs, which contain three different regions known as; 1) gap junctions, which provide a low resistance pathway for the rapid conductance through, which ionic current can pass from one cell to the next (Levick, 1995), 2) intermediate junctions and 3) desmosomes (Sjostrand & Anderson-Cedergren, 1958), that hold the adjacent myocytes together by means of a proteoglycan matrix (Levick, 1995). Myocytes contract when stimulated, however, nodal cells are spontaneously active and are located in the sino-atrial (SA) node and AV node regions of the heart. These pacemaker cells initiate the contractile response for the working myocytes. The spontaneous activity of these cells can be modified by nerve impulses. The Purkinje fibres are a set of conducting cells enabling rapid penetration of electrical impulses through the heart. They appear very similar to nodal cells but contain only a few contractile filaments compared to a myocyte (Litwin *et al.* 1998; Vander *et al.* 1994; Katz, 1977).

Papillary muscle

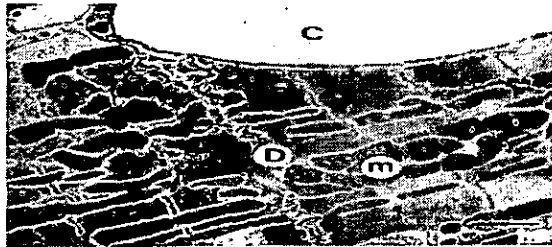
Control



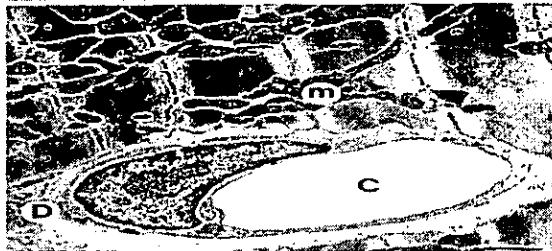
STZ



Control



STZ



Ventricular muscle

Figure 1.3. Electron microscope images of papillary muscle (top) and ventricular muscle (bottom), taken from STZ-induced type 1 diabetic and age-matched control rat hearts (Taken from Howarth *et al.* 2001).

1.4.3 The working myocyte

The working myocyte is full of long contractile bundles called myofibrils. Each myofibril is made up of smaller sarcomeres that are orientated across the cell giving a striated appearance. The sarcomere contains myofilaments that occupy between 45-60% of the cell volume (Bers, 2002a). The myofilaments are made of the thick myosin and thin actin filaments, along with other contractile and cytoskeletal components (Bers, 2002a). The myofilaments are responsible for contractility and changes in chemical energy to mechanical energy in the cardiac myocyte (Bers, 2002a). During contraction, the thin and thick filaments slide past each other, causing a change in muscle length. This movement is a consequence of cross bridge formation between the thin and thick filaments and is historically known as the sliding filament theory (Huxley, 2000).

The backbone of the thin filament consists of two chains of globular actin molecules (G-actin) to form a right-handed double stranded helical polymer (F-actin). Each turn of the actin molecule incorporates a molecule of tropomyosin that sits in the groove created by the double helices. At every seventh actin molecule, tropomyosin is attached to troponin. Troponin is a complex of three unidentical subunits; troponin-C, a Ca^{2+} binding unit, troponin-T, a tropomyosin binding unit and troponin-I, an inhibitory unit. Every thick filament is made up of around 300 myosin molecules along with other proteins including titin and C-protein. The tails of the myosin heavy chain (MHC) form the main core of the thick filament and the head region forms two light chains with binding sites for ATP and actin.

Ca^{2+} regulates the process of contraction brought about by the sliding of thin and thick filaments. In the resting state, with low $[\text{Ca}^{2+}]_i$, troponin-I binds to actin preventing the interaction of actin and myosin. Following a Ca^{2+} transient, $[\text{Ca}^{2+}]_i$ is raised, which causes the interaction of free Ca^{2+} with the troponin-C complex. Troponin-C then binds to troponin-I and causes the dissociation of it from actin. The change in troponin-C and troponin-I interaction instigate troponin-T, which causes positional change of the adjacent tropomyosin molecule, and in doing so exposes a myosin-binding site on the actin molecule. The head region of the myosin then attaches to the actin, which is followed by a change in the angle of the head. This causes the sliding of the actin and myosin over each other. The head is then disengaged and reattached at a different actin site. The requisite energy needed in the reaction comes from the hydrolysis of a molecule of ATP to ADP and a phosphate (P_i) (Huxley, 2000). Therefore the number of cross bridges formed is directly related to the Ca^{2+} content and causes a greater or lesser contraction in the presence of ATP.

1.4.4 Cardiac action potential

An Ap is a recording of the electrical membrane potential (E_m) of a cell (Katz, 1977). In a resting cardiac cell permeability favours potassium ion (K^+) entry and is relatively impermeable to sodium ions (Na^+), chloride ions (Cl^-) and Ca^{2+} . The Na^+/K^+ -ATPase pumps 3 Na^+ out and 2 K^+ into the cell and is responsible for the ionic concentration gradients for Na^+ and for K^+ , but it is the K^+ channels themselves that are responsible for the negative E_m in cardiac myocytes (Bers, 2002a). This results in a highly negative resting E_m nearing -90 mV. The cardiac action potential is characterised by four phases:

Phase (0) initial cardiac myocyte depolarisation is initiated by the spread of current from adjacent sarcolemmal membrane regions (Bers, 2002a) which, is associated with a rapid transient opening of fast Na^+ channels and slow Ca^{2+} channels so that inward Na^+ current (I_{Na}) exceeds outward K^+ current (I_{K}). This results in a large influx of Na^+ into the cell through voltage activated I_{Na} , driving the E_{m} nearer to that of the Na^+ equilibrium (+70 mV). At the peak of I_{Na} the E_{m} lies around +35 to 50 mV in ventricular myocytes, because of a small permeability of K^+ to the cell. The early repolarisation phase, Phase (1) coincides with the I_{Na} inactivation and activation of outward I_{to} and Ca^{2+} activated chloride current ($I_{\text{Cl}(\text{Ca})}$) and the slower influx of Ca^{2+} thus creating a plateau effect (phase 2). Ca^{2+} channels then close at this point and K^+ permeability increases resulting in the repolarisation of the cell (phase 3). Ionic balance is restored by a number of Na^+/K^+ -ATPase pumps. This is also a refractory period, which lasts from phase 0 until about halfway into phase 3. Between these points the heart muscle cannot be excited again and is absolutely refractory to stimulation. However, for a short period after this (during the relative refractory period) a critically timed stimulus may result in ventricular fibrillation and death (Litwin *et al.* 1998; Vander *et al.* 1994; Katz, 1977).

1.4.5 Rat ventricular action potentials

Action potentials profiles differ greatly according to differences in species and also regional variation within species (Oudit *et al.* 2001)(see Figure 1.4). In the ventricle of the rat, the amplitude of the action potential is shorter and is distinguishable by its “spike like” appearance, compared to other species including human (Li *et al.* 1998) and rabbits (Linz & Meyer, 2000), that have a longer and pronounced plateau phases of action potential. The rat ventricular action potential is characterised by a pronounced phase I repolarisation that precedes a very transient late plateau phase at E_{m} more negative than -20mV (Linz &

Meyer, 2000). The changes in action potential profiles are reflected in changes in variations in the types, kinetics and amplitudes of inward and outward currents although it appears that there are little differences in the I_{Na} and $I_{Ca,L}$ (Sah *et al.* 2003). In contrast however, repolarisation is primarily controlled by a number of K-channel properties, and differences in these channels appears to be the primary reason for the variation in Ap between species (Varro *et al.* 1993; Nerbonne *et al.* 2001; Oudit *et al.* 2001; Rosati *et al.* 2001). In particular the transient outward current (I_{to}), encoded by Kv4.2/4.3 genes, which is present in the rat has been reported to effect the duration and shape of the Ap (Josephson *et al.* 1984). It has been reported that the large I_{to} current densities in rat myocytes in comparison with other mammals is the major determinant to reduce the depolarising effects of the $I_{Ca,L}$, and in doing so reduce the plateau of the Ap in these species (Greenstein *et al.* 2000). However, in human and rabbit myocytes, where I_{to} is less prominent, homeostatic balance favours $I_{Ca,L}$, which results in a clear plateau phase (Greenstein *et al.* 2000). Studies in rodents where the I_{to} is removed have resulted in a long plateau phase of the Ap that is similar to that of the guinea-pig, which lacks I_{to} entirely (Wickenden *et al.* 1997; Gaughan *et al.* 1998). Differences in the Ap at the apex/base of the heart in the rat were first shown by Watanabe *et al.* (1983). More recent reports, have utilised isolate myocytes from sub-endocardium and sub-endocardial portions of the heart, and have reported that the Ap duration to be prolonged in the in sub-endocardial myocytes compared to that of sub-epicardial myocytes in normal rats (Clark *et al.* 1993; Shipsey *et al.* 1997; Natali *et al.* 2002). Moreover, it has also been shown that isolated myocytes from the mid-myocardium have Ap durations that lie between those of the sub-epi and sub-endocardium (Shipsey *et al.* 1997). A increase in expression of I_{to} (Antzelevitch *et al.*, 1991) and density of I_{to} (Clark *et al.* 1993; Shimoni *et al.* 1995) in sub-epicardial myocytes compared to sub-endocardial myocytes may well reflect the increase of Ap duration that has been reported in sub-endocardial myocytes compared to that of sub-epicardial myocytes (Clark *et al.*

1993; Shipsey *et al.* 1997; Natali *et al.* 2002). Changes in the duration and amplitude of the A_p , are mirrored by changes in the open probability of the L-type Ca^{2+} and $I_{Ca,L}$ (Sah *et al.* 2003). Because of this Ca^{2+} influx can be increased within the heart leading to increased trigger Ca^{2+} and SR load (Bouchard *et al.* 1995). Moreover, it has been reported that cell shortening is significantly greater in rat myocytes obtained from the sub-endocrinal compared to sub-epicardial portion of the heart (Clark *et al.* 1993; Natali *et al.* 2002). It is likely that a change in the expression of I_{to} is responsible for these changes in contractility.

1.4.6 Electrical conductance within the heart

The electrical stimulus needed for a heartbeat is initiated by the pacemaker conduction system. The dominant pacemaker region within the heart is the SA node. Spontaneous electrical activity generated in these cells causes the spread of electrical impulses through the gap junctions of the myocytes. The speed of the electrical input is fast enough to simultaneously initiate the contraction of the right and left atria. This wave of electrical conductance is responsible for the depolarisation of the AV node, which is positioned at the base of the right atrium. Depolarisation in this node is slower than other nodal cells, which results in a slight delay in electrical propagation and conductance through these cells in the heart. The mechanical consequences of this action are important, because this delay coincides with late atrial contraction and in doing so adds extra blood to the ventricle before they contract. The impulse then passes into the bundles of His, which divide into left and right branches that run down the entire ventricular septum into the network of Purkinje fibres. The conductance is finally passed on to the myocytes within the ventricle to initiate ventricular contraction. One of the important features of the heart is that the AV

node and the bundles of His are the only means by which electrical conductance can be carried from the atria through to the ventricles (Litwin *et al.* 1998; Vander *et al.* 1994; Katz, 1977).

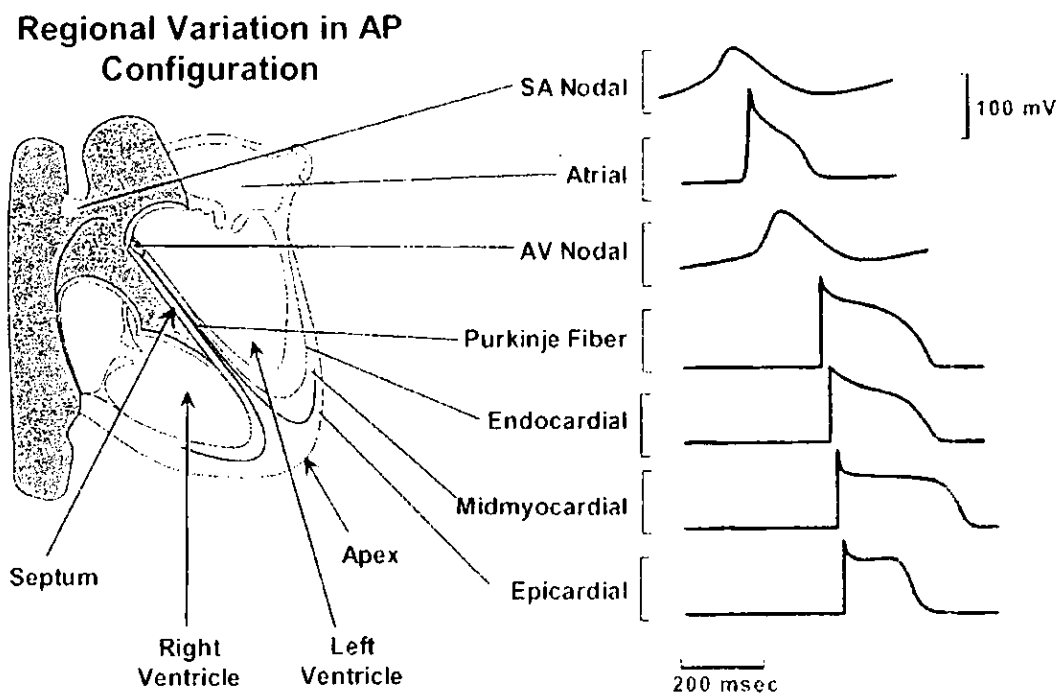


Figure 1.4. Representative recordings of differential sites of action potentials taken from specific regions within the heart (Taken from Bers, 2002a).

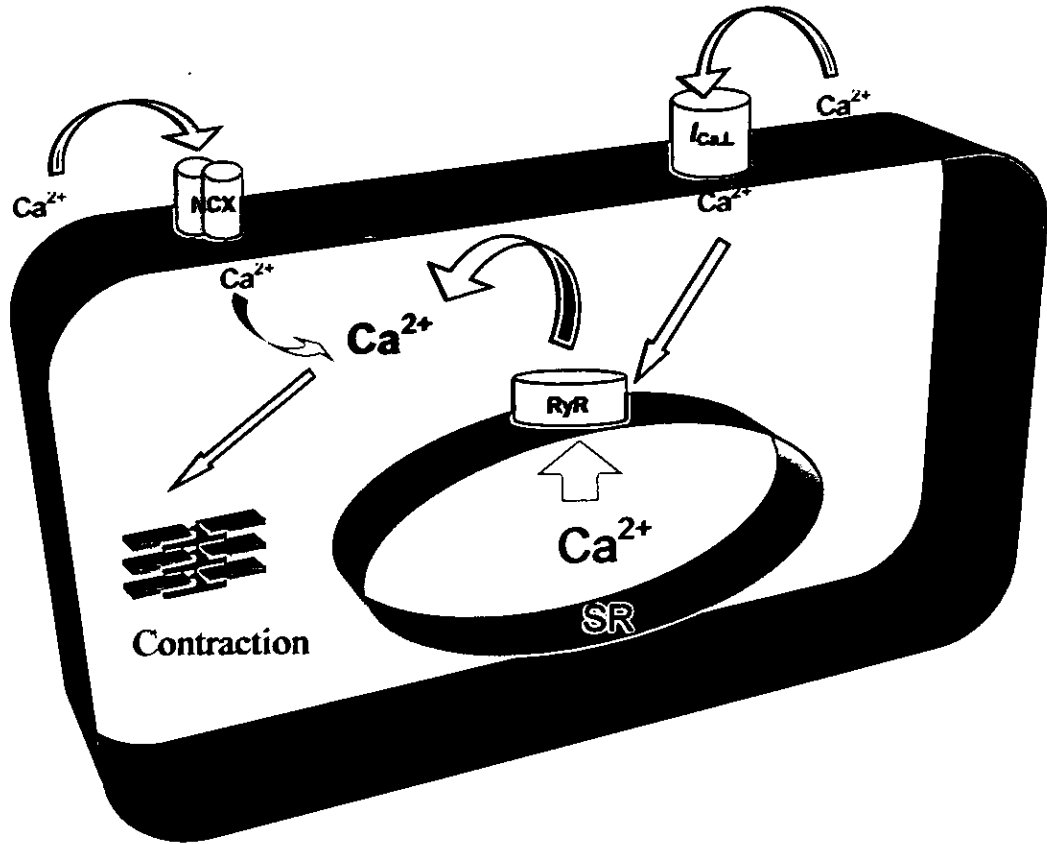


Figure 1.5.a Schematic model of E-C coupling in a normal ventricular cell, showing mechanisms that underpin Ca²⁺ transport following membrane depolarisation and contraction. *I*_{Ca,L} (L-type calcium current), NCX (Na⁺/Ca²⁺-exchanger), SR (sarcoplasmic reticulum), RyR (ryanodine receptor).

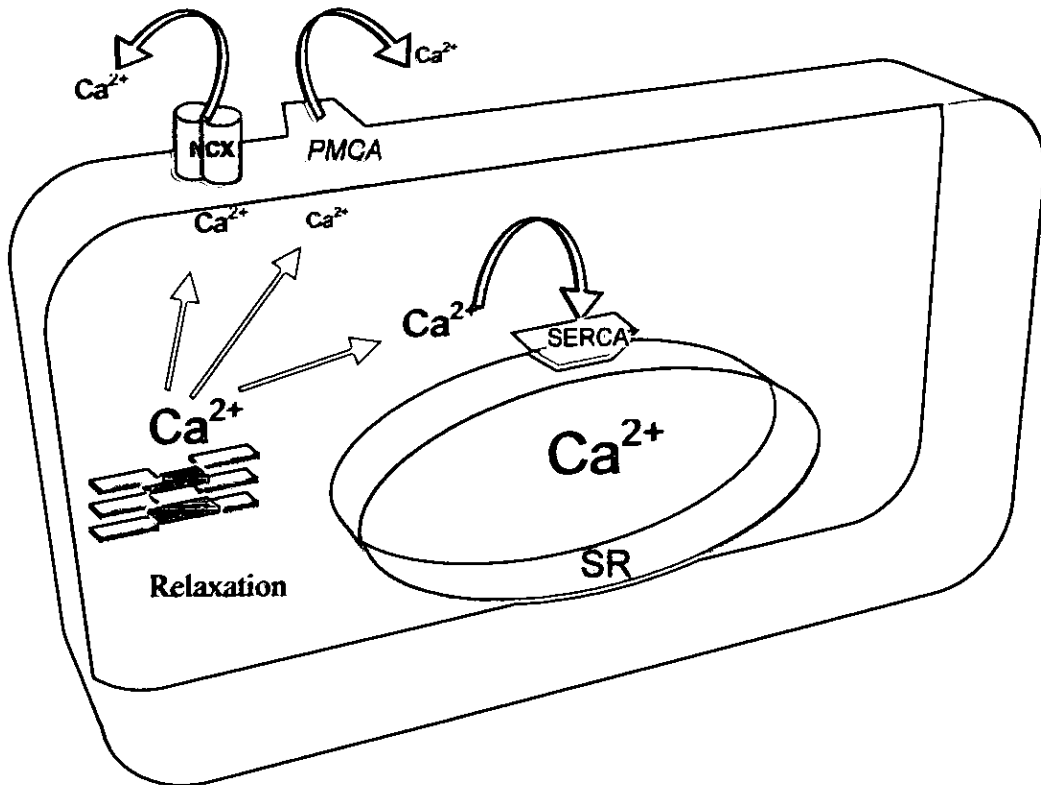


Figure 1.5.b Schematic model of E-C coupling in a normal ventricular cell, showing mechanisms that underpin Ca^{2+} transport following membrane repolarisation and relaxation. NCX ($\text{Na}^+/\text{Ca}^{2+}$ -exchanger), SR (sarcoplasmic reticulum), PMCA (plasma membrane Ca^{2+} -ATPase pump)

1.4.7 Excitation-contraction coupling in the normal heart

Cardiac E-C coupling is the process of electrical excitation of a cardiac myocyte that elicits contraction and enables the propulsion of blood out of the heart (Bers, 2002a). The initial rapid depolarisation of the cell membrane by an action potential triggers the signalling events of E-C coupling. This leads to a small entry of Ca^{2+} via the voltage-gated L-type channels (Barry & Bridge, 1993). There may also be a small entry of Ca^{2+} via the $\text{Na}^+/\text{Ca}^{2+}$ -exchanger operating in reverse mode (Nuss & Houser, 1992; Barry & Bridge, 1993; Kohmoto *et al.* 1994; Vornanen *et al.* 1994) although the magnitude and potency of this mechanism are still controversial (Levi *et al.* 1993a; Lipp & Niggli, 1994; Litwin *et al.* 1996; Wright *et al.* 1997). This small influx of Ca^{2+} triggers a much larger release of Ca^{2+} from the SR. When the SR is activated to release Ca^{2+} , there is a transient rise in $[\text{Ca}^{2+}]_i$; typically from a basal level of 100 nM to a peak between 1 and 2 μM within a period of 20 to 40 msec after depolarisation (Beuckelmann & Wier, 1988; Cannell *et al.* 1987a). This rise in $[\text{Ca}^{2+}]_i$ is commonly referred to as the Ca^{2+} transient. This process is referred to as “ Ca^{2+} -induced Ca^{2+} -release” (CICR) and is generally accepted as the main mechanism of Ca^{2+} release from the SR (Fabiato, 1983; Litwin *et al.* 1998; Muller, 1965). The process of contraction is initiated when Ca^{2+} binds to troponin-C. The decay of the Ca^{2+} transient is initiated by the re-uptake of Ca^{2+} into the SR by a SR Ca^{2+} -ATPase- dependent pump (SERCA)(Bers, 1991; Balke *et al.* 1994) and the extrusion of Ca^{2+} from the cell by the $\text{Na}^+/\text{Ca}^{2+}$ -exchanger (Barry & Bridge, 1993; Barcenas-Ruiz *et al.* 1987; Jorgensen *et al.* 1982). Recent studies have proposed that, as well as CICR, a voltage-activated Ca^{2+} release (VACR) mechanism (similar to that seen in skeletal muscle) may exist in cardiac muscle (Levi *et al.* 1997; Ferrier & Howlett, 1995).

1.4.8 Calcium sparks underlying local control in heart cells

The global Ca^{2+} transient within a cardiac myocyte is believed to be made up of the spatial and temporal summation of a number of individual Ca^{2+} sparks (Cannell *et al.* (1994). Ca^{2+} sparks were first described in single isolated cardiac myocytes by Cheng *et al.* (1993) as the spontaneous release of Ca^{2+} from a number(s) of RyR's on the SR. Subsequent work showed how Ca^{2+} sparks could be initiated through the activation of electrical stimulation, and synchronically regulated with the aid of Ap's and the $I_{\text{Ca,L}}$ (Cannell *et al.* 1994; Lopez-Lopez *et al.* 1994). Therefore, Ca^{2+} sparks can be described as an event(s) in the process of E-C coupling, which, when activated by Ca^{2+} efflux through $I_{\text{Ca,L}}$ and the $\text{Na}^+/\text{Ca}^{2+}$ -exchanger underlies the process of contraction. The relationship between $I_{\text{Ca,L}}$ and Ca^{2+} sparks has been described, to support the hypothesis that a single L-type Ca^{2+} -channel opening can lead to the initiation of a single Ca^{2+} spark (Lopez-Lopez *et al.* 1995; Cannell & Soeller, 1997; Collier *et al.* 1999). This phenomenon is however, favourable at more negative potentials (- 40mV), whereas a larger number of L-type Ca^{2+} -channels may be required to be open at more positive potentials (+ 60mV) (Guatimosim *et al.* 2002). The number of Ca ions that are required to bind to a RyR to initiate a Ca^{2+} spark remains controversial. It has been reported that the localised Ca^{2+} signal, produced by the opening of one L-type Ca^{2+} -channel (known as "Ca²⁺ sparklet") is enough to trigger a Ca^{2+} spark (Wang *et al.* 2001; Wang *et al.* 2002). Moreover, Fan & Palade, (1999) reported that a single Ca^{2+} was sufficient to activate RyR's and incur Ca^{2+} a transient release. The number of RyR's that is needed to be activated to initiate a Ca^{2+} spark is unresolved. Original theory suggested that a single RyR would be sufficient to initiate a release of a Ca^{2+} spark,, but more recent data have shown, that flux through a single RyR's is approx 4 pA whereas a single $I_{\text{Ca,L}}$ Ca^{2+} is approx 0.6 pA (Mejia-Alvarez *et al.* 1999). This suggests that the Ca^{2+} spark is due to a number or cluster of release channels on the SR. The termination of the Ca^{2+} spark is abrupt and is necessary for the relaxation of the cardiac muscle. The exact

process that underpins the termination of a Ca^{2+} are poorly understood, but it has been shown that the process cannot be explained by the depletion of the SR or the stochastic closure of the RyR's (Sham *et al.* 1998; Lukyaneko *et al.* 1999). One recent report using sarponin-permeabilised myocytes has shown that intra-SR Ca^{2+} buffering increased the amplitude and time course of Ca^{2+} sparks, which suggested that the termination of the Ca^{2+} spark is brought about by the control of local intra-SR Ca^{2+} regulated RyR openings (Terentyev *et al.* 2002).

1.5 Diabetic cardiomyopathy and cardiovascular disease

There is clear evidence of the negative influence of type 1 diabetes on the prevalence, severity and prognosis of cardiovascular disease (coronary heart disease (CHD), stroke, peripheral vascular disease) (Julien, 1997). Cardiovascular disease represents the commonest cause of morbidity and mortality within diabetic patients (Schaffer, 1991; Scherthaner, 1996; Mahgoub & Abd-Elfattah, 1998; Raman & Nesto, 1996; Laakso, 1999). Human and animal studies have shown that the excess risk of cardiovascular complications cannot be explained by conventional cardiovascular risk factors alone and therefore the diabetic state itself is likely to account for this alteration in cardiac function (Laakso, 1999; Albanna *et al.* 1998). This developing disease in the absence of any cardiovascular complications is termed diabetic cardiomyopathy (Kiss *et al.* 1988) and is defined as a decrease in cardiac contractile performance, which results in an abnormality in systolic function leading to a defect in expulsion of the blood (systolic heart failure), or by an abnormality in diastolic function leading to a defect in ventricular filling (diastolic heart failure) and resulting in congestive heart failure (CHF) (Schaffer, 1991). Many invasive and non-invasive clinical studies on human diabetic patients have reported alterations in cardiac performance. Studies in type 1 diabetes patients have reported an

increase in atrial contraction, impaired diastolic function of left ventricle and reduced rapid filling rate (Albanna *et al.* 1998; Kiss *et al.* 1988; Astorri *et al.* 1997; Nicolino *et al.* 1995). It is thought to be the diastolic dysfunction in the diabetic heart that is responsible for increased morbidity and mortality (Fein *et al.* 1980; Tahiliani *et al.* 1983).

1.5.1 Contractile dysfunction in the diabetic heart

Several mechanisms of contractile dysfunctions have been reported in experimentally-induced diabetic heart muscle. Depressed SV, aortic output (AO), positive (+dP/dt) and negative (-dP/dt) left ventricular developed pressure have all been reported in various type I diabetic heart preparations (Regan *et al.* 1974; Fein *et al.* 1985; Litwin *et al.* 1990; Miller 1979; Vadlamudi *et al.* 1982).

1.6 Cardiac myocyte in the resting state

In resting cells, $[Ca^{2+}]_i$ is determined by a Ca^{2+} leak that is compensated for by the sarcolemmal plasma membrane Ca^{2+} -ATPase (PMCA) pump and the sarcolemmal Na^+/Ca^{2+} -exchanger (Barry *et al.* 1986). In cultured cardiac myocytes the rate of Ca^{2+} extrusion by the myocardial membrane bound ATPase is around 1/10 that of the Na^+/Ca^{2+} -exchanger (Barry *et al.* 1986). Cannel (1991) reported that the Na^+/Ca^{2+} -exchanger accounts for as much as 75 % of the resting Ca^{2+} efflux within the cardiac cell. Therefore, the primary role of maintaining the basal $[Ca^{2+}]_i$ level is the responsibility of the Na^+/Ca^{2+} -exchanger (Cannell, 1991).

1.7 Mediators of calcium influx

Stimulated Ca^{2+} influx results in the release of Ca^{2+} from the SR, which in turn leads to contraction of the cardiac myocyte that contributes to E-C coupling in the heart. The underlying mechanisms associated with the transport of Ca^{2+} within the cell including the $I_{\text{Ca,L}}$, $\text{Na}^+/\text{Ca}^{2+}$ -exchanger and adrenergic receptor mediated events will be discussed:

1.7.1 Sarcolemmal calcium channels

There are two types of Ca^{2+} channels in cardiac tissue. The L (large conductance) and T (tiny conductance) type Ca^{2+} channels. T-type Ca^{2+} channels are present in various cardiac regions but are small or absent in ventricular myocytes, whereas L-type Ca^{2+} channels are very prominent in all regions of the heart (Bers, 2002a). L-type Ca^{2+} channels are highly sensitive to the dihydropyridines (DHP's) and most act as antagonists (e.g. nifedipine) to reduce L-type Ca^{2+} channel opening. Initial depolarisation of the cell membrane leads to the rapid activation of $I_{\text{Ca,L}}$ around $-40 \text{ mV } E_m$ and activates the opening of voltage-sensitive L-type channels (Bers, 1991). Ca^{2+} influx through L-type channels has been shown to be $13.8 \mu\text{mol/l}$ cytosol in rat ventricular myocytes (Yuan *et al.* 1996). However, during normal physiological conditions SR Ca^{2+} release inactivates Ca^{2+} influx by around 50 % in rabbit (Bers, 2002a) and rat (Sham *et al.* 1995).

In type 1 diabetic myocytes a few reports have suggested that L-type Ca^{2+} channel opening is impaired. Bergh *et al.* (1988) have reported that Ca^{2+} influx was significantly reduced in both acute and chronic diabetes compared to age-matched controls, while, Yu *et al.* (1995) proposed that the L-type Ca^{2+} channel in type 1 diabetes showed enhanced activity and was qualitatively and quantitatively altered. With regards to $I_{\text{Ca,L}}$, it has been suggested

that $I_{Ca,L}$ density-voltage relationships and steady-state inactivation curves of $I_{Ca,L}$ are not significantly altered in type 1 STZ-diabetic ventricular cells (Schneider & Sperelakis, 1975; Tamada *et al.* 1998; Jourdon & Feuvray, 1993). Moreover, Choi *et al.* (2002) reported that $I_{Ca,L}$ was not significantly different in 8 week treated STZ-induced ventricular myocytes at voltages from -40 to $+60$ mV. However, it has been reported that the $I_{Ca,L}$ was significantly decreased in 24-30 wk STZ-induced diabetic myocytes (Wang *et al.* 1995). The differences in reports may be attributable to the changes in treatment time, methods of acquiring $I_{Ca,L}$ recordings and changes in solutions used to perfuse and equilibrate cells. Any change in $I_{Ca,L}$ would alter the trigger Ca^{2+} on the SR and may also affect the reversal potential of the Na^+/Ca^{2+} -exchanger. Changes in these mechanisms may alter the amount of Ca^{2+} released from the SR and would therefore modify contraction. The response of Ca^{2+} channel activation and opening, is dependent on its phosphorylated state (Sperelakis 1988), which in turn regulates the length of time it is opened for and consequently the regulation of $I_{Ca,L}$. Phosphoprotein phosphatases 1, 2A, 2B and 2C, within the sarcolemmal regulate the life span of the opening time of the L-type Ca^{2+} channel, which, in the normal heart is likely to be around a few milli seconds (Allo & Schaffer, 1990). If the phosphorylation rate is altered, then the time span of opening may be affected in the diabetic heart and therefore contribute to changes in Ca^{2+} influx.

1.7.2 Sarcolemmal sodium/calcium exchanger

The Na^+/Ca^{2+} -exchanger on the sarcolemmal membrane is a reversible pump that generates the transportation of three Na^+ to one Ca^{2+} (3:1) (Philipson & Nicoll, 2000). However, recent data suggest a higher ratio rate ($>3:1$)(Fujioka *et al.* 2000). The isoform of the gene, which generates the Na^+/Ca^{2+} -exchanger in the heart is the NCX1 and consists of 970 amino acids with a molecular mass of 110 kDa (Nicoll *et al.* 1990). Ca^{2+} extrusion is

recognised as inward $\text{Na}^+/\text{Ca}^{2+}$ -exchanger current ($I_{\text{Na/Ca}}$) as one Ca^{2+} extruded being replaced by three Na^+ , so therefore Na^+ extrusion is named outward $I_{\text{Na/Ca}}$ (Bers, 2002b). The $\text{Na}^+/\text{Ca}^{2+}$ -exchanger is sensitive to current changes and therefore, has been implicated in the contribution of Ca^{2+} influx and SR Ca^{2+} release during cell membrane depolarisation (Litwin *et al.* 1998). High $[\text{Ca}^{2+}]_i$ favours Ca^{2+} efflux while a positive E_m and high $[\text{Na}^+]_i$ favour Ca^{2+} influx (Bers, 2002b). Therefore, in normal physiological conditions the $\text{Na}^+/\text{Ca}^{2+}$ -exchanger works to decrease $[\text{Ca}^{2+}]_i$ by an inward $I_{\text{Na/Ca}}$. However, if the AP duration is increased through changes in either $I_{\text{Ca,L}}$, SR Ca^{2+} release or if $[\text{Na}^+]_i$ is elevated, Ca^{2+} influx will occur (Bers, 2002b).

1.7.3 Adrenergic response and calcium mobilisation in the heart

Agonist occupation of β -adrenoceptors leads to the activation of GTP binding protein (G_s) and the dissociation of the α subunit ($G_{s\alpha}$) to activate adenylate cyclase, increasing the production of adenosine 3',5'-cyclic-monophosphate (cAMP). Elevated levels of cAMP leads to the dissociation of the regulatory and catalytic sub units of cAMP-dependent protein kinase A (PKA), which, phosphorylates a number, and variety of regulatory proteins. These include the phosphorylation of the L-type Ca^{2+} channel, ryanodine receptor (RyR), phospholamban (PLB) and troponin-I (Trautwein & Hescheler, 1990). The phosphorylation of the L-type Ca^{2+} channel results in the increased probability of its opening within normal activation voltages. This in turn increases the Ca^{2+} availability for CICR. Similarly, phosphorylation of PLB (Kranias & Solaro, 1982), results in an increase in Ca^{2+} uptake by SERCA (Tada & Katz, 1982). Elevated SR Ca^{2+} increases the availability of Ca^{2+} for release by phosphorylated, RyR (Philbin *et al.* 2000) therefore increasing the speed of SR Ca^{2+} release. Phosphorylation of troponin-I (Okazaki *et al.* 1990) results in decreased sensitivity of the myofilaments to Ca^{2+} . The net result of

myocardial β -adrenoceptor stimulation is a systolic increase in cytoplasmic $[Ca^{2+}]_i$ and an increase in contractility (Tamada *et al.* 1998).

The mechanism associated with increased sympathetic drive represents an important factor in maintaining cardiac output (CO) in the malfunctioning heart (Ha *et al.* 1999). A number of reports have documented impaired cardiac responsiveness to β -adrenoceptor stimulation in experimental-induced diabetic hearts. Reports using STZ-induced type 1 diabetic hearts suggested that stimulation with isoprenaline resulted in a decrease in the force of contraction in whole heart preparations (Atkins *et al.* 1985), in 4-6 week (Gando *et al.* 1997) and 8 week (Heyliger *et al.* 1982) STZ-treated papillary muscles and in isolated cardiomyocytes following 8-10 weeks of STZ treatment compared to control preparations (Horackova & Murphy, 1988). The rate at which, isoprenaline induced SR Ca^{2+} uptake was depressed in 180-day STZ-induced whole hearts when compared to age-matched controls (Vadlamudi & Mcneill, 1984). Therefore, β -adrenergic sensitivity seems to be defective in the STZ-induced type 1 diabetic heart. The inotropic responses to dibutyryl-adenosine 3',5'-cyclic-monophosphate (DBcAMP) and forskolin (an activator of the adenylate cyclase supply) were also prominently reduced in the type 1 diabetic heart compared to control (Gando 1994; Tamada *et al.* 1998). Competitive binding studies have shown that β -adrenergic receptor number are significantly decreased in the myocardial membrane (Gando, 1994; Caterson *et al.* 1982; Savarese & Berkowitz, 1979; Nishio *et al.* 1988) taken from type 1 diabetic hearts, although it appears that β -adrenergic receptor affinity for agonists is not compromised (Nishio *et al.* 1988). Competitive binding studies have shown (Gando, 1994) that the interaction between β -adrenoceptor and Gs-protein is not altered in type 1 diabetic hearts. This observation implies that the dysfunctional responsiveness associated with type 1 diabetic hearts may not necessarily be caused by an alteration in

cAMP or changes in G- proteins but is more likely to be caused by a defect, distal to the adenylate cyclase system. This would seem to implicate an alteration in Ca^{2+} homeostasis in the cardiac cell during diabetes. Gando *et al.* (1994) have also postulated that this dysfunctional response may be associated with impaired phosphorylation of phosphoproteins including PLB.

1.8 Mediators of systolic calcium

The trigger and release of Ca^{2+} from the SR into the cytosol contributes to myofilament activation, which leads to contraction in the heart. The mechanisms associated with this process will be discussed:

1.8.1 Ryanodine receptor activation and sarcoplasmic reticulum release

Ryanodine is a neutral plant alkaloid, which is a specific and selective ligand for the Ca^{2+} release-channel, RyR within the SR (Yu *et al.* 1994a). Ryanodine produces a progressive decline in cardiac muscle contraction (Yu *et al.* 1994a). At low concentrations (1-30 nM), ryanodine is thought to bind to high affinity sites resulting in the release of Ca^{2+} from the SR. [^3H] ryanodine has been employed previously to show that the number of high affinity binding sites in type I diabetic heart is reduced compared to control (Yu *et al.* 1994a). This observation suggests that the density of RyR's is lowered in type I diabetic hearts. Ca^{2+} influx accumulates around the RyR at the SR, where it binds to RyR's to trigger the SR Ca^{2+} release. Reduced density of RyR's may lead to an impairment of Ca^{2+} release from the SR, although it has yet to be reported if the decrease in numbers of RyR's (reported in type I diabetic hearts) is indicative of the sensitivity of Ca^{2+} release from the SR.

Fabiato (1983), carried out preliminary studies using caffeine to assess SR Ca^{2+} content in skinned cardiac muscle fibres and more recently caffeine-induced Ca^{2+} response has been used to assess SR Ca^{2+} content in single cardiomyocytes. Caffeine increases SR Ca^{2+} channel opening, thus promoting Ca^{2+} leakage into the cytoplasm. The permanent opening of Ca^{2+} channels prevents accumulation of Ca^{2+} into the SR (Rousseau & Meissner, 1987). The peak $[\text{Ca}^{2+}]_i$ induced by caffeine can be used as a measurement of an index of releasable Ca^{2+} from the SR, although it should be noted that caffeine also effects myofilaments sensitisation as well as inhibiting phosphodiesterase (which can increase cAMP and in turn activate of cAMP dependent PKA) (Yu *et al.* 1995). Several studies have demonstrated that the amplitude of the caffeine-induced Ca^{2+} transient is depressed in type 1 diabetic cardiomyocytes (Tamada *et al.* 1998; Lagadic-Gossmann *et al.* 1996; Woodbury & Hecht, 1952). Yu *et al.* (1994) reported that caffeine-induced contracture and subsequent Ca^{2+} transient in diabetic myocytes to be 75% that of control cells. Rapid cooling contracture (RCC) are another established method of assessing SR Ca^{2+} release in the contracted cell. Rapid cooling (from 30°C - 1°C) of the SR (in situ) results in the rapid release of Ca^{2+} from the SR, this is followed by a contracture. Bouchard & Bose (1991) showed a 50 % reduction of RCC in diabetic cells, while Yu *et al.* (1994a) observed a reduction in the amplitude of RCC in the diabetic heart that was 68% that of control cells. This evidence suggests that a reduction in caffeine and RCC seen in type 1 diabetic cardiac cells may be indicative of a diminished Ca^{2+} storage mechanism in the SR.

1.8.2 Myofilament interaction

A rise in Ca^{2+} transient raises the probability of free Ca^{2+} interacting with the troponin-C complex and initiating the sliding action of the actin and myosin, culminating in

contraction. This process may be greatly altered by a change in the pharmacological environment and an alteration in the pathological state (Morgan *et al.*, 2000). Therefore, changes in myofilament sensitivity may contribute to cardiac contractile abnormalities in the diabetic heart. Myosin, the thick filament associated with contraction is comprised of two heavy chains molecules, MHC and four light chain molecules (MLC). In cardiac myocytes there are two isoforms of MHC (α -MHC and β -MHC) that are distinguished by their heavy chain composition and Ca^{2+} -dependent ATPase activity (Schaffer, 1991). α -MHC or V1 has around four times the activity of the β -MHC or V3 isoform. In the adult rat heart over 90% of the adult isoform is made up of α -MHC and it is this isoform that predominantly contributes to contraction in normal conditions (Depre *et al.* 2000a). It has been reported that in the type 1 diabetic state, expression of the MHC is switched from the active α -MHC to the less active β -MHC isoform, (Goffman *et al.* 1999; Depre *et al.* 2000a; Pierce & Dhalla, 1981) which has been reported as a factor in cardiac dysfunction (Brouty-Boye *et al.* 1995). It has been suggested that a change in isoform expression may contribute to disturbances in ventricular dysfunction and ultimately lead to a specific diabetic cardiomyopathy (Schaffer, 1991). A change in $[\text{Ca}^{2+}]_i$ may be indicative of this change (from α -MHC to β -MHC), which is seen in diabetic cells (Malhotra & Sanghi, 1997).

1.9 Mediators of relaxation

During the relaxation phase of contraction, there is intracellular competition to decrease the $[\text{Ca}^{2+}]_i$ between the SERCA pump, the $\text{Na}^+/\text{Ca}^{2+}$ -exchanger, PMCA and mitochondrial uptake. The role each has to play in lowering $[\text{Ca}^{2+}]_i$ is discussed below.

1.9.1 Sarcoplasmic reticulum uptake

The SR possesses a pump (SERCA), which is distinct from the sarcolemmal PMCA pump. The SERCA pump is a member of the P-type ion transporting ATPase family that includes the Na^+/K^+ -ATPase, PMCA and the H/K-ATPase (Bers, 2002a). The only isoform of SERCA in the cardiac muscle is SERCA2a. The decay of the Ca^{2+} transient is initiated by the re-uptake of Ca^{2+} into the SR by SERCA (Bers, 1991; Balke *et al.* 1994) and the extrusion of Ca^{2+} from the cell by the $\text{Na}^+/\text{Ca}^{2+}$ -exchanger (Barceñas-Ruiz *et al.* 1987; Jorgensen *et al.* 1982; Barry & Bridge, 1993). In rat ventricular myocytes re-uptake of Ca^{2+} into the SR accounts for between 87 and 92 % of the total removal of Ca^{2+} from the cytosol, while the $\text{Na}^+/\text{Ca}^{2+}$ -exchanger accounts for approximately 9-7 % (Negretti *et al.* 1993; Bassani *et al.* 1994).

Defects in the activity of SERCA are likely to impair accumulation of Ca^{2+} into the SR leading to a steady-state decline in SR Ca^{2+} load. Several studies have observed decreased activity of the SERCA pump of the SR in STZ-induced type 1 diabetic cells (Ganguly *et al.* 1983; Lopaschuk *et al.* 1983b; Takeda *et al.* 1996; Misra *et al.* 1999). Zarain-Herzberg *et al.* (1994) reported that 3 and 5 week STZ- induced diabetic rat hearts exhibited a decrease of SERCA activity although Northern blot analyses failed to significantly show a reduction in the relative level of SERCA mRNA expression in either diabetic or insulin-treated rat hearts. Moreover, quantification of SERCA protein by Western blot did not reveal any change between diabetic and insulin treated animals. These results would therefore suggest that any defect within the SERCA pump may not be attributed to alterations at transcriptional or translational levels within the diabetic heart (Zarain-Herzberg *et al.* 1994). Although the SERCA pump is important in decreasing the beat-to-beat $[\text{Ca}^{2+}]_i$ levels, it is incapable of extruding Ca^{2+} from the cell. Therefore, steady-state

increases of $[Ca^{2+}]_i$ in diabetic myocytes cannot be explained by a defective SR Ca^{2+} transport system alone (Schaffer, 1991).

1.9.1.1 Phospholamban

Ca^{2+} uptake into the SR is regulated by PLB. PLB is an endogenous protein that inhibits SERCA pump activity and therefore decreases Ca^{2+} transport in the cardiac myocyte. When phosphorylated, PLB reverses its inhibitory effects on the SERCA pump and therefore, potentiates the uptake of Ca^{2+} from the cytoplasm into the SR (Tada & Katz, 1982). PLB can be phosphorylated by cAMP dependent PKA at the serine-16 residue (Tada *et al.* 1974).

It has been reported that isoprenaline enhanced the rise of $[Ca^{2+}]_i$ in response to a rapid caffeine induction in control myocytes more markedly than in type 1 diabetic cells (Tamada *et al.* 1998). In agreement with this, Gando *et al.* (1997) showed that stimulation with isoprenaline resulted in a 3-fold increase in PLB phosphorylation in control myocytes. Moreover, the same workers also demonstrated that type 1 diabetic hearts were less responsive to forskolin (Gando *et al.* 1997). This would suggest that the SR Ca^{2+} uptake through the SERCA pump might be impaired in the type 1 diabetic heart.

1.9.2 Sodium calcium exchanger

Although the Na^+/Ca^{2+} -exchanger has been suggested to be a mechanism of Ca^{2+} influx and a trigger for SR Ca^{2+} release, its main role is to reduce Ca^{2+} during diastole and therefore increasing $[Na^+]_i$ (Bridge *et al.* 1990). A few workers have demonstrated depressions in the activity of the Na^+/Ca^{2+} -exchanger pump in type 1 diabetic ventricular

cells (Takeda *et al.* 1996; Pierce *et al.* 1990). Chattou *et al.* (1999) have reported that the I_{Na-Ca} is significantly decreased in the 3-4 week treated STZ-induced diabetic myocytes similarly Hattori *et al.* (2000) have also observed that the I_{Na-Ca} was reduced in ventricular myocytes taken from the diabetic heart when compared to control. Activity of the Na^+/Ca^{2+} -exchanger is partly regulated by the intracellular sodium concentration ($[Na^+]_i$) showed that the level of $[Na^+]_i$ was significantly lower in diabetic myocytes (9.2 mM) than that in normal myocytes (12.0 mM) and it has been suggested (Kato *et al.* 1995) that the decrease in $[Na^+]_i$ in diabetic myocytes may be due to an attenuation of the activity in the Na^+/H^+ exchanger system. Pierce *et al.* (1990) have demonstrated a depression in Na^+/H^+ exchanger isolated from chronically diabetic rats, suggesting an imbalance of pH and Na^+ concentration within the cell. A reduction in $[Na^+]_i$ would favour operation of the exchanger in forward mode (influx of Na^+ efflux of Ca^{2+}) and may explain the decreases in cytoplasmic Ca^{2+} concentration (Pierce *et al.* 1990), which have been demonstrated in diabetic cells (Lagadic-Gossmann *et al.* 1996). Other reports however, suggest an increase in $[Ca^{2+}]_i$ (Allo *et al.* 1991). Increased $[Na^+]_i$ would result in the increase of $[Ca^{2+}]_i$ through the Na^+/Ca^{2+} -exchanger. Allo *et al.* (1991) have suggested that a significant decrease in the ability of the Na^+/K^+ -ATPase activity would lead to increased levels of $[Na^+]_i$.

1.9.3 PMCA pump

The PMCA is a P-type ATPase that uses energy ATP to drive Ca^{2+} out of the cell during relaxation. The pump is coupled to a proton counter flux that transports 1 proton in and 1 Ca^{2+} out of the cell (Kuwayama, 1988). In the rat heart, the PMCA is likely to account for approximately 10% of the total Ca^{2+} efflux and contribute around 1% to overall Ca^{2+} decrease in diastole (Bassani *et al.* 1994). In the STZ-induced type 1 diabetic heart, the PMCA pump has been reported to be significantly depressed following 18 and 24 days of

treatment (Takeda *et al.* 1996) and in 8 week (Heyliger *et al.* 1987; Makino *et al.* 1987) diabetic preparations. This alteration in the sarcolemmal (Heyliger *et al.* 1987) PMCA pump would contribute to a small defect in the Ca^{2+} efflux across the myocardial membrane in the diabetic heart.

In conclusion, there is clear evidence of the negative influence of type 1 diabetes on the severity of cardiovascular disease. Several mechanisms of contractile dysfunctions have been reported in experimentally-induced diabetic heart muscle and current evidence reviewed in the introduction suggests that an altered process that underpins the mechanism(s) of E-C coupling are responsible for the contractile dysfunction seen in diabetic heart cells. In particular, it has been suggested that abnormal Ca^{2+} movement is responsible for the impairment seen in diabetic hearts.

1.10 The story so far

To date, several studies have utilised the STZ-induced model of diabetes to look at the effects of diabetes in the heart. Unfortunately many studies appear to contradict each other in their reports and it appear that the degree and variety of experimental procedures may underpin, to some extent the apparent changes that have been observed. It is therefore worth while tabulated a number of reports to educate the reader in recent publications that have arisen from this model of diabetes.

Table 1.1. A comparison of studies looking at the effect of STZ-induced diabetes on the isolated cardiac myocytes from the rat heart

<i>Study</i>	<i>Findings</i>	<i>Treatment time</i>	<i>Author(s)</i>
Contraction	Reduced	8 weeks	Choi <i>et al.</i> (2002)
		8 weeks	Ren & Davidoff, (1997)
		5 months	Okayama <i>et al.</i> (1994)
	No change	6 weeks	Yu <i>et al.</i> (1994a)
		4-6 weeks	Tamada <i>et al.</i> (1998)
	Increased	4-6 weeks	Ishitani <i>et al.</i> (2001)
Calcium transient	Reduced	8-12 weeks	Howarth <i>et al.</i> 2001
		8 weeks	Choi <i>et al.</i> (2002)
		8 weeks	Noda <i>et al.</i> (1992)
	No change	6 weeks	Lagadic-gossman <i>et al.</i> (1996)
		4-6 weeks	Tamada <i>et al.</i> (1998)
		4-6 weeks	Hattori <i>et al.</i> (2000)
Ap duration	Prolonged	4-6 days	Shimoni <i>et al.</i> (1994)
		8 weeks	Magyar <i>et al.</i> (1992)
		3-4 weeks	Jourdan & Feuvray, (1993)
$I_{Ca,L}$	Reduced	4-6 days	Shimoni <i>et al.</i> (1994)
		24-30 weeks	Wang <i>et al.</i> (1995)
	No change	3-4 weeks	Chattou <i>et al.</i> (1999)
		8 weeks	Choi <i>et al.</i> (2002)
		4-6 weeks	Tamada <i>et al.</i> (1998)
I_{to}	Reduced	3-4 weeks	Jourdan & Feuvray, (1993)
		8 weeks	Magyar <i>et al.</i> (1992)
		4-6 days	Shimoni <i>et al.</i> (1994)
		24-30 weeks	Wang <i>et al.</i> (1995)
$I_{Na/Ca}$	Reduced	3-4 weeks	Chattou <i>et al.</i> (1999)
		4-6 weeks	Hattori <i>et al.</i> (2000)

1.11 Changes in Cation distribution within the diabetic heart

It has been reported that a change in specific cations within the body can result in a disruption of the contractile machinery of the heart (Elamin & Tuvemo, 1990). If this is

the case then it is reasonable to presume that changes in specific cations brought on by a diabetic state may synergistically lead to alteration in contraction that has been reported in the diabetic heart. One of the most abundant cations within the body is magnesium (Mg^{2+}) (Sasaki *et al.* 1999). In the heart, Mg^{2+} plays a pivotal role in myocardial functioning (Topalov *et al.* 2000). It has been reported changes in Mg^{2+} can, induce changes in membrane integrity and in doing so alter Ca^{2+} homeostasis (Altura & Altura, 1996), change the resting membrane and alter AP duration (Altura & Altura, 1985). Moreover, $[Mg^{2+}]_i$ has been reported to be important in the regulation of the Na^+/Ca^{2+} -exchanger. Therefore, any changes in Mg^{2+} levels may contribute to changes in the Na^+/Ca^{2+} -exchanger and cause a reduced or increased concentration of Ca^{2+} within the cell (Howarth & Levi, 1998). Therefore, any perturbation of Mg^{2+} within the heart may lead increased cardiac failure (Altura & Altura, 1985; Chakraborti *et al.* 2002).

It has been reported that Fe^{2+} when increased within the heart can result in heart failure. It has been reported that Fe^{2+} overload can result in heart failure and diabetes mellitus (Phatak & Cappuccio, 1994; Vonherbay *et al.* 1996).

Copper (Cu^{2+}) can act as a specific co-factor for over 20 enzymes that contribute to the normal function of the heart (Prohaska *et al.* 1990). Deficiency of this important cation has been implicated in a variety of cardiovascular complications including, IHD (Klevay, 2000), cardiac hypertrophy, cardiac fibrosis and changes in cardiac myofibrils (Saari *et al.* 1999). Copper deficiency has also been implicated in reducing cardiac action by altering Na^+ and K^+ transport through changes in $Na^+-K^+-ATPase$ isoform expression (Huang *et al.* 1995). In the whole heart, it has been reported that reducing $[Cu^{2+}]$ resulted in reduced contractile function (Allen *et al.* 1993; Prohaska *et al.* 1982). However, it has also been reported that isolated cardiac myocytes from Cu^{2+} deficient rats exhibit enhanced

contraction and speed of contraction (Wold *et al.* 2001). This implies that a change in Cu^{2+} content within the diabetic heart may contribute to changes in contractile function.

Zinc (Zn^{2+}) also acts as an important co-factor that is involved in numerous important physiological processes (Pras *et al.* 1983). It has been reported that changes in Zn^{2+} metabolism may be important in the induction of atherosclerosis (Paolisso *et al.* 1999). Whether or not changes in Zn^{2+} metabolism occur in diabetes, it is clear that changes in dietary Zn^{2+} can bring about changes in cardiac behaviour. One study reported that isoprenaline induced stimulation of the adenylate-cyclase activity, was significantly lower in diabetic rats that were given a low Zn^{2+} diet comparable to age-matched controls (Mooradian *et al.* 1988). This report would indicate that alterations in Zn^{2+} may directly effect the working of the cell through the β -adrenergic responsiveness of the diabetic heart (Mooradian *et al.* 1988) and therefore, any changes in Zn^{2+} metabolism in diabetes may contribute to changes at the cellular level.

Therefore, it can be seen that a changes in the total amount and variety of cations can have a profound effect on the normal functioning of the heart. Changes in the contractile dysfunction that has been reported in the diabetic heart may in part be brought about by altered cation metabolism

1.12 The effect of halothane on the heart

In patients that are attending elective surgical procedures under general anaesthesia, the commonest cause of significant morbidity and mortality corresponds to cardiovascular complications (Mangano & Goldman, 1995). Many volatile anaesthetics have been used in

the clinical environment to promote unconsciousness in patients undergoing surgical operations on the heart (Davies *et al.* 2000). It is well established that volatile anaesthetics have a potent negative inotropic effect on the heart, not only in clinical situations (Eger *et al.* 1970) and in animal, in situ hearts (Mahaffrey *et al.* 1961), but also in isolated heart muscle preparations (Housmans & Murat, 1988; Bosnjak *et al.* 1992), isolated cardiac myocytes (Harrison *et al.* 1999; Davies *et al.* 1999) and regionally isolated cardiac myocytes (Rithalia *et al.* 2001). Halothane is one such volatile anaesthetic that is widely used in a clinical and research environment and is reported to have a potent negative inotropic effect on the heart (Harrison *et al.* 1999; Davies *et al.* 1999). The negative inotropic effects of halothane on the heart are brought about by either a reduction in the Ca^{2+} transient, through altered Ca^{2+} homeostasis or by a change in myofilament sensitivity for Ca^{2+} (Davies *et al.* 2000). Moreover, it has been reported that myofilament sensitivity for Ca^{2+} is reduced in isolated rat cardiac myocytes in the presence of halothane (Harrison *et al.* 1999; Davies). It is well established that volatile anaesthetics such as halothane have a depressive effect on the $I_{\text{Ca,L}}$ (Ikemoto *et al.* 1985; Terrar *et al.* 1988; Bosnjak *et al.* 1991; Kanaya *et al.* 1998). Reductions in $I_{\text{Ca,L}}$ in the presence of halothane may contribute to a decrease in Ca^{2+} influx, SR Ca^{2+} content (Connelly *et al.* 1994), fractional Ca^{2+} release (Han *et al.* 1994), and Ca^{2+} transients (Wheeler *et al.* 1988), that have been reported in the heart preparations in the presence of halothane. As well as $I_{\text{Ca,L}}$, it has also been shown that halothane also affects other current, such as $I_{\text{Ca,L}}$ (Eskinder *et al.* 1991), I_{Na} (Weigt *et al.* 1997) and the I_{to} (Davies *et al.* 2000). Changes in current status in the presence of halothane are likely to account for changes in Ap characteristics that have been reported in the heart (Harrison *et al.* 1999). Moreover, it has recently been shown that halothane shortens the Ap duration to a greater extent in the sub-endocardial myocytes compared to sub-epicardial myocytes of the ventricle (Rithali *et al.* 2001). Any halothane-induced changes in Ap may contribute to the negative inotropic response that has been described

in the heart. Overall it has been shown that halothane-induced changes in current activity, Ca^{2+} mobilisation and Ca^{2+} myofilament sensitivity synergistically contribute to the negative inotropic effect in the heart.

It has been shown that changes in pathological disease states such as myocardial ischemia (Kissin *et al.* 1983;) and congestive heart failure have altered the negative inotropic effects of volatile anaesthetics. It is noteworthy that little is known about the effect of volatile anaesthetic on the diabetic heart. It has however been reported that halothane, isoflurane and enflurane did not significantly effect the papillary muscles of STZ-induced diabetic rat heart but increased the time course of contraction (Hattori *et al.* 1989).

1.13 Aims of the study

It has been reported in human patients and animal models with diabetes that contractility and Ca^{2+} homeostasis are compromised in the heart. A chemically induced model of type I diabetes will be employed by using the antibiotic STZ in the rat. To test the hypothesis that the underlying mechanisms of E-C are corrupt in the diabetic heart we will utilise cardiac myocytes that will be enzymically isolated from the ventricle of the heart. To date, there appears to be a great deal of contradiction surrounding changes in contractile dysfunction within the STZ-induced type I diabetic rat. We will therefore set up a time-course study to compare the effects of STZ-induced type I diabetes following, acute (4 week and 8-12 week) mid (4 and 5 month) and chronic (10 months) treatment on the mechanism of contraction in isolated ventricular myocytes. A cation imbalance is associated with cardiac dysfunction. This study will therefore test the hypothesis that the STZ-induced model of diabetes in the rat causes a specific cation imbalance. To test the hypothesis that there is a derangement in contractile function and Ca^{2+} mobilisation within the heart of the STZ-

induced diabetic rat, a video-edge detection system and a fluorescence system will be set up to measure contraction and Ca^{2+} simultaneously. The simultaneous recording of contraction and Ca^{2+} will allow the myofilament sensitivity Ca^{2+} to be measured and test the hypothesis that these may be affected in the STZ-induced diabetic heart. Pharmacological tools such as caffeine, NiCl_2 will then be employed to pinpoint changes in Ca^{2+} homeostasis, in particular to changes in Ca^{2+} efflux out of the cell within the STZ-induced diabetic heart. In some experiments isolated ventricular myocytes will be patched in whole cell mode and the voltage dependence of contraction will be measured to test the hypothesis that changes in membrane voltage are associated with differences in contractile function in the STZ-induced diabetic heart compared to age matched control. Throughout the series of experiments, the volatile anaesthetic halothane will be employed to test the hypothesis that the STZ-induced diabetic heart is more vulnerable to the inotropic effect of halothane compared to that seen in the normal heart.

Chapter 2

Materials and Methods

2.1 Materials

Streptozotocin; Sigma, S-0130, Collagenase; Worthington, LS004196, Protease, Sigma, P-5147, Insulin; Actrapid, 2-Bromo-2-chloro-1, 1,1-trifluoroethane (halothane); Sigma, B4388, stock 99%), Fura-2 AM; (Molecular probes, Leiden, The Netherlands), Nickel chloride; Sigma, N-5756.

2.2 Induction of diabetes

Diabetes was induced in male Wistar rats (200-250 g) by a single i.p. injection of STZ (60 mg kg⁻¹; Sigma, S-0130). STZ was dissolved in a citrate acid buffer solution (0.1 M citric acid; Sigma, C-0759 and 0.1 M sodium citrate; Sigma, S-4641 pH 4.5) (Ren & Davidoff, 1997; Tamada *et al.* 1998; Yu *et al.* 1994a; Noda *et al.* 1993). Age-matched control rats received an equivalent volume of citrate acid buffer solution alone. Control and diabetic animals were caged separately but housed under similar conditions. Both groups were fed the same diet and water *ad libitum* until they were used 1, 2, 4, 5 and 10 months later. All experiments had relevant ethical clearance from the Ethics Committees at the University of Central Lancashire and United Arab Emirates University.

2.2.1 Measurement of blood glucose, plasma osmolarity and plasma insulin

Glucose was measured in whole blood with a glucose meter (One Touch II glucose meter, Lifescan Inc) prior to administration of STZ, 3-5 days following administration of STZ to confirm diabetic state and immediately after humanely killing of the animal, prior to experiments. Blood plasma osmolarity was measured with a vapour pressure osmometer (Westcor Inc, Model 5500XR). Plasma insulin analysis was measured with a standard ¹²⁵I radioimmunoassay kit (Coat-A-Count Insulin, Diagnostic Products Corp, CA).

2.3 *Preparation of heart tissue for cation analysis*

At 2 and 4 month intervals diabetic and control animals were anaesthetised by an i.p. administration of pentobarbitone (60 mg kg^{-1} body weight) and also received $200 \mu\text{l}$ heparin (Leo Pharmaceutical Products, $5000 \text{ i.u. ml}^{-1}$). Hearts were rapidly excised, before being blot dried and weighed. These hearts were then used for the analysis of cardiac cation contents.

2.4 *Cardiac myocyte isolation for contractility study and calcium measurement*

Rats were humanely killed by a blow to the head followed by cervical dislocation and the hearts rapidly removed. Samples of blood were taken at this stage for subsequent measurement of whole blood glucose, osmolarity and plasma insulin. Cardiac myocytes were isolated according to previously described techniques (Frampton *et al.* 1991a). In brief, hearts were perfused retrogradially at a constant flow rate by Langendorff's method (Langendorff, 1895) with a physiological solution (Appendix) containing Ca^{2+} (0.75 mM) at 37°C . Perfusion flow rates were adjusted to $8 \text{ ml g heart}^{-1} \text{ min}^{-1}$ to allow for differences in heart weight between the diabetic and control animals. When the preparation appeared stable (regular contractions $300 \text{ beats min}^{-1}$), perfusion was switched to a nominally Ca^{2+} -free physiological salt solution (Appendix) containing ethylene glycol-bis(2-aminoethylether)-N,N,N',N'-tetraacetic acid (EGTA, 0.1 mM ; Sigma, E-0396) for 4 min. The heart was then perfused with a physiological salt solution (Appendix) containing Ca^{2+} (0.05 mM), collagenase (0.75 mg ml^{-1} ; Worthington, LS004196) and protease (0.075 mg ml^{-1} ; Sigma, P-5147). This solution was then re-circulated to give a total enzyme exposure of 6 min (see Figure 2.1.)

2.4.1 Isolation of ventricular myocytes

Following enzyme perfusion, the heart was cut down free from the perfusion apparatus and ventricles excised and cut into small pieces (1-5 mm). The ventricular tissues were then shaken (300 osc/min) in 5 ml enzyme solution (Appendix) containing 1% bovine serum albumin (BSA; Sigma, A-4503) for 4 min at 37°C. The mixture was then filtered through gauze (300 µm aperture, Cadish precision meshes, Finchley, London) and suspended in a physiological salt solution (Appendix) containing 0.75 mM Ca²⁺. The filtrate was then centrifuged (400 rpm, 1 min), the supernatant was removed and the cell pellet was re-suspended in physiological salt solution (Appendix) containing 0.75 mM Ca²⁺. The process was repeated a total of four times. Myocytes from shakes 2 and 3 were accumulated and stored at 4°C prior to use. Cells were used during a period of 1-8 hr after the isolation. Rod cell viability was measured (viability of the ratio of living cells (rods) to dead cells (rounds)) with an improved Neubauer haemocytometer within 1 hr after completion of the cell isolation (see Figure 2.2).

2.4.2 Isolation of sub-endocardial and sub-epicardial myocytes.

In a number of experiments sub-endocardial (endo) and sub-epicardial (epi) myocytes were isolated in preference to ventricular myocytes. Following enzyme perfusion, the heart was removed from the perfusion apparatus and the ventricle excised. The outer and inner layers of the left ventricle were dissected free and cut into small pieces. Endo and epi portions were then isolated (as total ventricular myocytes) separately to give two cohorts of cells (Rithalia *et al.* 2001).

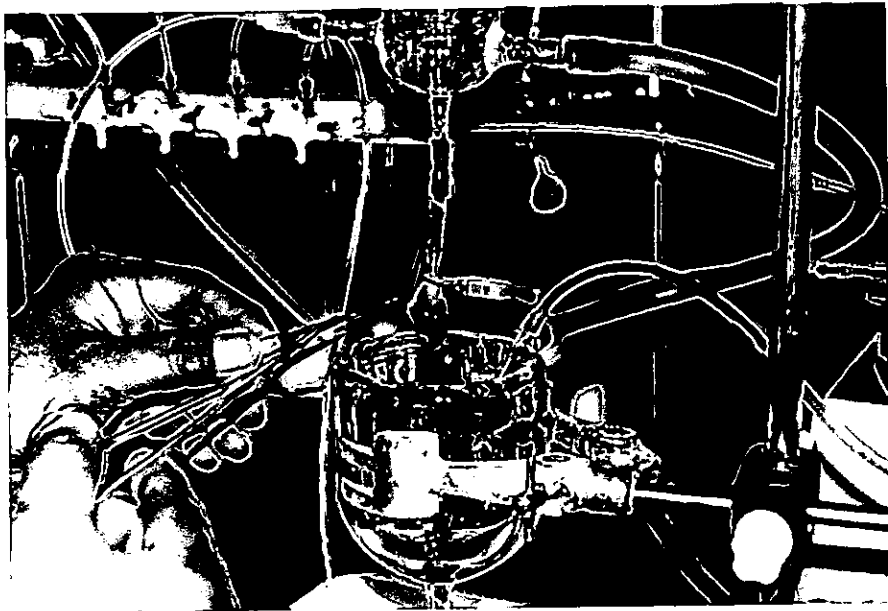
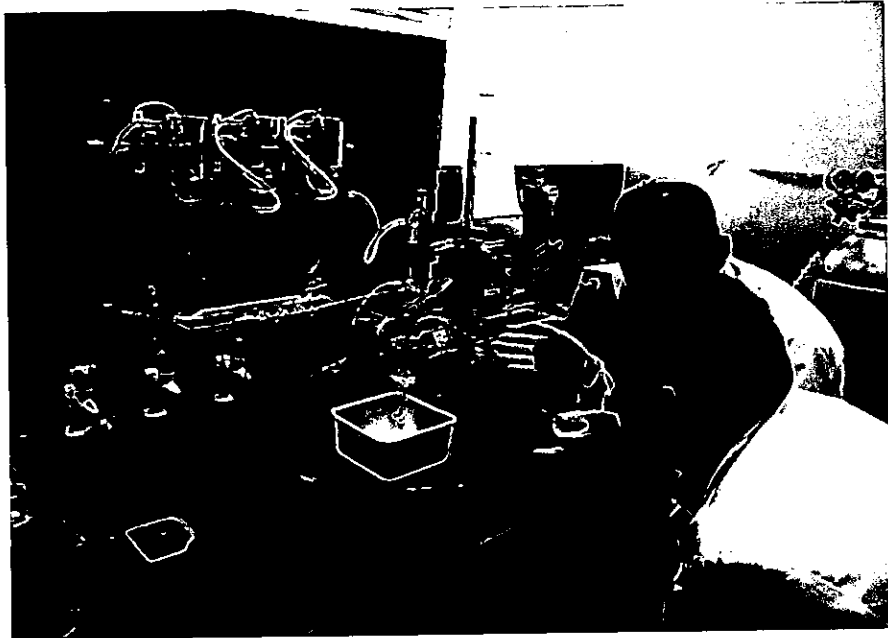


Figure 2.1. Apparatus used for perfusion of isolated heart (top) and close up photograph of heart on cannula (bottom).

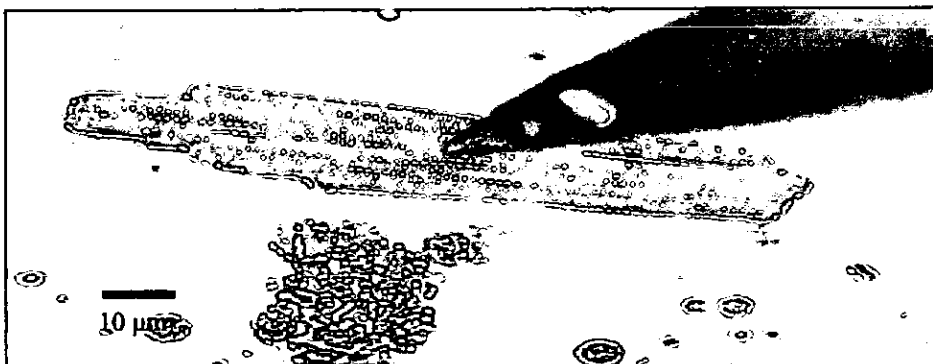
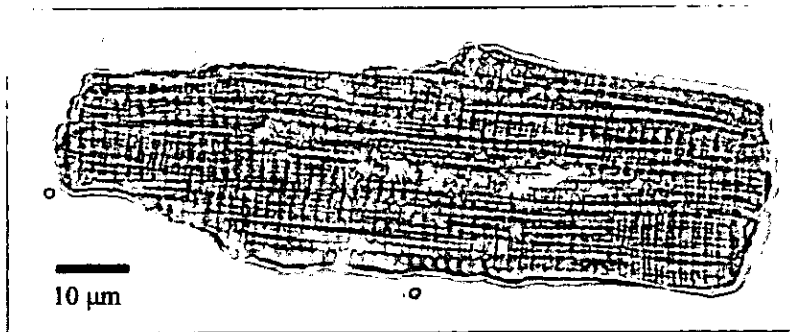


Figure 2.2. Close up of isolated heart (top), isolated ventricular myocyte (middle) and isolated ventricular myocyte attached to a patch pipette in whole cell mode (bottom).

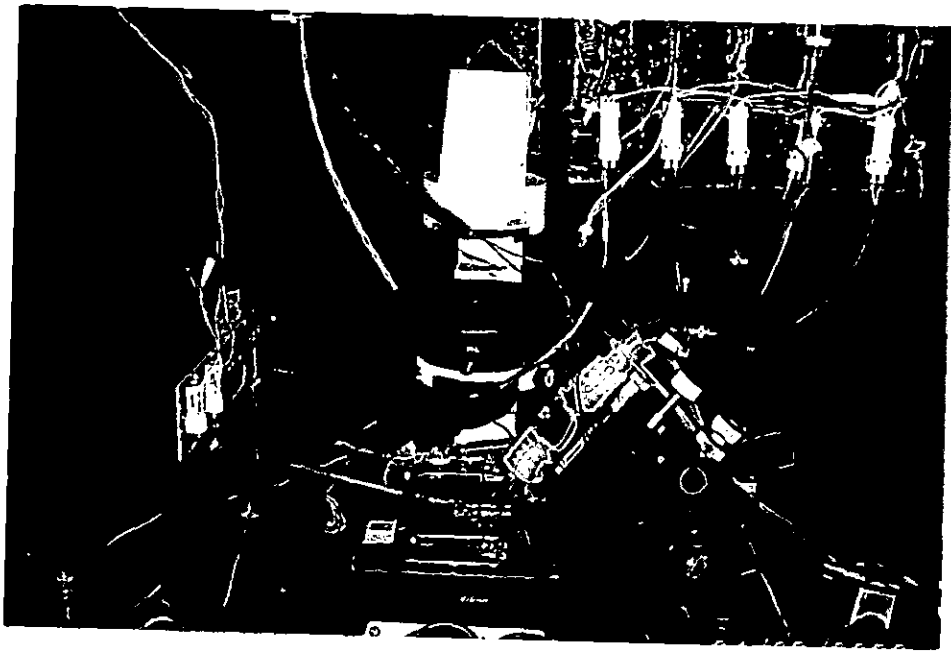
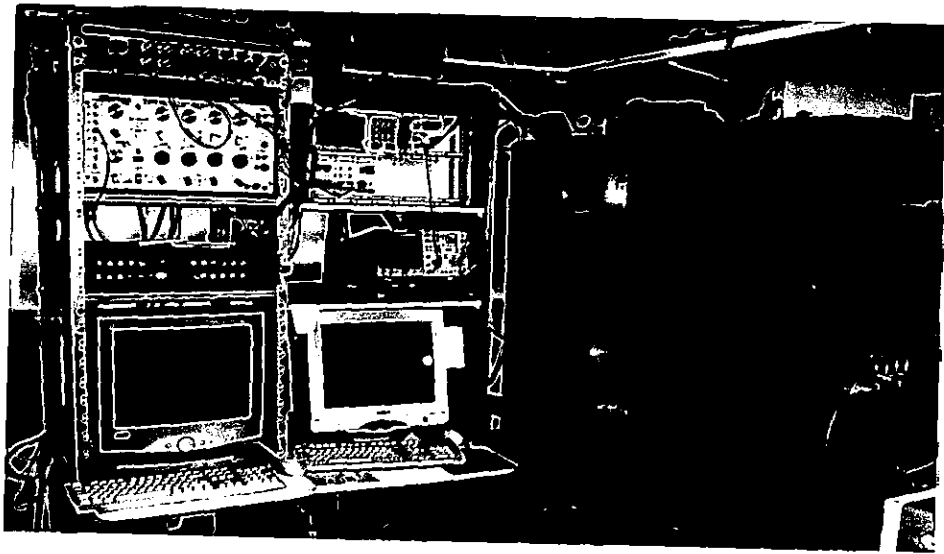


Figure 2.3. Apparatus system used for measuring contraction and calcium in ventricular myocytes. The whole rig (top) and the inside of the rig showing the cell chamber and solution switcher (bottom).

2.5 Measurement of total cardiac calcium, copper, iron, magnesium and zinc

Heart tissue was placed in 10 ml of Analar grade nitric acid (10 g tissue 100 ml⁻¹ nitric acid; VWR, 45004) and left to digest overnight at room temperature. Appropriate dilutions were made with Milli-Q grade water prior to measurement of cations. Total cardiac Ca²⁺, Mg²⁺, Fe²⁺; Cu²⁺ and Zn²⁺ concentrations were measured by atomic absorption spectrophotometry (PYE Unicam, Model SP9) using air/acetylene and nitrous oxide/acetylene flames, respectively. Calibration standards (Ca²⁺, Mg²⁺, Fe²⁺, Cu²⁺ and Zn²⁺) were obtained from VWR Laboratory Suppliers. Values for cation contents were expressed as mg (100 mg of heart tissue)⁻¹.

2.6 Measurement of contraction in cardiac myocytes

Cardiac (either epi, endo or total ventricular) myocytes were allowed to settle on the glass bottom of a chamber mounted on the stage of an inverted microscope (Nikon Diaphot-TMD, Japan) with X40 (Nikon, Japan) objective lens. Myocytes were superfused (3-5 ml min⁻¹) with a normal Tyrode (NT) solution (Appendix) containing 1 mM Ca²⁺ using a power driven magnetic micro pump (Cole-Parmer instrument Co.Ltd, London) system, maintained at 35-37°C with a heating system coupled to a temperature controller (Medical systems corp., USA) and field stimulated (S88 stimulator, Grass-Telefactor, USA) via two platinum electrodes located on either side of the chamber. Contraction was measured with a video edge detection system (Crystal Biotech, VED-114) (Howarth & Levi, 1996). SIGNAL software (Cambridge Electronic Design, England) was used to acquire and analyse data (see Figure 2.3.).

2.6.1 Effects of insulin and STZ on contraction

Ventricular myocytes isolated from diabetic and age-matched control hearts were incubated with either STZ (10 μ M) or with insulin (1 μ M; Actrapid) for 2-3 hr at room temperature prior to experiments. Contraction was measured with a video edge detection system (Crystal Biotech, VED-114) (Howarth & Levi, 1996). SIGNAL software (Cambridge Electronic Design, England) was used to acquire and analyse data.

2.6.2 Effect of halothane, glucose and perturbation of external calcium on contraction

In separate experiments a rapid solution changer (Levi *et al.* 1996) was used to apply either 2-Bromo-2-chloro-1,1,1-trifluoroethane (0.6 mM, halothane; Sigma, B4388, stock 99%) (Appendix) or different concentrations of either glucose (25 mM; VWR, 1011747) or Ca^{2+} (0.25, 1 and 5 mM; VWR, 100703-H) to perfused ventricular myocytes. Contraction was measured with a video edge detection system (Crystal Biotech, VED-114) (Howarth & Levi, 1996). SIGNAL software (Cambridge Electronic Design, England) was used to acquire and analyse data. Osmolarity of the NT solution and NT (25mM) glucose was measured using a calibrated Burnett osmometer.

2.7 Measurement of intracellular calcium transients in cardiac myocytes

In order to measure the $[\text{Ca}^{2+}]_i$ transients, cardiac myocytes were firstly loaded with the fluorescent indicator fura-2-AM (Molecular probes, Leiden, The Netherlands) using an established method (Howarth *et al.* 1999). Briefly, a volume of 6.25 μ l of a 1.0 mM stock solution of fura-2-AM (dissolved in dimethylsulphoxide, (DMSO; Sigma, D-5879)) was added to 2.5 ml of cells to give a final fura-2-AM concentration of 2.5 μ M. Myocytes were

shaken gently for 10 min at room temperature. Following loading, the cells were centrifuged at 400 rpm for 1 min, the supernatant was removed and cells were resuspended in NT (1 mM Ca^{2+}) (Appendix). Cells were then incubated for at least 30 min at room temperature to ensure complete hydrolysis of the intracellular ester.

$[\text{Ca}^{2+}]_i$ transients were measured by alternately illuminating the loaded myocytes with light at 340 and 380 nm using a dichromatic mirror (Cairn Research Ltd., Faversham, Kent, UK) and an inverted microscope with X40 (fluo) oil objective lens. The resultant fluorescence emission at 510 nm was recorded by a photomultiplier tube (PMT; Cairn research Ltd., Faversham, Kent, UK). The ratio of emitted fluorescence at the two-excitation wavelengths (340/380 ratio) was calculated to provide an index of $[\text{Ca}^{2+}]_i$ (see Figure 2.3.). A time course of Ca^{2+} analysis was measured by taking the time taken from stimulation to the peak of the Ca^{2+} . The decay of the Ca^{2+} transient was measured as either the time taken from the peak amplitude of Ca^{2+} transient to half its decay or the rate of decay measured by plotting a gradient of at least 8 points on the decay of the Ca^{2+} transient.

2.7.1 Effect of halothane and calcium on cardiac calcium transients

In separate experiments a rapid solution changer (Levi *et al.* 1996) was used to apply either halothane (0.6 mM) or different concentrations of extracellular Ca^{2+} (0.25, 1 and 5 mM) throughout the experiments.

2.8 Simultaneous measurement of contraction and calcium in cardiac myocytes

In some experiments it was possible to measure contraction and Ca^{2+} transient simultaneously using a long pass illumination filter (P810 ,Cairn Research Ltd.,

Faversham, Kent, UK) fitted in the path of the microscope light source, therefore transmitting infra-red light whilst block light of shorter wavelength. This enabled viewing of myocytes via a CCD camera, which is sensitive to infrared light.

2.9 *Effect of caffeine on fractional calcium release in cardiac myocytes*

Following a train of steady-state Ca^{2+} transients, stimulation was abbreviated for 10 sec and a rapid application of caffeine (10 mM; Sigma C-1778) was applied to myocytes (10 sec) to assess fractional Ca^{2+} release from the SR. Following the application of caffeine, cells were switched to a NT (1 mM Ca^{2+}) solution (Appendix) re-stimulated (1 Hz) and allowed to recover prior limits. The decay of the caffeine induced Ca^{2+} transient was measured as either the time taken from the peak amplitude of caffeine-induced Ca^{2+} transient to half its decay or the rate of decay measured by plotting a gradient of at least 8 points on the decay of the Ca^{2+} transient.

2.10 *Effects of nickel chloride on caffeine-induced calcium release*

In some experiments, following the recovery of myocytes from a caffeine-induced Ca^{2+} release, stimulation was abbreviated for 10-20 sec while, Nickel chloride (NiCl_2 , 10 mM; Sigma, N-5756) was rapidly applied to cells before a 10 sec re-application of caffeine (10 mM). Myocytes were then re-perfused with a NT (1 mM Ca^{2+}) solution (Appendix) and re-stimulated (1 Hz) to allow recovery to prior steady state.

2.11 Voltage dependence of contraction and calcium current in cardiac myocytes

Voltage dependence of contraction was measured in patch-clamped ventricular myocytes in whole cell mode. Patch pipettes (Harvard patch glass capillaries PG1-5OT-10) were pulled (Narishege, Japan PP-83) and fire polished (Narishege, Japan MF-79 microfuge) to between 2 and 5 Ω . Patch pipettes were filled with a cesium based pipette solution (Appendix). Patch-clamp recordings were made in whole cell, voltage clamp mode using an EPC-7 patch amplifier and headstage (HEKA, Germany). The “pipette to bath” junction potential was corrected before negative pressure was applied to cells which were then subjected to a holding potential of -40 mV to inactivate the sodium current (I_{Na}) and T-type Ca^{2+} current ($I_{Ca,T}$) (Brown *et al.* 1981). Test pulses (200 msec duration) were applied at potentials between -30 and $+60$ mV in 10 mV increments. Membrane capacitance (compensated for differences in cell size using c-slow/c-fast with a slow range of 100 pF), series resistance (g-series compensation) ($<15M\Omega$) and capacitance compensation (30-40%) were corrected before recordings were taken. A train of four conditioning pulses were applied before each test pulse to standardise SR Ca^{2+} load (Howarth & Levi, 1998). $I_{Ca,L}$ was measured using WINWCP (version 3.2) electrophysiological software (John Dempster, Strathclyde University, Glasgow, UK) at the same time as measuring the voltage dependence of contraction using a video edge detection system. The time to peak of the $I_{Ca,L}$ was measured from the start of the test pulse to the time at the peak of $I_{Ca,L}$. The amplitude of the $I_{Ca,L}$ was measured as the difference between $I_{Ca,L}$ at peak and $I_{Ca,L}$ at the end of the depolarising pulse.

2.11.1 Effects of halothane on calcium current and voltage dependence of contraction

In another series of experiments $I_{Ca,L}$ and contraction was measured in ventricular myocytes prior and during incubation with 0.6 mM halothane.

2.12 Data analysis and statistics

All data are expressed as mean \pm S.E.M. of (n) preparations/cells. Statistical comparisons were made (SPSS software) using independent samples Student's t-test, paired t-test or ANOVA followed by Bonferroni post hoc analysis. P-values of less than 0.05 were considered significant, while P-values of less than 0.01 were considered very significant.

Chapter 3

General characteristics of the streptozotocin-induced diabetic rat

3.1 General characteristics of the streptozotocin-induced diabetic rat heart and ventricular myocytes at differing treatment times

3.1.1 Introduction

A single dose of STZ (between 40 and 60 mg Kg⁻¹) administered to young adult rats is sufficient to initiate a stable model of type 1 diabetes (Szkudelski 2001). STZ acts to disrupt and destroy pancreatic β -cells, which leads to alterations in glucose and insulin (Szkudelski 2001). It has been reported that two hours, post injection of STZ, there is a fall in plasma insulin level leading to a rise in blood glucose, which is should be followed, around 6 hours later by a transient decrease in blood glucose and concurrent elevation in levels of circulating insulin. Finally, blood chemistry stabilises to a state of hyperglycaemia and hypoinsulinaemia (West *et al.* 1996). Therefore, induction of diabetes results in a state of β -cell necrosis that is manifested by a temporary return of responsiveness, which appears to be followed by a permanent disruption and/or destruction of the β -cells (West *et al.* 1996). Following a short incubation of up to 3 days, STZ-induced rats present symptoms, which include severe hyperglycaemia and polydipsia. Within the next two weeks, rats start to show symptoms of muscle wastage increased food consumption, decrease in muscle mass and after a number of weeks some rats appear to acquire a cataract like condition (some features associated with type-1 diabetes) (Bracken *et al.* 2003). Data, which follow show the general characteristics associated with the induction of STZ-induced diabetes. These include glucose, insulin and plasma osmolarity and there differences according to the different treatment times (4 and 8-12 weeks, 4 and 10 months) comparing age-matched with STZ-induced diabetic rat.

3.1.2 Methods

See *chapter 2* for details.

3.1.3 Results

The general characteristics of age-matched controls and diabetic rats and ventricular myocytes following 4 and 8-12 weeks, 4 and 10 months of treatment are shown in table 3.1.a, b, c and d. All rats within each group were supplied or bred together and weighed the same weight (± 15 g) at the start of treatment. Figure 3.1. shows the typical weight gained over a period of 8 weeks of treatment. It can be seen that STZ-induced rats gained significantly ($P < 0.01$) less body weight at each week (week 3-8) of treatment compared to age-matched control rats. Moreover, table 3.1. a, b, c and d shows that diabetic animals had reduced body weights and had smaller hearts in all treatment time periods (not significantly ($P > 0.05$) different in 4 weeks of treatment), compared to age-matched controls. Whole blood glucose was significantly ($P < 0.05$) elevated in all treatment times compared to controls. Plasma osmolarity measured in 8-12 weeks and 10 month STZ-treated rats was significantly ($P < 0.05$) higher than in age-matched controls. Cell viability measured by the percentage (%) of viable myocytes was significantly decreased ($P < 0.01$) in 4 week (43.3% *Vs.* 66.0 %) and 8-12 week (25.3% *Vs.* 49.4 %) STZ-treated hearts compared to controls. This trend was decreased in the 10 month treatment to 32.2% in control and 23.8% viability in diabetic cells, although no significant ($P > 0.05$) difference was reported. Plasma insulin was significantly ($P < 0.05$) decreased following 8-12 weeks and 4 months of treatment, but was unchanged after 10-month STZ treatment compared to age-matched controls.

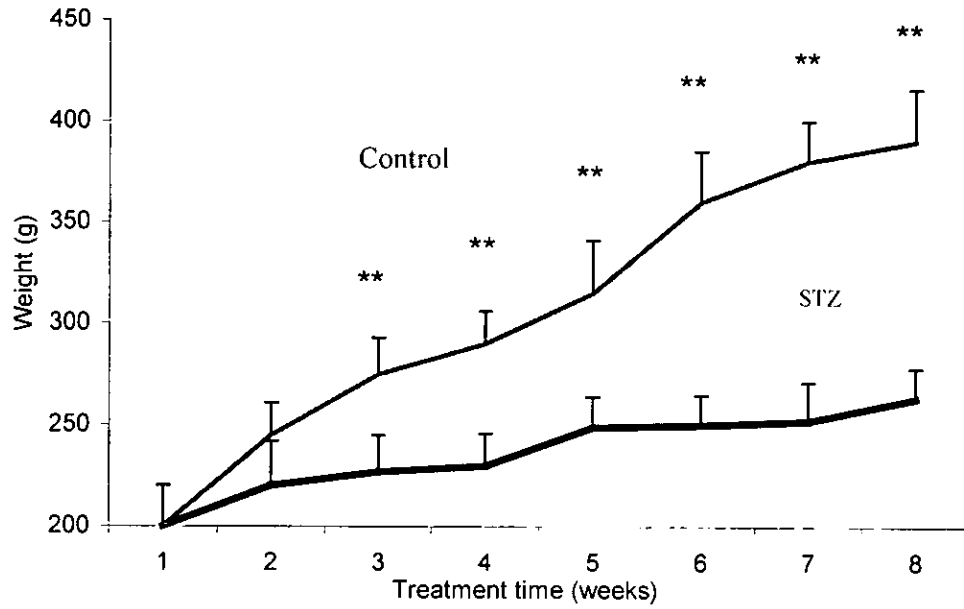


Figure 3.1. Typical, time dependent effects of STZ-induced (n=16) diabetes on mean body weight of Wistar rats compared to age-matched controls (n=16). Data shown are mean \pm SEM. Statistical significance showing control *vs.* STZ using independent samples t-test is represented by **P<0.01.

Table 3.1.a General characteristics of control and STZ-treated rat heart and ventricular myocytes following 4 weeks of treatment.

	Control	STZ-treated
Body Wt. (g)	371.0 +/-5.72 (4)	267.5 +/-6.55 (4)*
Heart Wt. (g)	1.2 +/- 0.01 (4)	1.2 +/- 0.04 (4)
Blood glucose (mg/dl)	87.7 +/- 5.4 (4)	441.4 +/-51.3 (4)**
Cell viability (% rod cells)	66.0 +/-5.7 (5)	43.3 +/-6.5 (4)*

Table 3.1.b General characteristics of control and STZ-treated rat heart and ventricular myocytes following 8-12 weeks of treatment.

	Control	STZ-treated
Body Wt. (g)	381.4 +/-12.5 (5)	232.8 +/-7.2 (6)**
Heart Wt. (g)	1.1 +/- 0.04 (5)	1.0 +/- 0.03 (6)**
Blood glucose (mg/dl)	92.4 +/- 2.42 (5)	407.5 +/-39.9(6)**
Cell viability (% rod cells)	49.4+/-3.5 (5)	25.3+/-1.2 (6)**
Plasma Osmolarity (osmol kg ⁻¹)	308.3 +/- 3.6 (4)	330.0 +/- 3.5 (4)**
Plasma Insulin (ng ml ⁻¹)	20.63 +/- 7.52 (7)	4.80 +/- 1.28 (4)*

In table 3.1.a and 3.1.b, data are means \pm S.E.M. Number in parenthesis indicates number of rats or ventricular myocytes. All data were obtained at the end of the treatment period. Control *Vs.* STZ compared using Student's independent samples *t* test. * $P < 0.05$, ** $P < 0.01$.

Table 3.1.c General characteristics of control and STZ-treated rat heart and ventricular myocytes following 4 months of treatment.

	Control	STZ-treated
Body Wt. (g)	420.3 +/-8.6 (6)	285. 5+/- 9.4 (6)**
Heart Wt. (g)	1.0 +/- 0.03 (6)	0.9 +/- 0.03 (6)**
Blood glucose (mg/dl)	120.0 +/-3.8 (6)	381.0 +/-18.7(6)**
Plasma Insulin (ng ml ⁻¹)	11.86 +/- 1.09 (6)	7.25 +/- 0.87 (6)**

Table 3.1.d General characteristics of control and STZ-treated rat heart and ventricular myocytes following 10 months of treatment.

	Control	STZ-treated
Body Wt. (g)	414.6 +/-21.2 (5)	270.0 +/-12.6 (5)**
Heart Wt. (g)	1.3 +/- 0.02 (5)	1.0 +/- 0.02 (5)**
Blood glucose (mg/dl)	81.2 +/- 3.1 (5)	415.0 +/-52.8 (5)**
Cell viability (% rod cells)	32.2+/-4.8 (5)	23.8+/-6.2 (5)
Plasma Osmolarity (osmol kg ⁻¹)	311.6 ±1.3 (5)	332.0 ± 7.3(5)*
Plasma Insulin (ng ml ⁻¹)	10.67 +/- 3.36 (7)	8.300 +/- 2.92 (8)

In table 3.1.c and 3.1.d, data are means ± S.E.M. Number in parenthesis indicates number of rats or ventricular myocytes. All data were obtained at the end of the treatment period. Control *Vs.* STZ compared using Student's independent samples *t* test.

* P<0.05, **P<0.01.

3.1.4 Discussion

STZ-induced diabetic rats displayed typical characteristic features, which have been previously reported in STZ-treated animals (Yu *et al.* 1994b; Howarth *et al.* 2001; Howarth *et al.* 2002). The results of this study have shown that there is a reduction in body and heart weights in the STZ-induced diabetic rats after 8-12 weeks and 4 and 10 months following treatment compared to healthy age-matched controls. Other workers have also reported decreases in heart and body weights at 1 and 2 weeks, (Gordon & Guppy, 1999) 4-6 weeks, (Tamada *et al.* 1998) 8-12 weeks (Howarth *et al.* 2001) and 7 months (Satoh *et al.* 2001) following STZ-treatment. An increase in blood glucose and a reduction in serum insulin levels are indicative of a diabetic state (Choi *et al.* 2002). It has been reported that blood glucose levels are 3-times as high in STZ-induced diabetic rats compared to control (Choi *et al.* 2002), which, is in agreement with this study, that has shown elevated blood glucose in all treatment times. Insulin levels were significantly depressed at 8-12 weeks and 4 months in agreement with other reports who have also shown hypoinsulinaemia in this model of diabetes (Shimoni *et al.* 1998; Howarth *et al.* 2001; Choi *et al.* 2002). Although there was a reduction of insulin at 10 months of treatment, it was not significant. This could be a result of some adaptive mechanism associated with the regenerative action of the pancreas, similar to that which has been reported in the STZ-induced type 2 model of diabetes (Schaffer, 1991). The viability of cardiac myocytes, when comparing good (rod) cells with dead (round) cells has shown to be significantly decreased at 4 and 8-12 weeks, in agreement with Yu *et al.* (1994) who also reported a reduction in rod cell viability. Any changes in cell viability may be a consequence of the fragility of the diabetic state. Hence, the cell becomes more disrupted and sensitive to any enzymic and mechanical disruption within the isolation process itself. Some reports (Okayama *et al.* 1994; Tamada *et al.* 1998) have suggested that though viability was altered from experiment to experiment, no significant changes were seen between control and diabetic cells, which mirrors what we

have seen in 10 months of STZ-treatment. The normalised insulin levels that were noted in 10 month treated rats may act to protect the heart in some way, and in doing so decrease its vulnerability in the isolation process and hence increase cell viability to levels similar to that of control myocytes.

3.1.5 Conclusion

The STZ-induced diabetic rat undergoes severe changes in body mass, muscle tone and eating/drinking habits that are underpinned by the destruction of the insulin producing pancreatic β -cells. Decreased circulating insulin gives rise to massively high amounts of unutilised blood glucose, which is transported around the body and some of which is excreted in the urine. The combination of changes in blood chemistry synergistically leads to altered physiological properties in the body's infrastructure and most importantly, notable changes in the heart functioning.

3.2 *Distribution of specific divalent cation within the streptozotocin-induced diabetic rat heart*

3.2.1 *Introduction*

It is known that an imbalance in specific cations can cause disruption to the contractile mechanisms of the heart (Elamin & Tuvemo, 1990). It is therefore reasonable to presume that any alteration in specific cations within diabetes may contribute to the alteration in contraction that has been reported in the diabetic heart.

3.2.1.1 *Magnesium*

Mg²⁺ is the fourth most abundant total cation in the human body and the second most abundant intracellular cation (Sasaki *et al.* 1999). Mg²⁺ regulates over 300 enzyme systems directly or indirectly (via Mg-ATP transport) (Nemesanszky & Gerencser, 1992; Altura & Altura, 1996). Mg²⁺ is predominantly found in three forms; bound to protein complexes, complexed to anion ligands and in its free ionised form. The concentration of intracellular magnesium ([Mg²⁺]_i) in whole blood is on average around 0.5-0.7 mmol l⁻¹ and approximately 65-72% of total Mg²⁺ being free or biologically-active Mg²⁺ (Altura & Altura, 1996). In the heart, Mg²⁺ plays a key role in myocardial functioning (Topalov *et al.* 2000). Perturbation of Mg²⁺ can effect contractility in cardiac cells by; inducing alterations in membrane and intracellular organelle binding, changes in Ca²⁺ transport, including actions of Ca²⁺ release from the SR (Altura & Altura, 1996), changes in resting membrane and Ap's and disrupting E-C coupling cascades (Altura & Altura, 1985). Therefore, any changes in Mg²⁺ can act to, or contribute to the aetiology of cardiac and vascular disorders (Altura & Altura, 1985; Chakraborti *et al.* 2002). Moreover, a dietary deficiency of Mg²⁺ can result in a loss of intracellular K⁺ ([K⁺]_i) and concurrent gain in

cellular Na^+ and Ca^{2+} (Chakraborti *et al.* 2002), which can induce electrolyte imbalance leading to changes in membrane integrity (Chakraborti *et al.* 2002). Mg^{2+} deficiency has been implicated in many cardiovascular-related disorders including; IHD, CHF, sudden cardiac death, hypertension, eclampsia, atherosclerosis, cardiac arrhythmias and ventricular complications in diabetes mellitus (Altura *et al.* 1981; Chakraborti *et al.* 2002). Measurement of total cardiac Mg^{2+} will indicate whether this cation contributes to the changes in contractility that has been reported in the diabetic heart.

3.2.1.2 Calcium

Ca^{2+} represents perhaps the most important ion within the heart. Ca^{2+} is crucial to the normal process of heart chamber, contraction and relaxation (Bers, 2002b). Consequently, perturbation of Ca^{2+} within the heart can contribute to alterations in contractile kinetics. In the normal heart Ca^{2+} levels are controlled by a number of transport systems including L-type Ca^{2+} channel (through $I_{\text{Ca,L}}$ activity), PMCA channels, $\text{Na}^+/\text{Ca}^{2+}$ -exchanger and SERCA pump on the SR. Therefore, in a normal heart beat, Ca^{2+} homeostasis is controlled by any or all of these system. Any alteration or modulation to any of these Ca^{2+} transport systems may contribute to both contractile dysfunction and arrhythmic pathological conditions (Pogwizd *et al.* 2001). This study will evaluate the total cardiac Ca^{2+} in STZ-treated rats after 2 and 4 months treatment. A change in total Ca^{2+} may be indicative of an underlying diseased state.

3.2.1.3 Copper

A deficiency in dietary Cu^{2+} can lead to cardiac disorder such as hypertrophy, fibrosis, derangement of myofibrils, and impaired contractile and electrophysiological function (Wold *et al.* 2001). It has been suggested that such disorders are directly related to the decrease in a specific a Cu^{2+} -dependent enzyme reaction (Saari, 2000).

3.2.1.4 Iron

Fe^{2+} is an important trace element in the body. However, changes in Fe^{2+} metabolism can lead to clinical problems. Haemochromatosis is an autosomal-recessive hereditary disorder, which is characterised by excessive increases in amounts of absorbed dietary Fe^{2+} . This induces a state of Fe^{2+} overload, which, over a period of time manifests increased deposits of Fe^{2+} in tissue. This can result in skin discoloration, arthropathy, hepatic cirrhosis, heart failure, diabetes mellitus and impotence (Phatak & Cappuccio, 1994; Vonherbay *et al.* 1996). It is not clear in the literature if diabetes mellitus is a true cause or consequence of increases in heart Fe^{2+} content. We have therefore determined total cardiac Fe^{2+} content in STZ-induced diabetic rats at 2 and 4 month treatment.

3.2.1.5 Zinc

Zn^{2+} acts as an important co-factor that is involved in numerous important physiological processes (Pras *et al.* 1983). Although little data are available to suggest any direct evidence of diabetes-induced cardiomyopathy with cardiac Zn^{2+} content, it has been observed that Zn^{2+} metabolism may be important in the induction of atherosclerosis (Paolisso *et al.* 1999).

3.2.2 Method

See *chapter 2* for details.

3.2.3 Results

Figure 3.2.a shows the time dependent changes in total concentration of total Cu^{2+} at 2 and 4 months following diabetes induction with STZ. The results show that diabetic heart tissue has a significantly ($P < 0.01$) elevated level of Cu^{2+} in 2 ($0.0056 \pm 0.0002 \text{ mg (100 mg tissue)}^{-1}$) and 4 months ($0.0049 \pm 0.0008 \text{ mg (100 mg tissue)}^{-1}$) compared to control heart tissue at 2 ($0.0021 \pm 0.0001 \text{ mg (100 mg tissue)}^{-1}$) and 4 months ($0.0030 \pm 0.00009 \text{ mg (100 mg tissue)}^{-1}$), respectively. Figure 3.2.b shows a significantly ($P < 0.01$) elevated level, of Fe^{2+} at 2 months ($0.011 \text{ mg} \pm 0.0005 \text{ (100 mg tissue)}^{-1}$) and 4 months ($0.013 \pm 0.0004 \text{ mg (100 mg tissue)}^{-1}$) in STZ-treated heart tissue compared to age-matched controls at the same treatment time. Figure 3.2.c shows a significant ($P < 0.01$) increase in total Ca^{2+} in 2 month STZ treated hearts ($0.015 \pm 0.001 \text{ mg (100 mg tissue)}^{-1}$) compared to age-matched controls ($0.0076 \pm 0.0007 \text{ mg (100 mg tissue)}^{-1}$). Similarly, significant increases were obtained in 4 month STZ treated hearts ($0.016 \pm 0.001 \text{ mg (100 mg tissue)}^{-1}$) compared to age-matched controls ($0.0089 \pm 0.0008 \text{ mg (100 mg tissue)}^{-1}$). Figure 3.3.a shows that Mg^{2+} levels remain similar at both 2 months and 4 months. At 2 months treatment, the total Mg^{2+} content in control and STZ-treated heart tissues was $0.010 \pm 0.0003 \text{ mg (100 mg tissue)}^{-1}$ and $0.010 \pm 0.0005 \text{ mg (100 mg tissue)}^{-1}$, respectively but in 4 month control heart tissues it was $0.012 \pm 0.0002 \text{ mg (100 mg tissue)}^{-1}$ compared to $0.011 \pm 0.0002 \text{ mg (100 mg tissue)}^{-1}$ in the diabetic tissue. Figure 3.3.b shows total Zn^{2+} content and reports a significant ($P < 0.05$) rise in Zn^{2+} content from $0.015 \pm 0.0007 \text{ mg (100 mg tissue)}^{-1}$ in control to $0.019 \pm 0.001 \text{ mg (100 mg tissue)}^{-1}$ in the 2-month treated diabetic heart. At 4 months no significance was seen between Zn^{2+} content in control ($0.019 \pm 0.0007 \text{ mg (100 mg tissue)}^{-1}$) and diabetic ($0.020 \pm 0.001 \text{ mg (100 mg tissue)}^{-1}$) tissue.

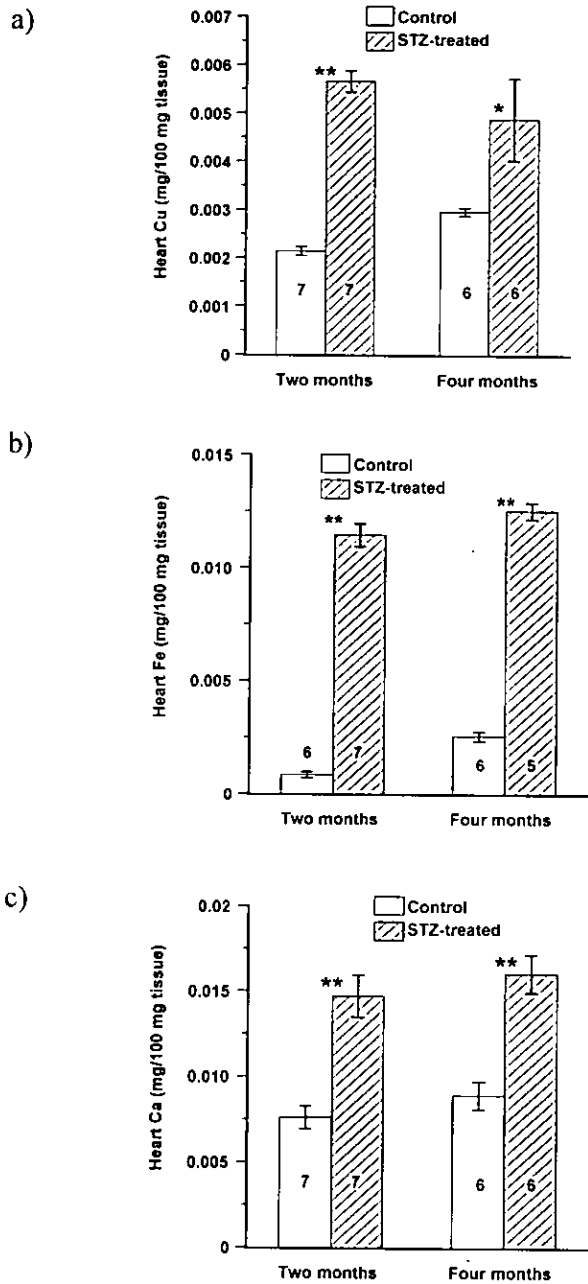


Figure 3.2. Time dependent effects of STZ-induced diabetes on (a) Cu^{2+} content, (b) Fe^{2+} content and (c) Ca^{2+} content in rat heart. Data shown are mean \pm SEM. Numbers within bars represent number of experiments. Statistical significance showing control vs. STZ using independent samples t-test is represented by * $P < 0.05$ and ** $P < 0.01$.

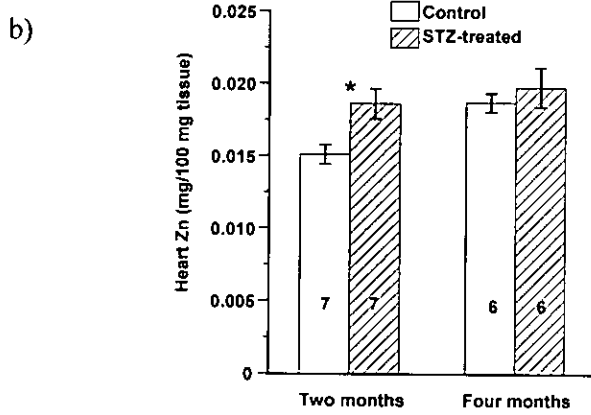
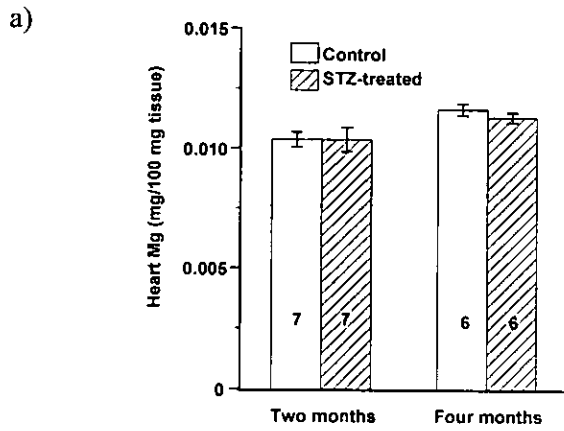


Figure 3.3. Time dependent effects of STZ-induced diabetes on (a) Mg^{2+} content and (b) Zn^{2+} content in rat heart. Data shown are mean \pm SEM. Numbers within bars represent number of experiments. Statistical significance showing control vs. STZ using independent samples t-test is represented by * $P < 0.05$ and ** $P < 0.01$.

3.2.4 Discussion

3.2.4.1 Magnesium content

Total cardiac Mg^{2+} levels within this study were not significantly different between control and STZ-treated rats after 2 and 4 months of treatment. The data in this study would suggest that cardiac Mg^{2+} is not affected in STZ-induced diabetes. Hypomagnesaemia, characterised by reduced serum Mg^{2+} has been reported in a number of human patients with diabetes (Saito, 1996; Sasaki *et al.* 2000; Nagase, 1996) as well as experimental-induced models of diabetes (Altura & Altura, 1995). Reports in experimental-induced diabetes have shown a significant decrease in cardiac Mg^{2+} levels from STZ (Bhimji *et al.* 1986) and alloxan (Bhimji *et al.* 1985) treated animals compared to controls. However, in another study it has been shown (Ewis & AbdelRahman, 1995) that there were no significant changes in heart Mg^{2+} in STZ-induced and controls. These later findings are in agreement with the results obtained in the present study.

$[Mg^{2+}]_i$ and extracellular Mg^{2+} ($[Mg^{2+}]_o$) concentrations play an important role on a variety of cellular events and are also an important co-factor for ATP in many cellular enzyme systems (Howarth & Levi, 1998). $[Mg^{2+}]_i$ has been reported to be important in the regulation of the Na^+/Ca^{2+} -exchanger. Therefore, any changes in Mg^{2+} levels may contribute to changes in the Na^+/Ca^{2+} -exchanger and consequently cause a reduced or increased concentration of Ca^{2+} within the cell (Howarth & Levi, 1998). It has also been reported that Mg^{2+} deficiency can induce the rise of $[Ca^{2+}]_i$, changes in cell membrane permeability and transport processes in cardiac cells. It has been suggested that the reason for the opposing effect of Ca^{2+} and Mg^{2+} is that there is competitive for the same site of action proteins such as troponin-C (Chakraborti *et al.* 2002).

3.2.4.2 Calcium content

The total Ca^{2+} concentration following 2 and 4 months of diabetes was significantly elevated after STZ treatment. Total tissue Ca^{2+} transient has also been reported in type 2 diabetic hearts were a 35 % increase in Ca^{2+} was reported (Schaffer *et al.* 1989). Moreover, ventricular muscle stiffness (Schaffer *et al.* 1989), as measured by changes in left ventricular pressure, is more rigid in diabetic hearts. Brady & Farnsworth (1986) have suggested that the increase in muscle stiffness may be caused by an elevation in basal $[\text{Ca}^{2+}]_i$ and partial activation of myosin. Because this experiment has reported an elevated Ca^{2+} content in both treatment times, it is tempting to suggest that Ca^{2+} influx through leak channels and reductions in the $\text{Na}^+/\text{Ca}^{2+}$ -exchanger working to shunt Ca^{2+} out of the cell is compromised in the diabetic heart and may contribute to the results reported in our experiments.

3.2.4.3 Copper content

Total cardiac Cu^{2+} concentrations in this study were significantly elevated versus age-matched control after 2 and 4 months STZ-treatment. It has been shown that a decrease in Cu^{2+} within the diet and subsequent Cu^{2+} deficiency leads to IHD (Klevay, 2000). As a result of decreased Cu^{2+} intake, hearts would also appear to have lesser amounts of Cu^{2+} . We, however, have shown an increase in Cu^{2+} in the diabetic heart. Moreover, It has been shown (Ford, 2000) that elevated levels serum Cu^{2+} concentrations may be associated with higher incidence of cardiovascular disease. There is little data available to directly link experimental diabetes with elevated levels of cardiac Cu^{2+} ; however, it has been shown that Cu^{2+} is elevated in the liver of diabetic animals (Hallmans & Lithner, 1980). From the literature and results presented in this study it seems unclear if there is a direct link with alterations in Cu^{2+} and an increase in diabetic-induced cardiomyopathy.

3.2.4.4 Iron content

This experiment would suggest that Fe^{2+} metabolism is changed in the diabetic state but if or how these changes affect the diabetic state or contractility within the cardiac cell need further investigation. Previous reports suggest that an alteration in Fe^{2+} levels is not implicated in the pathophysiology of diabetes (Tuvemo & Gebre-Medhin, 1983).

3.2.4.5 Zinc content

The direct implication of changes in Zn^{2+} metabolism and diabetes is unclear. The present study has demonstrated that total Zn^{2+} content in the heart is shown to be significantly elevated in 2 months, while, Zn^{2+} content was similar in 4 months following STZ-induced diabetes compared to control.

Though little data are available to compare cardiac Zn^{2+} content, it has reported that serum Zn^{2+} levels are unchanged in diabetic patients (Golik *et al.* 1993; Pras *et al.* 1983), whereas plasma Zn^{2+} concentrations have been reported to be significantly reduced in diabetic patients (Williams *et al.* 1995; Chen *et al.* 1995). However, other reports that showed no significant differences in plasma Zn^{2+} from with patients who had type 2 diabetes. It is widely accepted that during diabetes significantly high amounts of Zn^{2+} are lost through the urine (Tuvemo & Gebre-Medhin, 1983; Chen *et al.* 1995; Golik *et al.* 1993).

3.2.5 Conclusion

In conclusion, this study has demonstrated that STZ-induced diabetes elicits a state of hyperglycaemia and hypoinsulinaemia in the rat and also alters specific metabolic cations within the heart compared to healthy age-matched controls. It is proposed that these

metabolic disturbances may alter the mechanical functioning, that has been reported in the diabetic hearts. This study has reported differences in cation content in the diabetic heart. It is also clear that any perturbation of cardiac cation content can influence the cells ability to function “normally”. It is suggested that specific alterations in cation imbalance may lead to changes in cardiac heart function that has been reported in the STZ-induced diabetic rat heart.

Chapter 4

Effects of streptozotocin-induced diabetes on contraction in rat cardiomyocytes

4.1 Time dependent effects of streptozotocin-induced diabetes on the kinetics of contraction in ventricular myocytes isolated from rat heart

4.1.1 Introduction

Derangement of cardiac functionality is a common feature associated with experimentally-induced diabetes. Contractile responses have been measured in many different animal models of diabetes with varying methods, different treatment times and consequently different results. In the STZ-induced diabetic rat model of diabetes alone there are many contradictory results, but most are consistent to agree that there is underlying contractile dysfunction or alteration in the diabetic model, to serve as a valid tool to investigate diabetic-induced cardiomyopathy. Contractile defects have been reported in a wide range of STZ-induced diabetic tissues. These include the intact animal (Al Shafei *et al.* 2002), isolated perfused heart (Choi *et al.* 2002), papillary muscle preparations (Hattori *et al.* 2000; Marshall, 2000) and single isolated cardiac myocytes (Tamada *et al.* 1998; Yu *et al.* 1994a; Hattori *et al.* 2000; Choi *et al.* 2002). By using single isolated cardiac myocytes it is possible to investigate and study contraction consistently without possible problems e.g. extrinsic factors such as, changes in circulating hormones and metabolites in the *in vivo* preparation and changes in perfusion rates associated with intact hearts (Choi *et al.* 2002). Isolated cardiac myocytes from STZ-induced diabetic hearts have been reported as having depressed shortening (44% decrease compared with controls), reduced maximum rates of shortening and re-lengthening (58 and 56% decrease, respectively) and prolonged t_{pk} shortening (47% increase)(Yu *et al.* 1994a). Decreased shortening and a reduction in rates of contraction and relaxation have also been demonstrated by (Okayama *et al.* 1994) while, Ren & Davidoff (1997) showed that diabetes markedly prolonged both the contraction and relaxation phases of isolated ventricular myocytes. However, other groups (Tamada *et al.* 1998; Ishitani *et al.* 2001) have reported that STZ-induced diabetic hearts have no

significant differences in cell shortening. A significant increase in the amplitude of contraction has also been reported in conjunction with an increase in the t_{pk} of contraction (Howarth *et al.* 2000; Howarth *et al.* 2001). Importantly, it has been reported that STZ-induced diabetic rats treated with daily doses of insulin (to normalise blood glucose) have attained normal contractile function, thus indicating that defects associated with STZ-induced diabetes are specific to the disease state itself (Yu *et al.* 1994a).

This study investigated contractile characteristics associated with short (4 and 8-12 weeks), mid (5 months) and long-term (10 months) STZ-induced diabetes.

4.1.2 Method

See *Chapter 2* for details.

4.1.3 Results

The amplitude of contraction (compared as a % of resting cell length-RCL) was increased in all STZ-treated myocytes following each period of treatment (see Figure 4.1.a). Following 4 weeks treatment, the amplitude of contraction was significantly ($P < 0.01$) increased ($9.72 \pm 1.04\%$ Vs. $5.01 \pm 0.53\%$) compared to control, respectively. After 8-12 weeks of treatment the amplitude of contraction was markedly reduced in diabetic myocytes compared to 4 weeks of treatment, but was still significantly ($P < 0.01$) increased in diabetic myocytes ($6.8 \pm 0.5\%$) compared to that of age-matched controls ($4.1 \pm 1.04\%$) over the 8-12 weeks of diabetes. Following 5 months of treatment, the amplitude of contraction was similar to that after 8-12 weeks, with a significant ($P < 0.01$) increase in the diabetic cells versus control ($6.4 \pm 0.6\%$ Vs. $3.2 \pm 0.4\%$), and although reduced slightly after 10 months treatment. This was also significantly ($P < 0.01$) increased in diabetic

myocytes compared to age-matched controls, respectively ($4.7 \pm 0.3 \%$ Vs. $3.3 \pm 0.3 \%$). The t_{pk} of contraction was significantly ($P < 0.01$) increased in diabetic myocytes (207.2 ± 8.0 ms) following 4 weeks of treatment compared to control (167.2 ± 8.1 ms) (see Figure 4.1.b). This trend, although blunted was seen after 8-12 weeks of treatment as well, in diabetic and control myocytes (164.1 ± 7.4 ms Vs. 132.3 ± 5.9 ms), respectively. Following 5 months of treatment, t_{pk} of contraction was significantly ($P < 0.05$) longer in diabetic myocytes (134.7 ± 6.6 ms) compared to control myocytes (110.3 ± 6.2 ms). Following 10 months of treatment no significance ($P > 0.05$) difference was observed between diabetic and control myocytes.

The $t_{1/2\ relax}$ was not significantly ($P > 0.05$) altered after 4 weeks (95.8 ± 7.1 ms Vs. 106.4 ± 8.7 ms), 8-12 weeks (60.6 ± 4.1 ms Vs. 70.6 ± 5.6 ms) and 5 months (53.8 ± 1.6 ms Vs. 55.4 ± 4.3 ms) following induction of diabetes in myocytes from diabetic and control hearts, respectively (see Figure 4.1.c). However, following 10 months of treatment the $t_{1/2\ relax}$ was significantly ($P < 0.01$) shorter in diabetic (55.32 ± 2.7 ms) myocytes compared to control (85.1 ± 7.1 ms).

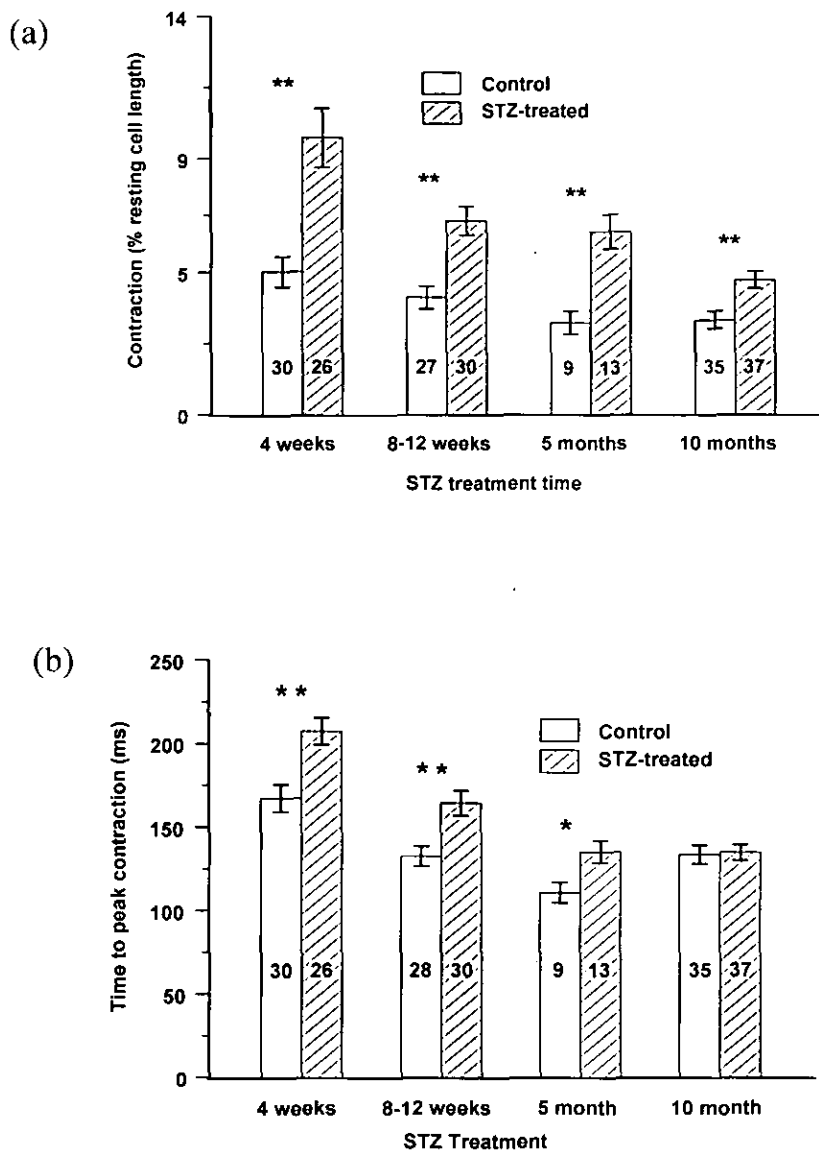


Figure 4.1. Time-dependent effects of STZ-induced diabetes after 4, 8-12 weeks and 5 and 10 months of treatment on amplitude of contraction (a) and t_{pk} of contraction (b) in electrically stimulated myocytes (1 Hz) perfused at 35-37°C with a NT solution containing 1 mM Ca^{2+} . Age-matched control myocytes are also shown in the figure for comparison. Data are mean \pm SEM. Numbers of cells are shown in bars. * $P < 0.05$, ** $P < 0.01$

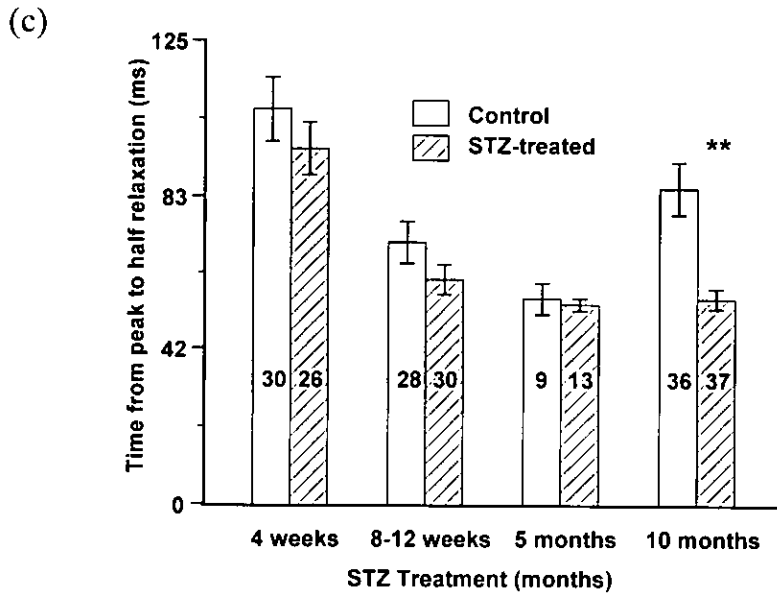


Figure 4.1.c. Time-dependent effects of STZ-induced diabetes after 4, weeks, 8-12 weeks and 5 and 10 months of treatment (c) on the $t_{1/2\text{ relax}}$ in electrically stimulated myocytes (1 Hz) in isolated ventricular cardiomyocytes perfused at 35-37°C with a NT solution containing 1 mM Ca^{2+} . Data from age-matched control myocytes are also shown in the figure for comparison. Data are mean \pm SEM. Numbers of cells are shown in bars.

** $P < 0.01$

4.1.4 Discussion

Contraction was measured as a % of RCL in isolated ventricular myocytes and was increased in each treatment time of STZ-induced diabetes. This is in agreement with previous studies (Howarth *et al.* 2001), which demonstrated an increase in contraction following 2 and 10 months of treatment. The increase in contraction in diabetic myocytes was more marked at shorter time periods compared to control. Increase in contraction is an indication of either altered or an increased amount of $[Ca^{2+}]_i$ or changes in myofilament sensitivity to Ca^{2+} during systole in the contractile phase. Other reports suggest that contractility is decreased in the STZ-induced diabetic cardiac myocyte following 5 months (Okayama *et al.* 1994), 6 weeks (Yu *et al.* 1994a) and 8-weeks (Noda *et al.* 1993; Choi *et al.* 2002) of STZ-treatment, while other reports suggest that there is no change in contraction following 4-6 weeks and 8 weeks of STZ-treatment (Tamada *et al.* 1998), respectively (Ishitani *et al.* 2001). Inconsistencies in data may well reflect differences in dose, time treatment, experimental protocol, and strains of animals used. What does seem evident is that in most reports there is either an alteration or/and disturbance in contraction in the diabetic heart. The t_{pk} of contraction was significantly increased in STZ-induced diabetes following 4, 8-12 weeks and 5 months but not following 10-months of STZ-treatment. An increase in the t_{pk} has also been reported in STZ-induced diabetic myocytes following 4-6 days (Ren & Davidoff, 1997), 6 weeks (Choi *et al.* 2002) and 8 weeks of treatment (Yu *et al.* 1994a; Ren & Davidoff, 1997; Howarth *et al.* 2000). However, in this study, it has also been observed that following 10-months of STZ-treatment there was no significant difference in the t_{pk} contraction between diabetic and age-matched control myocytes. The $t_{1/2\text{ relax}}$ was not significantly altered by STZ-induced diabetes following 4, 8-12 weeks and 5 months of treatment, but was significantly ($P<0.01$) decreased after 10 months of treatment. This is in agreement with a previous study (Howarth *et al.* 2000), which, reported an increase in the relaxation phase following 10 months of STZ-

treatment. Either way little/or no other data are currently available to compare the effect of such chronic treatment times on the type 1 model of diabetes. However, longer relaxation phases have been reported in shorter periods (8 weeks) of treatment (Choi *et al.* 2002).

The changes in the amplitude and the time-course of contraction would suggest that over time the STZ-induced diabetic rat heart undergoes a compensatory adaptive process to try and secure the integrity of the heart. It could be that a change in blood glucose and insulin instigates a slow change in gene regulation that is characterized by changes in contractile performance. This is an interesting hypothesis needing future investigation. Furthermore, because contraction is ultimately dependent on Ca^{2+} homeostasis, it is likely that a change in $[\text{Ca}^{2+}]_i$ regulation and or a change in myofilament sensitivity may explain differences seen in the STZ-induced diabetic model of diabetes versus age-matched control.

4.2 Post rest potentiation in STZ-induced diabetic heart

4.2.1 Introduction

E-C coupling is the process underlying contraction in the heart (Bers, 2002a). In the steady-state, contraction is followed by a short period of rest, which is characterised, by a refractory period (restitution). The predominant factor responsible for this is the recovery of the RyR from an inactivated or adapted state (Bers, 2002a). In the non-steady-state, cardiac cells are left in a quiescent phase for artificially long periods. Thus, the subsequent amplitude of contraction is greatly increased versus prior steady state in the rat (Yu & Mcneill, 1991; Bassani & Bers, 1994; Bers *et al.* 1993; Maier *et al.* 2000) and human (Pieske *et al.* 1999) but is diminished in the rabbit heart (Bassani & Bers, 1994; Bers *et al.* 1993; Maier *et al.* 2000). It is thought that an increase in amount of fractional Ca^{2+} release coupled together with the total available SR Ca^{2+} is likely to contribute to the increase in the amplitude of contraction. Increased availability of Ca^{2+} in the SR leads to an increase in contracture and therefore, longer periods of resting phases produce larger contractions. This phenomenon is referred to as the post rest potentiation (PRP), and is an indication of the degree of stored Ca^{2+} available for contraction (Yu & Mcneill, 1991). This study investigated the contractile characteristics of PRP in the STZ-induced diabetic rat heart compared to age-matched control. Changes in the STZ-induced diabetic heart may have implications regarding SR loading and Ca^{2+} release from SR stores.

4.2.2 Method

See *Chapter 2* section for details.

4.2.3 Results

In all figures, unless otherwise stated, relate to 8-12 weeks STZ-induced diabetic ventricular myocytes and age-matched controls. Myocytes were stimulated at 1 Hz until steady state contraction was attained. Stimulation was then abbreviated for periods between 2 and 60 s (Figure 4.2.). PRP was assessed by comparing the amplitude of the first PRP contraction with pre steady-state. t_{pk} of contraction and $t_{1/2\ relax}$ were also measured after each of the rest periods in control and diabetic myocytes. Figure 4.3. shows (a) PRP shortening, (b) t_{pk} and (c) $t_{1/2\ relax}$ of myocytes. The amplitude of PRP shortening increased progressively in diabetic and control myocytes as rest periods increased between 2 and 60 s. PRP increases of shortening were not as marked in myocytes from diabetic cells compared to control although at no stage were changes significant (Figure 4.3.a). The t_{pk} of PRP contraction was consistently longer in myocytes from the diabetic heart compared to control. Following 20 sec rest interval, t_{pk} contraction was 173 ± 4 ms and 143 ± 8 ms in diabetic and control myocytes, respectively (Figure 4.3.b). $t_{1/2\ relax}$ of PRP contraction after 2 months was not significantly different ($P > 0.05$) in myocytes from diabetic compared to control following all rest periods (Figure 4.3.c).

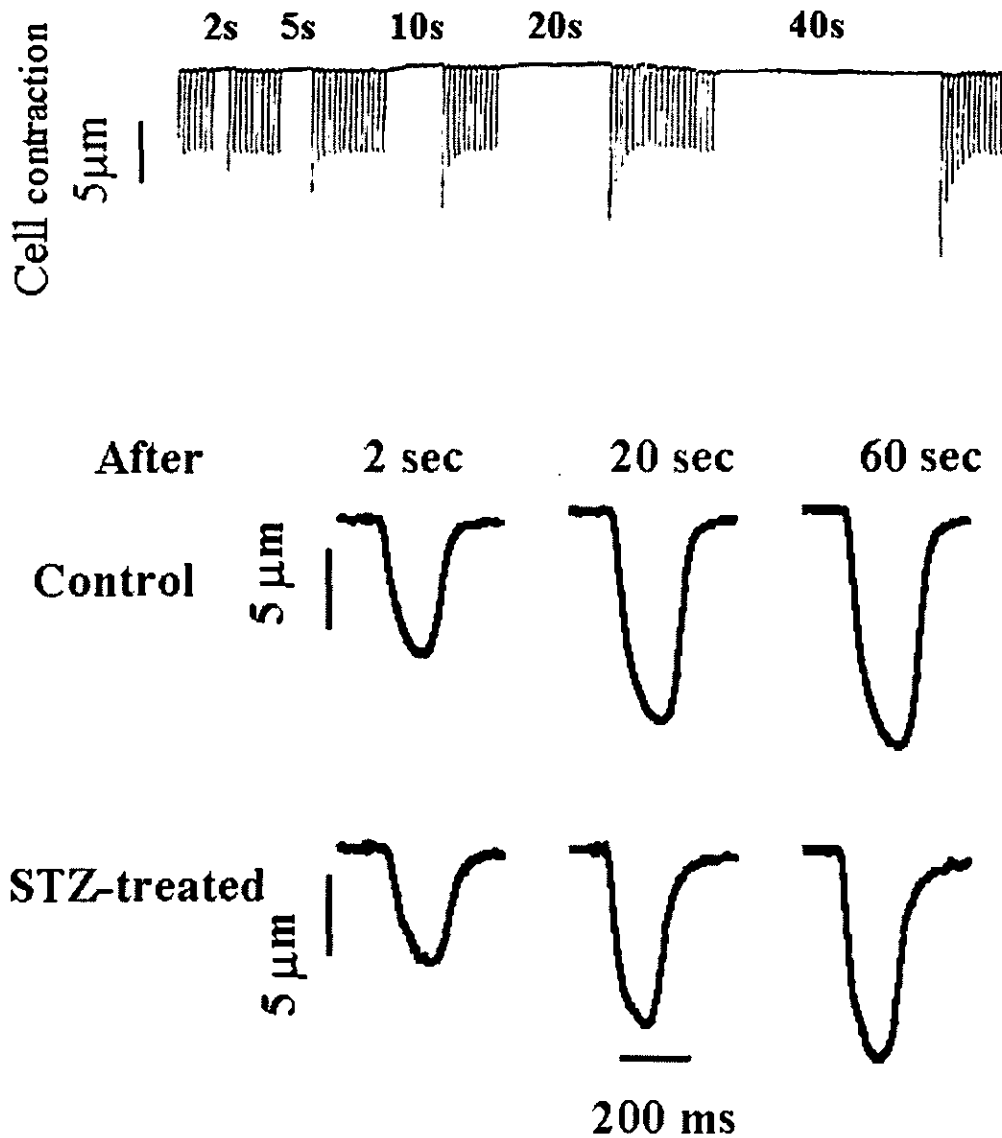
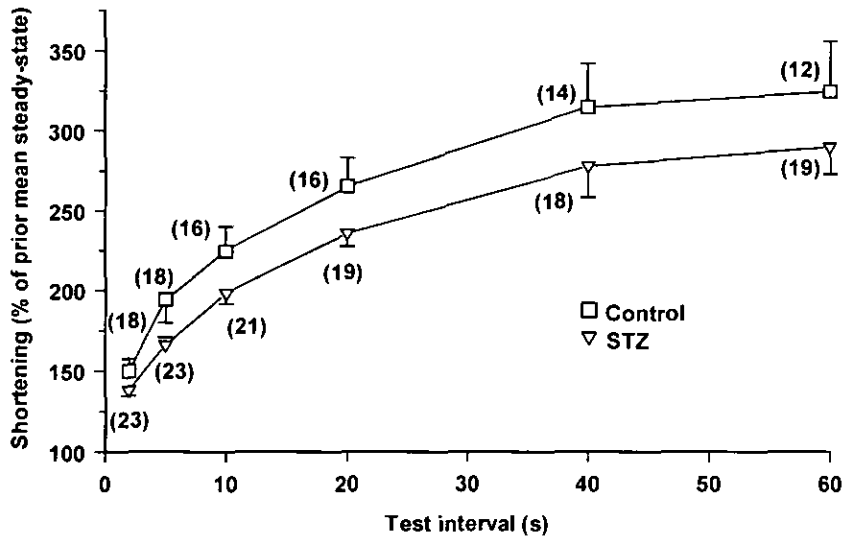
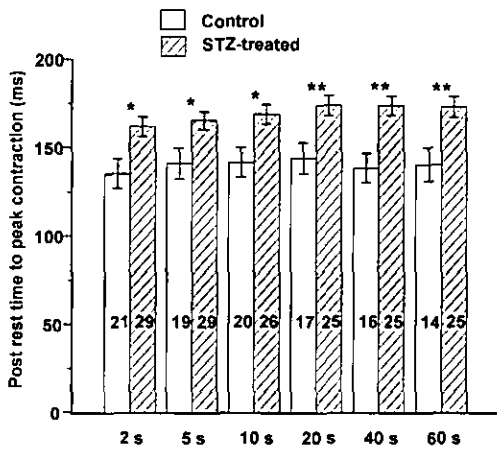


Figure 4.2. Determination of mechanical restitution in isolated rat ventricular myocytes. The trace shows the cell contraction (μm) from an isolated myocyte. After steady-state contractions (1Hz) extra systoles were interpolated after the test intervals above. Traces are typical of 15-25 such myocytes taken from 6-8 diabetic and 6-8 control hearts.

(a)



(b)



(c)

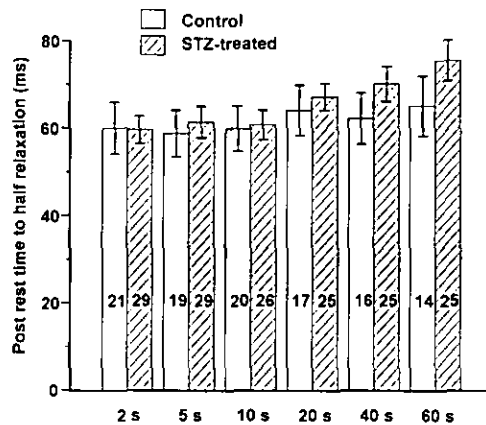


Figure 4.3. Time course of (a) shortening, (b) post rest t_{pk} of contraction and (c) post rest $t_{1/2\ relax}$ in ventricular myocytes from STZ-treatment and age-matched control rat hearts. Data are mean \pm SEM. Numbers of cells are shown in parentheses or in bars. They were obtained from 6-8 diabetic and 6-6 control hearts. * P < 0.05, ** P < 0.01

4.2.4 Discussion

PRP of shortening was observed in control and diabetic myocytes, however, shortening was less marked in diabetic cells versus control. Yu & McNeill (1991) have also reported a change in PRP contractions in diabetic papillary muscles from Wistar and spontaneously hypertensive rats. In contrast, the same workers have reported no change in PRP contraction in the left atria suggesting that there may be species as well as regional differences in PRP contraction in the heart. The t_{pk} of contraction has been shown to be significantly longer in diabetic myocytes following PRP at all periods. The t_{pk} in diabetic myocytes markedly increased over the increase in time period, however, in the control myocytes there was no increase in the t_{pk} . A change in the t_{pk} may indicate a slower sustained release of Ca^{2+} from the SR.

The two factors contributing to changes in the amplitude of PRP contraction in the rat heart are the amount of SR Ca^{2+} and the degree of fractional release (Bers, 2002a). During rest periods Ca^{2+} leaks out of the SR into the cytosolic compartment where it competes with other Ca^{2+} to be either transported back into the SR or out of the cell via the Na^+/Ca^{2+} -exchanger and the PMCA (Bassani & Bers, 1995). Because the SR pump predominates over the other mechanisms in the rat heart (Bassani *et al.* 1994), the great majority of Ca^{2+} leak is pumped back into the SR which ultimately contributes to unaltered Ca^{2+} flux that has been reported in the rat heart (Bassani & Bers, 1994). Another reason for the predominance of the SERCA pump over the Na^+/Ca^{2+} -exchanger is the high resting $[Na^+]_i$ that has been reported in the heart (Shattock & Bers, 1989). This would contribute to an influx of Ca^{2+} during quiescent phases. The marked decrease in the PRP amplitude of shortening (although not significant) and the significant changes in the t_{pk} of PRP contraction in myocytes from the STZ-induced diabetic heart may be associated with one

or more changes in $[\text{Na}^+]_i$, SERCA pump activity and fractional Ca^{2+} release as well as a alteration in myofilament sensitivity.

4.3 Effects of chronic streptozotocin-induced diabetes on contraction-frequency relationships in ventricular myocytes isolated from rat heart

4.3.1 Introduction

Force-frequency relationships have been studied for many years in many different animals models. In rabbit (Maier *et al.* 2000), guinea-pig (Kurihara & Sakai, 1985) and non-failing human hearts (Pieske *et al.* 1999), it has been shown that following an increase in the frequency of stimulation, contractile response, as well as SR Ca^{2+} content increase up to a point where a maximum frequency response is reached (Bers, 2002a), known as the positive staircase response (Bers, 2002a). However, in some rat cardiac myocytes, following an increase in frequency stimulus, it has been reported that there is a decrease in contractile force (Frampton *et al.* 1991), although SR Ca^{2+} does not appear to alter significantly (Maier *et al.* 2000). This response has therefore been named a negative staircase effect. One of the main reasons why some rat cardiac tissue should behave in this way is due to the loading of the SR with Ca^{2+} . In the rat heart, SR Ca^{2+} is relatively high (Maier *et al.* 2000) which, is due to a predominately strong SERCA pump that mops up the greatest percentage of Ca^{2+} leak from the SR. This is mirrored by a high level of $[\text{Na}^+]_i$ (Shattock & Bers, 1989) that drives $\text{Na}^+/\text{Ca}^{2+}$ -exchanger to reduce Ca^{2+} efflux from the cell. The aim of this part of the study was to investigate the effect of STZ-induced diabetes on the force frequency relationship in isolated ventricular myocytes. A significant change in force frequency within the diabetic heart may be associated with a derangement of SR Ca^{2+} release sequestration or alterations in myofilament sensitivity.

4.3.2 Method

See *Chapter 2* section for details.

4.3.3 Results

In all figures, unless otherwise stated, relate to 8-12 weeks STZ-induced diabetic ventricular myocytes and age-matched controls. Figure 4.4. shows the (a) amplitude of contraction (b) t_{pk} of contraction and (c) $t_{1/2\ relax}$ in myocytes of STZ-treated and age-matched control rat hearts. The amplitude of contraction was significantly ($P < 0.01$) larger in myocytes from diabetic heart during electrical stimulation at 1 Hz and 2 Hz frequency, compared to age-matched control, but was not significantly altered following 0.2 Hz stimulation (Figure 4.4.a). The t_{pk} of contraction was significantly ($P < 0.01$) longer in diabetic myocytes at all (0.2, 1 and 2 Hz) frequency ranges compared to age-matched control (figure 4.4b). Although $t_{1/2\ relax}$ was markedly decreased in diabetic myocytes at all frequencies (0.2, 1 and 2 Hz) it was found not to be to a significant level (Figure 4.4.c). There was a significant difference in the amplitude on contraction in control myocytes when frequency stimulation was switched from 0.2 to 1 Hz, but was not significantly altered between 1 and 2 Hz. In STZ-induced diabetic myocytes there was no significant differences between all (0.2 Hz to 1 Hz and 1Hz to 2 Hz) frequencies of stimulation.

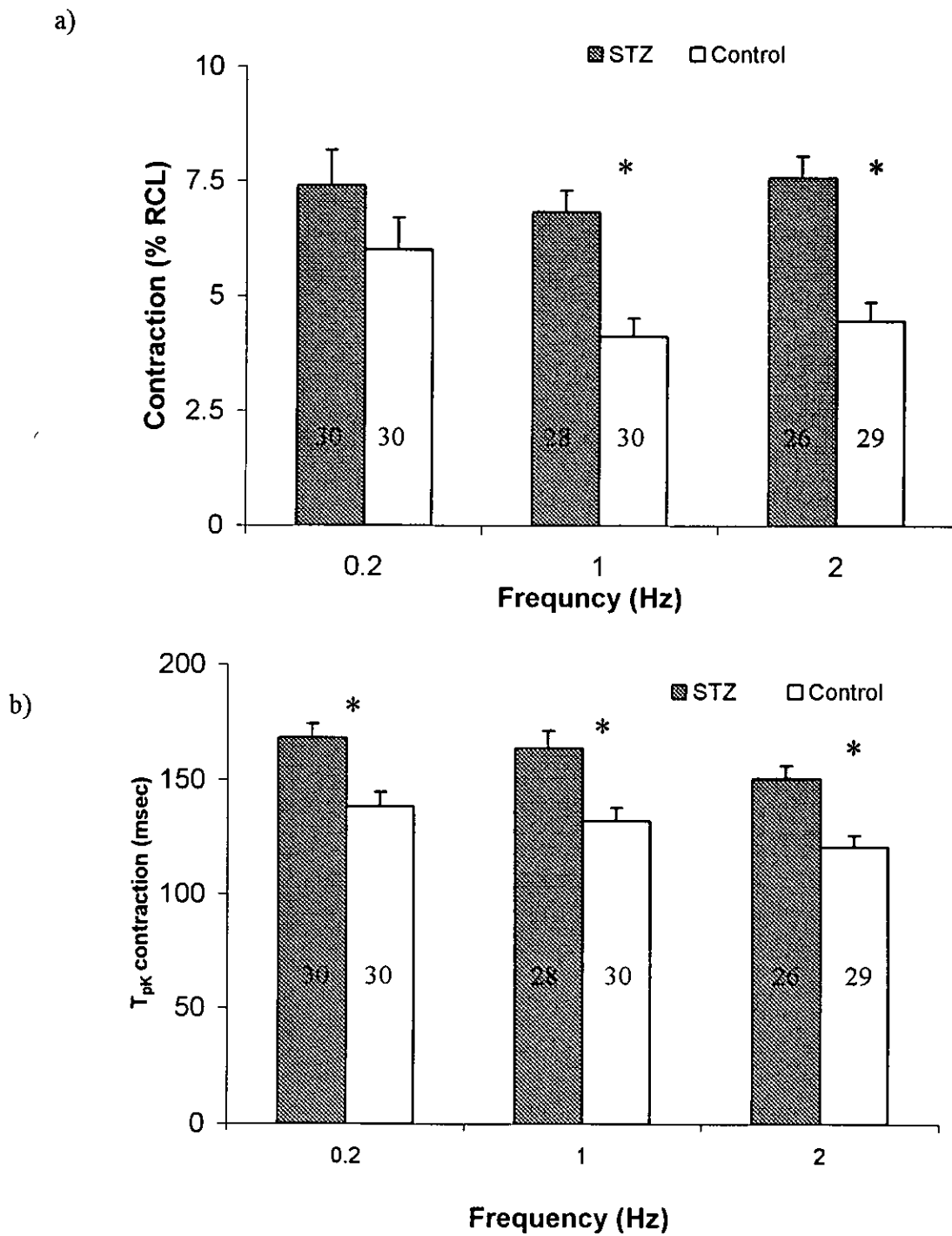


Figure 4.4. Effect of changes in stimulation frequency (0.2, 1 & 2 HZ) on amplitude of contraction (a) and t_{pk} of contraction (b) in control and STZ-induced ventricular myocytes perfused at 35-37°C with a NT solution containing 1 mM Ca^{2+} . Data are mean \pm SEM. Numbers of cells are shown in bars. Cells were obtained from 6-8 diabetic and 6-8 control hearts * $P < 0.05$

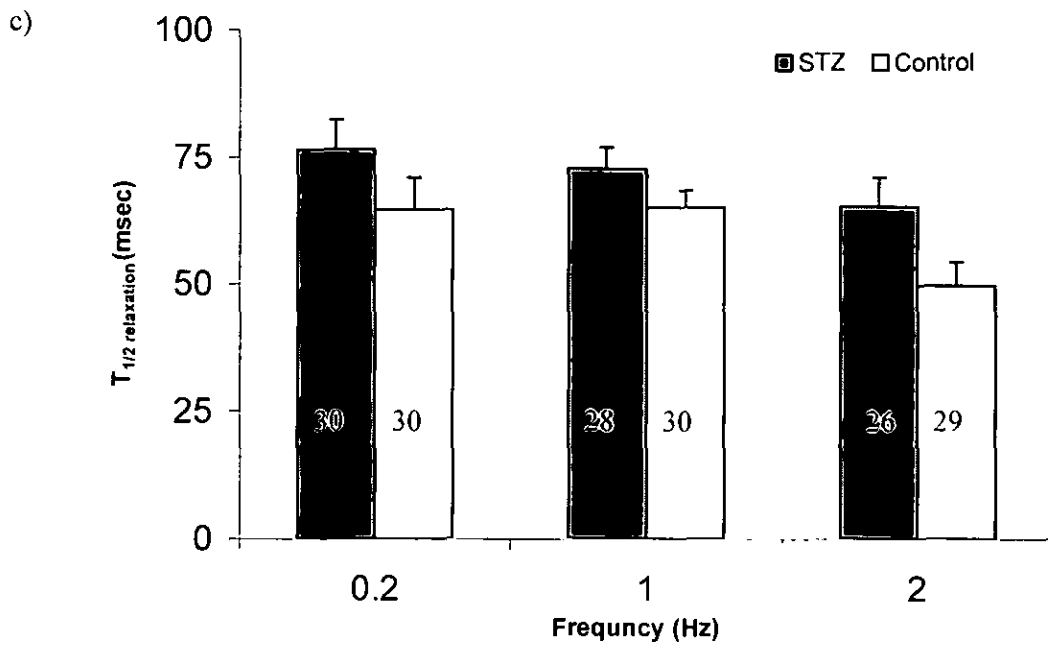


Figure 4.4. Effect of changes in stimulation frequency (0.2, 1 & 2 Hz) on time from peak to half relaxation (c) in control and STZ-induced ventricular myocytes at 35-37°C perfused with a NT solution containing 1 mM Ca^{2+} . Data are mean \pm SEM. Numbers of cells are shown in bars.

4.3.4 Discussion

The results from this study have shown that the amplitude of contraction is significantly greater in STZ-induced diabetic myocytes compared to age-matched control at frequencies of 1 and 2 Hz. However the amplitude of contraction was not significantly different between control and STZ-induced myocytes following 0.2 Hz stimulation. This would indicate that at lower frequencies (0.2 Hz) differences in contractile function are normalized between the control and diabetic heart. In contrast, it has been reported that the amplitude of contraction is significantly reduced in the STZ-induced diabetic myocytes compared to control. Differences in reports may reflect changes in experimental procedures. Within this study, myocytes obtained from 8-12 weeks STZ-induced diabetic hearts did not exhibit either a significantly positive or negative contraction-frequency response. However, in age-matched control myocytes there was significantly negative contraction-frequency response in control myocytes, when stimulation was changed between 0.2 and 1 Hz. Frampton *et al.* (1991), showed that around 40% of isolated ventricular myocytes responded in a negative manner when stimulation was switched from 0.2 Hz – 1Hz. It has been shown that the reduction in contraction that is seen in a negative force-frequency response is coupled with a modest change in the size of the Ca^{2+} transient (Frampton *et al.* 1991). In the rat heart, SR Ca^{2+} is relatively high (Maier *et al.* 2000) which, is due to a predominately strong SERCA pump that mops up the greatest percentage of Ca^{2+} leak from the SR. This is mirrored by a high level of $[\text{Na}^+]_i$ (Shattock & Bers, 1989) that drives $\text{Na}^+/\text{Ca}^{2+}$ -exchanger to reduce Ca^{2+} efflux from the cell. Therefore, when stimulation is increased in cells that respond in a negative manner the SR load is similar, which usually results in a similar release of SR Ca^{2+} . In the diabetic heart, a small change in $[\text{Na}^+]_i$ or/and SR loading may underpin differences between control and diabetic myocytes. The t_{pk} of contraction was significantly longer in the diabetic cells. This observation agrees with other workers who have reported significant increase in t_{pk} at

frequencies ranging from 0.1-5 Hz (Ren & Davidoff, 1997) in myocytes following 8 weeks STZ-treatment. This may reflect binding properties associated with myofilament binding. In this study $t_{1/2\text{ relax}}$ reduced (not to a significant level) in both control and diabetic cells as the stimulation frequencies increased from 0.2 Hz to 1 Hz and from 1Hz to 2 Hz. This is in agreement with Frampton *et al.* (1991), who also reported quicker rates of relaxation as stimulation of frequency was increased. There were however, no significant differences between control and diabetic myocytes, suggesting that the processes that underpin relaxation are not affected by the increase in stimulation frequency between control and diabetic cardiomyocytes.

4.4 Effect of insulin, streptozotocin and perturbation of external calcium concentration on the contractility of streptozotocin-induced diabetic ventricular myocytes.

4.4.1 Introduction

Insulin is a key regulator of the metabolic pathways associated with glucose transport homeostasis, and the synthesis and storage of many carbohydrates, lipids and proteins (Aulbach *et al.* 1999; Ren *et al.* 1999). Insulin also participates in gene expression, ionic flux as well as cell proliferation and apoptosis (Myers, Jr. & White, 1996). In mammalian heart preparations insulin has been reported to exert positive inotropic effect including, increases in left ventricular function, SV, CO, isometric tension, contractility as well as faster relaxation times (Lucchesi *et al.* 1972; Reikeras & Gunnes, 1986; Lee & Downing , 1976; Rieker *et al.* 1975).

This study investigated the effects of exogenous applications of insulin on the contractility of isolated ventricular myocytes from STZ-induced diabetic and age-matched control rat hearts.

4.4.2 Method

See *Chapter 2* for details.

4.4.3 Results

In all figures, unless otherwise stated, relate to 8-12 weeks STZ-induced diabetic ventricular myocytes and age-matched controls. Figure 4.5. shows a typical fast time base recording of a twitch contraction in (a) control, (b) STZ and (c) STZ + insulin treated ventricular myocytes stimulated at 1 Hz. Table 4.1. shows amplitude of the contraction, the t_{pk} of contraction and the $t_{1/2\ relax}$. The t_{pk} myocyte shortening was significantly ($P<0.01$) longer in STZ myocytes and was further prolonged in STZ myocytes that had been incubated with insulin compared with controls (Figure 4.6. b). Insulin had no significant effect on $t_{1/2\ relax}$ (Figure 4.6. c). The amplitude of cell shortening was significantly larger in STZ myocytes and was not significantly affected by exogenous insulin treatment (Figure 4.6. a).

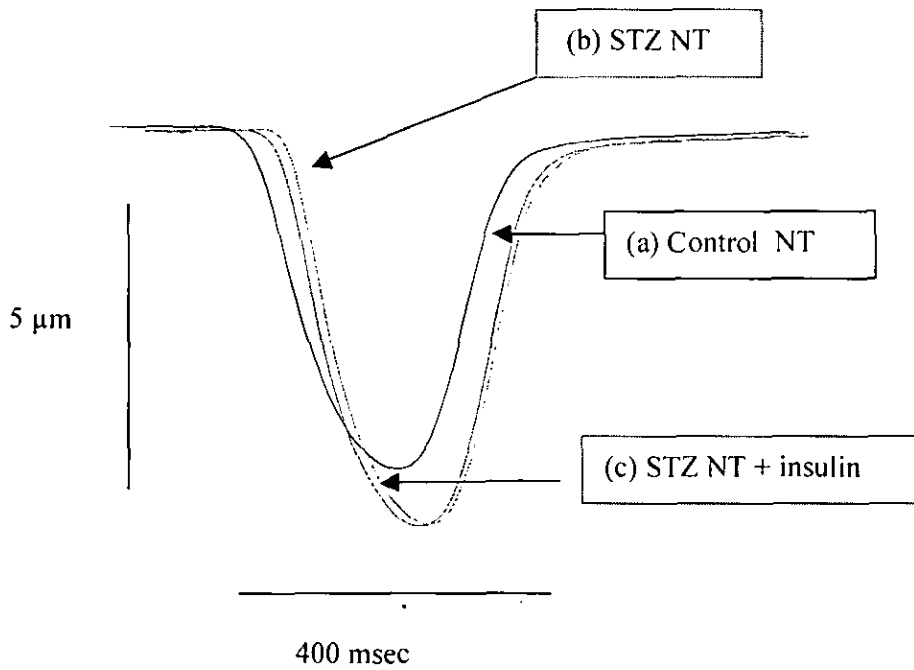


Figure 4.5. Typical fast time base records of shortening in (a) control (NT), (b) STZ (NT) and (c) STZ myocytes incubated and superfused in insulin (1 μM) Cells were stimulated at 1 Hz and perfused at 35-37°C. Traces are typical of 9-15 myocytes from 4-6 hearts

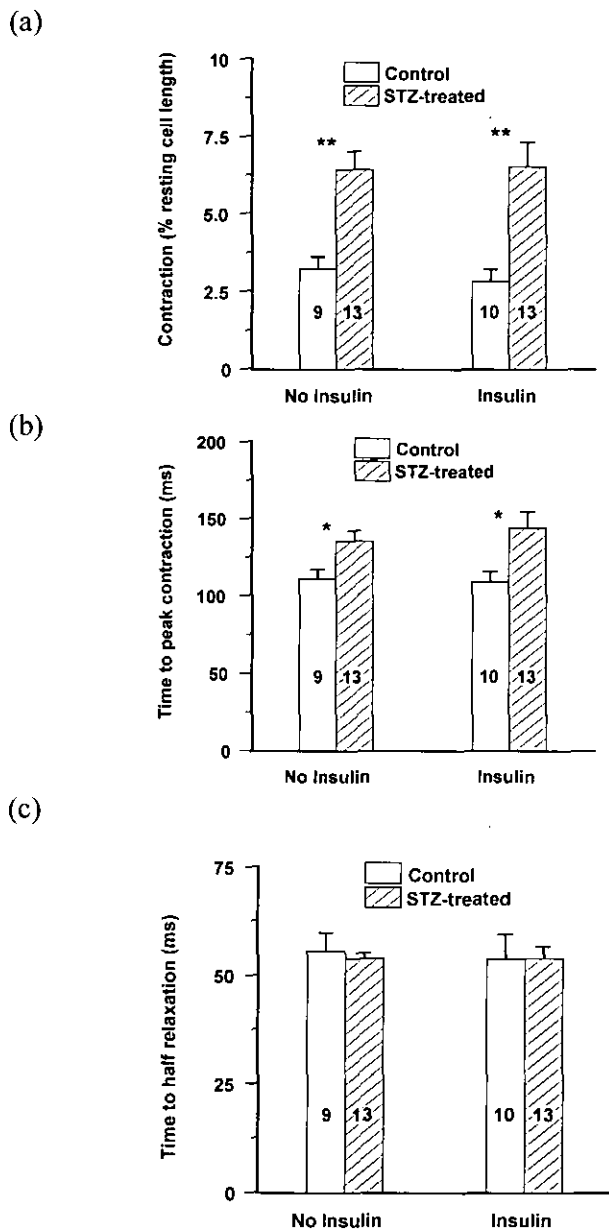


Figure 4.6. The effects of exogenous insulin application ($10 \mu\text{M}$) on (a) the amplitude of contraction, (b) t_{pk} of contraction and (c) $t_{1/2\text{ relax}}$ in ventricular myocytes isolated from age-matched control and STZ-induced diabetic hearts. Data shown are mean \pm SEM. Numbers within bars represent number of cells. Statistical significance showing control *Vs.* STZ using independent samples t-test is represented by * $P < 0.05$ and ** $P < 0.01$

In separate experiments we established that 2-3 h incubation of STZ-induced and control myocytes with exogenous STZ (1×10^{-5} M) had no significant effects on t_{pk} , $t_{1/2\ relax}$ or the amplitude of myocyte shortening.

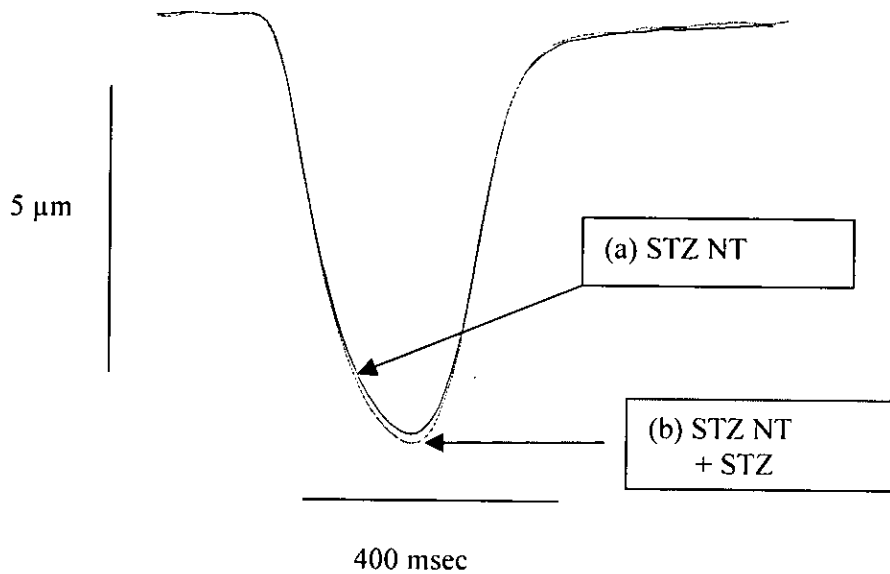


Figure 4.7. Typical fast time base records of shortening in (a) STZ (NT) and (b) STZ incubated in exogenous STZ ($10 \mu\text{M}$) Cells were stimulated at 1 Hz and perfused at $35\text{-}37^\circ\text{C}$. Traces are typical of 9-15 myocytes taken from 4-6 hearts

In a further separate study the effect of perturbation of $[Ca^{2+}]_o$ on the contractility was assessed in control and STZ-induced ventricular myocytes following 8-12 weeks of treatment. Table 4.1 shows the effect of perturbation of $[Ca^{2+}]_o$ on the amplitude of shortening, t_{pk} of contraction and $t_{1/2\ relax}$.

	CNT 0.25 mM $[Ca^{2+}]_o$	STZ 0.25 mM $[Ca^{2+}]_o$	CNT 1 mM $[Ca^{2+}]_o$	STZ 1 mM $[Ca^{2+}]_o$	CNT 2.5 mM $[Ca^{2+}]_o$	CNT 2.5 mM $[Ca^{2+}]_o$
Shortening (% RCL)	2.32±/0.3 (15)	3.1±/0.2 (15)*	5.2±/0.3 (15)	6.9±/0.4 (15)*	10.2±/0.7 (15)	11.9±/0.6 (15)*
t_{pk} contraction	100.2±/ 2.3 (15)	109.6±/ 2.4 (15)*	108.2±/ 3.1 (15)	117.1±/ 2.5 (15)*	115.5±/ 3.8 (15)	125.5±/ 2.1 (15)*
$t_{1/2\ relax}$	47.5±/3.0 (15)	48.0±/2.8 (15)	47.1±/3.6 (15)	43.9±/1.4 (15)	51.9±/3.4 (15)	48.9±/2.3 (15)

Table 4.1. The effects of changes in $[Ca^{2+}]_o$ (0.25, 1, and 2.5 mM) on the amplitude on contraction, t_{pk} of contraction and $t_{1/2\ relax}$ in ventricular myocytes obtained from age-matched control and STZ-induced diabetic rat hearts. Data are means ± S.E.M. Number in parenthesis indicates number of cells. Control *Vs.* STZ was compared using Student's independent samples *t* test and, ANOVA and Bonferroni analysis. * $P < 0.05$.

4.4.4 Discussion

Many studies have reported that daily administration of insulin to diabetic rats reverses the symptoms of the disease and normalises the contractile dysfunction that has been reported in the diabetic hearts (Lee *et al.* 1992; Litwin *et al.* 1990; Tamada *et al.* 1998; Yu *et al.* 1994b; Yu *et al.* 1994a). Therefore, this series of experiments was undertaken to see if the effect of exogenous application of insulin could reverse the contractile dysfunction seen in the STZ-induced hearts at the level of the myocyte. It has been reported that insulin has positive inotropic effect on various cardiac preparations. It has also been shown that myocardial contractility and the amplitude of cardiomyocyte shortening is enhanced in diabetes (Ren *et al.* 1999). This study, has found that insulin, does not significantly affect contractility in diabetic and control myocytes. One possibility for this may lie in the treatment time of the diabetic rats. In this study, diabetes treatment with STZ-treatment was performed for 5 months, while, other reports have utilised myocytes from 5-7 day treated animals (Ren *et al.* 1999). The myocytes used in this particular experiment were isolated and used fresh within 5 hours of isolation, where other reports have used cells that have been in a primary culture for up to 24 hrs (Ren *et al.* 1999). It has been shown that in some cases the contractility of the cardiac myocytes have been irreversibly altered when stored in primary culture (Ellingsen *et al.* 1993). Any such change could affect the results acquired from these cells.

When administered to young adult rats, STZ (60 mg/kg) destroys the insulin producing β -cells of the pancreas and produces symptoms, which include severe insulinopaenia, hyperglycaemia, glycosuria, polydipsia and muscle wasting (features associated with type 1 diabetes) (Bracken *et al.* 2003). In this series of experiments, incubating control and STZ myocytes had no significant effect on the contractility of the cell.

It has been shown in table 4.1 that a increasing the $[Ca^{2+}]_o$ from 0.25 mM to 1 mM to 2.5 mM significantly increases the amplitude of contraction and t_{pk} of contraction in control and STZ-induced ventricular myocytes. However it can be seen that the amplitude of shortening and the t_{pk} of contraction in STZ-induced myocytes is significantly greater compared to that of control myocytes in all the $[Ca^{2+}]_o$ ranges. Table 4.1 also shows that increasing the $[Ca^{2+}]_o$ ranges has no significant effect on the $t_{1/2\ relax}$ in ventricular myocytes obtained from age-matched control and STZ-induced diabetic rat hearts following 8-12 weeks treatment. This study would therefore suggest that changes in the amplitude of contraction and the t_{pk} of contraction that have been reported in this study may not be directly associated with the concentration of $[Ca^{2+}]_o$ and is more likely to be associated with changes in mechanism associated with Ca^{2+} mobilisation.

4.5 Effects of varying glucose concentrations on the kinetics of contraction in ventricular myocytes isolated from streptozotocin-induced diabetic rat heart

4.5.1 Introduction

Following the administration of STZ to young adult rats, after a number of days, whole blood glucose levels rise to a hyperglycemic status, between 20-30 mmol l⁻¹. Chronic hyperglycemia is a potent initiator of diabetic micro vascular complications including retinopathy, neuropath and nephropathy (Sheetz & King, 2002). Hyperglycemia has been linked to the aetiology of a variety of cardiovascular complications, which are associated with the diabetic state (Gerstein 1997; Pacher *et al.* 2002). This is hardly surprising as glucose metabolism and its metabolites contribute to a vast number of cellular pathways. It is however, unclear whether the effects of hyperglycemia are in response to direct toxic effects of glucose including change in oxidants, hyperosmolarity or glycosylation products or if hyperglycemia is directly related to alteration in sustained signaling pathway changes (Sheetz & King, 2002). Increases in glucose concentration in the STZ-induced diabetic heart have been shown to potentiate certain cellular pathways including diacylglycerol (DAG) (Inoguchi *et al.* 1992) and PKC (Kang *et al.* 1999) production. Changes in contractility have also been reported in the isolated STZ-induced diabetic heart, where the perfusion of high glucose concentration caused a significant prolongation of the Q-T (measure of cardiac repolarisation) interval (D'Amico *et al.* 2001).

This series of experiments investigated the effect of high glucose concentration on the contractility in the control and STZ-induced diabetic isolated ventricular myocytes. Altered glucose metabolism may underlie contractile dysfunction that has been reported in the diabetic heart.

4.5.2 Method

See *Chapter 2* for details.

4.5.3 Results

In all figures, unless otherwise stated, relate to 8-12 weeks STZ-induced diabetic ventricular myocytes and age-matched controls. Figure 4.8. shows real time traces of contraction in (a) control and (b) STZ-induced diabetic ventricular myocytes following 8-12 weeks treatment before and after the incubation with glucose (25 mM). The RCL of control and STZ-induced diabetic myocytes was not significantly ($P>0.05$) changed. The amplitude of cell shortening (% of RCL) was significantly ($P<0.05$) increased in the diabetic heart compared to the control ($7.30 \pm 0.59\%$ *Vs.* $4.83 \pm 1.12\%$), respectively with NT solution (Appendix). Following the addition of 25 mM glucose the amplitude of cell shortening in the control myocyte significantly ($P<0.01$) increased ($8.88 \pm 1.38\%$). In contrast, elevated extracellular glucose (25 mM) had no effect on the amplitude of shortening in STZ-induced myocytes (Figure 4.9.c). The rate and t_{pk} of contraction measured was significantly ($P<0.05$) increased in control myocytes following the addition of the high (25 mM) glucose concentration (Figure 4.9.a). The rate of relaxation was significantly ($P<0.05$) increased in control myocytes following the addition of high glucose concentration (25 mM). Changes in glucose concentration did not significantly ($P>0.05$) affect the time course of contraction or relaxation in STZ-induced diabetic myocytes. Osmolarity of the NT solution was 303 ± 5 mosmol kg^{-1} with the addition of 25 mM glucose was 323 ± 5 mosmol kg^{-1} .

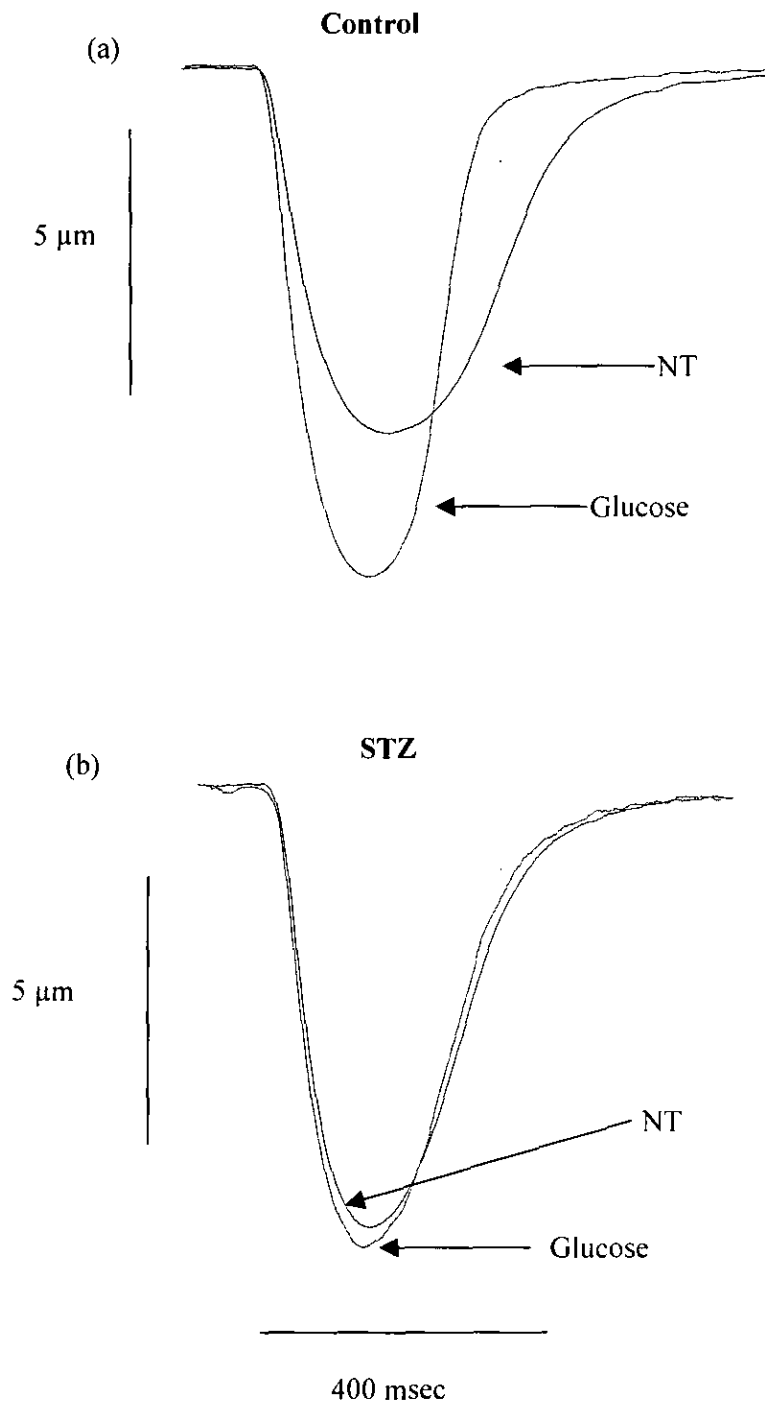


Figure 4.8. Representative real time traces of contraction in (a) control and (b) STZ-induced diabetic ventricular myocytes (Bottom) pre and post incubation with glucose (25 mM) at 35-37°C. Traces are typical of 8 (control) and 22 (STZ) some myocytes from at least 4 different rat hearts.

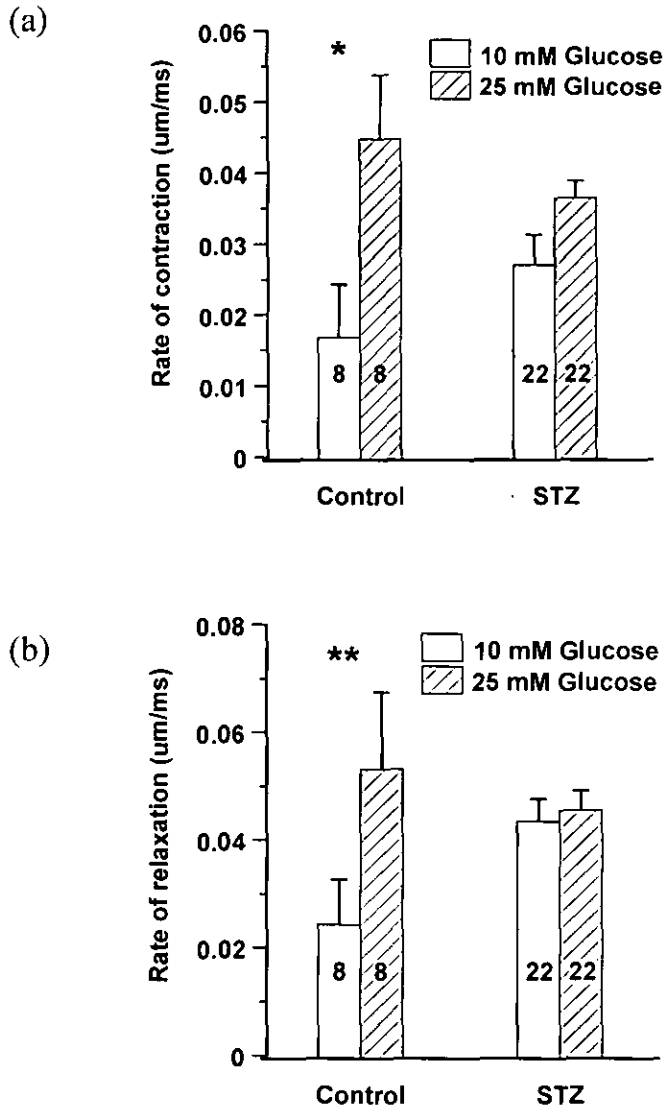


Figure 4.9. Effects of normal and high glucose concentration on (a) the rate of contraction and (b) the rate of relaxation in isolated ventricular myocytes from STZ-induced and age-matched controls at 35-37°C. Data are mean \pm SEM. Numbers of cells are shown in bars. ** $P < 0.01$ * $P < 0.05$.

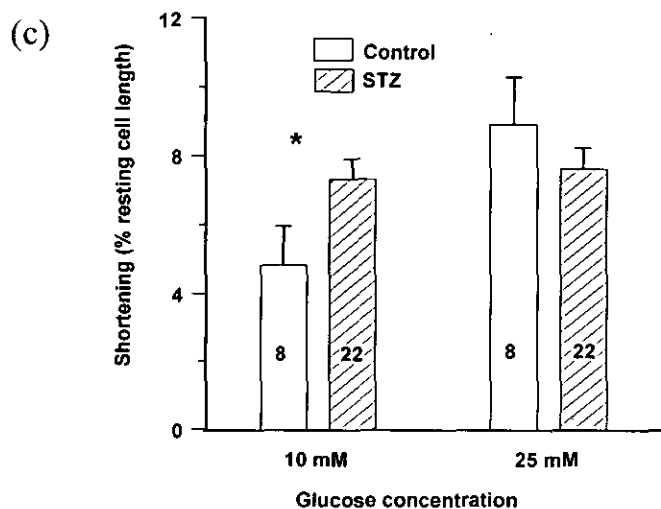


Figure 4.9. Effects of normal and high glucose concentration on (c) amplitude of shortening (% RCL) in isolated ventricular myocytes from STZ-induced and age-matched control hearts at 35-37°C. Data are mean \pm SEM. Numbers of cells are shown in bars. ** $P < 0.01$ * $P < 0.05$.

	<i>Control</i> <i>10mM Glucose</i>	<i>STZ</i> <i>10mM Glucose</i>	<i>Control</i> <i>25 mM Glucose</i>	<i>STZ</i> <i>25 mM Glucose</i>
t_{pk} contraction	167.6 \pm 4.0 (8)	199.6 \pm 7.6 (22)*	212.1 \pm 17.3 (8)a	208.8 \pm 9.4 (22)a
$t_{1/2}$ relaxation	103.8 \pm 8.5 (8)	88.8 \pm 6.3 (22)	95.9 \pm 10.3 (8)	87.6 \pm 5.3 (22)

Table 4.2. The effects of normal (10 mM) and high (25 mM) glucose on the amplitude on contraction, t_{pk} of contraction and $t_{1/2\ relax}$ in ventricular myocytes obtained 8-12 weeks STZ-induced and age-matched control rat hearts. Data are means \pm S.E.M. Number in parenthesis indicates number of cells. Control *Vs.* STZ was compared using Student's independent samples *t* test. * $P < 0.05$.

4.5.4 Discussion

Within this study, it has been previously shown that in control conditions, the amplitude of contraction is significantly increased in the STZ-induced diabetic heart compared to age-matched control. However, following the incubation of control and STZ-induced myocytes in a NT solution containing high glucose (25 mM) (similar to that found in the whole blood chemistry of diabetic rats), the amplitude of shortening and the rate and t_{pk} of contraction was significantly increased in control myocytes, but appeared to be unchanged in STZ-induced diabetic myocytes. In fact following the application of high glucose, control cells exhibited similar amplitude of contraction and t_{pk} of contraction to that observed in the STZ-induced diabetic. The rate of relaxation following the addition of high glucose concentration was significantly increased in control myocytes but had no significant effect in STZ-induced myocytes. This is in agreement with Davidoff and Ren (1997) who reported markedly longer relaxation in control myocytes culture incubated for 4 days in high glucose and low insulin medium. A decrease in Ca^{2+} transient decay was also reported in control myocytes subjected to high glucose and low insulin for 4 days in culture (Davidoff & Ren, 1997). An increase in glucose concentration is mirrored by an increase in Osmolarity. An increase in the osmolarity is associated with cell shrinkage and has reported to lead to a decrease in contraction and an increase in the time of contraction in control and STZ-induced diabetic myocytes (Howarth *et al.* 2001). It is therefore unlikely that the effects of high glucose concentration can be attributable, purely to a change in osmotic effects. One possible explanation for the results seen in this study is that the STZ-induced diabetic myocytes may be more acclimatized or adapted to high levels of glucose, due to the high level of circulating glucose in the blood and therefore they become more sensitized. An increase in the amplitude of contraction is likely to be due to an increase in SR load and subsequent releasable Ca^{2+} from the SR. In a agreement with this, it has been shown that the cytosolic $[Ca^{2+}]_i$ in control cardiac myocytes significant increased following

the incubation of cardiac myocytes in high glucose (30 mM) (Smogorzewski *et al.* (1998). Moreover, the increased response of high glucose was abolished when myocytes were superfused with either low extracellular Ca^{2+} or Ca^{2+} channel blockers, suggesting that increases in $[\text{Ca}^{2+}]_i$ are likely to be associated with a changes in Ca^{2+} influx through $\text{Na}^+/\text{Ca}^{2+}$ -exchanger or L-type Ca^{2+} channels. It has also been reported that control cells incubated with a high glucose concentration had significantly longer Ap duration's compared to control (Ren *et al.* (1997). Prolonged Ap's have been reported in STZ-induced diabetic myocytes following 8 weeks treatment (Magyar *et al.* 1992), probably through a decrease in I_{to} (Jourdan & Feuvray, 1993). In the STZ-induced diabetics heart it has been shown that the expression and activity of PKC is significantly increased compared to control (Liu *et al.* 1999; Kang *et al.* 1999; Guo *et al.* 2003). Moreover it is known that PKC inhibits the I_{Kto} , (Ren *et al.* 1997). This suggests that in the STZ-induced diabetic heart, hyperglycaemia may increase PKC activity, which may lead to increased Ap duration. However, it is suggested that in control myocytes a transient application high glucose is unlikely to alter expressional changes of PKC and it is therefore more likely that increases in $[\text{Ca}^{2+}]_i$ may increase SR load and subsequent SR Ca^{2+} release, which may lead to an increase in contraction.

4.6 Regional differences in the streptozotocin –induced diabetic heart

4.6.1 Introduction

The heart is made up of a variety of specific myocardial cells according to their position and electrical properties. The largest portion of the heart, the left ventricle largely governs the contractile propulsion of blood around the body in a heartbeat (Katz, 1977). The plateau phase of an Ap in ventricular cells of the heart is far longer than in other areas including the atria. The reason for this is two fold, firstly it prevents the re-excitation of another Ap, by prolonging the depolarised membrane and therefore inactivating the Na⁺ and Ca²⁺ channels on the cell membrane, thus not allowing any tetanic twitch effects that can be seen in skeletal muscle. Secondly, it allows the heart to relax, so that the ventricles can be filled with blood for the next heart beat (Bers, 2002a). The three main regions within the ventricle are the epi, endo and myocardium. The regions differ according to their differential ion channel expression, which in turn leads to a differential in electrical properties that is seen in a typical action potential. The plateau phase of the ventricular Ap is shortest in the epi cells, increased in the endo cells and longest still in the myocardial cells.

The aim of this study was to ascertain if STZ-induced diabetes effects regional specificity within the ventricle from the endo and epi portions of the ventricle. Any changes in contractile characteristics seen in specific regions of the heart may underpin alterations of contractile characteristics that have been reported in the diabetic heart.

4.6.2 Method

See *Chapter 2* for details.

4.6.3 Results

In all figures, unless otherwise stated, relate to 8-12 weeks STZ-induced diabetic ventricular myocytes and age-matched controls. Figure 4.10 shows (a) cell shortening, (b) t_{pk} of contraction and (c) $t_{1/2\ relax}$ relaxation in endo and epi cell taken from STZ-induced diabetic and age-matched control hearts following 8-12 weeks treatment. Cell shortening as a % of RCL was not significant ($P>0.05$) altered between in endo and epi cardiac cells in control ($5.94 \pm 0.42\%$ Vs. $6.46 \pm 0.59\%$), respectively and STZ-induced ($6.59 \pm 0.5\%$ Vs. $6.22 \pm 0.35\%$) diabetic hearts and comparing endo and epi cells with diabetic counterparts (Figure 4.6.a).

The t_{pk} of contraction was significantly ($P<0.05$) longer in endo compared to epi cells in age-matched control heart, respectively ($103.5 \pm 3.1\text{ ms}$ Vs. $94.1 \pm 2.76\text{ ms}$). Moreover, endo ($137 \pm 4.32\text{ ms}$ Vs. $103.5 \pm 3.1\text{ ms}$) and epi ($139.6 \pm 5.2\text{ ms}$ Vs. $94.1 \pm 2.76\text{ ms}$) myocytes from STZ-induced hearts were significantly ($P>0.01$) longer than age-matched control, respectively, however, there was no significant ($P>0.05$) difference between t_{pk} of endo and epi cells in STZ-induced hearts (Figure 4.6.b).

The $t_{1/2\ relax}$ was significantly ($P>0.05$) increased in endo compared with epi cells in control ($48.1 \pm 2.54\text{ ms}$ Vs. $40.7 \pm 1.51\text{ ms}$) and STZ-induced cells ($52.3 \pm 2.66\text{ ms}$ Vs. $45.1 \pm 1.80\text{ ms}$) respectively, however, there was no significant ($P>0.05$) difference in the $t_{1/2\ relax}$ between control and STZ-induced epi and endo cells (Figure 4.6.c).

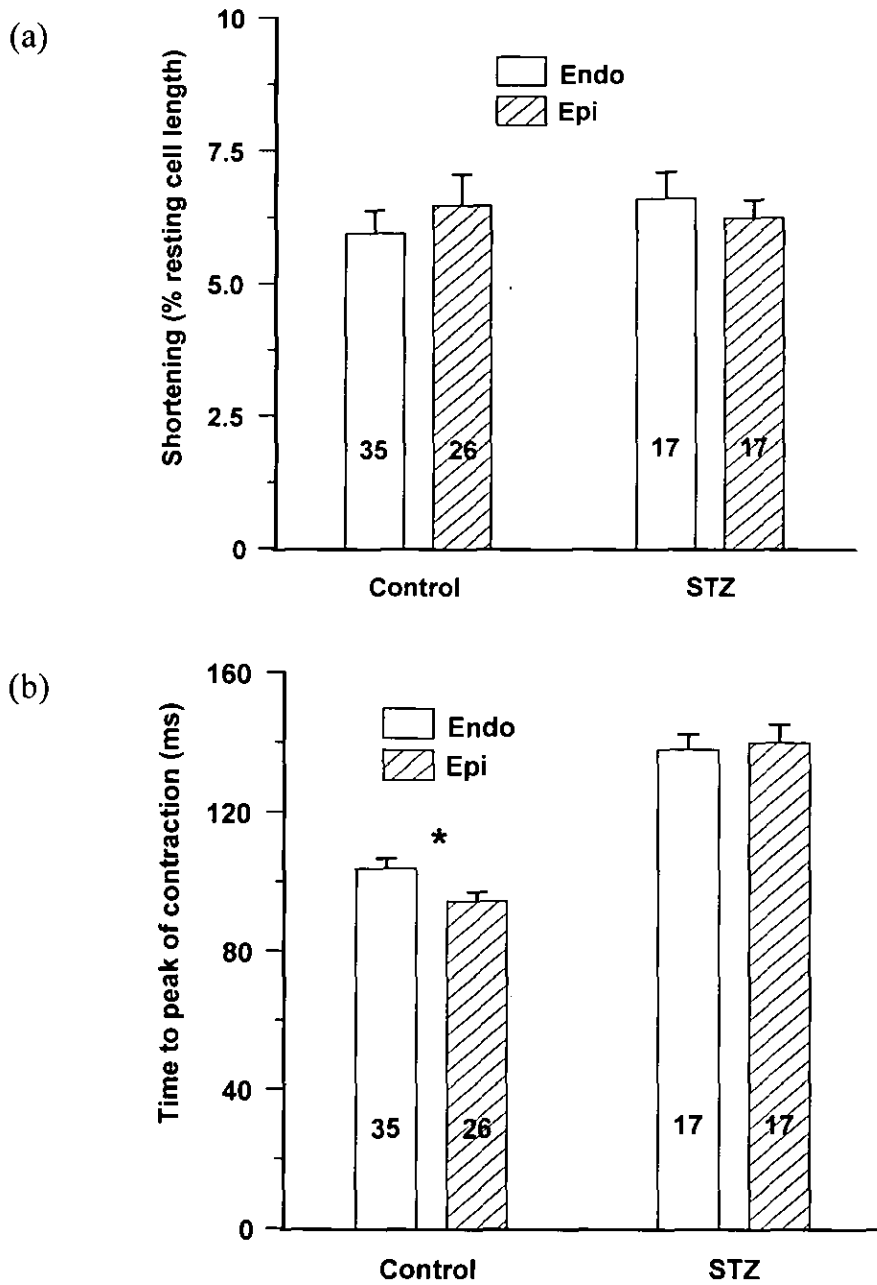
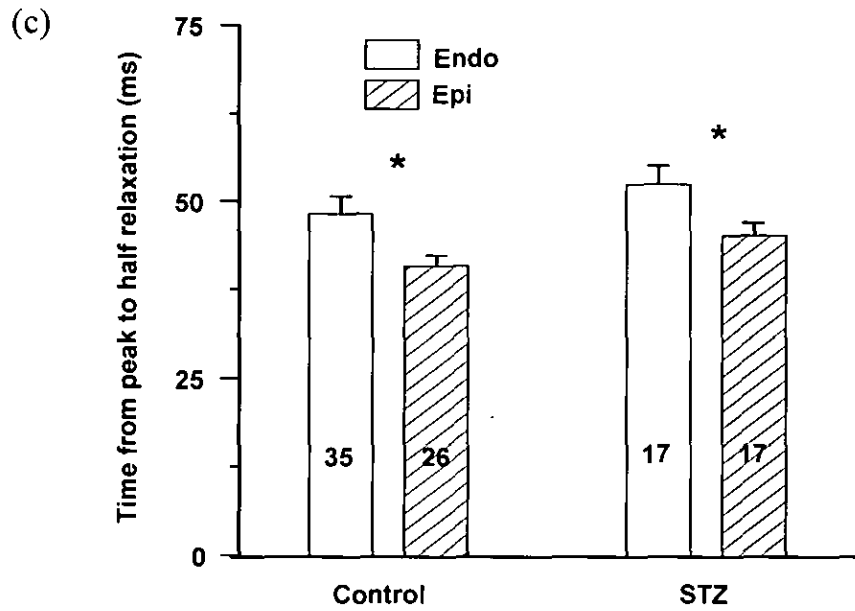


Figure 4.10. Regional specific changes in contractile characteristics of control and STZ-induced diabetic following 8-12 weeks treatment on shortening (a) and time to peak of contraction (b) in isolated endo and epi myocytes at 35-37°C perfused with a NT solution containing 1 mM Ca^{2+} . Cells from age-matched control myocytes are also shown for comparison. Data are mean \pm SEM. Numbers of cells are shown in bars. Cells were obtained from 10-12 hearts. *



4.10.c. Regional specific changes in contractile characteristics of control and STZ-induced diabetic from peak to half relaxation in isolated endo and epi myocytes at 35-37°C perfused with a NT solution containing 1 mM Ca^{2+} . Control myocytes are also shown in figure 4.6.c for comparison. Data are mean \pm SEM. Numbers of cells are shown in bars. Cells were obtained from 10-12 hearts. * $P < 0.05$.

4.6.4 Discussion

Cell shortening as a % of RCL was not significantly altered between epi and endo myocytes in control and diabetic hearts. This is agreement with other workers who found no difference in the shortening of control and diabetic hearts (Tamada *et al.* 1998; Ishitani *et al.* 2001). Moreover, it has also been reported that there were no significant changes in peak amplitude between endo and epi myocytes (Bryant *et al.* 1997). Results presented in this chapter have shown that there is an increase in shortening in STZ-induced myocytes. Hence, it is apparent that both epi and endo cells are not affected by diabetes. The t_{pk} of contraction was significantly longer in endo cells from control heart, but not in the diabetic heart. However, STZ-induced diabetes significantly increased the t_{pk} in both endo and epi cells compared to control. This observation suggests that the rate at which Ca^{2+} is released from the RyR is longer than in normal endo cells. Moreover, the Ap plateau is longer in the endo cells, so therefore it may be suggested that increased Ap plateau contributes to a slower sustained release trigger for Ca^{2+} from the SR. The increase in t_{pk} in the diabetic heart is in agreement with other workers (Choi *et al.* 2002; Yu *et al.* 1994a) who have also reported similar findings. This suggests that the transport mechanisms that contribute to the speed of contraction are affected in diabetes. Alteration in t_{pk} of contraction may be associated with either a change in SR Ca^{2+} release or a change in triggered Ca^{2+} induced SR Ca^{2+} release. The $t_{1/2\ relax}$ was increased in endo compared to epi cells in control and diabetic heart but this was not altered between groups. This may well be associated with a longer Ap that has been reported in the endo heart cells. Moreover, it can be seen from the present results that diabetes has no significant effect on the $t_{1/2\ relax}$, which, is in agreement with other workers (Howarth *et al.* 2000).

Overall regional differences in the age-matched control and diabetic hearts may contribute to changes in the speed of contraction and relaxation. Moreover, this study has shown that

STZ-induced diabetes abolishes the speed of contraction in the heart, and this in turn may be associated with contractile abnormalities that have been reported in the diabetic heart (Choi *et al.* 2002)

4.7 Conclusion

Contraction as a percentage of RCL length was significantly increased in diabetic myocytes. This may be due to altered sensitivity of Ca^{2+} to myosin activation or an increase in the available Ca^{2+} during the Ca^{2+} transient within systole. Although a slower Ca^{2+} transient in acute type 1 STZ-induced cardiomyocytes has been reported (Ren & Davidoff, 1997), other workers have observed little or no significant differences in the characteristics of the Ca^{2+} transient (Tamada *et al.* 1998). The amount of Ca^{2+} released by the SR is thought to be graded and dependent upon the amount of trigger Ca^{2+} entering the cardiac cell via the single L-type channel and possibly through the $\text{Na}^+/\text{Ca}^{2+}$ -exchanger operating in reverse mode (Levi *et al.* 1993b). Defects in the mechanisms which are involved in Ca^{2+} transport including sarcolemmal PMCA, L-type Ca^{2+} channels, $\text{Na}^+/\text{Ca}^{2+}$ -exchanger or SR Ca^{2+} uptake or release mechanisms, may have significant effects on contractile function of heart muscle. The t_{pk} of contraction was longer in diabetic cells with STZ treatment. A reduction in $I_{\text{Ca,L}}$ and/or SR Ca^{2+} release may underlie the increase of t_{pk} of contraction. However, it has been reported that the $I_{\text{Ca,L}}$ is not effected after STZ-treatment (Schneider & Sperelakis, 1975; Tamada *et al.* 1998). The $t_{1/2\text{ relax}}$ was not altered significantly within the STZ-induced myocytes. Any alterations in the removal of Ca^{2+} by the $\text{Na}^+/\text{Ca}^{2+}$ -exchanger or by increased uptake of Ca^{2+} through the Ca^{2+} -ATPase pump back into the SR would alter $[\text{Ca}^{2+}]_i$ within diastole.

Chapter 5

Effects of streptozotocin-induced diabetes on calcium homeostasis in rat cardiomyocytes

5.1 General introduction

The homeostatic control of $[Ca^{2+}]_i$ is crucial in the management of contraction and relaxation in the heart. Ca^{2+} homeostasis is regulated by mechanisms associated with Ca^{2+} transport into and out of the cell and its intracellular compartments (Bers, 2002). If this equilibrium is unaltered the heart is capable of normal contraction and relaxation. However, if any of the mechanisms are impinged, a state of imbalance can arise, which can ultimately lead to an alteration in the contractile kinetics of the cell. In order to measure the specific mechanisms involved in Ca^{2+} homeostasis it is necessary to measure the amounts of $[Ca^{2+}]_i$ at any given point in the contraction/relaxation process. In recent years many indicators (including fura and indo) have been manufactured that enable the worker to ascertain the relative amounts on $[Ca^{2+}]_i$.

Following depolarisation of the cardiac cell, the L-type Ca^{2+} channels open, leading to a small influx of Ca^{2+} into the cell. Ca^{2+} influx contributes to the increased probability of RyR opening, which leads to SR Ca^{2+} release and a Ca^{2+} transient (Fabiato, 1983). The release of SR Ca^{2+} is graded and dependent upon triggered stimulation from the Ca^{2+} influx (Fabiato 1983). When the SR releases Ca^{2+} there is a transient rise of $[Ca^{2+}]_i$ from resting levels of around 60-100 nmol l⁻¹ to 600-1000 nmol l⁻¹ (Cannell *et al.* 1987b). An elevation in $[Ca^{2+}]_i$ following SR Ca^{2+} release increases the probability of myofilament sensitive sites to alter functional properties, which results in the induction of contraction (Bers, 2002a). A decrease in Ca^{2+} in the repolarisation phase induces the decrease in $[Ca^{2+}]_i$ and the dissociation of Ca^{2+} away from the myofilaments. The same amount of Ca^{2+} entering the cell during L- type channel opening and SR Ca^{2+} release must either be taken out of the cell or pumped back into the SR leading to relaxation. Any changes in these mechanisms

may contribute to derangement in the E-C coupling process and this in turn can lead to a diseased state.

The effects of type I diabetes on the levels of diastolic $[Ca^{2+}]_i$ are still unclear. It has been reported that diastolic $[Ca^{2+}]_i$ is either reduced or unchanged. Significant reductions (approx. 52%) in diastolic levels of $[Ca^{2+}]_i$ in type I diabetic heart cells have been reported (Lagadic-Gossmann *et al.* 1996; Hayashi & Noda, 1997; Noda *et al.* 1992). However, in another report Yu *et al.* (1995), reported no significant changes in diastolic $[Ca^{2+}]_i$ between, type I diabetic and control cardiomyocytes. The effects of diabetes on systolic $[Ca^{2+}]_i$ in ventricular myocytes obtained from type I diabetic hearts are not well understood. It has been reported that the peak systolic Ca^{2+} transient was reduced in type I STZ-induced rat cardiomyocytes by 43 % compared to control (Lagadic-Gossmann *et al.* 1996), while other reports have observed little or no significant differences in the characteristics of the Ca^{2+} transient obtained diabetic hearts (Tamada *et al.* 1998). Many of these discrepancies may be due to several factors including; varied nature of the experimental protocols and in particular, treatment time of the STZ-induction, the type of fluorescence indicator employed in the study and the temperature at which experiments were carried out.

This study was designed mainly to investigate Ca^{2+} homeostasis in the STZ-induced diabetic and age-matched control ventricular cardiomyocytes.

5.2 *Effect of perturbation of extracellular calcium on calcium transients in the streptozotocin induced ventricular myocytes in the diabetic heart*

5.2.1 *Introduction*

The amount of Ca^{2+} entering the cell, during cell depolarisation acts as a trigger for SR Ca^{2+} release (Fabiato, 1983). A model for CICR was initially described by Fabiato *et al.*, (1983), showing how free Ca^{2+} can trigger SR Ca^{2+} release from skinned cardiac myocytes (Fabiato, 1983). In the presence of high free extracellular Ca^{2+} ($[\text{Ca}^{2+}]_o$) the trigger for SR Ca^{2+} is diminished or inhibited due to the specific binding attributes of Ca^{2+} on RyR (Fabiato 1985). The RyR has two binding sites, a fast low affinity site and a slow high affinity site. If Ca^{2+} binds to the fast sites the channel is activated and allows SR Ca^{2+} release, however, if the high affinity site is occupied then the channel becomes deactivated and reduces Ca^{2+} release (Fabiato 1985). Therefore, altering extracellular Ca^{2+} below or above the physiological standard may change the binding and release parameters of Ca^{2+} from the SR. It may then be possible to study the affects this has on the control and diabetic heart.

The aim of this section of the study was to investigate the effects of $[\text{Ca}^{2+}]_o$ on Ca^{2+} handling in the diabetic heart. To pin point any dysfunction, the amplitude (peak ratio minus resting ratio), t_{pk} and $t_{1/2}$ decay of Ca^{2+} transient were recorded and analysed.

5.2.2 *Method*

See *chapter 2* for details.

5.2.3 Results

In all figures, unless otherwise stated, relate to 8-12 weeks STZ-induced diabetic ventricular myocytes and age-matched controls. Figure 5.1. shows typical Ca^{2+} transients recorded in control and STZ-induced ventricular myocytes, perfused with (a), 0.25 mM $[\text{Ca}^{2+}]_o$, (b), 1 mM $[\text{Ca}^{2+}]_o$ and (c) 5 mM $[\text{Ca}^{2+}]_o$. Ventricular myocytes isolated from 8-12 week STZ-induced diabetic hearts and age-matched controls were superfused with a NT solution containing 1 mM $[\text{Ca}^{2+}]_o$. Subsequent Ca^{2+} transients were recorded during the application of electrical stimulation at 1 Hz. In some cells a rapid solution switcher was used to change $[\text{Ca}^{2+}]_o$ (0.25, 1, and 5 mM) throughout the experiment. Figure 5.2. shows (a) the amplitude of the Ca^{2+} transient (ratio units), (b) the t_{pk} of the Ca^{2+} transient, and (c) the $t_{1/2}$ decay of Ca^{2+} transient in age-matched control and STZ-induced myocytes with differing $[\text{Ca}^{2+}]_o$. Basal resting Ca^{2+} (measure by fluorescence ratio units) was significantly ($P < 0.01$) increased in STZ-induced diabetic myocytes following 8 weeks of treatment compared to control (0.599 ± 0.009 ratio units, $n=23$ Vs. 0.521 ± 0.012 ratio units), respectively. The amplitude of Ca^{2+} release from the SR, induced by electrical stimulation was not significantly ($P > 0.05$) different between control and STZ-induced myocytes in the presence of different concentrations of $[\text{Ca}^{2+}]_o$. There was however, a significant ($P < 0.05$, ANOVA and Bonferroni) difference between the amplitude of Ca^{2+} release seen in the STZ-induced myocytes superfused with 0.25 mM Ca^{2+} and 1 mM Ca^{2+} . The t_{pk} of Ca^{2+} transient was not significantly ($P > 0.05$) altered between control and diabetic myocytes in each group, nor was it significantly ($P > 0.05$) different between groups of cells (ANOVA). The decay of the Ca^{2+} transient was significantly longer in STZ myocytes perfused with 0.25 mM $[\text{Ca}^{2+}]_o$ ($P < 0.01$), 1 $[\text{Ca}^{2+}]_o$ ($P < 0.05$) and 5 mM $[\text{Ca}^{2+}]_o$ ($P < 0.05$). However, there were no significant ($P > 0.05$) differences in control and STZ-induced diabetic groups (ANOVA-Bonferroni).

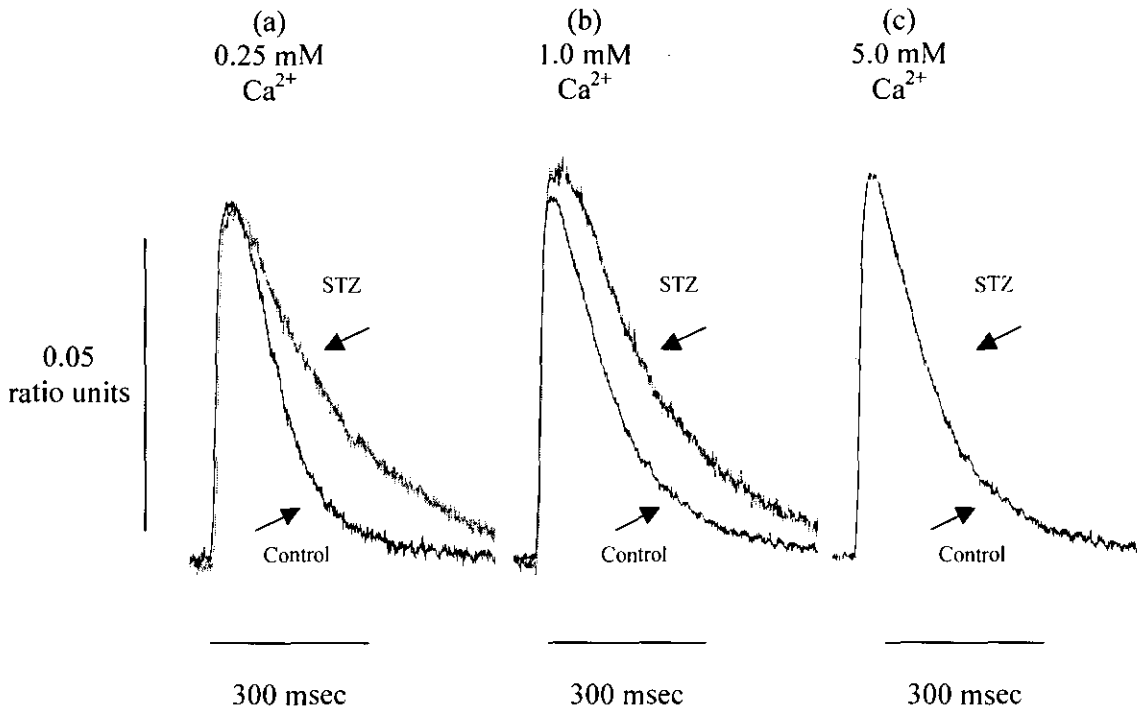


Figure 5.1. The effects of perturbation of extracellular calcium concentration (a) 0.25 mM, (b) 1 mM, and (c) 5 mM on electrically stimulated (1 Hz) Ca^{2+} transients in ventricular myocytes isolated from age-matched control and STZ-induced diabetic rat hearts at 35-37 °C. Traces are typical of 10-20 such myocytes obtained from 6-8 hearts.

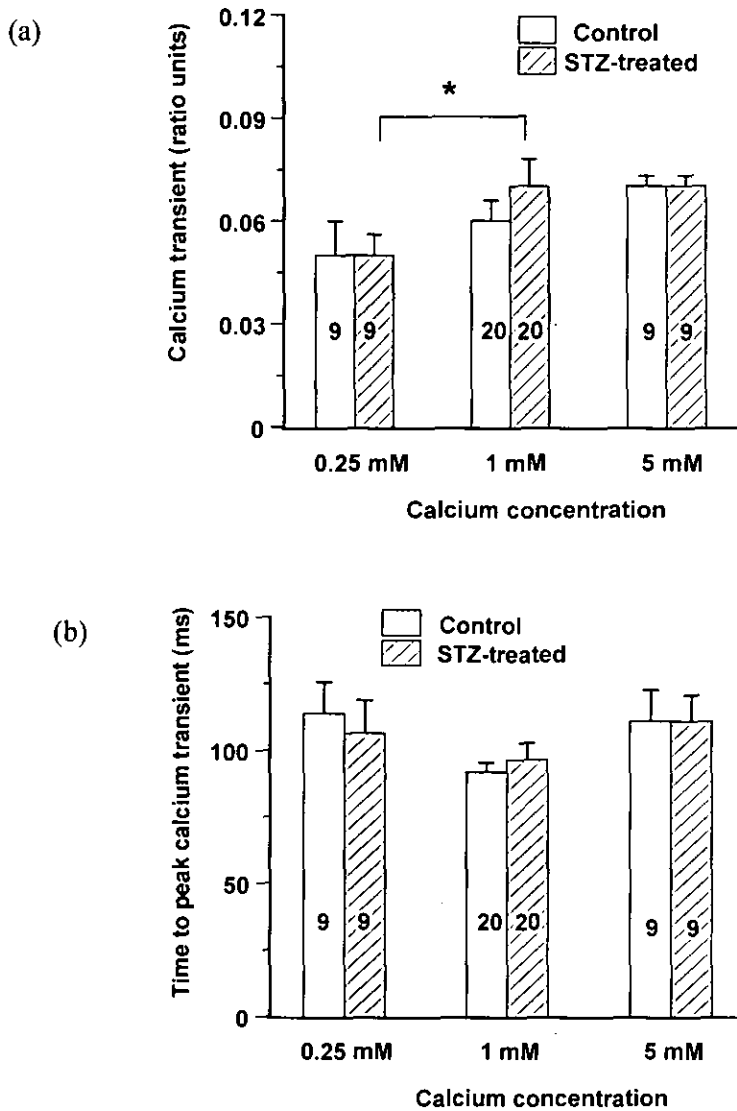


Figure 5.2. The effects of changes in $[Ca^{2+}]_o$ (0.25, 1, and 5 mM) on, (a) amplitude of the Ca^{2+} transient (ratio units) and (b) t_{pk} of Ca^{2+} transient in ventricular myocytes isolated from age-matched control and STZ-induced diabetic rat hearts. Data are means \pm S.E.M. Number in bars indicates number of cells. Control *Vs.* STZ was compared using Student's independent samples *t* test and, ANOVA and Bonferroni analysis. * $P < 0.05$.

(c)

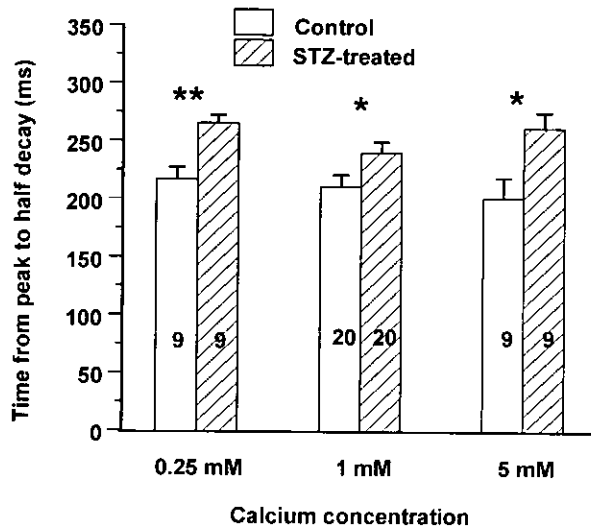


Figure 5.2. The effects of changes in $[Ca^{2+}]_o$ (0.25, 1, and 5 mM) on, (C) $t_{1/2}$ decay of Ca^{2+} transient in ventricular myocytes isolated from age-matched control and STZ-induced diabetic rat hearts. Data are means \pm S.E.M. Number in bars indicates number of cells. Control *Vs.* STZ was compared using Student's independent samples *t* test and, ANOVA and Bonferroni analysis. * $P < 0.05$, ** $P < 0.01$.

5.2.4 Discussion

It has been shown within this report, that contractility is deranged in the experimentally induced diabetic heart. It is envisaged that an alteration in Ca^{2+} handling within the cardiomyocyte is responsible for this change in contractility. The effects of diabetes on systolic $[\text{Ca}^{2+}]_i$ in ventricular myocytes obtained from type 1 diabetic hearts are still somewhat unclear and contradictory. The amplitude of Ca^{2+} release and the t_{pk} of the Ca^{2+} transient in electrically stimulated (1 Hz) ventricular myocytes were not significantly altered at varying concentrations of $[\text{Ca}^{2+}]_o$ in 8-12 week STZ-induced diabetic ventricular myocytes. This is in agreement with Tamada *et al.* (1998), who observed little or no significant differences in the characteristics of the Ca^{2+} transient from diabetic hearts compared to control. However, this study has shown that an increase in $[\text{Ca}^{2+}]_o$ from a low (0.25 mM) up to normal (1 mM), significantly increased the amplitude of Ca^{2+} transient in STZ-induced diabetic myocytes. This observation suggests that an elevation in external Ca^{2+} from 0.25 mM to 1 mM in the diabetic myocyte may contribute to a greater amount of trigger Ca^{2+} , which, may ultimately lead to a greater fractional release of Ca^{2+} from the SR compared to control. The diabetic heart, therefore, may be more sensitive to changes in extracellular Ca^{2+} compared to the control heart. It is worth noting that the amplitude of the Ca^{2+} transient in the presence of 5mM $[\text{Ca}^{2+}]_o$ was similar to that observed when perfusing with 1 mM $[\text{Ca}^{2+}]_o$. It is likely, in this case, that the high (5 mM) $[\text{Ca}^{2+}]_o$ may have saturated the internal system, as it would be expected that a 5 fold increase (compared to 1 mM $[\text{Ca}^{2+}]_o$) in $[\text{Ca}^{2+}]_o$ would have significantly increased increase the amplitude of the Ca^{2+} transient. Moreover, the amplitude of contraction was significantly increased in both diabetic and control myocytes when perfusing with 2.5 mM $[\text{Ca}^{2+}]_o$ when compared to the amplitude of contraction in myocytes perfused with 1 mM $[\text{Ca}^{2+}]_o$ (Table 4.1.). This study

it has also demonstrated that the basal level of Ca^{2+} is increased in the diabetic heart. Increased levels of basal Ca^{2+} would increase available Ca^{2+} for contraction. Resting Ca^{2+} is governed mainly by the $\text{Na}^+/\text{Ca}^{2+}$ -exchanger. If this transport mechanism were corrupt, or if $[\text{Na}^+]_i$ was high, it would benefit Ca^{2+} influx and may lead to an increase in basal Ca^{2+} . The decay of the Ca^{2+} transient measured from the $t_{1/2}$ decay is longer in diabetic cells superfused with Ca^{2+} (0.25, 1 and 5 mM) compared to control cells. This is in agreement with other workers who have also shown a slower decay of Ca^{2+} transient in type 1 STZ-induced ventricular myocytes (Lagadic-Gossmann *et al.* 1996; Kotsanas *et al.* 2000; Choi *et al.* 2002; Ren & Davidoff, 1997; Ha *et al.* 1999). A slower decay in Ca^{2+} transient is likely to be caused by a discrepancy in the homeostatic control mechanisms within the cell. It appears likely that either, the SERCA pump situated on the SR membrane (or one of its components) and/or the $\text{Na}^+/\text{Ca}^{2+}$ -exchanger on the sarcolemmal membrane is disrupted in the diseased state. This would result in a reduced amount of Ca^{2+} being taken up by the SR and out of the cell through the $\text{Na}^+/\text{Ca}^{2+}$ -exchanger. The consequence of this would be a greater amount of Ca^{2+} within the cytosol in diastole, which has been reported in this study.

5.3 Time dependent effects of STZ-induced diabetes

The aim of this part of the study was to investigate whether, the contractile changes that have been reported (chapter 4) in 4 weeks STZ-induced diabetic is a consequence of altered Ca^{2+} homeostasis as early as 4 week post injection.

5.3.1 Results

Figure 5.3. shows a typical Ca^{2+} transient following 4 weeks STZ-treatment and age-matched controls in electrically stimulated (1 Hz) ventricular myocytes (bottom). Basal, resting Ca^{2+} (measured by fluorescence ratio units) was significantly ($P < 0.01$) increased in

STZ-induced diabetic myocytes following 4 weeks of treatment compared to control (0.738 ± 0.017 ratio units, $n=10$ Vs. 0.472 ± 0.07 ratio units, $n=10$), respectively. The amplitude and t_{pk} of Ca^{2+} transient were not significantly ($P>0.05$) altered in 4-week STZ-induced diabetic myocytes compared to control. However, the decay of the Ca^{2+} transient measured as the rate of ratio units/sec was significantly ($P<0.05$) longer in the diabetic myocytes versus control (Figure 5.4). Moreover, there was no significant difference between STZ-induced myocytes following 4 and 8-12 weeks treatment of STZ (Figure 5.5).

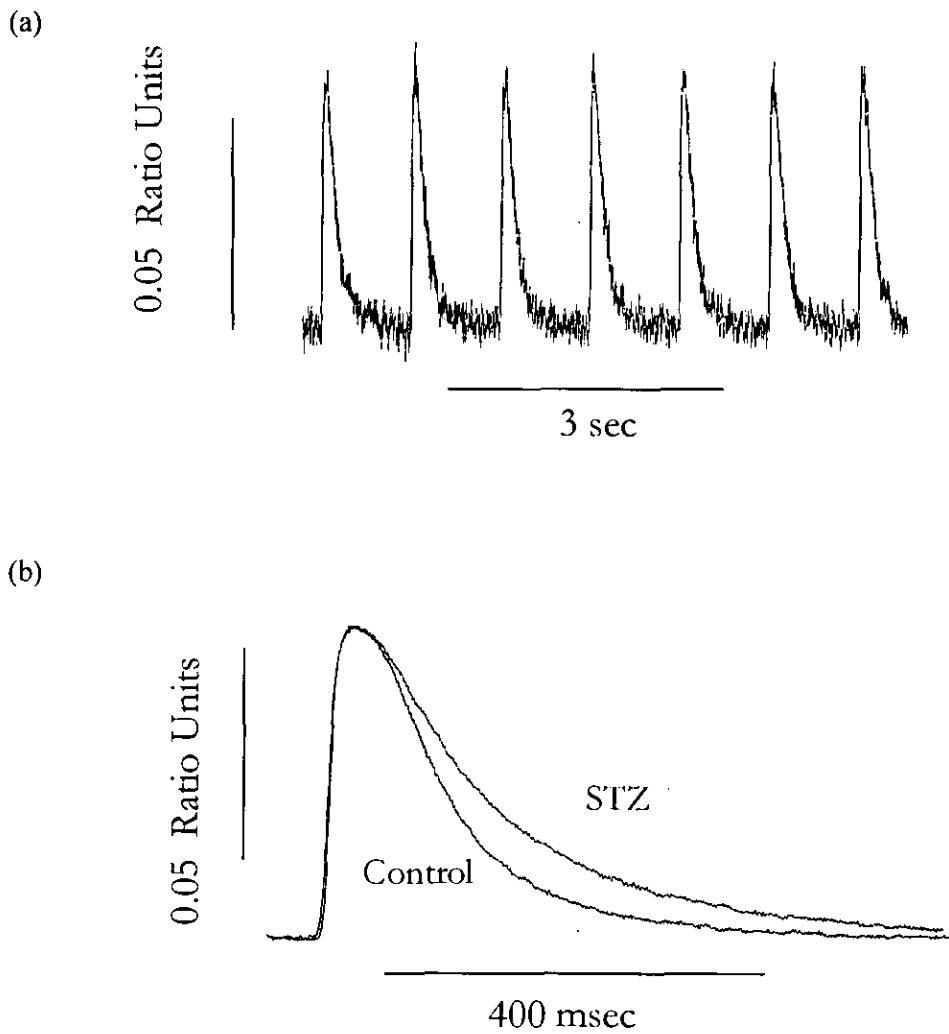


Figure 5.3 Fast time base recordings of a train (a) and a single extrapolated Ca^{2+} transient (b) in electrically stimulated (1 Hz) ventricular myocytes isolated from age-matched control and STZ-induced diabetic rat hearts. Cells were superfused with a NT solution (1 mM Ca^{2+}) at 35–37 °C. Traces are typical of 7-10 such myocytes obtained from 3-5 hearts

Table 5.1. The effects of 4 and 8-12 weeks STZ-induced diabetes on Ca^{2+} homeostasis in ventricular myocytes stimulated at 1 Hz perfused with a NT solution (1 mM Ca^{2+}) at 35-37°C

	Control	STZ 4 weeks	STZ 8weeks
Ca^{2+} release	19.9±2.9 (10)	14.8±1.4 (7)	18.5±1.1 (23)
(% rise <i>Vs.</i> basal)			
t_{pk} of Ca^{2+} transient	109.6±7.5 (10)	98.6±8.4 (7)	102.6±6.3 (23)
(msec)			
Rate of Ca^{2+} decay	0.56±0.07 (10)	0.32±0.07 (7)*	0.37±0.02 (23)
(ratio units/sec)			
$t_{1/2}$ Ca^{2+} decay (msec)	91.8±4.8(10)	166.5±12.9 (7)*	156.1±8.4 (23)

Data are means ± S.E.M. Number in parenthesis indicates number of cells. Controls *Vs.* STZ and STZ (8 weeks) *Vs.* STZ (4 weeks) were compared using Student's independent samples *t* test. *P<0.05.

Discussion This study has shown that the amplitude and t_{pk} of Ca^{2+} transient was not significantly altered in 4 week STZ-induced diabetic myocytes compared to control, similar to results observed for the 8-12 weeks treated rats. However, basal Ca^{2+} is significantly increased in the diabetic heart following 4 weeks STZ treatment compared to age-matched controls. It is proposed that increases in basal Ca^{2+} , may contribute to the increase in contraction that has been reported in the diabetic heart. Moreover, this study has shown that resting $[Ca^{2+}]_i$ is higher following 4 weeks STZ compared to 8 weeks. Furthermore, the amplitude of contraction is bigger after 4 weeks compared to 8 weeks STZ treatment. The rate of Ca^{2+} transient decay is also significantly slower in the diabetic heart following 4 weeks of treatment. This study has shown that the defects associated with changes in Ca^{2+} homeostasis and contractions are in place after 4 weeks post injection of STZ. Therefore, the slower decay of the Ca^{2+} and the increase in resting Ca^{2+} may lead to an increase in contraction that has been reported within this study.

5.4 The effects of caffeine-induced calcium transients in isolated ventricular myocytes from streptozotocin-induced diabetic rat heart

5.4.1 Introduction

The velocity and measure of Ca^{2+} released from the SR following an action potential, is indicative of the speed of Ca^{2+} release from the SR but not an overall measure of the total amount of Ca^{2+} in the SR. The rapid application of caffeine however, activates the SR RyR channels to open and initiate a total release of Ca^{2+} from the SR (O'Neill & Eisner, 1990). If the caffeine application is sustained, Ca^{2+} re-sequestered back into the SR (via the SERCA pump) will be spontaneously released back into cytosol (Rousseau & Meissner, 1987). Therefore, a caffeine-induced Ca^{2+} release will enable the worker to assess: (a) total capacity of Ca^{2+} within the SR and (b) an indication of the speed or rate of Ca^{2+} efflux from the cell and back into the mitochondria (although the relative amount of Ca^{2+} pumped into the mitochondria is so little, that it does not contribute to changes in Ca^{2+} homeostasis and will therefore will not be discussed). Caffeine also effects myofilaments sensitisation as well as inhibiting phosphodiesterase (which can increase cAMP and in turn activate of cAMP dependent PKA) (Yu *et al.* 1995).

The aim of this part of the study was to investigate the effects of caffeine-induced Ca^{2+} release in isolated ventricular myocytes from age-matched control and STZ-induced diabetic myocytes following 8-12 weeks of STZ-treatment.

5.4.2 Method

See *Chapter 2* for details.

5.4.3 Results

In all figures, unless otherwise stated, relate to 8-12 weeks STZ-induced diabetic ventricular myocytes and age-matched controls. Figure 5.6. shows an original chart recording of the time course of the experimental protocol used to investigate the effects of caffeine (10 mM) on age-matched control and STZ-induced ventricular myocytes. Myocytes were electrically stimulated at 1 Hz before stimulation was abbreviated and the myocytes were rapidly superfused with 10 mM caffeine. Following a 10 sec application of caffeine, myocytes were re-stimulated and superfused with NT solution (1 mM Ca^{2+}) until Ca^{2+} transients reached pre-caffeine levels.

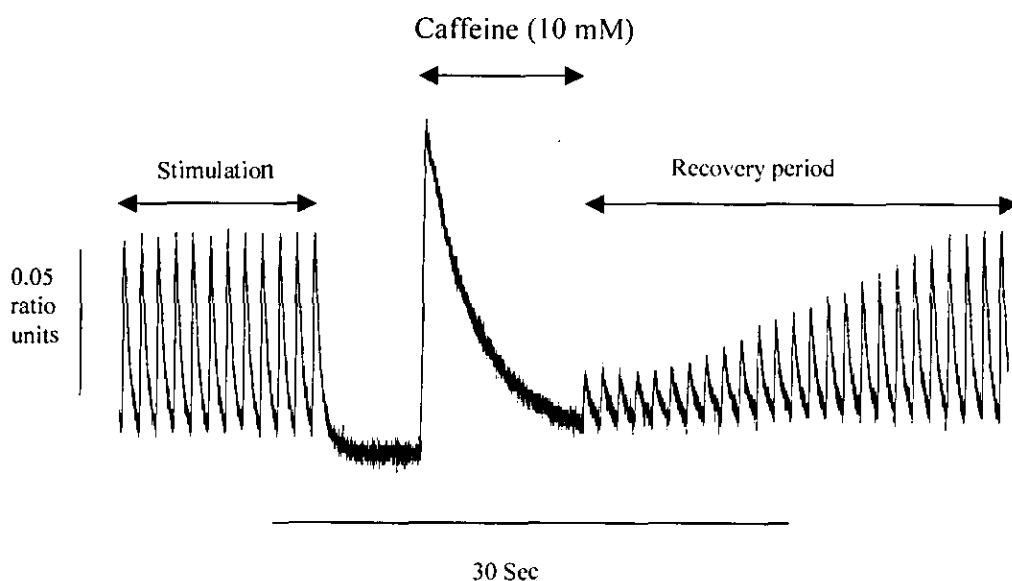


Figure 5.6. Original trace showing the time course protocol for caffeine-induced Ca^{2+} release and recovery in rat ventricular myocyte. Myocytes were stimulated and superfused with NT solution (1 mM Ca^{2+}) at 35°C-37°C. The trace is typical of 18 such myocytes from 6 rats.

Table 5.2. shows that the amplitude of caffeine-induced Ca^{2+} release was not significantly ($P>0.05$) altered between control and STZ-induced myocytes. Moreover, fractional release of Ca^{2+} was not altered significantly in control and STZ myocytes. The t_{pk} of the Ca^{2+} transient was not significantly ($P>0.05$) altered between control and STZ-induced. However, the $t_{1/2}$ decay of Ca^{2+} transient following the application of caffeine was significantly longer (43%) in myocytes obtained from STZ-induced compared to age-matched controls (Figure 5.7). Moreover, the rate of relaxation was significantly ($P<0.05$) smaller in diabetic myocytes compared to control (Table 5.2).

Table 5.2. The effects of 8-12 weeks STZ-induced diabetes on caffeine-induced Ca^{2+} release in isolated ventricular myocytes obtained from rat heart at 35-37°C

	Age-matched control	STZ-induced (8 weeks)
Amplitude of Ca^{2+} release (% rise Vs. Basal)	25.7±1.9 (18)	25.9±2.2 (17)
Fractional Ca^{2+} release	89.7±14.8 (18)	83.5±8.8 (17)
t_{pk} of Ca^{2+} transient (msec)	250.3±50.1 (18)	330.1±48.2 (17)
Rate of Ca^{2+} decay (ratio units/sec)	0.73±0.07 (18)	0.56±0.04 (17)*
$t_{1/2}$ Ca^{2+} decay (msec)	91.8±4.8(18)	156.1±8.4 (17)*

Data are means ± S.E.M. Number in parenthesis indicates number of cells. Controls Vs. STZ were compared using Student's independent samples *t* test. * $P<0.05$

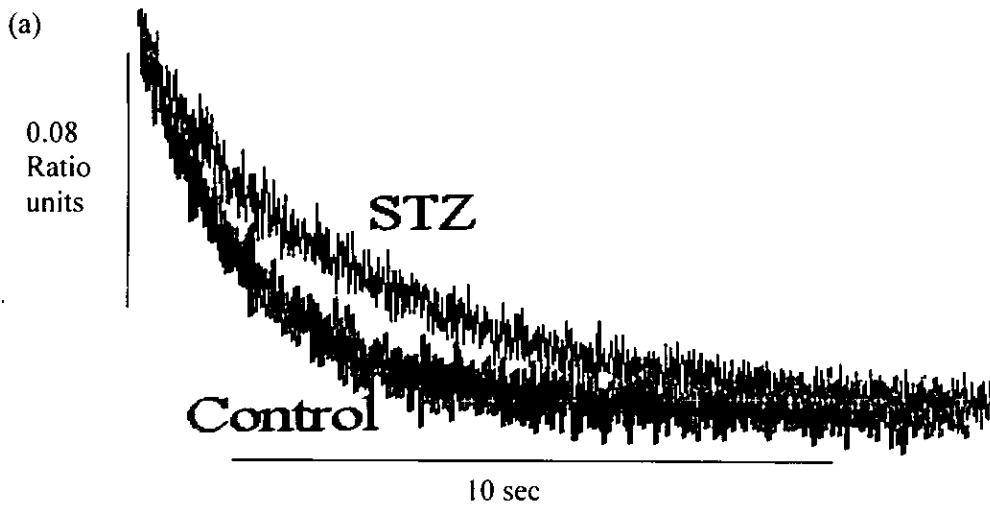


Figure 5.7.a Original chart recording of Ca^{2+} transient in age-matched controls (black) and STZ-induced (green) myocytes. Traces are typical of 18 such myocytes obtained from 6-8 rat hearts.

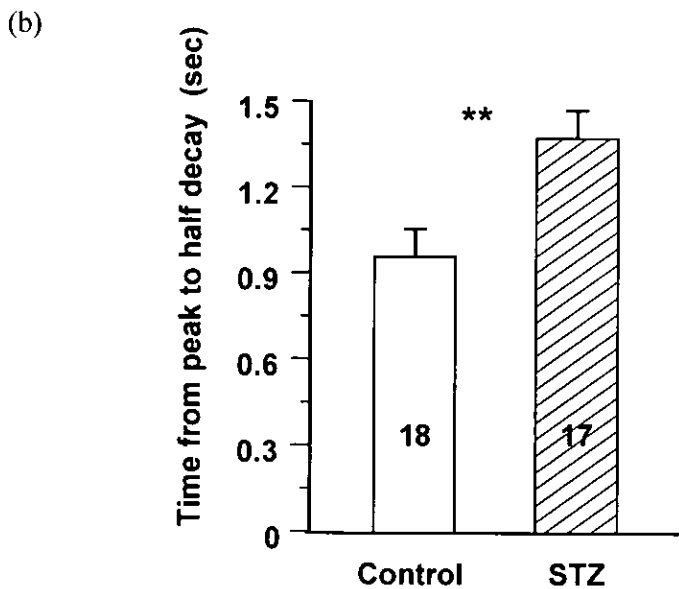


Figure 5.7.b shows the $t_{1/2 \text{ decay}}$ of a caffeine-induced Ca^{2+} release in STZ-induced and age-matched control myocytes. Data are means \pm S.E.M. Number in bars indicates cells. Control *Vs.* STZ was compared using Student's independent samples *t* test.

5.4.4 Discussion

The amount of Ca^{2+} released by the SR is dependent on the SR Ca^{2+} content and the magnitude and duration of the trigger stimulus (Baartscheer *et al.* 2000). A rapid application of caffeine activates the SR RyR channels to open and initiate a total release of Ca^{2+} from the SR (O'Neill & Eisner, 1990). In this study, the amplitude of the caffeine-induced Ca^{2+} release was not significantly altered in control and diabetic myocytes. In contrast, it has been reported that, following a caffeine-evoked Ca^{2+} transient the amount of Ca^{2+} released from the SR is reduced in the diabetic heart (Lagadic-Gossmann *et al.* 1996; Tamada *et al.* 1998; Yu *et al.* 1995; Choi *et al.* 2002). The reported changes in caffeine-induced SR Ca^{2+} release may be attributable to the rest period preceding an application of caffeine. In this study, stimulation was abbreviated for 10 sec, prior to a rapid caffeine pulse, but in other reports there was a 30 sec (Choi *et al.* 2002) and 40 sec (Lagadic-Gossmann *et al.* 1996) quiescent phase. Longer rest periods may be associated with alterations in SR loading abilities and may contribute to a change in releasable SR Ca^{2+} . Interestingly, Choi *et al.* (2002) reported that the decrease in caffeine-induced Ca^{2+} release was mirrored by a decrease in the amplitude of contraction. In contrast, this present study has shown that the amplitude of contraction is significantly larger in the diabetic heart compared to age-matched controls. It seems likely that alterations in Ca^{2+} release and myofilament sensitivity may contribute to changes in contractile dysfunction. Fractional Ca^{2+} release was not significantly different in STZ-induced diabetic myocytes compared to control. This suggests that the triggered response and release of Ca^{2+} from the SR is similar in the diabetic heart. It has been shown that the gain of CICR is dependent on the $I_{\text{Ca,L}}$ and subsequent influx of Ca^{2+} to trigger Ca^{2+} release from the SR (Wier *et al.* 1994). This study has shown that stimulated Ca^{2+} release and caffeine-induced Ca^{2+} release are similar, therefore any changes in $I_{\text{Ca,L}}$ may be indicative of changes in the gain in the diabetic heart. The t_{pk} of a Ca^{2+} transient following a rapid application of caffeine is an

indication of RyR release sensitivity/activity. In this study, it has been reported that the t_{pk} of a caffeine-evoked Ca^{2+} transient was increased in the STZ-induced diabetic myocytes but not to a significant level. It has however, been reported that the time course of the caffeine-induced Ca^{2+} transient decay was significantly prolonged in the diabetic myocytes (Choi *et al.* 2002). Similarly, in this study it has also been shown that the $t_{1/2}$ decay of the caffeine-induced Ca^{2+} was significantly longer in the diabetic myocytes compared to control (Figure 5.7.b). This is in agreement with, other workers who have also reported longer rates of Ca^{2+} transient decay in 8 weeks (Choi *et al.* 2002) STZ-induced diabetic myocytes.

Caffeine application causes the release of Ca^{2+} from the SR and causes the SR to become “leaky”. However, the SR is still functional and can sequester Ca^{2+} back into the SR, where it is then expelled out into the cytosol through RyR channels affected by caffeine. It is worthwhile to note that a series of experiments were undertaken to look at the effects of thapsigargin on the decay of Ca^{2+} release during the application of caffeine. However following a 10 min incubation of thapsigargin, caffeine induced Ca^{2+} release was reduced and the measure of the decay of the Ca^{2+} transient was impossible to measure accurately due to an increase in noise. Moreover, it has been reported that the rate of decay of a caffeine induced Ca^{2+} transient is largely dependent on the Na^+/Ca^{2+} -exchanger (Bassani *et al.* 1992; Bassani *et al.* 1994; Negretti *et al.* 1993; Choi & Eisner, 1999) and therefore, the decay of the Ca^{2+} transient during a caffeine-evoked response in the absence of thapsigargin provides a direct measure of the rate of Ca^{2+} efflux out of the cell, although a tiny proportion of Ca^{2+} is sequestered back into the mitochondria. It can therefore, be said that in this study the prolonged time course of $[Ca^{2+}]_i$ decay is associated with a derangement in efflux pathways. The prolonged decay of $[Ca^{2+}]_i$ may also contribute to the change in contractile function that is a feature of human and experimentally induced

diabetes (Albanna *et al.* 1998; Kiss *et al.* 1988; Astorri *et al.* 1997; Nicolino *et al.* 1995; Regan *et al.* 1974; Fein *et al.* 1985; Litwin *et al.* 1990; Miller 1979; Vadlamudi *et al.* 1982).

5.5 *Effects of nickel on caffeine-induced calcium transients in the isolated ventricular myocytes from streptozotocin-induced diabetic rat heart*

5.5.1 *Introduction*

In order to isolate the mechanism responsible for the delay in $[Ca^{2+}]_i$ efflux, following an application of caffeine, it is useful to use a pharmacological tool to block Ca^{2+} pathways. The main transport mechanisms involved in Ca^{2+} efflux are the Na^+/Ca^{2+} -exchanger and the PMCA pump. The Na^+/Ca^{2+} -exchanger is the main mechanism by which, Ca^{2+} is taken out of the cell. It has been reported that the Na^+/Ca^{2+} -exchanger accounts for between 68 and 87 % of Ca^{2+} efflux, while the PMCA pump and mitochondria, collectively, accounts for between 13 and 32 % (Bassani *et al.* 1992; Bassani *et al.* 1994; Negretti *et al.* 1993; Choi & Eisner, 1999). $NiCl_2$ (10 mM) blocks the Na^+/Ca^{2+} -exchanger (as well as the L-type Ca^{2+} channel) but has no effect on the PMCA (Egger *et al.* 1999; Leoty *et al.* 2001). Therefore, following caffeine-induced Ca^{2+} transient, the rate of efflux in the presence of $NiCl_2$ is indicative of the rate at which, Ca^{2+} is taken up by the mitochondria and passed out of the cell via the PMCA.

Therefore, the main aim of this part of the study was to initiate caffeine-induced Ca^{2+} release in the presence of $NiCl_2$, in control and STZ-induced diabetic ventricular myocytes. An alteration between control and diabetic myocytes may implicate the PMCA and mitochondria to be deranged, while, a similar rate of Ca^{2+} efflux would imply that the Na^+/Ca^{2+} -exchanger may contribute to changes in Ca^{2+} efflux that has been reported in the diabetic heart.

5.5.2 *Method*

See Chapter 2 for details.

5.5.3 Results

In all figures, unless otherwise stated, relate to 8-12 weeks STZ-induced diabetic ventricular myocytes and age-matched controls. Figure 5.8. shows a time course trace of the protocol used for this series of experiments. Following a caffeine protocol (see Figure 5.6) electrical stimulation is stopped and NiCl_2 (10 mM) is applied to cells for 10 sec, caffeine (10 mM) is then rapidly applied to cells for 10 sec, before NT solution is re applied to the cells and cell re-stimulated (1 Hz) until pre caffeine controls are reached.

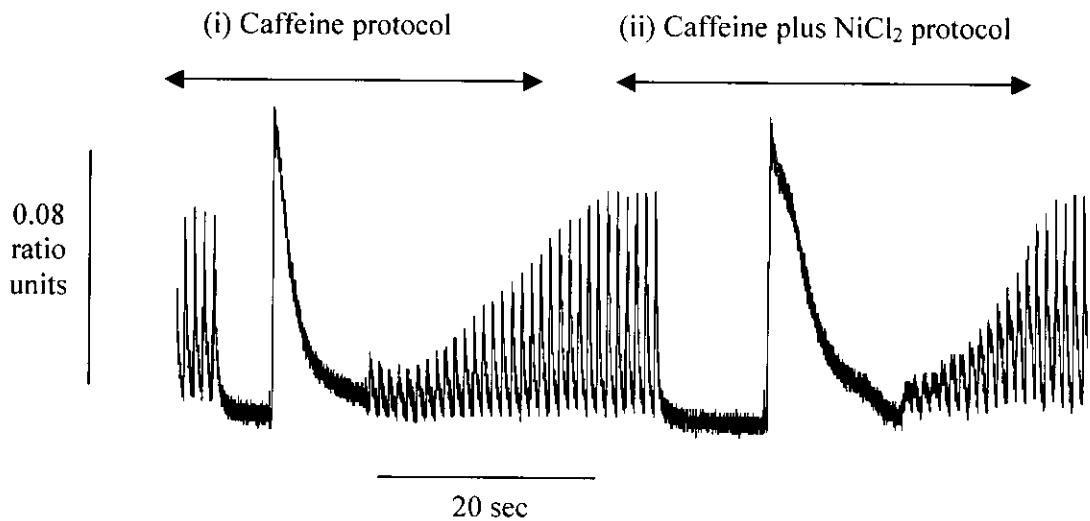


Figure 5.8. Original trace showing the time course protocol for (i) caffeine-induced Ca^{2+} release and for (ii) caffeine-induced Ca^{2+} release in the presence of NiCl_2 (10 mM) and recovery in rat ventricular myocyte. Myocytes were stimulated and superfused with NT solution (1 mM Ca^{2+}) at 35°C - 37°C . The trace is typical of 18 such myocytes from 6 rats.

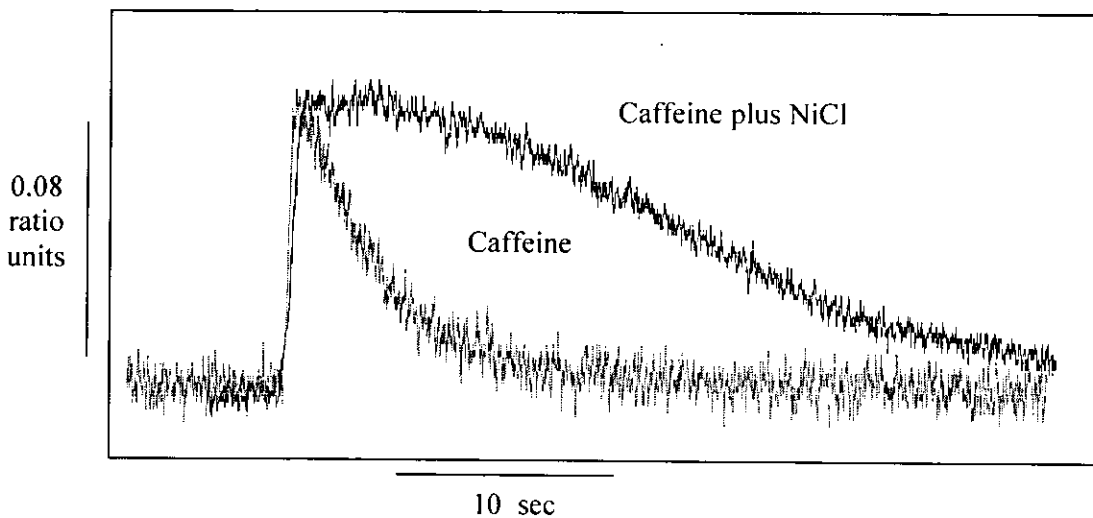


Figure 5.9. The effects of NiCl on the caffeine induced Ca^{2+} release. Superimposed traces of caffeine induced SR Ca^{2+} release in the absence (blue) and presence of nickel (black) from isolated ventricular myocytes. Traces are typical of 18 cells taken from at least 5 rat hearts.

In the presence of NiCl_2 , the amplitude of Ca^{2+} release measured by the percentage change versus pre caffeine pulse was not significantly ($P > 0.05$) altered in control and diabetic myocytes, respectively (Table 5.1). Moreover, there was no significant ($P > 0.05$, Paired t-test) difference in the amplitude of caffeine-induced Ca^{2+} release between the pre and post application of NiCl_2 in control and STZ-induced myocytes. The t_{pk} of the caffeine-induced Ca^{2+} release (peak taken from first point of peak transient) in the presence of NiCl_2 was significantly ($P < 0.05$) longer in diabetic myocytes compared to control (Table 5.1). Moreover, the t_{pk} was significantly ($P < 0.01$, Paired t-test) increased in both control and diabetic myocytes between pre and post application of NiCl_2 . The $t_{1/2}$ and rate of decay of the Ca^{2+} transient was not significantly ($P > 0.05$) altered in STZ-induced myocytes in the presence of NiCl_2 (Table 5.1). However, both control and STZ-induced myocytes had

significantly ($P < 0.01$, Paired t-test) longer decays in the rate of Ca^{2+} transient decline following an application of NiCl_2 .

Table 5.2. The effects of STZ-diabetes on the caffeine-induced Ca^{2+} transient in the presence of NiCl_2 of isolated ventricular myocytes obtained from rat heart at 35-37°C.

	Age-matched control	STZ-induced
Amplitude of Ca^{2+} transient (% rise Vs. stimulated)	25.6 ± 1.9 (18)	25.8 ± 2.0 (17)
Fractional Ca^{2+} release	90.7 ± 15.4 (18)	82.3 ± 8.7 (17)
Time to peak (t_{pk}), (sec)	0.49 ± 0.06 (18)	0.71 ± 0.08 (17) *
Time to half decay ($t_{1/2}$), (sec)	2.5 ± 0.23 (18)	2.9 ± 0.26 (17)
Rate of Ca^{2+} decay (ratio units /sec)	0.03 ± 0.003 (18)	0.03 ± 0.002 (17)

Data are means ± S.E.M. Number in parenthesis indicates number of cells. Control Vs. STZ was compared using Student's independent samples *t* test. * $P < 0.05$.

5.5.3.1 Comparison of rate of decay

The rate of cytosolic Ca^{2+} decay in electrically stimulated (1 Hz) ventricular myocytes taken from control hearts was significantly ($P < 0.01$) quicker (39.8 %) than that of STZ-induced diabetic hearts (Figure 5.10.a) Moreover, the rate of decay following an application of caffeine was significantly ($P < 0.05$) faster (23.6 %) in control compared to diabetic myocytes. However, the rate at which, Ca^{2+} efflux and uptake in caffeine in the

presence of NiCl_2 was not significantly ($P>0.05$) altered in diabetic and control. versus control (Figure 5.10.).

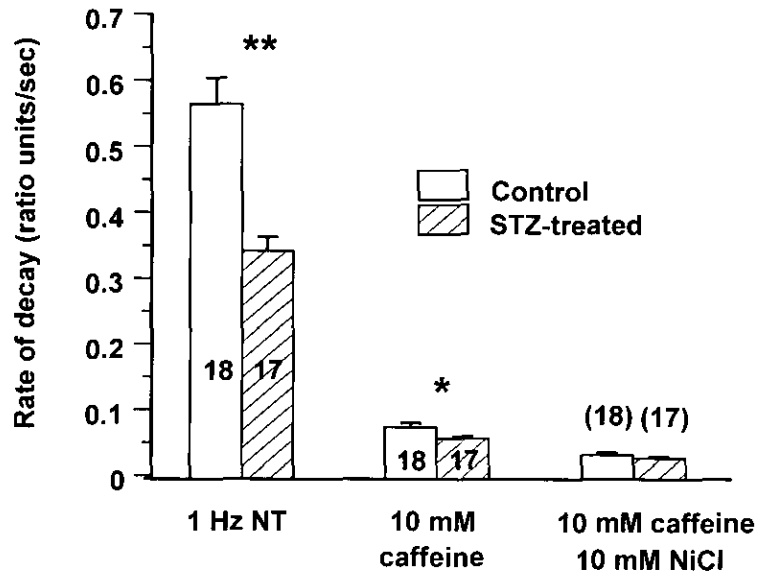


Figure 5.10. The rate of Ca^{2+} decay in electrically stimulated, caffeine-induced and caffeine-induced Ca^{2+} transient in the presence of NiCl in ventricular myocytes isolated from control and STZ-induced rat heart perfused with a NT (1 mM Ca^{2+}) at 35-37°C. Data are means \pm S.E.M. Numbers in bars indicates number of cells. Control vs. STZ was compared using Student's independent samples *t* test. * $P<0.05$, ** $P<0.01$.

5.5.4 Discussion

From the results, it can be seen that, in the presence of NiCl_2 the amplitude of Ca^{2+} released from the SR, in control myocytes following an application of caffeine was not significantly different than in STZ-induced myocytes. Therefore, it would seem that the total available amount of Ca^{2+} is similar in the normal and diabetic heart and that the $\text{Na}^+/\text{Ca}^{2+}$ -exchanger does not contribute to changes in caffeine-induced Ca^{2+} release in ventricular myocytes. However, it has been reported that in the diabetic heart caffeine-induced Ca^{2+} release is significantly diminished (Choi *et al.* 2002). In the presence of NiCl_2 , the t_{pk} of the caffeine-induced Ca^{2+} transient is longer in both control and diabetic myocytes (compared to caffeine-induced Ca^{2+} release without NiCl_2) but is significantly increased in the STZ-induced myocyte compared to control. This would suggest that either NiCl_2 itself or the action of NiCl_2 on the $\text{Na}^+/\text{Ca}^{2+}$ -exchanger changes the t_{pk} of the a caffeine-induce Ca^{2+} release in STZ-myocytes significantly more than control myocytes. Because, the speed of Ca^{2+} release of the SR is indicative of RyR, sensitivity, it is suggested that in the diabetic heart the sensitivity of RyR release channels is altered though the action of NiCl_2 itself or through changes in $[\text{Ca}^{2+}]_i$ through the $\text{Na}^+/\text{Ca}^{2+}$ -exchanger blockade. The rate of decay of the caffeine-induced Ca^{2+} transient is longer in diabetic myocytes versus control, but in the presence of NiCl_2 the rate of decay is not significantly altered. Because NiCl_2 blocks the $\text{Na}^+/\text{Ca}^{2+}$ -exchanger, the rate of decay during caffeine-induced Ca^{2+} release in the presence of NiCl_2 is a rate of efflux from the PMCA and uptake into the mitochondria. Therefore, it is tempting to suggest that in this series of experiments the sustained elevation in $[\text{Ca}^{2+}]_i$ following caffeine treatment is directly associated with the $\text{Na}^+/\text{Ca}^{2+}$ -exchanger, but not the changes in PMCA Ca^{2+} efflux or mitochondrial Ca^{2+} uptake.

Chapter 6

*Effects of halothane on $I_{Ca,L}$,
 $[Ca^{2+}]_i$ and contraction in the
streptozotocin-induced diabetic
and age-matched control
cardiomyocyte*

6.1 Introduction

Volatile anaesthetics have been used in the clinical environment to produce unconscious effects in patients undergoing clinical procedures including surgery on the heart (Davies *et al.* 2000). However, cardiovascular complications are a major source of morbidity and mortality in patients in surgery under anaesthesia (Campling *et al.*, 1993). Halothane is a well known modern volatile anaesthetic, but has been reported to produce several adverse side effects within the heart (Davies *et al.* 2000). Several reports suggest that halothane can induce a negative inotropic (contraction) effect in the heart (Housmans & Murat, 1988). The negative inotropic and lusitropic (relaxation) effects of halothane (Harrison *et al.* 1999; Davies *et al.* 1999) have been reported to be attributable to alterations in Ca^{2+} sarcolemmal influx (Ikemoto *et al.* 1985), SR Ca^{2+} uptake (Connelly & Coronado, 1994) and release, and changes in sensitivity of contractile myofilament sensitivity (Davies *et al.* 2000).

The rate of inward $I_{\text{Ca,L}}$ determines the rate of Ca^{2+} influx leading to the triggered response of Ca^{2+} from the SR, following depolarisation of the sarcolemmal. Initial depolarisation of the cell membrane leads to the rapid activation of $I_{\text{Ca,L}}$ around $-40 \text{ mV } E_m$ (Bers, 1991). Ca^{2+} influx through L-type channels has been shown to be around $13.8 \mu\text{mol/l}$ cytosol in rat ventricular myocytes (Yuan *et al.* 1996). Given that the rate of inward $I_{\text{Ca,L}}$ is the trigger for SR Ca^{2+} release (in normal conditions), any alteration in the $I_{\text{Ca,L}}$ may effect its opening and subsequent ability to trigger Ca^{2+} release. Moreover, a reduction $I_{\text{Ca,L}}$ has been reported in the heart in the presence of halothane (Ikemoto *et al.* 1985).

Following the triggered release of Ca^{2+} from the SR, cytosolic free Ca^{2+} increases, leading to the binding of Ca^{2+} with the troponin-C complex, which, results in the sliding of actin

and myosin over each other, and subsequent contraction. These processes have the potential to be altered by changes in pharmacological environment and alterations in the pathological state (Morgan *et al.*, 2000). It has also been reported that myofilament sensitivity to Ca^{2+} is altered in the normal rat heart in the presence of halothane (Harrison *et al.* 1999). Therefore, changes in myofilament sensitivity may contribute to cardiac contractile abnormalities in the diabetic heart and may be attenuated by halothane.

During surgical procedures, the concentration of plasma halothane ranges between 0.05 and 0.7 mmol l^{-1} (Davies *et al.* 1972). It has been reported that, two times minimum alveolar concentration (MAC)(2) concentration in the rat is 0.6 mmol l^{-1} (Rithalia *et al.* 2001). Therefore, in this study, a clinically relevant concentration of halothane (0.6 mmol l^{-1}) has been employed to characterise the effects of halothane on the diabetic heart compared to age-matched control. The diabetic heart is characterised by an alteration or disruption of contractility that is underpinned by changes in Ca^{2+} homeostasis. The intracellular mechanisms underlying the changes in cardiac function in the presence of halothane in the diabetic heart are not fully understood. It is hoped that changes associated with inotropic effects of halothane in normal and diabetic myocytes may provide a greater understanding of the underlying mechanisms of dysfunction in the STZ-induced diabetic heart.

The aim of this study was to investigate the effects of a clinically relevant concentration of halothane on isolated ventricular myocytes from age-matched control and STZ-induced diabetic hearts. Specifically this study has investigated the effects of halothane on: (1) $I_{\text{Ca,L}}$, voltage dependence of contraction, inotropy an lusitropy, stimulated Ca^{2+} transient and myofilament sensitivity for Ca^{2+} .

6.2 Results

In all figures, unless otherwise stated, relate to 8-12 weeks STZ-induced diabetic ventricular myocytes and age-matched controls. In a number of tissues it is established that membrane Ca^{2+} conductance decreases progressively over time and is mainly due to artificially perfusing cells as thus washing away of molecules that are important in maintaining the function of channels, which can result in a loss of $I_{\text{Ca,L}}$ (Kameyama *et al.* 1997). This process is known as “run-down”. Rundown was assessed in a number of experiments, and it was shown there was no significance difference between the $I_{\text{Ca,L}}$ in control and STZ-induced myocytes following wash off periods compared to time-tested controls. Cell volume (V) was measured by using a formula based on the observations of Satoh *et al.* (1996), that the shape of a rat ventricular myocyte is an elongated ellipse, of which the volume is equal to 54 % of the volume of a block. This is defined as the length X Width X Depth. Depth was calculated as a prediction of the cell width. Therefore, the formula was; $V = L \times W \times (W/W:D) \times 5.4 \times 10^{-4} \text{ pl } \mu\text{m}^3$ or $V = L \times W^2/2667 \text{ pl}^{-1} \mu\text{m}^3$. Cell volume in ventricular myocytes obtained from control hearts were not significantly different to those obtained from STZ-induced diabetic hearts, respectively. Control $15.2 \pm 0.8 \text{ pl}$, (n=9) and STZ $14.9 \pm 0.31 \text{ pl}$, (n=9).

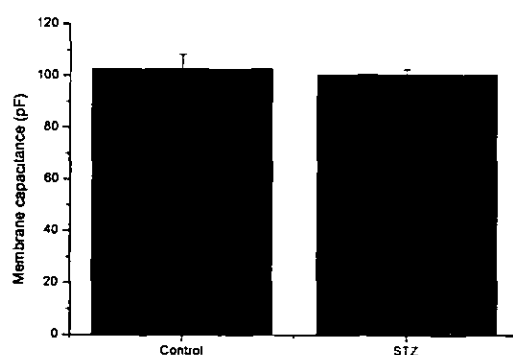


Figure 6.1. Membrane capacitance (pF) measured in control and STZ-induced diabetic ventricular myocytes: Control $102.7 \pm 5.64 \text{ pF}$, (n=9) and STZ $100.6 \pm 2.09 \text{ pF}$, (n=9).

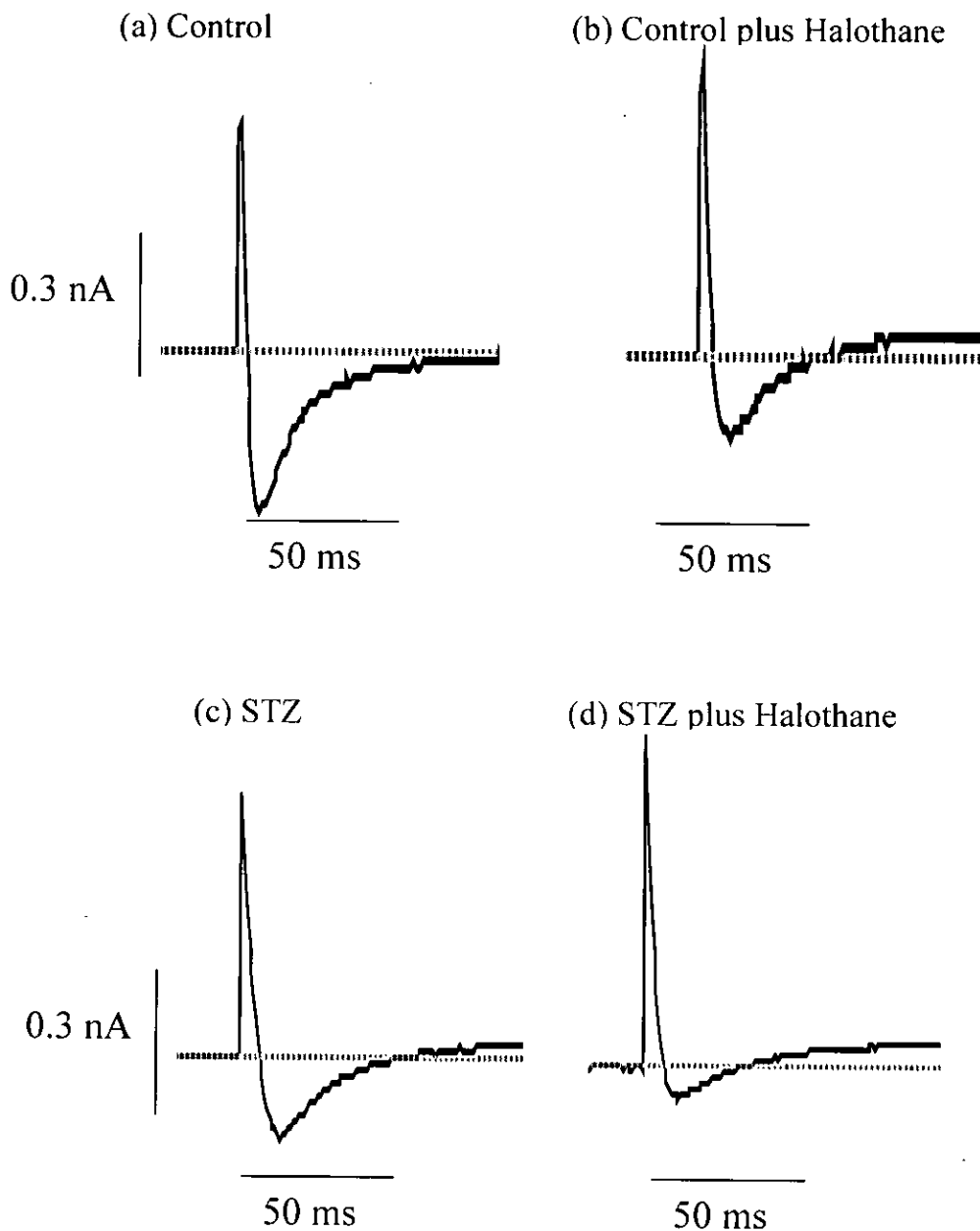


Figure 6.2. Typical chart traces of $I_{Ca,L}$ following a test pulse of 0 mV from a holding potential of -40 mV in (a) control and (c) STZ-induced ventricular myocytes and the effects of halothane (0.6 mM) on $I_{Ca,L}$ in (b) control and (d) STZ-induced myocytes at room temperature. Traces are typical of 8-10 cells from taken from 3-4 rat hearts.

6.2.1 Current function

Figure 6.2. shows typical $I_{Ca,L}$ traces obtained from either in (a) age-matched control, (b) age-matched control plus halothane, (c) STZ-induced or (d) STZ-induced plus halothane myocytes. The t_{pk} of $I_{Ca,L}$ was not significantly ($P>0.05$) altered between control and STZ-induced diabetic myocytes in the absence or presence of halothane (Table 6.1.).

Table 6.1. The effects of 8-12 weeks STZ-induced diabetes and halothane on the time to peak of the $I_{Ca,L}$ compared to age-matched controls in isolated ventricular myocytes patched clamped in whole cell configuration at room temperature.

	Time to peak of the $I_{Ca,L}$ (msec)
Control	7.97±0.97(9)
STZ	9.25±1.35(9)
Control plus halothane	10.31±0.79(9)
STZ plus halothane	8.91±0.91(9)

Data are means ± S.E.M. Number in parenthesis indicates number of cells. Control *Vs.* STZ was compared using Student's independent samples *t* test. Control *Vs.* Control plus halothane (0.6 mM) and STZ *Vs.* STZ plus halothane (0.6 mM) was compared using a paired *t* test.

6.2.2 Current Amplitude

Figure 6.3. Shows the peak $I_{Ca,L}$ amplitude (difference between the peak $I_{Ca,L}$ and the $I_{Ca,L}$ at the end of the depolarising pulse) in age-matched control and STZ-induced diabetic ventricular myocytes in the presence and absence of halothane (0.6 mM). The amplitude

of peak $I_{Ca,L}$ was significantly ($P < 0.05$) reduced in STZ-induced myocytes (-3.03 ± 0.19 pA/pF, $n = 9$ Vs. -4.87 ± 0.32 pA/pF, $n = 9$) compared to age-matched control, respectively. Following the application of halothane (hal), peak $I_{Ca,L}$ amplitude was significantly ($P < 0.05$) to -3.24 ± 0.29 pA/pF, $n = 7$ in control myocytes and to -1.81 ± 0.23 pA/pF, $n = 7$ in STZ-induced diabetic myocytes (Figure 6.2.).

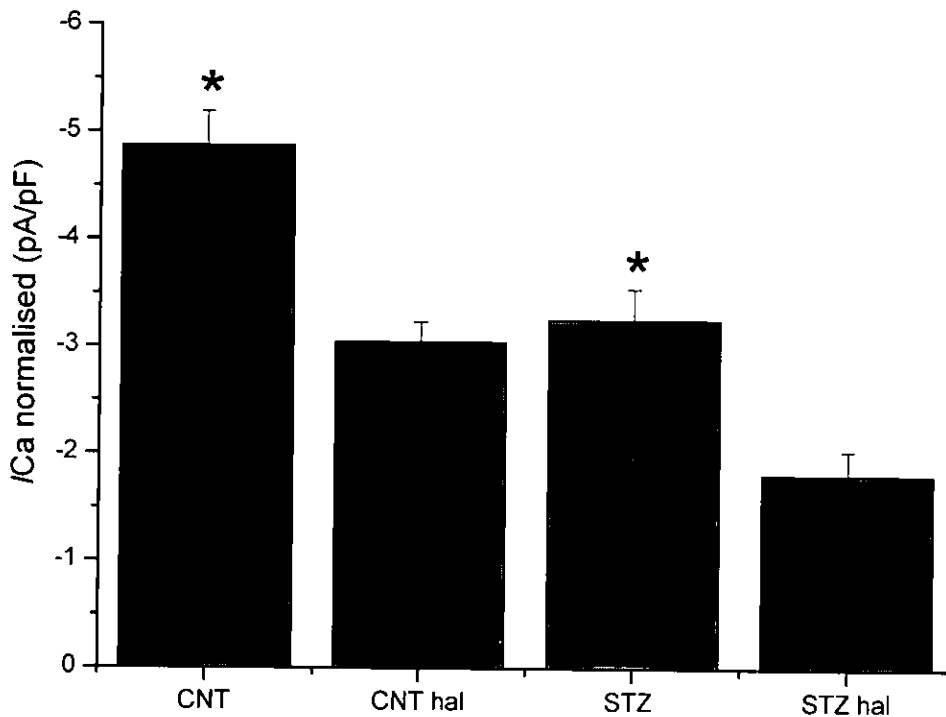


Figure 6.3. The effect of halothane (hal, 0.6 mM) on the mean voltage dependence of $I_{Ca,L}$ in control-CNT (b) and STZ-induced diabetic (c) ventricular myocytes. Respective control for each group (either control (b) or STZ (c)) is shown for comparison. Data shown are mean \pm SEM. Statistical significance showing control ($n=8$) vs. control plus halothane ($n=8$) and STZ ($n=7$) vs. STZ plus halothane ($n=7$) compared using paired t test is represented by $*P < 0.05$.

6.2.3 Current/voltage relationship

Figure 6.4. shows the $I_{Ca,L}$ voltage relationship in (a) control versus STZ, (b) control versus control plus halothane and (c) STZ versus STZ plus halothane. The $I_{Ca,L}$ was significantly ($P < 0.05$) reduced throughout voltage ranges (0 mV and 40 mV) in STZ-induced myocytes when compared to age-matched controls (Figure 6.4.a). However, there was no significant difference in $I_{Ca,L}$ between control and STZ-induced myocytes in the presence of halothane. In age-matched control myocytes, $I_{Ca,L}$ was further reduced at voltages between 10 mV and 40 mV in the presence of halothane (Figure 6.4.b). Halothane also significantly ($P > 0.05$) reduced the $I_{Ca,L}$ further in STZ-induced myocytes at 10 mV test pulse, but in contrast did have not any significant effect at all other voltages (Figure 6.4.c).

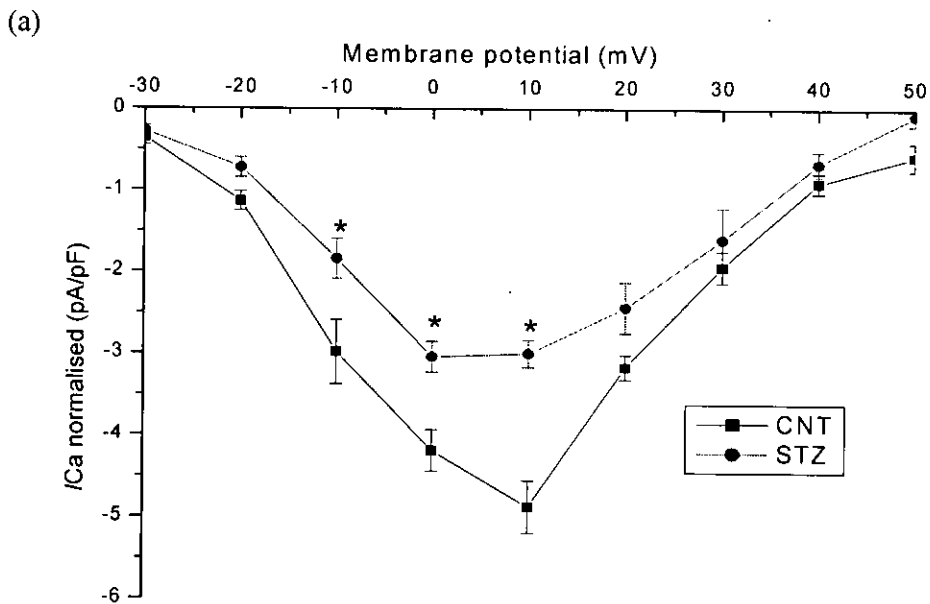


Figure 6.4.a. Mean voltage dependence of $I_{Ca,L}$ plotted as current density (pA/pF) for test potentials between -30 and $+50$ mV between control-CNT and STZ-induced diabetic ventricular myocytes at room temperature. Data shown are mean \pm SEM. Statistical significance showing CNT ($n=7$) vs. STZ ($n=7$) were compared using independent t test. $*P < 0.05$.

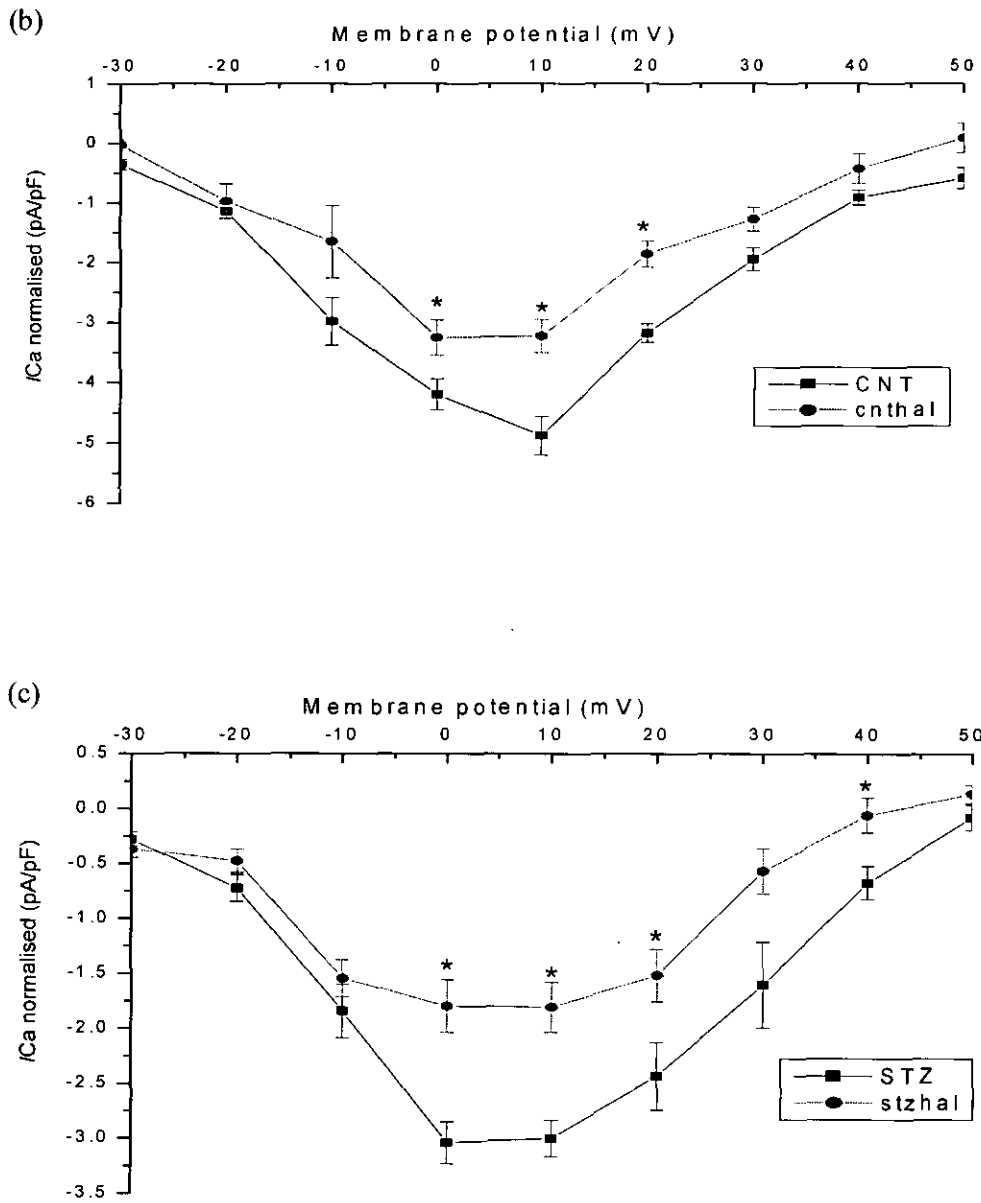


Figure 6.4. Mean voltage dependence of $I_{Ca,L}$, plotted as current density (pA/pF) for test potentials between -30 and $+50$ mV in (b) control-CNT and (c) STZ-induced diabetic ventricular myocytes, pre and post application of halothane (hal) at room temperature. Data shown are mean \pm SEM. Statistical significance showing CNT (n=7) vs. CNT plus hal (n=7) and STZ vs. STZ plus hal (n=7) were compared using paired t test. * $P < 0.05$.

6.2.4 Voltage dependence of contraction

Figure 6.5. shows the effect of halothane on the voltage dependence of contraction in 8-12 weeks STZ-induced and age-matched control myocytes at room temperature. Contraction was examined in these cells by measuring the amplitude of contraction in relation to resting cell length elicited at each test voltage (mV) step in the $I_{Ca,L}$ /voltage data. Contraction was significantly ($P<0.05$) greater in control myocytes compared to STZ-induced myocytes at all test potentials. Following the application of halothane (0.6 mM), the amplitude of contraction significantly decreased between -10 mV and -50 mV potentials in control myocytes. Moreover in STZ-induced diabetic myocytes, following the application of halothane also resulted in a significant reduction in the amplitude of contraction at -20 mV, 0 mV and $+10$ mV potentials. Furthermore, contraction was significantly decreased at test potentials between -20 and $+10$ mV when comparing control myocyte with STZ-induced myocytes in the presence of halothane.

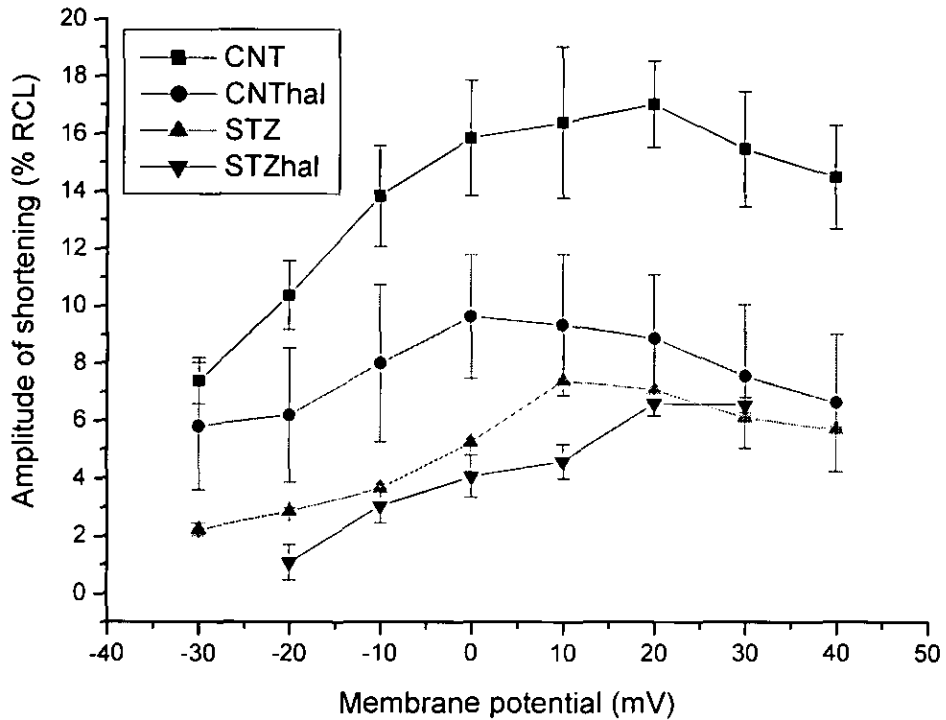


Figure 6.5. Mean voltage dependence of contraction, plotted as percentage of resting cell length for test potentials between -30 and $+50$ mV in control-CNT and 8-12 weeks STZ-induced diabetic ventricular myocytes, in the absence and presence of halothane (hal) at room temperature. Data shown are mean \pm SEM. Statistical significance was analysed (see commentary) CNT ($n=7$) vs. STZ ($n=7$) were compared using independent t test. CNT ($n=7$) vs. CNT plus hal ($n=7$) and STZ vs. STZ plus hal ($n=7$) were compared using paired t test.

6.2.5 Contraction

Figure 6.6. shows (a) original fast time based chart recordings of contraction, (b) t_{pk} of contraction and (c) contraction as percentage remaining following the application of 0.6 mM halothane in ventricular myocytes isolated from age-matched control and STZ-induced diabetic. Figures 6.7 and 6.8 show (a) original fast time based chart recordings and the (b), t_{pk} of contraction and $t_{1/2}$ decay of contraction (c) in age-matched control and STZ-induced cardiomyocytes in the absence and presence of 0.6 mM halothane. The results show that the t_{pk} of myocyte shortening was significantly ($P < 0.01$) prolonged in STZ myocytes (137.2 ± 4.1 msec, $n = 32$) compared to control (105.5 ± 2.0 msec, $n = 31$) (Figure 6.6.a). However, t_{pk} of contraction were significantly ($P < 0.01$) reduced in control (105.5 ± 2.0 msec, $n = 31$ Vs. 94.6 ± 2.4 msec, $n = 31$) (Figure 6.7.b) and STZ-induced (137.2 ± 4.1 msec, $n = 32$ Vs. 119.3 ± 3.4 msec, $n = 32$) (Figure 6.8.b) myocytes in the absence and presence of halothane, respectively. Halothane significantly ($P < 0.01$) reduced amplitude of contraction in both control (from 100% to 65.9 ± 2.7 %, $n = 31$) and STZ-induced (from 100% to 40.9 ± 3.2 %, $n = 32$) myocytes. This reduction in contraction was significantly ($P < 0.01$) greater in STZ-induced myocytes compared to control (Figure 6.6.c). The $t_{1/2}$ decay was not significantly altered between control and STZ-induced myocytes in the presence of halothane, but was significantly ($P < 0.01$) decreased in control (46.5 ± 2.1 msec, $n = 31$ Vs. 42.5 ± 2.0 msec, $n = 31$) (Figure 6.7.c) and STZ-induced (48.6 ± 1.8 msec, $n = 32$ Vs. 45.1 ± 1.9 msec, $n = 32$,) (Figure 6.8.c) myocytes before and after the application of halothane, respectively.

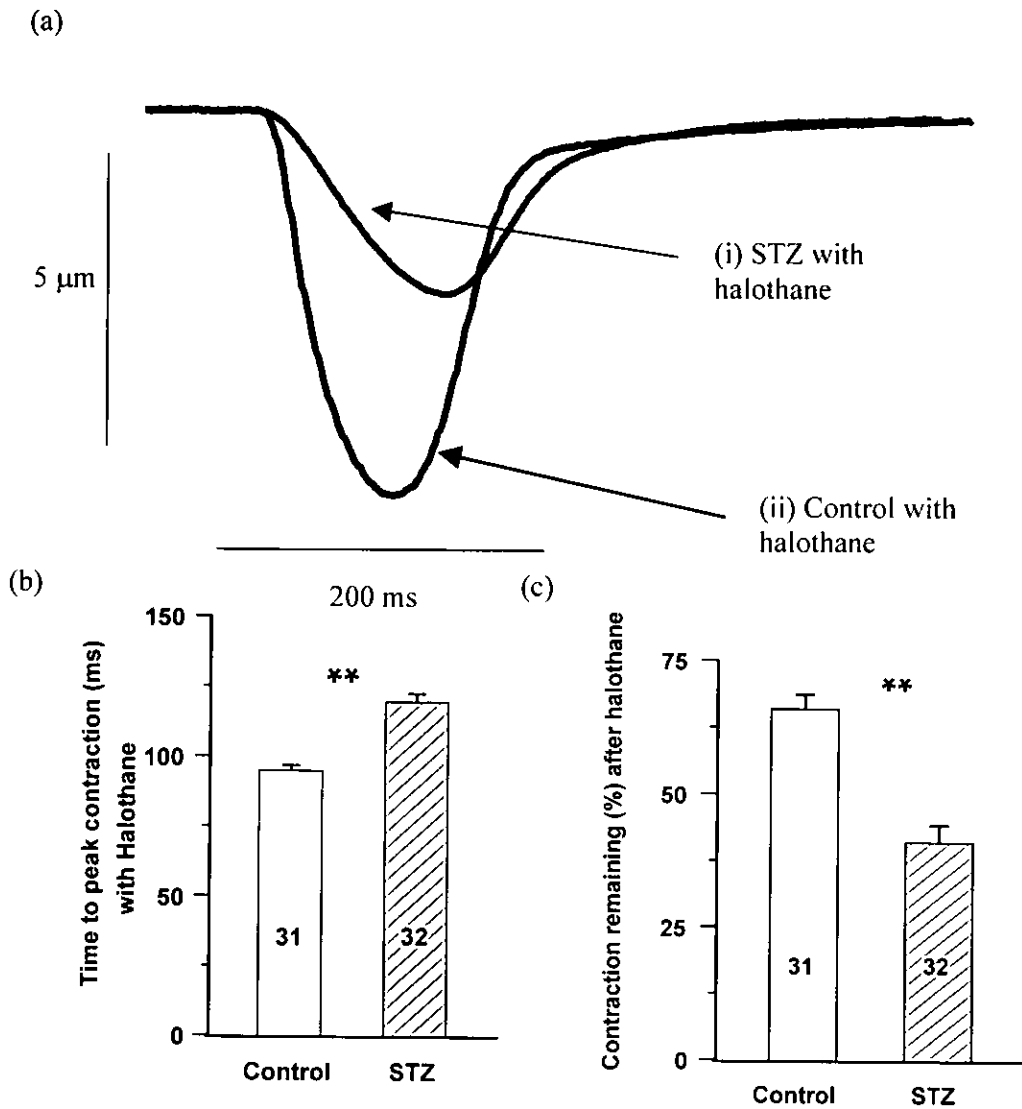


Figure 6.6.a Representative fast time-base recordings of contraction in electrically stimulated (1 Hz) rat ventricular myocytes, superfused with NT containing 0.6 mM halothane at 35-37°C, from (i) STZ-induced diabetic compared with (ii) control rats. (b), t_{pk} of contraction and (c), contraction as a percentage remaining after the application of halothane. Data shown are mean \pm SEM. Numbers within bars represent number of cells. Statistical significance showing control vs. STZ, independent samples t test is represented by $**P < 0.01$. Frames in (a) are typical of 31 control myocytes and 32 STZ treated myocytes.

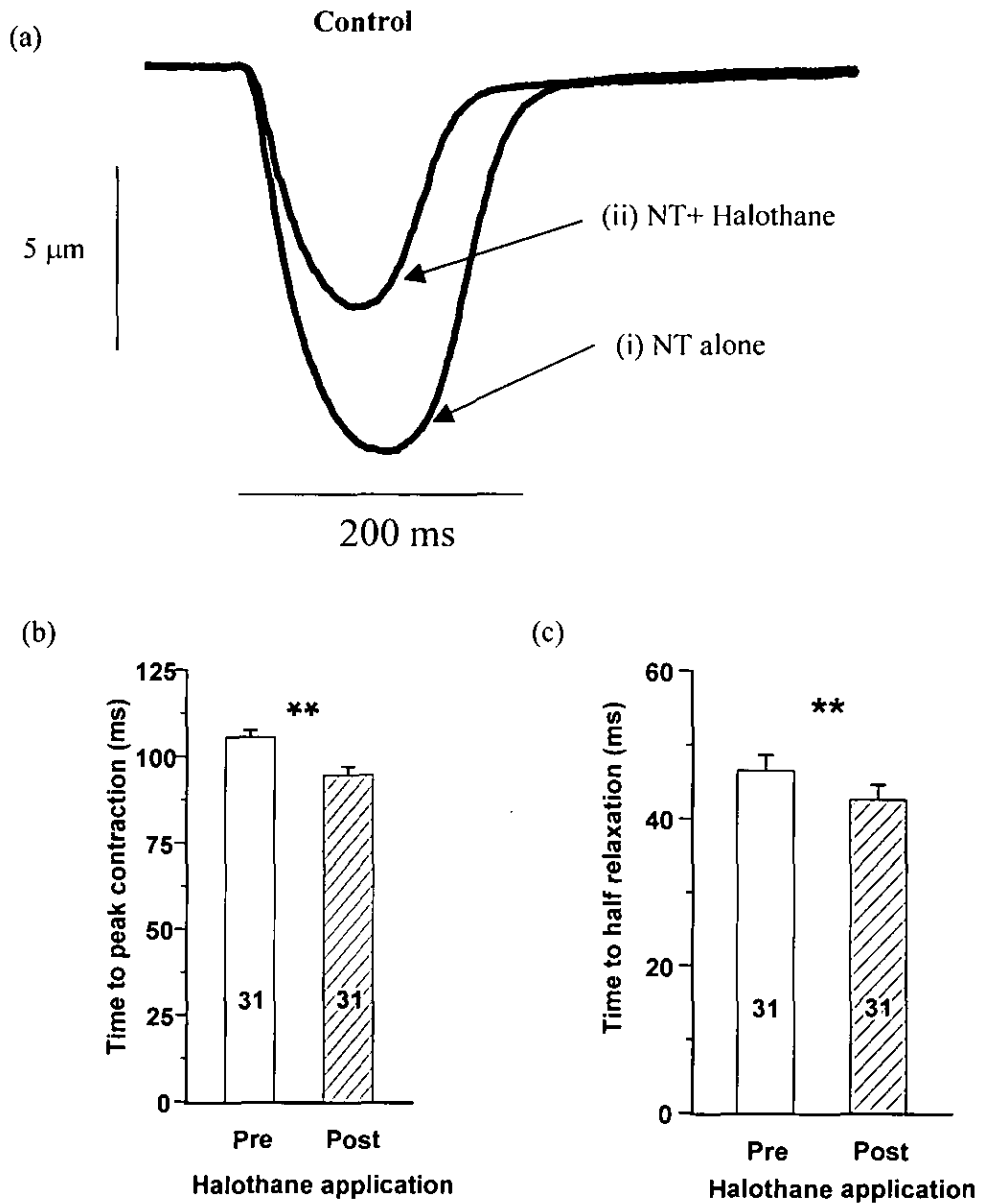


Figure 6.7. (a) Representative fast time-base recordings of contraction in electrically stimulated (1 Hz) rat ventricular myocytes, superfused with either normal Tyrode (NT) alone (Pre) or containing 0.6 mM halothane (Post) at 35-37°C, from age-matched control rat hearts. (b) t_{pk} of contraction and (c), $t_{1/2\text{ relax}}$. Data shown are mean \pm SEM. Numbers within bars represent number of cells. Statistical significance showing Pre *Vs.* Post application of halothane using paired *t* test is represented by ** $P < 0.01$.

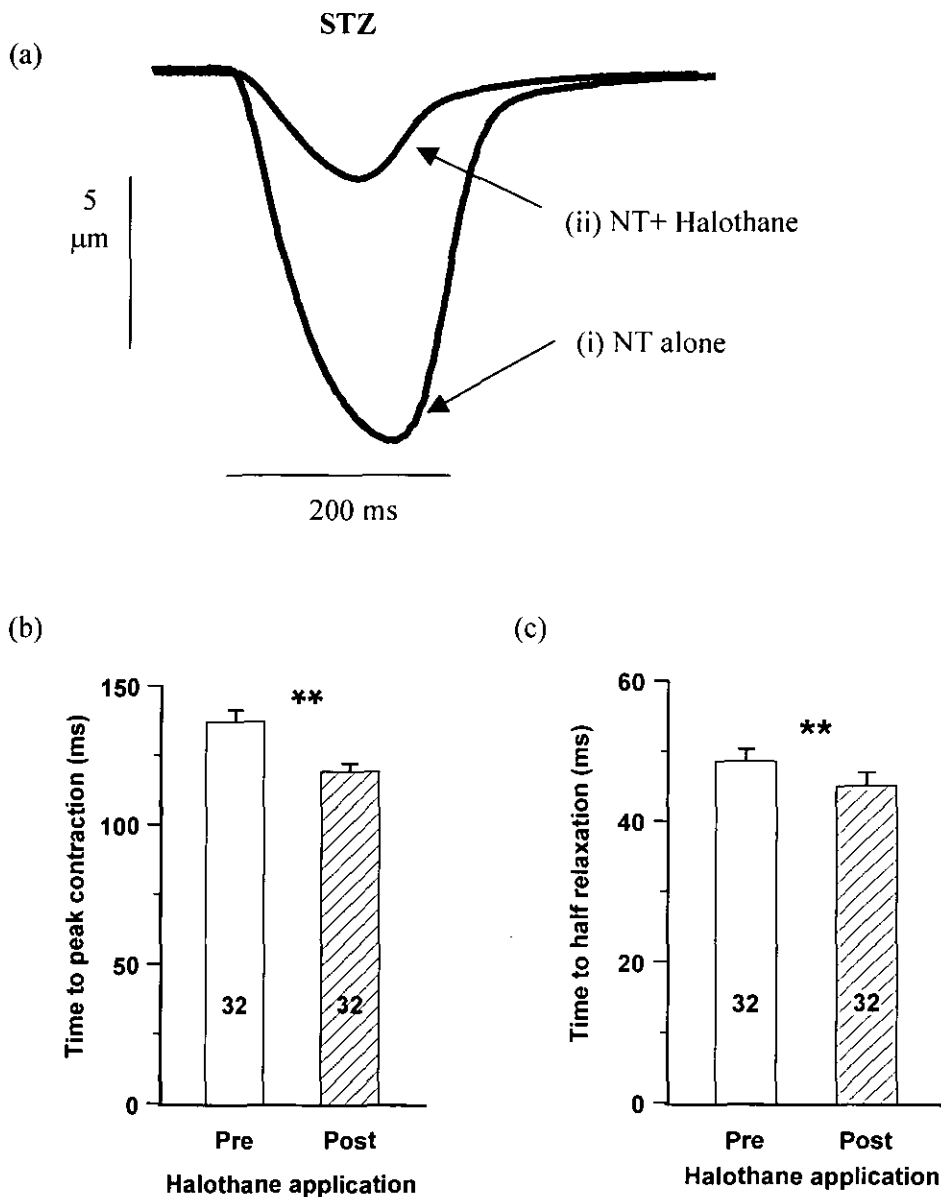


Figure 6.8. (a) Representative fast time-base recordings of contraction in electrically stimulated (1 Hz) rat ventricular myocytes, superfused with either NT alone or NT containing 0.6 mM halothane at 35-37°C, from STZ-induced diabetic rat hearts. (b) t_{pk} of contraction and (c), $t_{1/2, relax}$. Data shown are mean \pm SEM. Numbers within bars represent number of cells. Statistical significance showing Pre Vs. Post application of halothane using paired t test. $**P < 0.01$. Frames in (a) are typical of 32 STZ-treated such myocytes.

6.2.6 Calcium

Figure 6.9. shows typical chart recordings of Ca^{2+} transient in ventricular myocytes taken from age-matched control and STZ-induced diabetic rat heart superfused with either NT solution alone or NT solution containing 0.6 mM halothane. Figure 6.10. shows (a) the amplitude of Ca^{2+} transient measured in ratio units, (b) t_{pk} of Ca^{2+} transient (ms) and (c), $t_{1/2}$ decay of Ca^{2+} transient in the absence and presence of halothane in ventricular myocytes isolated from age-matched control and STZ-induced diabetic rat hearts. The resting level of $[\text{Ca}^{2+}]_i$ (measured as basal ratio units) was not ($P>0.05$) significantly affected by the application of halothane in control and STZ-induced cardiac myocytes. The amplitude of Ca^{2+} transient was significantly reduced in both age-matched control ($P<0.01$) (0.507 ± 0.078 ratio units, $n=13$, *Vs* 0.374 ± 0.054 ratio units, $n=13$) and STZ-induced ($P<0.05$) myocytes (0.513 ± 0.061 ratio units, $n=13$, *Vs* 0.437 ± 0.058 ratio units, $n=13$), in the absence and presence of halothane, respectively (Figure 6.10.a). However, there was no significant ($P>0.05$, paired test) difference between the amplitude of Ca^{2+} in age-matched control and STZ-induced myocytes in the absence and presence of halothane (Figure 6.10.a). The t_{pk} of Ca^{2+} transient was not significantly ($P>0.05$) altered in STZ myocytes (74.7 ± 6.5 msec *Vs*. 68.3 ± 5.4 msec, $n=13$) and age-matched control (66.0 ± 2.8 msec *Vs*. 61.4 ± 3.4 msec, $n=13$) myocytes in the absence and presence of halothane (Figure 6.10.b). Moreover, there is no significant ($P>0.05$, paired test) difference between the t_{pk} of Ca^{2+} transient in age-matched control and STZ-induced myocytes either before or after the application of halothane (Figure 6.10.b). In contrast, the $t_{1/2}$ decay of Ca^{2+} transient was significantly ($P<0.01$) longer in STZ-induced cardiac myocytes (148.4 ± 10.2 msec *Vs*. 160.5 ± 9.93 msec, $n=13$) and control myocytes (104.8 ± 4.5 msec *Vs*. 109.0 ± 4.0 msec, $n=13$), in the absence and presence of halothane, respectively (Figure 6.10.c).

However, the application of halothane did not significantly ($P>0.05$) alter the $t_{1/2}$ decay of Ca^{2+} transient the results obtained in the absence and presence of halothane (Figure 6.10.c).

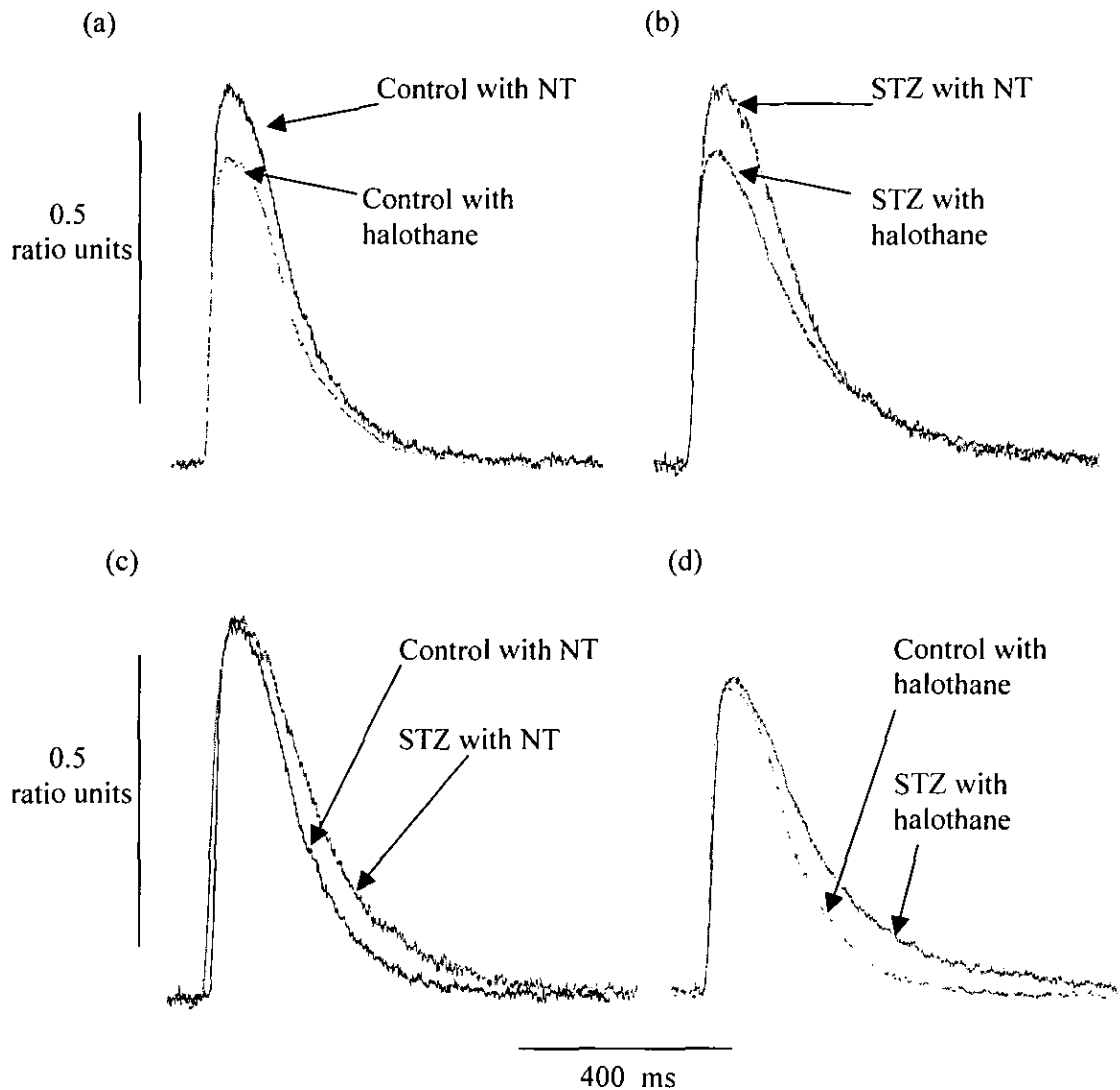


Figure 6.9. Effect of 0.6 mM halothane on Ca^{2+} transients (1 Hz) in control and STZ-induced ventricular myocytes perfused at 35-37°C. Traces are typical of 13 such myocytes from at least 4 rats per group. (a) Control superfused with NT alone and control superfused with NT containing halothane, (b) STZ superfused with NT and STZ superfused with NT containing halothane (c) Control superfused with NT alone and STZ superfused with NT and (d) Control superfused with NT containing halothane and STZ superfused with NT containing halothane.

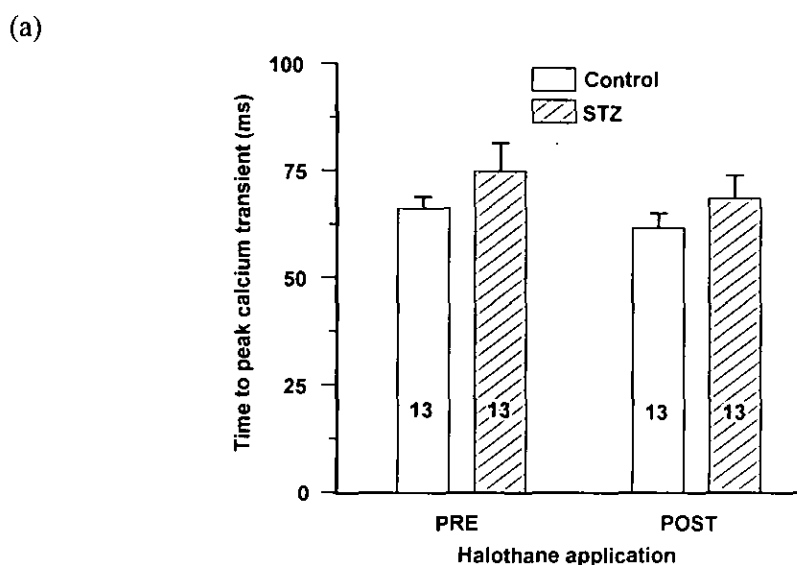
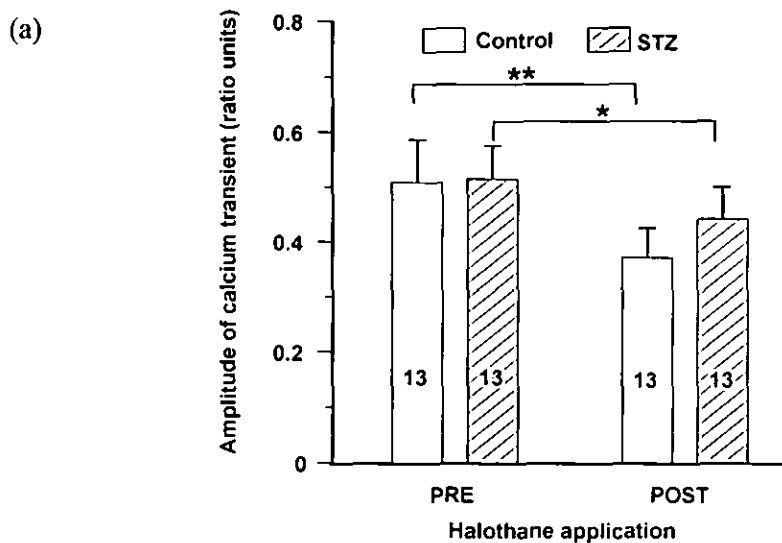


Figure 6.10. Effects of halothane on the (a) amplitude of Ca^{2+} transient and (b) the tpk of Ca^{2+} transient from ventricular myocytes taken from age-matched control (open) and STZ-induced (hatched) diabetic rat hearts perfused at 35-37°C with (a) Control with NT, (b) STZ with NT, (c) Control with 0.6 mM halothane and (d) STZ with 0.6 mM halothane. Data shown are mean \pm SEM. Numbers within bars represent number of cells. Statistical significance showing NT alone vs. NT plus halothane treatment halothane (paired *t* test) and control vs. STZ, (independent samples *t* test). **P* < 0.05 and ***P* < 0.01.

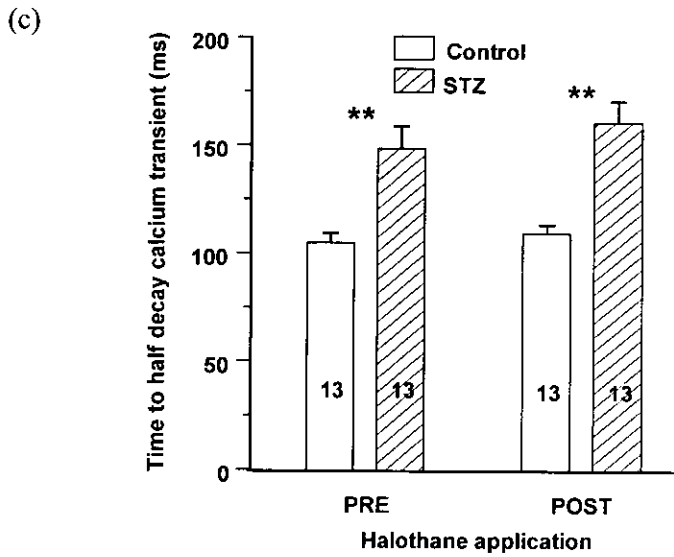


Figure 6.10. (c) Effects of halothane on the $t_{1/2}$ decay of Ca^{2+} transient from ventricular myocytes taken from age-matched control (open) and STZ-induced (hatched) diabetic rat hearts perfused at 35-37°C with (a) Control with NT, (b) STZ with NT, (c) Control with 0.6 mM halothane and (d) STZ with 0.6 mM halothane. Data shown are mean \pm SEM. Numbers within bars represent number of cells. Statistical significance showing NT alone vs. NT plus halothane treatment halothane (paired t test) and control vs. STZ, (independent samples t test). ** $P < 0.01$.

6.2.7 Myofilament calcium sensitivity

Previous reports have suggested that during the final phase of relaxation, cardiac myofilaments come into a quasi-equilibrium state with $[Ca^{2+}]_i$ (Spurgeon *et al.* 1992). Therefore, plotting myocyte cell length against the ratio of emitted fura-2 fluorescence during the final phase of relaxation of a contraction may provide an index of Ca^{2+} sensitivity of the myofilaments.

The relationship between the magnitude of cell length and analogous fura-2 fluorescence ratio from age-matched control and STZ diabetic rats hearts in the absence and presence of halothane are shown in table 6.2, Figure 6.11.a and Figure 6.12.a

	Slope of regression $\mu\text{m}/\text{fura-2}$ fluorescence ratio
Control	$-5.0 \pm 0.6 \mu\text{m}/\text{fura-2}$ fluorescence ratio, $n=13$
STZ	$-13.5 \pm 3.6 \mu\text{m}/\text{fura-2}$ fluorescence ratio, $n=6$ *
Control plus halothane	$-3.7 \pm 0.5 \mu\text{m}/\text{fura-2}$ fluorescence ratio, $n=13\#$
STZ plus halothane	$-9.0 \pm 2.3 \mu\text{m}/\text{fura-2}$ fluorescence ratio, $n=6$ *#

Table 6.2. The slope of regression during the final phase of relaxation in ventricular myocytes obtained from age-matched control and STZ-induced diabetic rat hearts following 8-12 weeks treatment in the absence and presence of halothane (0.6 mM). Data are means \pm S.E.M. Number in parenthesis indicates number of cells. Control *Vs.* STZ in the absence and presence of halothane (0.6 mM) was compared using Student's independent samples *t* test. * $P<0.05$. Control and STZ before and after the application of halothane (0.6 mM) was compared using paired *t* test. # $P<0.05$.

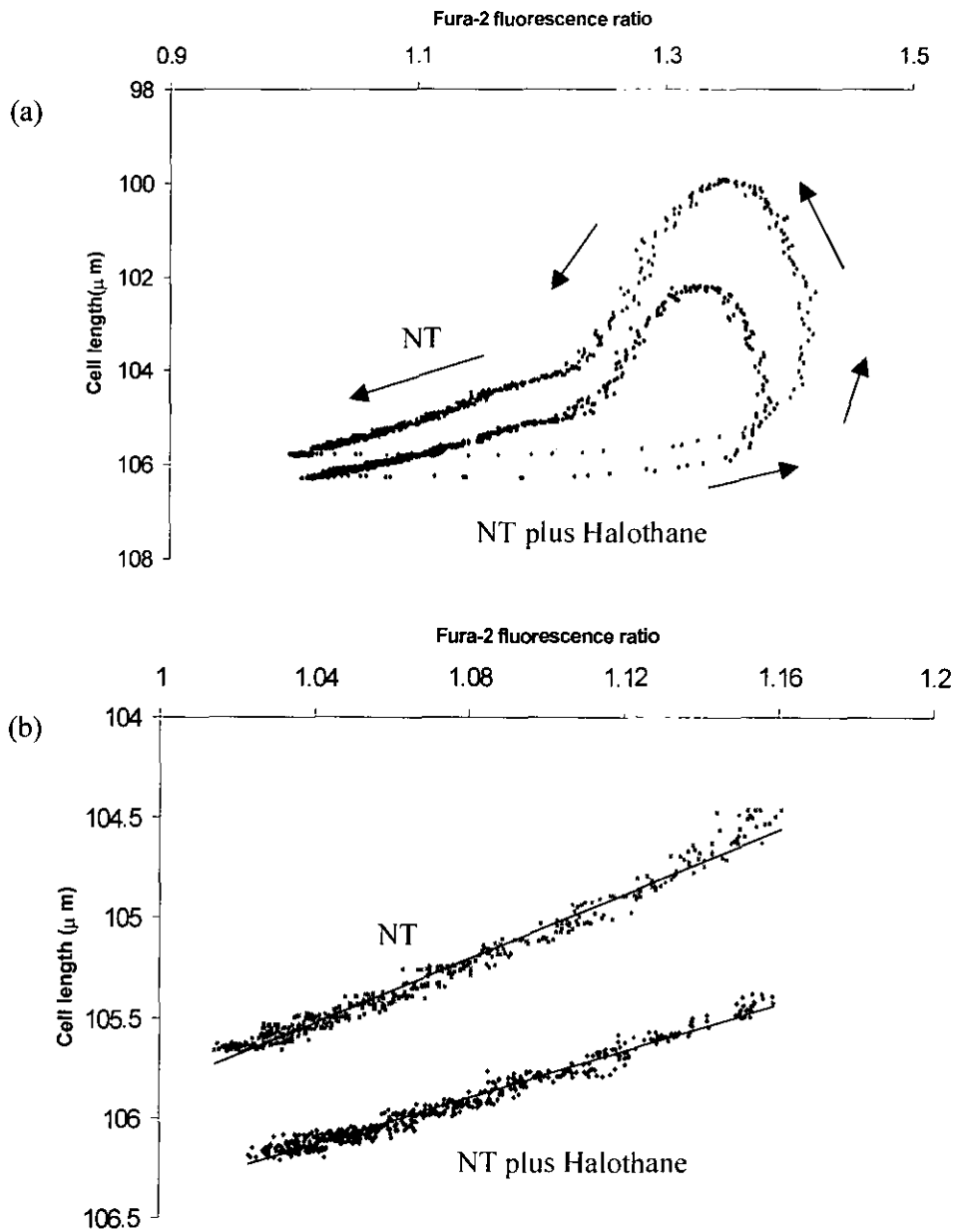


Figure 6.11. Effects of halothane on myofilament Ca^{2+} sensitivity in stimulated (1 Hz) cardiac myocytes from age-matched control rat heart perfused at 35-37°C. (a) Relationship between cell length and ratio obtained during perfusion of NT solution and NT solution plus halothane (0.6 mM) and (b) relationship between the cell length and of fluorescence ratio during the final relaxation phase obtained in myocytes perfused with NT or NT plus halothane. Data in b are fitted with a regression line. Traces are typical observations from 13 such myocytes from at least 4 hearts.

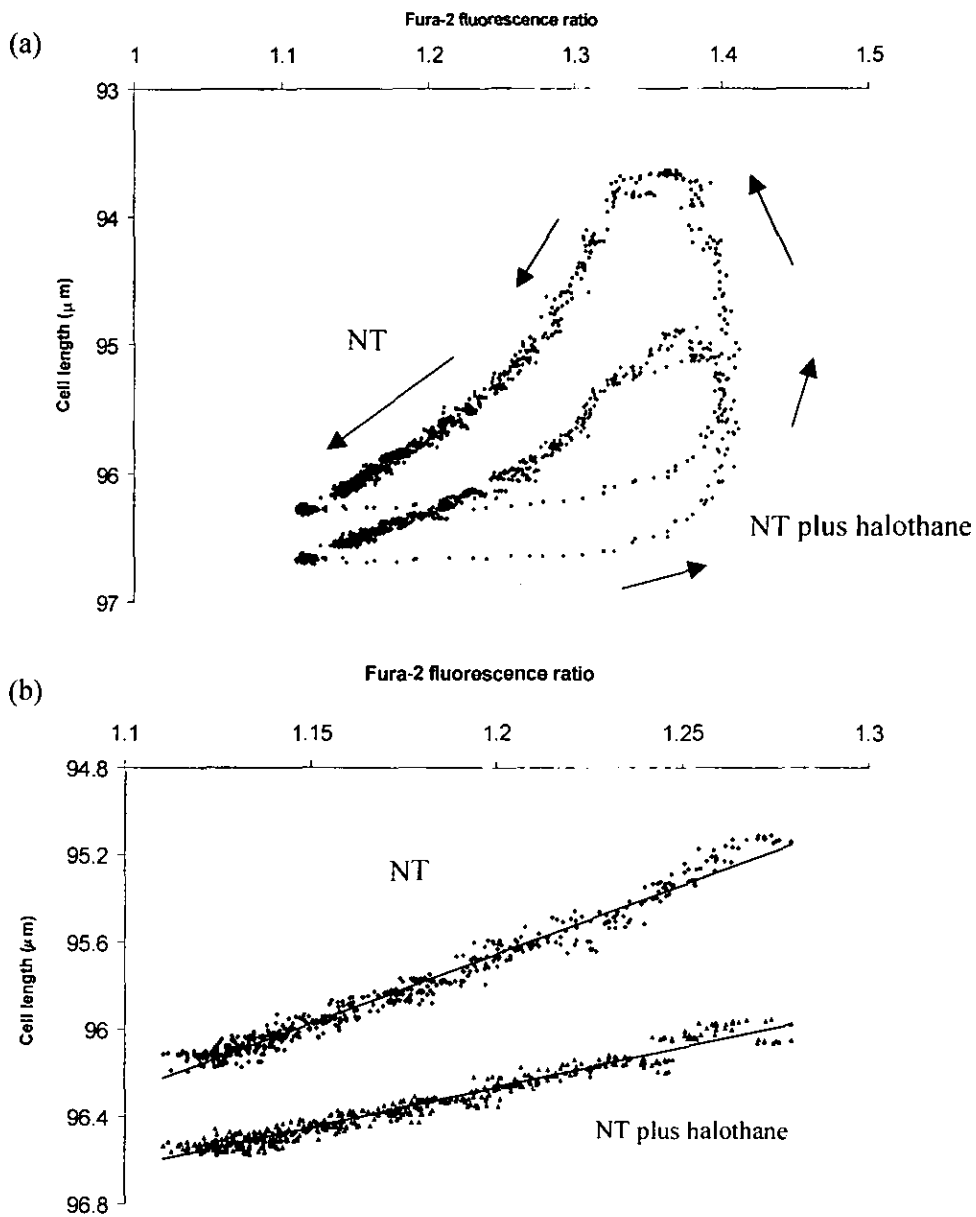


Figure 6.12. Effects of halothane on myofilament Ca^{2+} sensitivity in stimulated (1 Hz) cardiac myocytes from STZ-induced rat heart perfused at 35-37°C. (a) Relationship between cell length and ratio obtained during perfusion of NT solution and NT solution plus halothane (0.6 mM) and b relationship between the cell length and of fluorescence ratio during the final relaxation phase obtained in myocytes perfused with NT or NT plus halothane. Data in b are fitted with a regression line. Traces are typical observations from 13 such myocytes from at least 4 hearts.

6.3 Discussion

6.3.1 $I_{Ca,L}$ amplitude and t_{pk}

This study has reported that the t_{pk} of $I_{Ca,L}$ was not significantly affected by either the diabetic state or by the application of halothane. This would imply that the t_{pk} of $I_{Ca,L}$ does not have a role to play in the downstream characteristics reported in halothane-induced inotropic changes in the heart (Housmans *et al.*, 1988). The $I_{Ca,L}$ amplitude of the cell is indicative of increased $I_{Ca,L}$ and therefore is of direct significance to the influx of Ca^{2+} into the cell. Increased Ca^{2+} influx may lead to increased triggering of Ca^{2+} release from the SR (Bers, 2002). This study has reported that in STZ-induced diabetic myocytes, the amplitude of $I_{Ca,L}$ is significantly less than that of controls, moreover, the application of halothane further reduced the peak amplitude of the $I_{Ca,L}$ in control and STZ-induced diabetic myocytes. This reduction in peak $I_{Ca,L}$ amplitude was more pronounced in halothane treated diabetic myocytes compared to control. A reduction in the $I_{Ca,L}$ has been reported in the following the application of halothane in normal heart (Ikemoto *et al.* 1985; Bosnjak *et al.* 1991). A halothane-induced decrease in $I_{Ca,L}$ will lead to a reduction in SR Ca^{2+} content and may lead to a reduction in the fractional release of Ca^{2+} from the SR. Reduced SR Ca^{2+} release may ultimately contribute to a decrease in the amplitude of contraction.

6.3.2 Current voltage relationship

This study also investigated the relationship between $I_{Ca,L}$ and voltage in the diabetic heart in the presence of halothane. The $I_{Ca,L}$ was significantly reduced in all voltage ranges (-10 mV to 50 mV) in diabetic myocytes compared to control. Moreover, in the presence of halothane, the $I_{Ca,L}$ was further reduced in control myocytes (0 mV to 50 mV) and diabetic

myocytes (10 mV). Diabetes, therefore, in respect of the $I_{Ca,L}$ voltage relationship reduces the $I_{Ca,L}$ at test potentials associated with the opening of the L-type Ca^{2+} channel. This may result in a decrease in Ca^{2+} influx into the cell and contribute to a decrease in trigger Ca^{2+} needed to initiate Ca^{2+} release from SR. Moreover, reduced SR Ca^{2+} release may lead to reduced amounts of Ca^{2+} available for contraction. Following the application halothane, $I_{Ca,L}$ was also significantly reduced in both control and STZ-induced myocytes, which suggest the diabetic state may act synergistically with halothane.

6.3.3 Voltage dependence of contraction

The dependence of voltage on the amplitude of contraction was studied in the STZ-induced diabetic myocytes in the absence and presence of halothane. In this series of experiments the results show that STZ-induced diabetic myocytes displayed significant reduction in the amplitude of contraction at all test potentials tested compared to age-matched control myocytes. Moreover, myocyte shortening was further reduced in diabetic and control myocytes in the presence of halothane. This would suggest that the process by which a voltage test pulse causes the contraction is disrupted by the diabetic state and by the application of halothane. The reduction in contraction occurs because of a reduction in the amount of Ca^{2+} released from the SR or by a reduction in the myofilament sensitivity to Ca^{2+} . It has been reported that halothane reduces the peak $I_{Ca,L}$ amplitude. This would therefore imply that a reduction in Ca^{2+} influx results in a decreased amount of trigger Ca^{2+} and a subsequent decrease in SR Ca^{2+} release and contraction. Moreover, it has been reported in this study that the application of halothane reduces the amplitude of contraction in control and STZ-induced diabetic myocytes.

In contrast, it has been reported within this study that the amplitude of contraction is significantly increased in the STZ-induced diabetic heart compared to that of control in electrically cells. One possible reason for these apparent changes in results may lie with the properties of the diabetic Ap. In the myocardium the height and duration of the Ap greatly correlates to the strength and amplitude of contraction (Fabiato *et al.* 1985). Moreover, Bouchard & Giles, (1995), showed that increased Ap duration resulted in a two-fold decrease in the peak $I_{Ca,L}$, but an increase in the Ca^{2+} transient and the amplitude of contraction. In the diabetic heart it has been reported that the Ap duration is significantly longer than age-matched controls (Shimoni *et al.* 1994; Magyar *et al.* 1992; Jourdan & Feuvray, 1993). An increase in Ap duration in an STZ-induced diabetic myocyte, will be associated with a decrease in the $I_{Ca,L}$ but an increased flux of Ca^{2+} . The increase in Ca^{2+} influx may in turn compensate for any reduction in Ca^{2+} influx via $I_{Ca,L}$ that would be notable in voltage clamped myocytes. This would neutralise differences between control and diabetic myocytes and would result in a similar amount of trigger Ca^{2+} for both groups. Consequently, this may lead to a similar release of Ca^{2+} from the SR. This is in agreement with results detailed within chapter 5. An increase in contraction, in the electrically stimulated myocytes in the absence of any relative (compared to control) changes in Ca^{2+} released from the SR is likely to be due to a change in the myofilament sensitivity for Ca^{2+} . In the patch clamped myocyte, however, the Ap is not a factor due to the voltage clamp protocols. Therefore in these cells, reduced $I_{Ca,L}$ would lead to a reduction in Ca^{2+} influx and subsequent reduction in trigger Ca^{2+} . This may contribute to a reduction in SR Ca^{2+} release and a subsequent reduction in contraction that has been reported in this study in STZ-induced myocyte.

6.3.4 Contraction

In the diabetic state it has been reported that contractile function is significantly altered (Choi *et al.*, 2002). Moreover, other reports suggest that halothane has a negative inotropic effect on the normal heart (Harrison *et al.*, 1999). This study has investigated the effects of halothane on the STZ-induced diabetic heart. Although halothane was found to significantly depress the amplitude of contraction in both control and STZ-induced myocytes, the reduction in the amplitude of contraction was significantly greater in diabetic myocytes compared to age-matched controls. This interesting observation suggests that either the release of Ca^{2+} from the SR during stimulation is decreased (this may be due to either less influx of Ca^{2+} from the cellular medium) or myofilament sensitivity to Ca^{2+} is reduced. Either or both would bring about a decrease in contraction. Moreover, halothane significantly decreased the t_{pk} and $t_{1/2}$ decay of contraction in the diabetic heart, an observation that has been reported in the normal heart too (Housmans *et al.* 2000). A change in the t_{pk} of contraction may be a consequence of a change in RyR sensitivity for trigger Ca^{2+} . Interestingly, in the diabetic heart it has been reported that the t_{pk} is increased (Howarth *et al.* 2001). This suggests that STZ-induced diabetes affect cardiac myocytes contractility in opposing way with respect to halothane. In this study halothane reversed the increased contraction and the t_{pk} of contraction that has previously been reported in the diabetic heart (Howarth *et al.*, 2001).

6.3.5 Calcium

It has been reported in chapter 6 in this study that an alteration in contraction induced by halothane is likely to be caused by a change in Ca^{2+} homeostasis within the cell. Therefore, this study has investigated the effect of halothane on electrically stimulated (1 Hz) Ca^{2+} transients in control and STZ-induced myocytes, and has demonstrated that halothane can significantly reduce the amplitude of Ca^{2+} transient in both control and STZ-induced

cardiac myocytes. The application of halothane itself, therefore is likely to account for the reduction in the amplitude of Ca^{2+} release in stimulated myocytes. The reduction in Ca^{2+} may be attributable to a number of factors including, the reduction in trigger Ca^{2+} through $I_{\text{Ca,L}}$ (which has been reported in this study) or a reduction in SR Ca^{2+} content or fractional release. SR Ca^{2+} content has been reported to be reduced by halothane in normal rat ventricular myocytes (Davies *et al.*, 2000). In the present study, it has been shown that the peak amplitude of $I_{\text{Ca,L}}$ is reduced by halothane. Therefore, it is acceptable to suggest that a decrease in $I_{\text{Ca,L}}$ and therefore Ca^{2+} influx leads to a reduction in SR Ca^{2+} release in the presence of halothane. The t_{pk} and $t_{1/2}$ decay of Ca^{2+} transient were not significantly altered by halothane in control and STZ-induced diabetic myocytes. It is therefore likely that in the STZ-induced diabetic heart, halothane has no significant effect on either Ca^{2+} efflux or Ca^{2+} uptake during diastole.

6.3.6 Myofilament sensitivity

The results in this study have shown that the slope of regression during the final phase of relaxation in STZ-induced myocytes was significantly increased compared to age-matched controls. Therefore, this study is the first to suggest that the sensitivity of the cardiac myofilaments to $[\text{Ca}^{2+}]_i$ in the STZ-induced diabetic hearts is significantly increased compared to that of controls. We have thus far reported that within electrically stimulated STZ-induced diabetic myocytes, the amplitude of contraction is significantly increased compared to that of control. In contrast, this study has shown that the fractional release and total release of Ca^{2+} from the SR is not changed between control and diabetic myocytes. Therefore, the results from Ca^{2+} and contraction studies have reported that a similar increase in $[\text{Ca}^{2+}]_i$ is mirrored by greater contraction in the diabetic heart. The results in this study therefore suggest that the underlying mechanism that controls this change in

contraction within the diabetic heart is an increase in the sensitivity of the myofilaments for Ca^{2+} in myofilaments. In contrast, following the application of halothane, ventricular myocytes obtained from both age-matched control and STZ-induced diabetic hearts reported a significant reduction in the slope of regression. This would suggest that halothane directly decreases the sensitivity of the myofilament to $[\text{Ca}^{2+}]_i$. This is in agreement with Harrison *et al.* (1999) who reported that halothane induced a reduction in myofilament sensitivity in myocytes from a normal heart. The activity of the cardiac myofilaments is controlled by cross bridge cycling of actin and myosin. Moreover, a change in the affinity of Troponin-C for Ca^{2+} is a primary reason for changes in myofilament sensitivity. Within the diabetic heart it has been reported that the expression of the MHC is switched from the active α -MHC to the less active β -MHC isoform (Golfman *et al.* 1999; Depre *et al.* 2000b; Pierce & Dhalla, 1981) which, has been reported as a factor in cardiac dysfunction (Brouty-Boye *et al.* 1995). It may be that an alteration in MHC isoform and Troponin-C affinity for Ca^{2+} is altered by the diabetic state and may contribute to an increase in myofilament Ca^{2+} sensitivity, which ultimately is responsible for an increase in the amplitude of contraction that has been reported in this study

Chapter 7

General discussion and final comments

This study was developed principally to examine the underlying cellular mechanism(s) that are associated with contractile dysfunction in an experimentally-induced model of type-1 diabetes in the rat heart. A stable model of type-1 diabetes mellitus was induced in male Wistar rats by a single i.p. injection of STZ (60 mg Kg⁻¹) (Howarth *et al.* 2001). The STZ-diabetic heart was characterised by hyperglycaemia, hypoinsulinaemia and changes in osmolarity. Further more total cardiac Ca²⁺, Cu²⁺, Zn²⁺ and Fe²⁺, following 2 months STZ-treatment were significantly elevated compared to controls. Therefore, as well as changes in blood chemistry the diabetic heart is characterised by an alteration in specific cation imbalance. It is suggested these changes may contribute and lead to an alteration in heart function that has been reported in STZ-induced diabetes. To assess the relative contributions of particular parameters within the heart, cardiac myocytes were isolated from ventricular heart tissue, using an enzymatic method to produce single cardiomyocytes. In some experiments, the volatile general anaesthetic, halothane was applied to myocytes. Halothane is known to alter specific properties of E-C coupling in cardiac myocytes from normal hearts (Housmans & Murat, 1988), although very little is known about its effects on the diabetic heart.

Although contractility studies had been reported in human and animal models with diabetes, there appeared to be degree a degree of contradiction regarding results experimental design. Initial studies therefore focussed on measuring contraction. In ventricular myocytes taken from the STZ-induced diabetic rat following 4 weeks, 8-12 weeks, 5 months and 10 month of STZ-treatment, reported significant increases in the amplitude of contraction compared to control. Moreover, the t_{pk} of contraction was significantly longer following 4 and 8-12 weeks and 5 months of STZ-treatment. However, in the 10-month STZ-treated heart, the t_{pk} of contraction was not significantly

altered. Interestingly, the $t_{1/2\text{ relax}}$ was significantly longer following 10 months of STZ-treatment but appeared similar to age-matched controls following 4, 8-12 weeks and 5 months treatment of STZ. These time-dependent changes in the chronic (10 month STZ-induced) model of diabetes may be indicative of a some underlying compensatory process that is instigated within the heart to secure its integrity. Following the application halothane, the amplitude of contraction was depressed in both control and STZ-induced myocytes, but this was significantly more pronounced in the diabetic cells. Moreover the time course of contraction was also effected by the application of halothane in the diabetic heart, suggesting that the diabetic heart is more susceptible to the actions of halothane. In a separate study, it was shown that high glucose (25 mM) increased the amplitude of shortening, the rate of contraction and the rate of relaxation in control, but not in STZ-induced diabetic myocytes, showing that the diabetic heart may be more acclimatized to the increase in glucose.

An increase in contraction is a consequence of increased SR Ca^{2+} release and/or increased myofilament Ca^{2+} sensitivity. A change in Ca^{2+} influx via $I_{\text{Ca,L}}$ has been shown to alter the SR load and fractional Ca^{2+} release (Bouchard *et al.* 1995). Therefore, $I_{\text{Ca,L}}$ and the voltage-dependence of contraction was measured in the STZ-induced diabetic myocytes. The peak amplitude of $I_{\text{Ca,L}}$ was found to be significantly decreased in STZ-induced myocytes compared to age-matched controls. Moreover, following the application of halothane application was further reduced the $I_{\text{Ca,L}}$ in control and STZ-induced diabetic myocytes. The voltage-dependence of contraction was found to be decreased in STZ-myocytes compared to control, thus opposing the results that been obtained in electrically stimulated myocytes. In voltage-clamped myocytes, the depolarising pulse is identical. Reduced $I_{\text{Ca,L}}$ in the STZ-induced myocytes will therefore result in a decrease in Ca^{2+} influx. Reduced Ca^{2+} influx will lead to a decrease in SR Ca^{2+} load and reduced Ca^{2+} release from the SR. It

is therefore likely that a reduction in SR Ca^{2+} release in voltage clamped myocytes from STZ-induced diabetic hearts makes a major contribution in reducing the amplitude of contraction. In electrically stimulated myocytes, however, changes in AP duration may influence changes in the open probability of the L-type Ca^{2+} channel (Sah *et al.* 2003). The open probability of the L-type Ca^{2+} channel is dictated in part by the membrane potential. At more positive potentials there is an increased possibility of L-type Ca^{2+} channel opening. In normal rat myocytes, large $I_{\text{Ca,L}}$ spikes have a rapid membrane repolarisations that, consequently have a rapid phase within the more positive potential and are therefore likely to restrict the open probability and channel activation, as well as accelerating the channel deactivation (Bers, 2002). Moreover it has been shown that in normal rat myocytes, prolonging the AP leads to a reduction in peak $I_{\text{Ca,L}}$, but an increase in Ca^{2+} influx release (Bouchard *et al.* 1995). Increased Ca^{2+} leads to an increased SR load and release and contributes to a positive inotropic effect. In the diabetic heart it is well established that the AP duration is prolonged because of a decrease in I_{to} (Shimoni *et al.* 1994; Magyar *et al.* 1992). It is therefore suggested that in electrically stimulated STZ-induced myocytes, prolonged AP duration leads to a smaller $I_{\text{Ca,L}}$ but increased probability of L-type Ca^{2+} influx. Increased trigger Ca^{2+} is likely to act on the SR and may contribute to the changes in Ca^{2+} release.

To ascertain if changes in contractile function are partly due to alterations in trigger Ca^{2+} influx, Ca^{2+} measurements were taken in the control and diabetic heart. In this study, basal resting Ca^{2+} was increased in the diabetic heart, suggesting that increased $\text{Na}^+/\text{Ca}^{2+}$ -exchanger, possibly through increased $[\text{Na}^+]_i$ could reduce the rate of Ca^{2+} efflux. The amplitude and the t_{pk} of the Ca^{2+} transient through electrically stimulated myocytes or caffeine-induced release were not altered by the diabetic state, suggesting that triggered Ca^{2+} release from the RyR's and fractional Ca^{2+} release is not deranged in STZ-induced

diabetes. These results show that a similar amount of Ca^{2+} release released from the SR in control and diabetic myocytes have different effects on contraction and is therefore likely that myofilament Ca^{2+} sensitivity may play a role in the alteration in contraction within the STZ-induced diabetic heart. It was also observed that the decay of the Ca^{2+} transient in both caffeine-induced and electrically stimulated myocytes appeared significantly longer in STZ-induced diabetic myocytes. A prolonged decay that was observed in the STZ-induced myocytes in the presence of caffeine is an indirect measure of the speed of Ca^{2+} efflux from the cell. In order to ascertain if the prolongation in Ca^{2+} decay was partly or principally due to the $\text{Na}^+/\text{Ca}^{2+}$ -exchanger, NiCl_2 was employed to block this mechanism during a caffeine-induced Ca^{2+} release. In the presence of NiCl_2 , Ca^{2+} efflux in age-matched control myocytes was similar to that seen in diabetic myocytes. Moreover, NiCl_2 did not significantly alter the amplitude of Ca^{2+} release in the diabetic myocytes. This suggests that the $\text{Na}^+/\text{Ca}^{2+}$ -exchanger, but not the PMCA, contributes to a longer decay in Ca^{2+} transient in the diabetic heart.

Myofilament Ca^{2+} sensitivity was assessed by simultaneous measurement of contraction and Ca^{2+} . Plotting cell length with $[\text{Ca}^{2+}]_i$ generated in the final phase of relaxation provided an index of myofilament Ca^{2+} sensitivity (Sturgeon *et al.* 1992). In STZ-induced myocytes myofilament Ca^{2+} sensitivity was significantly increased compared to controls. Therefore, in the STZ-induced diabetic myocytes, increased contraction in the absence of increased $[\text{Ca}^{2+}]_i$ (compared to control) is primarily due to an increase in myofilament Ca^{2+} sensitivity. It is this overriding observation that underpins the differences between the diabetic heart and control within this study. It has been reported that changes in the cross-bridge cycling due to an alteration in MHC isoform (that has been reported in the diabetic heart, (Schaffer *et al.*, 1989a)) may underpin the change in myofilament Ca^{2+} sensitivity that has been demonstrated in this study. In the presence of halothane, myofilament Ca^{2+}

sensitivity was significantly decreased in both control and STZ-induced myocytes. Therefore, it is suggested that decreased in myofilament sensitivity in the following the application of halothane is the overriding mechanism by which contraction is depressed to a greater degree in the diabetic heart. Although a change in expression is a likely candidate for explains the perturbation of myofilament Ca^{2+} in diabetes, it is unlikely that the transient application of halothane would manipulate the filaments in such a manner. It is therefore suggested that direct action of halothane reduces the affinity of troponin-C for Ca^{2+} , and in doing so reduces contraction to a greater degree in the diabetic heart.

7.1 Final conclusion

This main focus of this study has looked at the effects of STZ-induced diabetes on isolated ventricular myocytes. The results of the study have shown that a decrease in $I_{\text{Ca,L}}$ led to an increase in the amplitude of contraction in electrically stimulated STZ-induced myocytes compared to controls and this was primarily due to an increase in myofilament sensitivity for Ca^{2+} and not due to an increase in Ca^{2+} release from the SR. Moreover, the prolonged decay in Ca^{2+} efflux following electrically stimulated and caffeine induced Ca^{2+} release in STZ-induced diabetic myocytes is in part due to dysfunctional $\text{Na}^+/\text{Ca}^{2+}$ -exchanger. It is suggested that prolonged Ap duration primarily through reduced I_{to} , may lead to increased Ca^{2+} influx albeit a reduced $I_{\text{Ca,L}}$. Increased Ca^{2+} influx through $I_{\text{Ca,L}}$ may overcompensate for a decrease in SERCA function (that has been reported in the diabetic heart, Misra *et al.* 1999) and may lead to a similar SR Ca^{2+} load and release in both diabetic and control myocytes. Following SR Ca^{2+} release it is suggested that the increased myofilament Ca^{2+} sensitivity in STZ-induced myocytes leads to an increase in contraction that has been reported in this study.

In voltage clamped myocytes from STZ-induced hearts, however, that are not influenced by the A_p , decreased $I_{Ca,L}$, may lead to a reduction in Ca^{2+} influx through $I_{Ca,L}$, leading to a reduction in trigger Ca^{2+} and subsequent SR Ca^{2+} release. Reduced Ca^{2+} release from the SR, may not be compensate for by the increase in myofilament Ca^{2+} sensitivity in the diabetic heart, and may ultimately lead to a reduction in the amplitude of contraction that has been reported in this study.

It has also been shown that, following the application of halothane, the $I_{Ca,L}$, Ca^{2+} transient and amplitude of contraction were significantly more decreased in STZ-induced myocytes compared to that of control. It is suggested that reduced myofilament Ca^{2+} sensitivity in the presence of halothane contributes to the changes in contraction. However, it is also likely that another mechanism such as fractional Ca^{2+} release and/or SR Ca^{2+} load may also be affected by the actions of halothane in the diabetic heart.

Chapter 8

Appendix

8.1 Solutions

8.1.1 Isolation solution

The composition of the physiological salt solution used during the cell isolation procedure was (in mM) 130, NaCl (VWR, 102415-R), 5.4, KCl (VWR, 1019842); 1.4, MgCl² (VWR, 220933-M); 0.4, NaH₂PO₄ (VWR, 102494-C); 5, HEPES (Sigma, H-3375); 10, glucose; 20, taurine (Sigma, T-0625); 10, creatine (Sigma C-0780) and 0.75 Cal set to pH 7.3 (Orion pH meter, 920-A) with 4 M NaOH (VWR, 10252).

8.1.2 Normal Tyrode (NT) solution

The NT solution used to perfuse cells during experiments contained (in mM) 140, NaCl; 5, KCl; 1, MgCl₂.6H₂O (VWR, 101494-V); 10, glucose; 5, HEPES; 1, CaCl₂; set to pH 7.4 with 4 M NaOH.

8.1.3 Patch pipette solution

Patch pipette solution contained (in mM) 120 mM, CsCl₂ (Sigma, C-3011); 8, K₂ATP (Sigma A-8937); 5, glucose; 10, NaCl; 8, MgCl₂; 10 HEPES set to pH 7.2 with CsOH (Sigma, C-8518).

8.1.4 Halothane solution

Halothane was made up by adding 132.5 µl stock solution halothane to 2.37 ml of stock DMSO. A 60 µl portion of this mixed solution was then added to 50 ml of NT (1 mM Ca²⁺) to give a final halothane concentration of 0.6 mM. All solutions were freshly prepared using either Milli-Q or Millipore grade water.

Chapter 9

References

9.1 References sited within this thesis

Al Shafei AI, Wise RG, Gresham GA, Carpenter TA, Hall LD, & Huang CL (2002).

Magnetic resonance imaging analysis of cardiac cycle events in diabetic rats: the effect of angiotensin-converting enzyme inhibition. *J Physiol* **538**, 555-572.

Albanna II, Eichelberger SM, Khoury PR, Witt SA, Standiford DA, Dolan LM, Daniels SR, & Kimball TR (1998). Diastolic dysfunction in young patients with insulin-dependent diabetes mellitus as determined by automated border detection. *J Am Soc Ech* **11**, 349-355.

Allen CB & Saari JT (1993). Isolated hearts from copper-deficient rats exhibit improved post-ischemic contractile performance. *J Nutr* **123**, 1794-1800.

Allo SN, Lincoln TM, Wilson GL, Green FJ, Watanabe AM, & Schaffer SW (1991). Non-insulin-dependent diabetes-induced defects in cardiac cellular calcium regulation. *Am J Physiol* **260**, C1165-C1171.

Allo SN & Schaffer SW (1990). Defective sarcolemmal phosphorylation associated with noninsulin- dependent diabetes. *Biochim Biophys Acta* **1023**, 206-212.

Altura BM & Altura BT (1985). New perspectives on the role of magnesium in the pathophysiology of the cardiovascular system. II. Experimental aspects. *Magnesium* **4**, 245-271.

Altura BM & Altura BT (1995). Magnesium and cardiovascular biology: an important link between cardiovascular risk factors and atherogenesis. *Cell Mol Biol Res* **41**, 347-359.

Altura BM & Altura BT (1996). Role of magnesium in patho-physiological processes and the clinical utility of magnesium ion selective electrodes. *Scand J Clin Lab Invest Suppl* **224**, 211-234.

Altura BM, Altura BT, Carella A, & Turlapaty PD (1981). Hypomagnesemia and vasoconstriction: possible relationship to etiology of sudden death ischemic heart disease and hypertensive vascular diseases. *Artery* **9**, 212-231.

Amos AF, Mccarty DJ, & Zimmet P (1997). The rising global burden of diabetes and its complications: estimates and projections to the year 2010. *Diabet Med* **14 Suppl 5**, S1-85.

Antzelevitch C, Sicouri S, Litovsky S H, Lukas A, Krishnan S C, Di Diego J M, Gintant G A & Liu D W (1991). Heterogeneity within the ventricular wall Electrophysiology and pharmacology of epicardial endocardial and M cells. *Circ Res* **69**, 1427-1449.

Astorri E, Fiorina P, Gavaruzzi G, Astorri A, & Magnati G (1997). Left ventricular function in insulin-dependent and in non-insulin-dependent diabetic patients: Radionuclide assessment. *Cardiology* **88**, 152-155.

Atkins FL, Dowell RT, & Love S (1985). β -adrenergic receptors, adenylate cyclase activity, and cardiac dysfunction in the diabetic rat. *J Card Pharm* **7**, 66-70.

Aulbach F, Simm A, Maier S, Langenfeld H, Walter U, Kersting U, & Kirstein M (1999). Insulin stimulates the L-type Ca^{2+} current in rat cardiac myocytes. *Cardiovasc Res* **42**, 113-120.

Baartscheer A, Schumacher CA, & Fiolet JW (2000). SR calcium depletion following reversal of the Na⁺/Ca²⁺-exchanger in rat ventricular myocytes. *J Mol Cell Cardiol* **32**, 1025-1037.

Balke CW, Egan TM, & Wier WG (1994). Processes that remove calcium from the cytoplasm during excitation-contraction coupling in intact rat heart cells. *J Physiol* **474**, 447-462.

Barceñas-Ruiz L, Beuckelmann DJ, & Weir WG (1987). Sodium-calcium exchange in the heart: Membrane currents and changes in [Ca²⁺]_i. *Science* **238**(4834), 1720-1722.

Barry WH & Bridge JHB (1993). Intracellular calcium homeostasis in cardiac myocytes. *Circulation* **87**(6), 1806-1815.

Barry WH, Rasmussen Caf J, Ishida H, & Bridge JHB (1986). External Na⁺-independent Ca²⁺ extrusion in cultured ventricular cells. Magnitude and functional significance. *J Gen Physiol* **88**, 393-411.

Bassani JW, Bassani RA, & Bers DM (1994). Relaxation in rabbit and rat cardiac cells: species dependent differences in cellular mechanisms. *J Physiol* **476**, 279-293.

Bassani RA, Bassani JW, & Bers DM (1992). Mitochondrial and sarcolemmal Ca²⁺ transport reduce [Ca²⁺]_i during caffeine contractures in rabbit cardiac myocytes. *J Physiol* **453**, 591-608.

Bassani RA & Bers DM (1994). Na⁺/Ca²⁺-exchanger is required for rest-decay but not for rest-potential of twitches in rabbit and rat ventricular myocytes. *J Mol Cell Cardiol* **26**, 1335-1347.

Bassani RA & Bers DM (1995). Rate of diastolic Ca release from the sarcoplasmic reticulum of intact rabbit and rat ventricular myocytes. *Biophys J* **68**, 2015-2022.

Berlin JR, Cannell MB, & Lederer WJ (1987). Regulation of twitch tension in sheep cardiac Purkinje fibres during calcium overload. *Am J Physiol* **253**, H1540-H1547.

Bers DM (1991). *Excitation-contraction coupling and cardiac contractile force*, 1st Edition. Kluwer Academic Publishers, Dordrecht, The Netherlands.

Bers DM (2002a). *Cardiac excitation-contraction coupling and cardiac contractile force*, 2nd Edition ed. Kluwer Academic Publishers, Dordrecht.

Bers DM (2002b). Cardiac excitation-contraction coupling. *Nature* **415**, 198-205.

Bers DM, Bassani RA, Bassani JW, Baudet S, & Hryshko LV (1993). Paradoxical twitch potentiation after rest in cardiac muscle: increased fractional release of SR calcium. *J Mol Cell Cardiol* **25**, 1047-1057.

Beuckelmann DJ & Wier WG (1988). Mechanism of release of calcium from sarcoplasmic reticulum of guinea-pig cardiac cells. *J Physiol* **405**, 233-255.

Bhimji S, Godin DV, & McNeill JH (1985). Biochemical and functional changes in hearts from rabbits with diabetes. *Diabetologia* **28**, 452-457.

Bhimji S, Godin DV, & Mcneill JH (1986). Insulin reversal of biochemical changes in hearts from diabetic rats. *Am J Physiol* **251**, H670-H675.

Bhimji S & Mcneill JH (1989). Isoproterenol-induced ultrastructural alterations in hearts of alloxan- diabetic rabbits. *Gen Pharmacol* **20**, 479-485.

Bosnjak Z J (1991). Effects of volatile anesthetics on the intracellular calcium transient and calcium current in cardiac muscle cells. *AdvExpMedBiol* **301**, 97-107.

Bosnjak Z J, Aggarwal A, Turner L A, Kampine J M & Kampine J P (1992). Differential effects of halothane enflurane and isoflurane on Ca^{2+} transients and papillary muscle tension in guinea pigs. *Anesthesiology* **76**, 123-131.

Bouchard RA, Clark R & Giles WR (1995). Effects of action potential prolongation on E-C coupling in rat ventricular myocytes. *Circ Res* **76**, 790-801.

Bracken NK, Singh J, Winlow W, & Howarth F C(2003). Mechanisms underlying contractile dysfunction in streptozotocin-induced type 1 and type 2 diabetic cardiomyopathy. In: *Atherosclerosis, Hypertension and Diabetes*, Eds. Pierce GN, Nagano M, Zahradka P, & Dhalla NS, pp. 387-408. Kluwer, Boston.

Brady AJ & Farnsworth SP (1986). Cardiac myocyte stiffness following extraction with detergent and high salt solutions. *Am J Physiol* **250**, H932-H943.

Bridge JHB, Smolley JR, & Spitzer KW (1990). The relationship between charge movements associated with I_{Ca} and I_{Na-Ca} in cardiac myocytes. *Science* **248**, 376-378.

Brouty-Boye D, Kolonias D, & Lampidis TJ (1995). Antiproliferative activity of taxol on human tumor and normal breast cells vs effects on cardiac cells. *Int J Cancer* **60**, 571-575.

Brown AM, Lee KS, & Powell T (1981). Sodium current in single rat heart muscle cells. *J Physiol* **318**, 479-500.

Bryant SM, Shipsey SJ, & Hart G (1997). Regional differences in electrical and mechanical properties of myocytes from guinea-pig hearts with mild left ventricular hypertrophy. *Card Res* **35**, 315-323.

Cannell MB (1991). Contribution of sodium-calcium exchange to calcium regulation in cardiac muscle. *Ann N Y Acad Sci* **639**, 428-443.

Cannell MB, Berlin JR, & Lederer WJ (1987a). Effect of membrane potential changes on the calcium transient in single rat cardiac muscle cells. *Science* **238**, 1419-1423.

Cannell MB, Berlin J R, & Lederer W J (1987b). Intracellular calcium in cardiac myocytes: calcium transients measured using fluorescence imaging. In: *Cell Calcium and the Control of Membrane Transport*, Eds. Mandel LJ & Eaton DC, pp. 201-214. The Rockefeller University Press, New York.

Cannell M B Cheng H & Lederer W J (1994). Spatial non-uniformities in $[Ca^{2+}]_i$ during excitation-contraction coupling in cardiac myocytes. *Biophys J* **67**, 1942-1956.

Cannell M B & Soeller C (1997a). Numerical analysis of ryanodine receptor activation by L-type channel activity in the cardiac muscle diad. *Biophys J* **73**, 112-122.

Caterson ID, Fuller SJ, & Randle PJ (1982). Effect of the fatty acid oxidation inhibitor 2-tetradecylglycidic acid on pyruvate dehydrogenase complex activity in starved and alloxan- diabetic rats. *Biochem J* **208**, 53-60.

Chakraborti S, Chakraborti T, Mandal M, Mandal A, Das S, & Ghosh S (2002). Protective role of magnesium in cardiovascular diseases: a review. *Mol Cell Biochem* **238**, 163-179.

Cheng H, Lederer W J & Cannell M B (1993). Calcium sparks: elementary events underlying excitation-contraction coupling in heart muscle. *Science* **262**, 740-744.

Chen MD, Lin PY, Tsou CT, Wang JJ, & Lin WH (1995). Selected metals status in patients with noninsulin-dependent diabetes-mellitus. *Bioll Trace Elem Res* **50**, 119-124.

Choi HS & Eisner DA (1999). The role of sarcolemmal Ca^{2+} -ATPase in the regulation of resting calcium concentration in rat ventricular myocytes. *J Physiol* **515 (Pt 1)**, 109-118.

Choi KM, Zhong Y, Hoit BD, Grupp IL, Hahn H, Dilly KW, Guatimosim S, Lederer WJ, & Matlib MA (2002). Defective intracellular Ca^{2+} signaling contributes to cardiomyopathy in Type 1 diabetic rats. *Am J Physiol* **283**, H1398-H1408.

Clark A H & Garland C J (1993). Ca^{2+} channel antagonists and inhibition of protein kinase C each block contraction but not depolarization to 5-hydroxytryptamine in the rabbit basilar artery. *Eur J Pharmacol* **235**, 113-116.

Collier M L, Thomas A P & Berlin J R (1999). Relationship between L-type Ca^{2+} current and unitary sarcoplasmic reticulum Ca^{2+} release events in rat ventricular myocytes. *J Physiol* **516 (Pt 1)**, 117-128.

Connelly TJ & Coronado R (1994). Activation of the Ca²⁺ release channel of cardiac sarcoplasmic reticulum by volatile anesthetics. *Anesthesiology* **81**, 459-469.

D'Amico M, Marfella R, Nappo F, Di Filippo C, De Angelis L, Berrino L, Rossi F, & Giugliano D (2001). High glucose induces ventricular instability and increases vasomotor tone in rats. *Diabetologia* **44**, 464-470.

Davidoff AJ & Ren J (1997). Low insulin and high glucose induce abnormal relaxation in cultured adult rat ventricular myocytes. *Am J Phys* **41**, H159-H167.

Davies DN, Steward A, Allott PR, & Mapleson WW (1972). A comparison of arterial and arterialized venous concentrations of halothane. *Br J Anaesth* **44**, 548-550.

Davies LA, Gibson CN, Boyett MR, Hopkins PM, & Harrison SM (2000). Effects of isoflurane, sevoflurane, and halothane on myofilament Ca²⁺ sensitivity and sarcoplasmic reticulum Ca²⁺ release in rat ventricular myocytes. *Anesthesiology* **93**, 1034-1044.

Davies LA, Hamilton DL, Hopkins PM, Boyett MR, & Harrison SM (1999). Concentration-dependent inotropic effects of halothane, isoflurane and sevoflurane on rat ventricular myocytes. *Br J Anaesth* **82**, 723-730.

Depre C, Young ME, Ying J, Ahuja HS, Han Q, Garza N, Davies PJ, & Taegtmeyer H (2000a). Streptozotocin-induced changes in cardiac gene expression in the absence of severe contractile dysfunction. *J Mol Cell Cardiol* **32**, 985-996.

Depre C, Young ME, Ying J, Ahuja HS, Han Q, Garza N, Davies PJ, & Taegtmeyer H (2000). Streptozotocin-induced changes in cardiac gene expression in the absence of severe contractile dysfunction. *J Mol Cell Cardiol* **32**, 985-996.

Dhalla NS, Pierce GN, Innes IR, & Beamish RE (1985). Pathogenesis of cardiac dysfunction in diabetes mellitus. *Can J Cardiol* **1**, 263-281.

Eger E I, Smith N T, Stoelting R K, Cullen D J, Kadis L B & Whitcher C E (1970). Cardiovascular effects of halothane in man. *Anesthesiology* **32**, 396-409.

Egger M, Ruknudin A, Niggli E, Lederer WJ, & Schulze DH (1999). Ni^{2+} transport by the human $\text{Na}^+/\text{Ca}^{2+}$ -exchanger expressed in Sf9 cells. *Am J Physiol* **276**, C1184-C1192.

Elamin A & Tuvemo T (1990). Magnesium and insulin-dependent diabetes mellitus. *Diab Res Clin Pract* **10**, 203-209.

Ellingsen O, Davidoff AJ, Prasad SK, Berger HJ, Springhorn JP, Marsh JD, Kelly RA, & Smith TW (1993). Adult rat ventricular myocytes cultured in defined medium: Phenotype and electromechanical function. *Am J Physiol* **265**, H747-H754.

Elsner M, Guldbakke B, Tiedge M, Munday R, & Lenzen S (2000). Relative importance of transport and alkylation for pancreatic beta- cell toxicity of streptozotocin. *Diabetologia* **43**, 1528-1533.

Eskinder H, Rusch N J, Supan F D, Kampine J P & Bosnjak Z J (1991). The effects of volatile anesthetics on L- and T-type calcium channel currents in canine cardiac Purkinje cells. *Anesthesiology* **74**, 919-926.

Ewis SA & AbdelRahman MS (1995). Effect of metformin on glutathione and magnesium in normal and streptozotocin-induced diabetic rats. *J App Tox* **15**, 387-390.

Fabiato A (1983). Calcium-induced release of calcium from the cardiac sarcoplasmic reticulum. *Am J Physiol* **14**, C1-C14.

Fabiato A (1985). Time and calcium dependence of activation and inactivation of calcium-induced release of calcium from the sarcoplasmic reticulum of a skinned canine cardiac Purkinje cell. *J Gen Physiol* **85**, 247-289.

Fan J S & Palade P (1999). One calcium ion may suffice to open the tetrameric cardiac ryanodine receptor in rat ventricular myocytes. *J Physiol* **516** (Pt 3), 769-780.

Fein FS, Kornstein LB, Strobeck JE, Capasso JM, & Sonnenblick EH (1980). Altered myocardial mechanics in diabetic rats. *Circ Res* **47**, 922-933.

Fein FS, Miller-Green B, & Sonnenblick EH (1985). Altered myocardial mechanics in diabetic rabbits. *Am J Physiol* **248**, H729-H736.

Ferrier GR & Howlett SE (1995). Contractions in guinea-pig ventricular myocytes triggered by a calcium-release mechanism separate from Na^+ and $I_{\text{Ca,L}}$. *J Physiol* **484**, 107-122.

Ford ES (2000). Serum copper concentration and coronary heart disease among US adults. *Am J Epidemiol* **151**, 1182-1188.

Frampton JE, Harrison SM, Boyett MR, & Orchard CH (1991b). Ca^{2+} and Na^+ in rat myocytes showing different force-frequency relationships. *Am J Physiol* **261**, C739-C750.

Frampton JE, Orchard CH, & Boyett MR (1991a). Diastolic, systolic and sarcoplasmic reticulum Ca^{2+} during inotropic interventions in isolated rat myocytes. *J Physiol* **437**, 351-375.

Fujioka Y, Komeda M, & Matsuoka S (2000). Stoichiometry of $\text{Na}^+/\text{Ca}^{2+}$ -exchanger in inside-out patches excised from guinea-pig ventricular myocytes. *J Physiol* **523 Pt 2**, 339-351.

Gando S (1994). Pharmacological studies on alterations in myocardial beta- adrenoceptors and their intracellular signal transduction in experimental diabetic rats. *Hokkaido Igaku Zasshi* **69**, 1140-1153.

Gando S, Hattori Y, Akaishi Y, Nishihira J, & Kanno M (1997). Impaired contractile response to beta adrenoceptor stimulation in diabetic rat hearts: Alterations in beta adrenoceptors-G protein adenylate-cyclase system and PLB phosphorylation. *J Pharm Expl Therap* **282(1)**, 475-484.

Ganguly PK, Pierce GN, Dhalla KS, & Dhalla NS (1983). Defective sarcoplasmic reticular calcium transport in diabetic cardiomyopathy. *Am J Physiol* **244**, E528-E535.

Gaughan J P, Hefner C A & Houser S R (1998). Electrophysiological properties of neonatal rat ventricular myocytes with alpha1-adrenergic-induced hypertrophy. *Am J Physiol* **275**, H577-H590.

Gerstein HC (1997). Glucose: a continuous risk factor for cardiovascular disease. *Diab Med* **14**, S25-S31.

Golfman L, Dixon IM, Takeda N, Chapman D, & Dhalla NS (1999). Differential changes in cardiac myofibrillar and sarcoplasmic reticular gene expression in alloxan-induced diabetes. *Mol Cell Biochem* **200**, 15-25.

Golik A, Cohen N, Ramot Y, Maor J, Moses R, Weissgarten J, Leonov Y, & Modai D (1993). Type II diabetes mellitus, congestive heart failure, and zinc metabolism. *Biol Trace Elem Res* **39**, 171-175.

Gordon EA & Guppy LJ (1999). Cardiomyopathic changes in streptozotocin-induced diabetes. *Proc West Pharmacol Soc* **42**, 83-86.

Greenstein J L, Wu R Po S, Tomaselli G F & Winslow R L (2000). Role of the calcium-independent transient outward current $I_{(to)}$ in shaping action potential morphology and duration. *Circ Res* **87**, 1026-1033

Guatimosim S, Dilly K, Santana L F, Saleet J M, Sobie E A & Lederer W J (2002). Local Ca^{2+} signaling and EC coupling in heart: Ca^{2+} sparks and the regulation of the $[Ca^{2+}]_i$ transient. *J Mol Cell Cardiol* **34**, 941-950.

Ha T, Kotsanas G, & Wendt I (1999). Intracellular Ca^{2+} and adrenergic responsiveness of cardiac myocytes in streptozotocin-induced diabetes. *Clin Exp Pharmacol Physiol* **26**, 347-353.

Hallmans G & Lithner F (1980). Early changes in zinc and copper metabolism in rats with alloxan diabetes of short duration after local traumatization with heat. *Ups J Med Sci* **85**, 59-66.

Han J, Leem C, So I, Kim E, Hong S, Ho W, Sung H & Earm Y E (1994). Effects of thyroid hormone on the calcium current and isoprenaline-induced background current in rabbit ventricular myocytes. *J Mol Cell Cardiol* **26**, 925-935.

Harris M & Zimmet P (1997). Classification of diabetes mellitus and other categories of glucose intolerance. In: *International Textbook of Diabetes Mellitus*, Eds. Zimmet AK, DeFronzo R, & Keen H, pp. 9-23. Wiley, Chichester.

Harrison SM, Robinson M, Davies LA, Hopkins PM, & Boyett MR (1999). Mechanisms underlying the inotropic action of halothane on intact rat ventricular myocytes. *Br J Anaesth* **82**, 609-621.

Hattori Y, Azuma M, Gotoh Y & Kanno M (1987). Negative inotropic effects of halothane enflurane and isoflurane in papillary muscles from diabetic rats. *Anesth Analg* **66**, 23-28.

Hattori Y, Matsuda N, Kimura J, Ishitani T, Tamada A, Gando S, Kemmotsu O, & Kanno M (2000). Diminished function and expression of the cardiac Na⁺/Ca²⁺-exchanger in diabetic rats: implication in Ca²⁺ overload. *J Physiol* **527 Pt 1**, 85-94.

Hayashi H & Noda N (1997). Cytosolic Ca²⁺ concentration decreases in diabetic rat myocytes. *Cardiovasc Res* **34**, 99-103.

Heller B, Burkle A, Radons J, Fengler E, Jalowy A, Muller M, Burkart V, & Kolb H (1994). Analysis of oxygen radical toxicity in pancreatic islets at the single cell level. *Biol Chem Hoppe Seyler* **375**, 597-602.

Heyliger CE, Pierce GN, Singal PK, Beamish RE, & Dhalla NS (1982). Cardiac alpha- and beta-adrenergic receptor alterations in diabetic cardiomyopathy. *Basic Res Cardiol* **77**, 610-618.

Heyliger CE, Prakash A, & McNeill JH (1987). Alterations in cardiac sarcolemmal Ca^{2+} pump activity during diabetes mellitus. *Am J Physiol* **252**, H540-H544.

Horackova M & Murphy MG (1988). Effects of chronic diabetes mellitus on the electrical and contractile activities, $^{45}\text{Ca}^{2+}$ transport, fatty acid profiles and ultrastructure of isolated rat ventricular myocytes. *Pflugers Arch* **411**, 564-572.

Housmans PR & Murat I (1988). Comparative effects of halothane, enflurane, and isoflurane at equipotent anesthetic concentrations on isolated ventricular myocardium of the ferret. II. Relaxation. *Anesthesiology* **69**, 464-471.

Howarth FC, Calaghan SC, Boyett MR, & White E (1999). Effect of the microtubule polymerizing agent taxol on contraction, Ca^{2+} transient and L-type Ca^{2+} current in rat ventricle cells. *J Physiol* **516.2**, 409-419.

Howarth FC & Levi AJ (1996). Intracellular magnesium modulates voltage dependence of Ca^{2+} release in rabbit ventricular myocytes. *J Mol Cell Cardiol* **28**, P11-A222.

Howarth FC & Levi AJ (1998). Internal free magnesium modulates the voltage dependence of contraction and Ca^{2+} transient in rabbit ventricular myocytes. *Pflugers Arch* **435**, 687-698.

Howarth FC, Qureshi MA, Bracken NK, Winlow W, & Singh J (2001). Time-dependent effects of streptozotocin-induced diabetes on contraction of ventricular myocytes from rat heart. *Emirates Med J* **19**, 35-41.

Howarth FC, Qureshi MA, Lawrence P, & Adeghate E (2000). Chronic effects of streptozotocin-induced diabetes on the ultrastructure of rat ventricular and papillary muscle. *Acta Diabetol* **37**, 119-124.

Howarth FC, Qureshi MA, & White E (2002). Effects of hyperosmotic shrinking on ventricular myocyte shortening and intracellular Ca^{2+} in streptozotocin-induced diabetic rats. *Pflugers Arch* **444**, 446-451.

Huang W, Lai C C, Wang Y, Askari A, Klevay L M, Askari A & Chiu T H (1995). Altered expressions of cardiac Na/K-ATPase isoforms in copper deficient rats. *Cardiovasc Res* **29**, 563-568.

Huxley AF (2000). Mechanics and models of the myosin motor. *Philos Trans R Soc Lond B Biol Sci* **355**, 433-440.

Ikemoto Y, Yatani A, Arimura H, & Yoshitake J (1985) Reduction of the slow inward current of isolated rat ventricular cells by thiamylal and halothane. *Acta Anaesthesiol Scand* **29**, 583-586.

Inoguchi T, Battan R, Handler E, Sportsman JR, Heath W, & King GL (1992). Preferential elevation of PKC isoform beta II and diacylglycerol levels in the aorta and heart of diabetic rats: differential reversibility to glycemic control by islet cell transplantation. *PNAS* **89**, 11059-11063.

Ishitani T, Hattori Y, Sakuraya F, Onozuka H, Makino T, Matsuda N, Gando S, & Kemmotsu O (2001). Effects of Ca^{2+} sensitizers on contraction, $[Ca^{2+}]_i$ transient and myofilament Ca^{2+} sensitivity in diabetic rat myocardium: potential usefulness as inotropic agents. *J Pharmacol Exp Ther* **298**, 613-622.

Jorgensen AO, Shen ACY, Daly P, & MacLennan DH (1982). Localization of Ca^{2+} + Mg^{2+} -ATPase of the sarcoplasmic reticulum in adult rat papillary muscle. *J Cell Biol* **93**, 883-892.

Josephson I R, Sanchez-Chapula J & Brown A M (1984). Early outward current in rat single ventricular cells. *Circ Res* **54**, 157-162.

Joslin EP (1948). *The Unknown Diabetic*, 4th Edition, pp. 302-306.

Jourdon P & Feuvray D (1993). Calcium and potassium currents in ventricular myocytes isolated from diabetic rats. *J Physiol* **470**, 411-429.

Julien J (1997). Cardiac complications in non-insulin-dependent diabetes mellitus. *J Diab Comp* **11**, 123-130.

Kameyama A, Yazawa K, Kaibara M, Ozono K & Kameyama M (1997). Run-down of the cardiac Ca^{2+} channel: characterization and restoration of channel activity and cytoplasmic factors. *Pflugers Arch* **433**, 547-556.

Kanaya N, Matsumoto M, Kawana S, Tsuchida H, Kimura H, Miyamoto A, Ohshika H & Namiki A (1998). Ca^{2+} channel modulation alters halothane-induced depression of ventricular myocytes. *Can J Anaesth* **45**, 584-591.

Kang N, Alexander G, Park JK, Maasch C, Buchwalow I, Luft FC, & Haller H (1999). Differential expression of protein kinase C isoforms in streptozotocin- induced diabetic rats. *Kid Int* **56**, 1737-1750.

Kassiri Z, Myers R, Kaprielian R, Banijamali HS, & Backx PH (2000). Rate-dependent changes of twitch force duration in rat cardiac trabeculae: a property of the contractile system. *J Physiol* **524 Pt 1**, 221-231.

Katoh H, Noda N, Hayashi H, Satoh H, Terada H, Ohno R, & Yamazaki N (1995). Intracellular sodium concentration in diabetic rat ventricular myocytes. *Jpn Heart J* **36**, 647-656.

Katz AM (1977). *Physiology of the Heart*, 1st ed. Raven Press, New York.

Kim HW, Ch YS, Lee HR, Park SY, & Kim YH (2001). Diabetic alterations in cardiac sarcoplasmic reticulum Ca^{2+} -ATPase and phospholamban protein expression. *Life Sci* **70**, 367-379.

King H, Aubert RE, & Herman WH (1998). Global burden of diabetes, 1995-2025: prevalence, numerical estimates, and projections. *Diabetes Care* **21**, 1414-1431.

Kiss A, Kertesz T, Koltai MZ, Cserhalmi L, Jermendy G, Kammerer L, Zrinyi T, & Pogatsa G (1988). Left ventricular diastolic function in diabetics. *Acta Physiol Hung* **71**, 227-232.

Kissin I, Thomson C T & Smith L R (1983). Effect of halothane on contractile function of ischemic myocardium. *J Cardiovasc Pharmacol* **5**, 438-442.

Klevay LM (2000). Cardiovascular disease from copper deficiency--a history. *J Nutr* **130**, 489S-492S.

Kohmoto O, Levi AJ, & Bridge JHB (1994). Relation between reverse $\text{Na}^+/\text{Ca}^{2+}$ -exchanger and sarcoplasmic reticulum calcium release in guinea-pig ventricular cells. *Circ Res* **74**, 550-554.

Kotsanas G, Delbridge LM, & Wendt IR (2000). Stimulus interval-dependent differences in Ca^{2+} transients and contractile responses of diabetic rat cardiomyocytes. *Cardiovasc Res* **46**, 450-462.

Kranias EG & Solaro RJ (1982). Phosphorylation of Troponin I and phospholamban during catecholamines stimulation of rabbit heart. *Nature* **298**(5870), 182-184.

Kroncke KD, Fehsel K, Sommer A, Rodriguez ML, & Kolb-Bachofen V (1995). Nitric oxide generation during cellular metabolism of the diabetogenic N-methyl-N-nitroso-

urea streptozotocin contributes to islet cell DNA damage. *Biol Chem Hoppe Seyler* **376**, 179-185.

Kurihara S & Sakai T (1985). Effects of rapid cooling on mechanical and electrical responses in ventricular muscle of guinea-pig. *J Physiol* **361**, 361-378.

Laakso M (1999). Hyperglycemia and cardiovascular disease in type 2 diabetes. *Diabetes* **48**, 937-942.

Lagadic-Gossmann D, Buckler KJ, Le Prigent K, & Feuvray D (1996). Altered Ca²⁺ handling in ventricular myocytes isolated from diabetic rats. *Am J Physiol* **270**, H1529-H1537.

Langendorff O (1895). Untersuchungen am berlebenden Saugtierherzen. *Pflugers Arch* **61**, 291-332.

Leblanc N & Hume JR (1990). Sodium current-induced release of calcium from cardiac sarcoplasmic reticulum. *Science* **248**, 372-376.

Lee JC & Downing SE (1976). Effects of insulin on cardiac muscle contraction and responsiveness to norepinephrine. *Am J Physiol* **230**, 1360-1365.

Lee SL, Ostadalova I, Kolar F, & Dhalla NS (1992). Alterations in Ca²⁺-channels during the development of diabetic cardiomyopathy. *Mol Cell Biochem* **109**, 173-179.

Leoty C, Huchet-Cadiou C, Talon S, Choisy S, & Hleihel W (2001). Caffeine stimulates the reverse mode of Na⁺/Ca²⁺-exchanger in ferret ventricular muscle. *Acta Physiol Scand* **172**, 27-37.

Levi AJ, Brooksby P, & Hancox JC (1993a). A role for depolarisation-induced calcium entry on the Na⁺/Ca²⁺-exchanger in triggering intracellular calcium release and contraction in rat ventricular myocytes. *Cardiovas Res* **27**, 1677-1690.

Levi AJ, Brooksby P, & Hancox JC (1993b). One hump or two? - The triggering of calcium release from the sarcoplasmic reticulum and the voltage-dependence of contraction in mammalian cardiac muscle. *Cardiovas Res* **27**, 1743-1757.

Levi AJ, Hancox JC, Howarth FC, Croker J, & Vinnicombe J (1996). A method for making rapid changes of superfusate whilst maintaining temperature at 37°C. *Pflügers Arch* **432**, 930-937.

Levi AJ, Hobai IA, Dalton GR, Howarth FC, Pabbathi VK, Hancox JC, & Ferrier GR (1997). Sarcoplasmic reticulum Ca²⁺ release activated by membrane depolarisation in the absence of Ca²⁺ entry, in heart cells from rabbit, rat and guinea-pig. *Biophys J* **72** (2), 161-166.

Levick JR (1995). *An Introduction into Cardiovascular Physiology*, 2nd ed. Butterworth-Heinemann, Oxford.

Li G R, Feng J, Yue L & Carrier M (1998). Transmural heterogeneity of action potentials and I_{to1} in myocytes isolated from the human right ventricle. *Am J Physiol* **275**, H369-H377

Linz K W & Meyer R (2000). Profile and kinetics of L-type calcium current during the cardiac ventricular action potential compared in guinea-pigs rats and rabbits. *Pflugers Arch* **439**, 588-599.

Lipp P & Niggli E (1994). Sodium current-induced calcium signals in isolated guinea-pig ventricular myocytes. *J Physiol* **474**, 439-446.

Litwin SE, Kohmoto O, Levi AJ, Spitzer KW, & Bridge JHB (1996). Evidence that reverse Na⁺/Ca²⁺-exchanger can trigger SR release. *Ann N Y Acad Sci* **779**, 451-463.

Litwin SE, Li J, & Bridge JH (1998). Na⁺/Ca²⁺-exchanger and the trigger for sarcoplasmic reticulum Ca²⁺ release: studies in adult rabbit ventricular myocytes. *Biophys J* **75**, 359-371.

Litwin SE, Raya TE, Anderson PG, Daugherty S, & Goldman S (1990). Abnormal cardiac function in the streptozotocin-diabetic rat. Changes in active and passive properties of the left ventricle. *J Clin Invest* **86**, 481-488.

Lopaschuk GD, Katz S, & Mcneill JH (1983a). The effect of alloxan- and streptozotocin-induced diabetes on calcium transport in rat cardiac sarcoplasmic reticulum. The possible involvement of long chain acylcarnitines. *Can J Physiol Pharmacol* **61**, 439-448.

Lopaschuk GD, Tahiliani AG, Vadlamudi RV, Katz S, & McNeill JH (1983b). Cardiac sarcoplasmic reticulum function in insulin- or carnitine- treated diabetic rats. *Am J Physiol* **245**, H969-H976.

Lopez-Lopez J R, Shacklock P S, Balke C W & Wier W G (1994). Local stochastic release of Ca^{2+} in voltage-clamped rat heart cells: visualization with confocal microscopy. *J Physiol* **480** (Pt 1), 21-29.

Lopez-Lopez J R, Shacklock P S, Balke C W & Wier W G (1995). Local calcium transients triggered by single L-type calcium channel currents in cardiac cells. *Science* **268**, 1042-1045.

Lucchesi BR, Medina M, & Kniffen FJ (1972). The positive inotropic action of insulin in the canine heart. *Eur J Pharmacol* **18**, 107-115.

Lukyanenko V & Gyorke S (1999). Ca^{2+} sparks and Ca^{2+} waves in saponin-permeabilized rat ventricular myocytes. *J Physiol* **521 Pt 3**, 575-585.

Magyar J, Rusznak Z, Szentesi P, Szucs G & Kovacs L (1992). Action potentials and potassium currents in rat ventricular muscle during experimental diabetes. *J Mol Cell Cardiol* **24**, 841-853.

Mahaffrey JE, Aldinger EE, Spronse JH, Darby TD & Thrower WB (1961). The cardiovascular effects of halothane. *Anesthesiology* **22**, 982-986.

Mahgoub MA & Abd-Elfattah AS (1998). Diabetes mellitus and cardiac function. *Mol Cell Biochem* **180**, 59-64.

- Maier LS, Bers DM, & Pieske B (2000). Differences in Ca^{2+} -handling and sarcoplasmic reticulum Ca^{2+} content in isolated rat and rabbit myocardium. *J Mol Cell Cardiol* **32**, 2249-2258.
- Makino N, Dhalla KS, Elimban V, & Dhalla NS (1987). Sarcolemmal Ca^{2+} transport in streptozotocin-induced diabetic cardiomyopathy in rats. *Am J Physiol* **253**, E202-E207.
- Malhotra A & Sanghi V (1997). Regulation of contractile proteins in diabetic heart. *Cardiovasc Res* **34**, 34-40.
- Mangano D T & Goldman L (1995). Preoperative assessment of patients with known or suspected coronary disease. *N Engl J Med* **333**, 1750-1756.
- Marshall SM (2000). HOPE for all people with diabetes? Heart Outcomes Prevention Evaluation. *Diabetes Med* **17** (2), 9-10.
- Mejia-Alvarez R, Kettlun C, Rios E, Stern M & Fill M (1999). Unitary Ca^{2+} current through cardiac ryanodine receptor channels under quasi-physiological ionic conditions. *J Gen Physiol* **113**, 177-186.
- Miller TBJ (1979). Cardiac performance of isolated perfused hearts from alloxan diabetic rats. *Am J Physiol* **236**, H808-H812.
- Misra T, Gilchrist JS, Russell JC, & Pierce GN (1999). Cardiac myofibrillar and sarcoplasmic reticulum function are not depressed in insulin-resistant JCR:LA-cp rats. *Am J Physiol* **276**, H1811-H1817.

Mooradian AD, Morley JE, & Scarpace PJ (1988). The role of zinc status in altered cardiac adenylate cyclase activity in diabetic rats. *Acta Endocrinol* **119**, 174-180.

Muller P (1965). Ouabain effects on cardiac contraction, action potential and cellular potassium. *Circ Res* **17**, 46-56.

Myers MA, Mackay IR, Rowley MJ, & Zimmet PZ (2001). Dietary microbial toxins and type 1 diabetes--a new meaning for seed and soil. *Diabetologia* **44**, 1199-1200.

Myers MG, Jr. & White MF (1996). Insulin signal transduction and the IRS proteins. *Annu Rev Pharmacol Toxicol* **36**, 615-658.

Nagase N (1996a). Hypertension and serum Mg in the patients with diabetes and coronary heart disease. *Hypertens Res* **19**, S65-S68.

Natali A J, Wilson L A, Peckham M, Turner D L, Harrison S M & White E (2002). Different regional effects of voluntary exercise on the mechanical and electrical properties of rat ventricular myocytes. *J Physiol* **541**, 863-875.

Negretti N, O'Neill SC, & Eisner DA (1993). The relative contributions of different intracellular and sarcolemmal systems to relaxation in rat ventricular myocytes. *Cardiovas Res* **27**, 1826-1830.

Nemesanszky E & Gerencser Z (1992). Clinical aspects of magnesium. *Orv Hetil* **133**, 1475-1479.

Nerbonne J M, Nichols C G, Schwarz T L & Escande D (2001). Genetic manipulation of cardiac K(+) channel function in mice: what have we learned and where do we go from here? *Circ Res* **89**, 944-956.

Netticadan T, Temsah RM, Kent A, Elimban V, & Dhalla NS (2001). Depressed levels of Ca²⁺ cycling proteins may underlie sarcoplasmic reticulum dysfunction in the diabetic heart. *Diabetes* **50**, 2133-2138.

Nicolino A, Longobardi G, Furgi G, Rossi M, Zoccolillo N, Ferrara N, & Rengo F (1995). Left-ventricular diastolic filling in diabetes-mellitus with and without hypertension. *Am J Hypertens* **8**, 382-389.

Nicoll DA, Longoni S, & Philipson KD (1990). Molecular cloning and functional expression of the cardiac sarcolemmal Na⁺/Ca²⁺-exchanger. *Science* **250**, 562-565.

Nishio Y, Kashiwagi A, Kida Y, Kodama M, Abe N, Saeki Y, & Shigeta Y (1988). Deficiency of cardiac beta-adrenergic receptor in streptozotocin-induced diabetic rats. *Diabetes* **37**, 1181-1187.

Noda N, Hayashi H, Miyata H, Suzuki S, Kobayashi A, & Yamazaki N (1992). Cytosolic Ca²⁺ concentration and pH of diabetic rat myocytes during metabolic inhibition. *J Mol Cell Cardiol* **24**, 435-446.

Noda N, Hayashi H, Satoh H, Terada H, Hirano M, Kobayashi A, & Yamazaki N (1993). Ca²⁺ transients and cell shortening in diabetic rat ventricular myocytes. *Jpn Circ J* **57**, 449-457.

Nukatsuka M, Sakurai H, Yoshimura Y, Nishida M, & Kawada J (1988). Enhancement by streptozotocin of O₂- radical generation by the xanthine oxidase system of pancreatic beta-cells. *FEBS Lett* **239**, 295-298.

Nukatsuka M, Yoshimura Y, Nishida M, & Kawada J (1990). Importance of the concentration of ATP in rat pancreatic beta cells in the mechanism of streptozotocin-induced cytotoxicity. *J Endocrinol* **127**, 161-165.

Nuss HB & Houser SR (1992). Sodium-calcium exchange-mediated contractions in feline ventricular myocytes. *Am J Physiol* **263**, H1161-H1169.

O'Neill SC & Eisner DA (1990). A mechanism for the effects of caffeine on Ca²⁺ release during diastole and systole in isolated rat ventricular myocytes. *J Physiol* **430**, 519-536.

Okayama H, Hamada M, & Hiwada K (1994). Contractile dysfunction in the diabetic-rat heart is an intrinsic abnormality of the cardiac myocyte. *Clin Sci* **86**, 257-262.

Okazaki O, Suda N, Hongo K, Konishi M, & Kurihara S (1990). Modulation of Ca²⁺ transients and contractile properties by beta- adrenoceptor stimulation in ferret ventricular muscles. *J Physiol* **423**, 221-240.

Oudit G Y, Kassiri Z, Sah R, Ramirez R J, Zobel C & Backx P H (2001). The molecular physiology of the cardiac transient outward potassium current (I_{to}) in normal and diseased myocardium. *J Mol Cell Cardiol* **33**, 851-872.

Pacher P, Liaudet L, Soriano FG, Mabley JG, Szabo E, & Szabo C (2002). The role of poly(ADP-ribose) polymerase activation in the development of myocardial and endothelial dysfunction in diabetes. *Diabetes* **51**, 514-521.

Paolisso G, Esposito R, D'Alessio MA, & Barbieri M (1999). Primary and secondary prevention of atherosclerosis: is there a role for antioxidants? *Diabetes Metab* **25**, 298-306.

Phatak PD & Cappuccio JD (1994). Management of hereditary hemochromatosis. *Blood Rev* **8**, 193-198.

Philbin EF, Weil HF, Francis CA, Marx HJ, Jenkins PL, Pearson TA, & Reed RG (2000). Race-related differences among patients with left ventricular dysfunction: observations from a biracial angiographic cohort. Harlem- Bassett LP(A) Investigators. *J Card Fail* **6**, 187-193.

Philipson KD & Nicoll DA (2000). Sodium-calcium exchange: a molecular perspective. *Annu Rev Physiol* **62**, 111-133.

Pierce GN & Dhalla NS (1981). Cardiac myofibrillar ATPase activity in diabetic rats. *J Mol Cell Cardiol* **13**, 1063-1069.

Pierce GN, Ramjiawan B, Dhalla NS, & Ferrari R (1990). Na⁺/H⁺-exchange in cardiac sarcolemmal vesicles isolated from diabetic rats. *Am J Physiol* **258**, H255-H261.

Pieske B, Maier LS, Bers DM, & Hasenfuss G (1999). Ca²⁺ handling and sarcoplasmic reticulum Ca²⁺ content in isolated failing and non failing human myocardium. *Circ Res* **85**, 38-46.

Pogwizd SM, Schlotthauer K, Li L, Yuan W, & Bers DM (2001). Arrhythmogenesis and contractile dysfunction in heart failure: Roles of sodium-calcium exchange, inward rectifier potassium current, and residual beta-adrenergic responsiveness. *Circ Res* **88**, 1159-1167.

Portha B, Blondel O, Serradas P, McEvoy R, Giroix MH, Kergoat M, & Bailbe D (1989). The rat models of non-insulin dependent diabetes induced by neonatal streptozotocin. *Diabetes Metab* **15**, 61-75.

Pras P, Bayada JM, Bertrand F, Lapalus P, Garaffo R, Savini EC, & Babeau P (1983). The effect of various diseases on the zinc plasma level. *Sem Hop* **59**, 1519-1522.

Prohaska J R (1990). Biochemical changes in copper deficiency. *J Nutr Biochem* **1**, 452-461.

Prohaska J R (1982). Mechanical properties of the copper-deficient rat heart. *J Nutr* **112**, 2142-2150.

Raman M & Nesto RW (1996). Heart disease in diabetes mellitus. *Endocrinol Metab Clin North Am* **25**, 425-438.

Regan TJ, Ettinger PO, Khan MI, Jesrani MU, Lyons MM, Oldewurtel HA, & Weber M (1974). Altered myocardial function and metabolism in chronic diabetes mellitus without ischemia in dogs. *Circ Res* **35**, 222-237.

Reikeras O & Gunnes P (1986). Effects of high doses of insulin on systemic haemodynamics and regional blood flows in dogs. *Clin Physiol* **6**, 129-138.

Ren J & Davidoff AJ (1997). Diabetes rapidly induces contractile dysfunctions in isolated ventricular myocytes. *Am Journal Phys* **41**, H148-H158.

Ren J, Walsh MF, Hamaty M, Sowers JR, & Brown RA (1999). Augmentation of the inotropic response to insulin in diabetic rat hearts. *Life Sci* **65**, 369-380.

Rieker RP, Lee JC, & Downing SE (1975). Positive inotropic action of insulin on piglet heart. *Yale J Biol Med* **48**, 353-359.

Rithalia A, Gibson CN, Hopkins PM, & Harrison SM (2001). Halothane inhibits contraction and action potential duration to a greater extent in subendocardial than subepicardial myocytes from the rat left ventricle. *Anesthesiology* **95**, 1213-1219.

Rosati B, Pan Z, Lypen S, Wang H S, Cohen I, Dixon J E & McKinnon D (2001). Regulation of KChIP2 potassium channel beta subunit gene expression underlies the gradient of transient outward current in canine and human ventricle. *J Physiol* **533**, 119-125.

Rousseau E & Meissner G (1987). Single cardiac sarcoplasmic reticulum Ca²⁺-release channel: activation by caffeine. *Am J Physiol* **256**, H328-H333.

Saari JT (2000). Copper deficiency and cardiovascular disease: role of peroxidation, glycation, and nitration. *Can J Physiol Pharmacol* **78**, 848-855.

Saari J T & Schuschke D A (1999). Cardiovascular effects of dietary copper deficiency. *Biofactors* **10**, 359-375.

Sah R, Ramirez R J, Oudit G Y, Gidrewicz D, Trivieri M G, Zobel C & Backx P H (2003). Regulation of cardiac excitation-contraction coupling by action potential repolarization: role of the transient outward potassium current (I_{to}). *J Physiol* **546**, 5-18.

Saito N (1996). Overview--suppression effect of essential trace elements on arteriosclerotic development and its mechanism. *Nippon Rinsho* **54**, 59-66.

Sandler S & Swenne I (1983). Streptozotocin, but not alloxan, induces DNA repair synthesis in mouse pancreatic islets in vitro. *Diabetologia* **25**, 444-447.

Sasaki S, Oshima T, Matsuura H, Ozono R, Higashi Y, Sasaki N, Matsumoto T, Nakano Y, Ueda A, Yoshimizu A, Kurisu S, Kambe M, & Kajiyama G (2000). Abnormal magnesium status in patients with cardiovascular diseases. *Clin Sci* **98**, 175-181.

Sasaki S, Oshima T, Teragawa H, Matsuura H, Kajiyama G, & Kambe M (1999). Magnesium (Mg) status in patients with cardiovascular diseases. *Rinsho Byori* **47**, 396-401.

Satoh N, Sato T, Shimada M, Yamada K, & Kitada Y (2001). Lusitropic effect of MCC-135 is associated with improvement of sarcoplasmic reticulum function in ventricular muscles of rats with diabetic cardiomyopathy. *J Pharmacol Exp Ther* **298**, 1161-1166.

Savarese JJ & Berkowitz A (1979). β -Adrenergic receptor decrease in diabetic rat hearts. *Life Sci* **25**, 2075-2078.

Schaffer SW (1991). Cardiomyopathy associated with noninsulin-dependent diabetes. *Mol Cell Biochem* **107**, 1-20.

Schaffer SW, Allo S, Punna S, & White T (1991). Defective response to cAMP-dependent protein kinase in non-insulin-dependent diabetic heart. *Am J Physiol* **261**, E369-E376.

Schaffer SW, Mozaffari MS, Artman M, & Wilson GL (1989). Basis for myocardial mechanical defects associated with non-insulin-dependent diabetes. *Am J Physiol* **256**, E25-E30.

Schernthaner G (1996). Cardiovascular mortality and morbidity in type-2 diabetes mellitus. *Diabetes Res Clin Pract* **31**, S3-13.

Schneider JA & Sperelakis N (1975). Slow Ca^{2+} and Na^{+} responses induced by isoproterenol and methylxanthines in isolated perfused guinea-pig hearts exposed to elevated K. *J Mol Cell Cardiol* **7**, 249-273.

Sham JSK, Cleemann L, & Morad M (1995). Functional coupling of Ca^{2+} channels and ryanodine receptors in cardiac myocytes. *PNAS* **92**, 121-125.

Sham J S, Song L S, Chen Y, Deng L H, Stern M D, Lakatta E G & Cheng H (1998). Termination of Ca^{2+} release by a local inactivation of ryanodine receptors in cardiac myocytes. *PNAS* **95**, 15096-15101.

Shattock MJ & Bers DM (1989). Rat vs. rabbit ventricle: Ca^{2+} flux and intracellular Na^{+} assessed by ion-selective microelectrodes. *Am J Physiol* **256**, C813-C822.

Sheetz MJ & King GL (2002). Molecular understanding of hyperglycemia's adverse effects for diabetic complications. *JAMA* **288**, 2579-2588.

Shimoni Y, Ewart HS, & Severson D (1998). Type I and II models of diabetes produce different modifications of K⁺ currents in rat heart: role of insulin. *J Physiol* **507**, 485-496.

Shimoni Y, Firek L, Severson D & Giles W (1994). Short-term diabetes alters K⁺ currents in rat ventricular myocytes. *Circ Res* **74**, 620-628.

Shimoni Y, Severson D & Giles W (1995). Thyroid status and diabetes modulate regional differences in potassium currents in rat ventricle. *J Physiol* **488 (Pt 3)**, 673-688.

Shimoni Y & Severson D L (1995). Thyroid status and potassium currents in rat ventricular myocytes. *Am J Physiol* **268**, H576-H583.

Shipsey S J, Bryant S M & Hart G (1997). Effects of hypertrophy on regional action potential characteristics in the rat left ventricle: a cellular basis for T-wave inversion? *Circulation* **96**, 2061-2068.

Sjostrand FS & Anderson-Cedergren E (1958). The ultra-structure of the intercalated disc of frog, mouse and guinea pig cardiac muscle. *J Ultrastruct Res* **1**, 271-287.

Smogorzewski M, Galfayan V, & Massry SG (1998). High glucose concentration causes a rise in [Ca²⁺]_i of cardiac myocytes. *Kidney Int* **53**, 1237-1243.

Sperelakis N (1988). Regulation of calcium slow channels of cardiac muscle by cyclic nucleotides and phosphorylation. *J Mol Cell Cardiol* **20 Suppl 2**, 75-105.

Spurgeon HA, DuBell WH, Stern MD, Sollott SJ, Ziman BD, Silverman HS, Capogrossi MC, Talo A, & Lakatta EG (1992). Cytosolic calcium and myofilaments in single rat

cardiac myocytes achieve a dynamic equilibrium during twitch relaxation. *J Physiol* **447**, 83-102.

Szkudelski T (2001). The mechanism of alloxan and streptozotocin action in B cells of the rat pancreas. *Physiol Res* **50** , 537-546.

Tada M & Katz AM (1982). Phosphorylation of the sarcoplasmic reticulum and sarcolemma. *Ann Rev Phys* **44**, 401-423.

Tada M, Kirchberger MA, Repke DI, & Katz AM (1974). The stimulation of calcium transport in cardiac sarcoplasmic reticulum by adenosine 3',5' monophosphate dependent protein kinase. *J Biol Chem* **249**, 6174-6180.

Tahiliani AG, Vadlamudi RV, & McNeill JH (1983). Prevention and reversal of altered myocardial function in diabetic rats by insulin treatment. *Can J Physiol Pharmacol* **61**, 516-523.

Takeda N, Dixon IC, Hata T, Elimban V, Shah KR, & Dhalla NS (1996). Sequence of alterations in subcellular organelles during the development of heart dysfunction in diabetes. *Diab Res Clin Prac* **30**, S113-S122.

Tamada A, Hattori Y, Houzen H, Yamada Y, Sakuma I, Kitabatake A, & Kanno M (1998). Effects of beta-adrenoceptor stimulation on contractility, $[Ca^{2+}]_i$, and Ca^{2+} current in diabetic rat cardiomyocytes. *Am J Physiol* **43**, H1849-H1857.

Terentyev D, Viatchenko-Karpinski S, Valdivia H H, Escobar A L & Gyorko S (2002). Luminal Ca^{2+} controls termination and refractory behavior of Ca^{2+} -induced Ca^{2+} release in cardiac myocytes. *Circ Res* **91**, 414-420.

Terrar D A & Victory J G (1988). Effects of halothane on membrane currents associated with contraction in single myocytes isolated from guinea-pig ventricle *Br J Pharmacol* **94**, 500-508.

Teshima Y, Takahashi N, Saikawa T, Hara M, Yasunaga S, Hidaka S, & Sakata T (2000). Diminished expression of sarcoplasmic reticulum Ca^{2+} -ATPase and ryanodine sensitive Ca^{2+} Channel mRNA in streptozotocin-induced diabetic rat heart. *J Mol Cell Cardiol* **32**, 655-664.

Thorsby P, Undlien DE, Berg JP, Thorsby E, & Birkeland KI (1998). Diabetes mellitus--a complex interaction between heredity and environment. *Tidsskr Nor Laegeforen* **118**, 2519-2524.

Topalov V, Kovacevic D, Topalov A, & Kovacevic D (2000). Magnesium in cardiology. *Med Pregl* **53**, 319-324.

Trautwein W & Hescheler J (1990). Regulation of cardiac L-type calcium current by phosphorylation and G proteins. *Ann Rev Physiol* **52**, 257-274.

Trost SU, Belke DD, Bluhm WF, Meyer M, Swanson E, & Dillmann WH (2002). Over expression of the Sarcoplasmic Reticulum Ca^{2+} -ATPase Improves Myocardial Contractility in Diabetic Cardiomyopathy. *Diabetes* **51**, 1166-1171.

Tuomilehto J, Lounamaa R, Tuomilehto-Wolf E, Reunanen A, Virtala E, Kaprio EA, & Akerblom HK (1992a). Epidemiology of childhood diabetes mellitus in Finland--background of a nationwide study of type I (insulin-dependent) diabetes mellitus. The Childhood Diabetes in Finland (DiMe) Study Group. *Diabetologia* **35**, 70-76.

Tuomilehto J, Podar T, Brigis G, Urbonaite B, Rewers M, Adojaan B, Cepaitis Z, Kalits I, King H, LaPorte R, & . (1992b). Comparison of the incidence of insulin-dependent diabetes mellitus in childhood among five Baltic populations during 1983-1988. *Int J Epidemiol* **21**, 518-527.

Tuvemo T & Gebre-Medhin M (1983). The role of trace elements in juvenile diabetes mellitus. *Pediatrician* **12**, 213-219.

Vadlamudi RV & Mcneill JH (1984). Effect of experimental diabetes on isolated rat heart responsiveness to isoproterenol. *Can J Physiol Pharmacol* **62**, 124-131.

Vadlamudi RV, Rodgers RL, & Mcneill JH (1982). The effect of chronic alloxan- and streptozotocin-induced diabetes on isolated rat heart performance. *Can J Physiol Pharmacol* **60**, 902-911.

Vander AJ, Sherman JH, & Luciano DS (1999). *Human Physiology*, 6th Edition. McGraw-Hill, New York.

Varro A Lathrop D A Hester S B Nanasi P P & Papp J G (1993). Ionic currents and action potentials in rabbit rat and guinea pig ventricular myocytes. *Basic Res Cardiol* **88**, 93-102.

Vonherbay A, Niederau C, Pilichowska M, Reinecke P, Perings C, Vester E, Strohmeyer G, & Haussinger D (1996). Cardiomyopathy as a cause of death in genetic hemochromatosis. *Zeitschrift Fur Gastroenterologie* **34**, 178-182.

Vornanen M, Sheperd N, & Isenberg G (1994). Tension-voltage relations of single myocytes reflect Ca^{2+} release triggered by $\text{Na}^+/\text{Ca}^{2+}$ -exchanger at 35°C but not at 23°C . *Am J Physiol* **267**, C623-C632.

Wang DW, Kiyosue T, Shigematsu S, & Arita M (1995). Abnormalities of K^+ and Ca^{2+} currents in ventricular myocytes from rats with chronic diabetes. *Am J Physiol* **269**, H1288-H1296.

Wang S Q, Song L S, Lakatta E G & Cheng H (2001). Ca^{2+} signalling between single L-type Ca^{2+} channels and ryanodine receptors in heart cells. *Nature* **410**, 592-596.

Wang S Q, Song L S, Xu L, Meissner G, Lakatta E G, Rios E Stern M D & Cheng H (2002). Thermodynamically irreversible gating of ryanodine receptors in situ revealed by stereotyped duration of release in Ca^{2+} sparks. *Biophys J* **83**, 242-251.

Watanabe T, Delbridge L M, Bustamante J O & McDonald T F (1983). Heterogeneity of the action potential in isolated rat ventricular myocytes and tissue. *Circ Res* **52**, 280-290.

Weigt H U, Rehmert G C, Bosnjak Z J & Kwok W M (1997b). Conformational state-dependent effects of halothane on cardiac Na^+ current. *Anesthesiology* **87**, 1494-1506.

West E, Simon OR, & Morrison EY (1996). Streptozotocin alters pancreatic beta-cell responsiveness to glucose within six hours of injection into rats. *West Indian Med J* **45**, 60-62.

Wheeler D M, Rice R T, Hansford R G & Lakatta E G (1988). The effect of halothane on the free intracellular calcium concentration of isolated rat heart cells. *Anesthesiology* **69**, 578-583.

Wickenden A D, Kaprielian R, Parker T G, Jones O T & Backx P H (1997). Effects of development and thyroid hormone on K⁺ currents and K⁺ channel gene expression in rat ventricle. *J Physiol* **504 (Pt 2)**, 271-286.

Williams G & Pickup JC (1999). *Handbook of Diabetes*, 2nd ed. Blackwell Science Ltd., London.

Williams NR, Rajputwilliams J, West JA, Nigdikar SV, Foote JW, & Howard AN (1995). Plasma, granulocyte and mononuclear cell copper and zinc in patients with diabetes-mellitus. *Analyst* **120**, 887-890.

Wold LE, Saari JT, & Ren J (2001). Isolated ventricular myocytes from copper-deficient rat hearts exhibit enhanced contractile function. *Am J Physiol* **281**, H476-H481.

Woodbury LA & Hecht HH (1952). Effects of cardiac glycosides upon the electrical activity of single ventricular fibres of the frog heart, and their relation to the digitalis effect of the electrocardiogram. *Circulation* **6**, 172-182.

Wright AR, Rees SA, & Powell T (1997). Sodium-calcium exchange in guinea-pig, marmoset and human cardiac cells. *Biophys J* **72**, A66.

Yu JZ, Quamme GA, & Mcneill JH (1995). Altered $[Ca^{2+}]_i$ mobilization in diabetic cardiomyocytes - responses to caffeine, KCl, Ouabain, and ATP. *Diab Res & Clin Prac* **30**, 9-20.

Yu Z & Mcneill JH (1991). Force-interval relationship and its response to ryanodine in streptozotocin-induced diabetic rats. *Can J Physiol Pharmacol* **69**, 1268-1276.

Yu Z, Quamme GA, & Mcneill JH (1994b). Depressed $[Ca^{2+}]_i$ responses to isoproterenol and cAMP in isolated cardiomyocytes from experimental diabetic rats. *Am J Physiol* **266**, H2334-H2342.

Yu Z, Tibbits GF, & Mcneill JH (1994a). Cellular functions of diabetic cardiomyocytes: contractility, rapid-cooling contracture, and ryanodine binding. *Am J Physiol* **266**, H2082-H2089.

Yuan W, Ginsburg KS, & Bers DM (1996). Comparison of sarcolemmal calcium channel current in rabbit and rat ventricular myocytes. *J Physiol* **493**, 733-746.

Zarain-Herzberg A, Yano K, Elimban V, & Dhalla NS (1994). Cardiac sarcoplasmic reticulum Ca^{2+} -ATPase expression in streptozotocin-induced diabetic rat heart. *Biochem Biophys Res Commun* **203**, 113-120.

Zhong Y, Ahmed S, Grupp IL, & Matlib MA (2001). Altered SR protein expression associated with contractile dysfunction in diabetic rat hearts. *Am J Physiol* **281**, H1137-H1147.

Zimmet P (2000). Globalization, coca-colonization and the chronic disease epidemic: can the Doomsday scenario be averted? *J Intern Med* **247**, 301-310.

Zimmet P, Alberti KG, & Shaw J (2001). Global and societal implications of the diabetes epidemic. *Nature* **414**, 782-787.

9.2 *List of publications arising from work which has been undertaken*

1. Qureshi MA, Bracken NK, Winlow W, Singh J, & Howarth FC (2000). Effects of chronic streptozotocin-induced force-frequency relationships in ventricular myocytes isolated from rat heart. *J Physiol* **523P**, 16P.
2. Bracken, NK, Qureshi, MA, Winlow, W, Singh, J and Howarth, FC (2000). Effects of insulin on contraction of ventricular myocytes from streptozotocin-induced diabetic rat heart. *J Physiol* **528P**, 17P.
3. Howarth FC, Qureshi, MA, Bracken, NK, Winlow, W & Singh, J (2001). Time dependent effects of streptozotocin-induced diabetes on contraction in rat ventricular myocytes. *Emirates Medical J* **19** (1), 35-41.
4. Bracken NK, Howarth FC, Qureshi MA, Winlow W & Singh J (2001). Effects of diabetes on cation contents and on contraction in the isolated rat heart. In *Adap Biol Med* **3**. New Frontier, Eds. Morovec J, Takeda N & Singal PK, Narosa Pub. House, India.
5. Singh J, Howarth FC, Bracken NK, Qureshi MA & Hustler BI (2001). Adaptation of the heart to osmotic shock. In *Adap Biol Med* **3**. New Frontier, Eds. Morovec J, Takeda N & Singal PK, Narosa Pub. House, India
6. Bracken NK, Singh J, Winlow W and Howarth FC (2001). Cellular mechanism of cardiac muscle dysfunction in streptozotocin-induced diabetes mellitus. *Bulletin of the BSCR* **14** (2), 4-13.

7. Bracken NK, Qureshi MA, Winlow W, Singh J & Howarth FC (2001). Effects of exogenous insulin on contraction in the diabetic heart. *J Mol Cell Cardiol* **33** (6), A15.
8. Singh J, Howarth FC, Qureshi MA, Winlow W & Bracken NK (2001). Effects of diabetes on contraction and cation metabolism in the isolated rat heart. *J Mol Cell Cardiol* **33** (6), A111.
9. Bracken, NK, Qureshi MA, Winlow W, Singh J and Howarth FC (2002). Altered Ca^{2+} homeostasis in heart from streptozotocin-induced diabetic rat heart. *J Physiol* **543**, 85P.
10. Bracken, NK, Qureshi MA, Winlow W, Singh J and Howarth FC (2002). The negative inotropic effects of halothane on contractile properties in the streptozotocin-induced diabetic rat heart. *J Physiol* **543**, 85P.
11. Bracken NK, Singh J, Winlow W, & Howarth FC (2003). Mechanisms underlying contractile dysfunction in streptozotocin-induced type 1 and type 2 diabetic cardiomyopathy. In *Atherosclerosis. Hypertension and Diabetes*, Eds. Pierce GN, Nagano M, Zahradka P, & Dhalla NS, pp. 387-408. Kluwer, Boston.
12. Bracken NK, Howarth FC, Qureshi MA, Singh J & Woodall AJ (2003). Effects of halothane on $I_{Ca,L}$, $[Ca^{2+}]_i$ and contraction in the STZ-induced diabetic rat ventricular myocytes. *J Physiol* (in preparation).

13. Bracken NK, Howarth FC, & Singh J (2003). Time course effects of STZ-induced diabetes on contraction and $[Ca^{2+}]_i$ in ventricular myocytes. *J Mol Cell Cardiol* (in preparation).

14. Bracken NK, Howarth FC, & Singh J (2003). Altered Ca^{2+} homeostasis in STZ-induced rat ventricular myocytes. *Exp Physiol* (in preparation).